DEPARTAMENTO DE INGENIERÍA QUÍMICA Y TECNOLOGÍA DEL MEDIO AMBIENTE

UNIVERSIDAD DE OVIEDO

INTERCAMBIO IÓNICO CON RESINAS COMERCIALES Y SINTETIZADAS PARA LA RETENCIÓN DE SULFAMIDAS Y TIOCIANATOS EN SISTEMAS INDIVIDUALES Y MEZCLADOS

TESIS DOCTORAL

POR

ANA MARÍA LÓPEZ FERNÁNDEZ

Febrero, 2014

DEPARTMENT OF CHEMICAL AND ENVIRONMENTAL ENGINEERING

UNIVERSITY OF OVIEDO

ION EXCHANGE WITH COMMERCIAL AND SYNTHESIZED RESINS FOR SULFAMIDES AND THIOCYANATE RETENTION IN INDIVIDUAL AND MULTICOMPONENT SYSTEMS

Ph.D. THESIS

BY

ANA MARÍA LÓPEZ FERNÁNDEZ

February, 2014

RESUMEN DEL CONTENIDO DE TESIS DOCTORAL

1.- Título de la Tesis	
Español/Otro Idioma: INTERCAMBIO IÓNICO CON RESINAS COMERCIALES Y SINTETIZADAS PARA LA RETENCIÓN DE SULFAMIDAS Y TIOCIANATOS EN SISTEMAS INDIVIDUALES Y MEZCLADOS	Inglés: ION EXCHANGE WITH COMMERCIAL AND SYNTHESIZED RESINS FOR SULFAMIDES AND THIOCYANATE RETENTION IN INDIVIDUAL AND MULTICOMPONENT SYSTEMS

2.- Autor	
Nombre: ANA MARÍA LÓPEZ FERNÁNDEZ	
Programa de Doctorado: Ingeniería de Procesos y Ambiental (Mención Calidad MCD2005-00213)	
Órgano responsable: Universidad de Oviedo	

RESUMEN (en español)

El incremento de la contaminación de las aguas debido a actividades industriales, vertidos humanos, prácticas agrícolas y ganaderas, es un fenómeno ambiental de importancia. Las aguas residuales de coquería procedentes de la industria siderúrgica se caracterizan por su alto contenido en tiocianatos y fenoles. Estos contaminantes han de ser tratados antes de su vertido para cumplir con los límites establecidos por la legislación vigente.

Por otro lado, el elevado consumo de antibióticos tanto en veterinaria como en medicina humana está generando gran cantidad de contaminantes conocidos como contaminantes emergentes. Está demostrada la presencia de fármacos en las aguas residuales, así como su baja eliminación en los procesos convencionales de depuración de aguas. También, se han detectado muchos de estos compuestos en aguas subterráneas y superficiales. El principal problema de la presencia de estos compuestos en el medio ambiente es la aparición de cepas bacterianas resistentes a los antibióticos, y además producen efectos tóxicos sobre la fauna acuática.

La creciente necesidad de reutilizar el agua y de cumplir con una legislación cada vez más estricta en términos medioambientales, han hecho necesario el desarrollo de técnicas de tratamiento de aguas alternativas a los tratamientos convencionales existentes. Entre los distintos métodos de tratamientos de aguas, en el presente trabajo se ha elegido la operación de intercambio iónico para eliminar estos contaminantes de las aguas, por las ventajas que presenta frente a otras técnicas como bajo coste, selectividad, fácil regeneración y sencillez en diseño y operación.

En primer lugar, se ha estudiado la viabilidad del proceso de intercambio iónico para eliminar sulfamidas, debido a que se han detectado en elevada concentración en las aguas residuales. Así, se ha analizado la capacidad de retención de las sulfamidas sulfametoxazol (SMX) y sulfametazina (SMZ) en disoluciones sintéticas, empleando la resina Lewatit MP500. Se ha estudiado el equilibrio y la cinética del proceso de intercambio iónico en tanque agitado. Se han modelizado los resultados de equilibrio empleando isotermas de adsorción, y la cinética se ajustó al modelo de transferencia de

masa a través de la película líquida y al modelo de difusión en poros. Se ha estudiado la operación en columna, realizando sucesivos ciclos de carga y elución, y modelizado los datos experimentales ajustándolos a un modelo de lecho fijo.

De igual modo, se ha estudiado la competitividad en el proceso de adsorción empleando disoluciones de mezclas SMX y SMZ. Se han empleado varios modelos basados en la ecuación de Langmuir para describir la adsorción en el sistema binario. También, se ha analizado el proceso de intercambio iónico de SMX en disolución en presencia de sales para simular su comportamiento en aguas reales. Los datos experimentales se han ajustado a la ecuación de Langmuir para sistemas multicomponentes.

Asimismo, se ha estudiado la operación de intercambio iónico para eliminar tiocianato y fenol presentes en disoluciones acuosas y en aguas residuales industriales, empleando las resinas comerciales Lewatit MP500 y Lewatit M610. Se ha evaluado el equilibrio y la cinética del proceso en tanque agitado. Los datos de equilibrio se ajustaron a las isotermas Langmuir y Factor de Separación Constante, y la cinética del proceso se describió empleando el modelo de transferencia de masa a través de la película líquida y el modelo de difusión en poros. A su vez, se estudió la operación en columna. Se realizaron sucesivos ciclos de carga y elución, se determinó las capacidades de retención y la capacidad de recuperación del eluyente.

Finalmente, se han sintetizado polímeros de metacrilato mediante fotopolimerización en forma de partículas esféricas: se han caracterizado y estudiado su capacidad de adsorción de SMX en disolución acuosa. Con el polímero con el que se obtuvieron mejores capacidades de retención, se realizaron ensayos en tanque agitado y en columna empleando disoluciones sintéticas de SMX, SMZ y mezclas de ambos. Se determinaron los parámetros de equilibrio y cinética y se modelizó la operación en columna usando un modelo de lecho fijo. Además, se ha estudiado la capacidad del polímero sintetizado para retener tiocianato y fenol presentes en disoluciones acuosas en tanque agitado y en columna.

RESUMEN (en Inglés)

Increased water pollution due to industrial activities, dumping human, farming practices, is an important environmental phenomenon. Coke wastewater from the steel industry is characterized by its high content of phenols and thiocyanates. These contaminants must be treated before discharge to comply with the limits established by current legislation.

On the other hand, the high consumption of antibiotics in veterinary and human medicine are generating large amount of contaminants known as emerging contaminants. It is demonstrated the presence of drugs in wastewater and their low removal in conventional water treatment processes. Also, many of these compounds have been detected in groundwater and surface water. The main problems of the presence of these compounds in the environment is the emergence of antibiotic resistant bacterial strains and also produce toxic effects on aquatic organisms.

The growing need to reuse water and to comply with increasingly stringent

legislation in environmental terms, have made it necessary development of water treatment techniques alternatives to existing conventional treatments.

Among the different water treatments existing methods, in this work we have chosen the ion exchange operation to remove these contaminants, which has the advantages over other techniques such as low cost, selectivity, easy regeneration and simplicity in design and operation.

Firstly, the feasibility of the ion exchange process to remove sulfonamides were studied due to they have been detected in high concentrations in wastewater. Thus, the retention capabilities of the sulfonamides sulfamethoxazole (SMX) and sulfamethazine (SMZ) were evaluated using synthetic solutions onto Lewatit MP500 resin. Equilibrium and kinetics of the ion exchange process was studied in batch. The equilibrium data were adjusted to isotherm, and kinetics data were modeled using the film mass transfer model through the liquid film and pore diffusion model. The column operation was studied, performing successive loading and elution cycles, and have been modeled using a fixed-bed model.

Similarly, the competition in the adsorption process was studied using mixtures solutions of SMX and SMZ. Several methods based on the Langmuir equation isotherm were used to correlate the binary adsorption data. In addition, the ion exchange process was analyzed using SMX in presence of salts to simulate real behavior in water. Multicomponent Langmuir model was used to describe the experimental data.

Likewise, the ion exchange operation was studied to remove thiocyanate and phenol present in aqueous solutions and in industrial wastewater, using the commercial resins Lewatit MP500 and Lewatit M610. Kinetics and equilibrium studies were carried out in batch. The equilibrium data were fit to the Langmuir and Constant Separation Factor isotherms, and kinetics of the process was described using the film mass transfer model through the liquid film and pore diffusion model. Furthermore, the column operation was evaluated. Successive loading and elution cycles were carried out in column, and the resin retention capacity and the regeneration capacity of the eluant were determined.

Finally, methacrylate polymer beads were synthesized by photopolymerization. They were characterized and its adsorption capacities were studied using SMX aqueous solutions. With the polymer which the highest retention capacity was obtained, tests were conducted in batch and in column using synthetic solutions of SMX, SMZ and mixtures of both compounds. The kinetics and equilibrium parameters were determined and the column operation was modeled using a fixed bed model. Also was studied the ability of the synthesized polymer to retain thiocyanate and phenol from synthetic aqueous solutions both in batch and column procedure.

Date: Sat, 28 Dec 2013 12:12:20 -0500
From: crames@rpi.edu
Subject: Separation Science and Technology - Decision on Manuscript ID LSST-2013-7165.R2
To: mrenduel@uniovi.es

28-Dec-2013

Dear Professor Rendueles:

Ref: SULFAMETHAZINE RETENTION FROM WATER SOLUTIONS BY ION EXCHANGE WITH A STRONG ANIONIC RESIN IN FIXED BED

I am pleased to inform you that your revised manuscript has been accepted for publication in Separation Science and Technology. Your manuscript will now be forwarded to the publisher for copy editing and typesetting.

You will receive proofs for checking, and instructions for transfer of copyright in due course.

The publisher also requests that proofs are checked and returned within 48 hours of receipt.

Many thanks for contributing to Separation Science and Technology. I have enjoyed working with you and I look forward to receiving your next submission.

Sincerely,
Steven Cramer, Ph.D.
Editor, Separation Science and Technology
crames@rpi.edu

AGRADECIMIENTOS

En primer lugar me gustaría agradecer al Prof. José Mario Díaz y al Dr. Manuel Rendueles por la dirección del trabajo, el apoyo prestado, y el tiempo dedicado a corregir los fallos y solucionar los problemas surgidos durante la investigación.

Al Dr. Manuel Rendueles quisiera agradecerle en especial su paciencia y dedicación, me ayudo a dar mis primeros pasos en una técnica desconocida para mí, el intercambio iónico e ir ganando confianza y autonomía en el laboratorio. Gracias por la paciencia, los buenos consejos y las palabras de ánimo durante estos años.

Asimismo quisiera agradecer a la Dra. Dña Angeles Villa por haberme enseñado e introducido en la síntesis de polímeros y poner a mi disposición su extensa experiencia en el campo de la caracterización de materiales.

Quisiera asimismo agradecer a la Prof. Maria Aurora Fernández por permitirme llevar a cabo una breve estancia en el Departamento de Ingeniería Química y Medioambiente del Institut National Des Sciences Apliquées de Toulouse, por su apoyo y sus consejos. Quisiera agradecer también a la doctoranda Manel Wakkel, por la ayuda prestada durante mi estancia en el INSA, por su colaboración en el laboratorio, su acogida y por hacerme sentir como en casa.

Quisiera agradecer a FICYT (Fundación para el Fomento en Asturias de la Investigación Científica Aplicada y la Tecnología) por el apoyo económico con la concensión de una beca del Programa Severo Ochoa para la realización de la Tesis doctoral.

Quiero agradecer mi enorme gratitud al Dr. Federico Gularte por su ayuda desde el primer día, así como por sus palabras de ánimo y consejos en los momentos difíciles, y al Dr. Sergio Collado por su inestimable ayuda y por su disponibilidad para atender cualquier duda. A Laura por su colaboración, compañía y por el apoyo prestado durante la realización del trabajo de investigación.

A mis compañeros de laboratorio del grupo TBR (Isma, Sergio, Carlos, Saúl, Paula,…) por su acogida desde el primer día, su ayuda desinteresada y por ser responsables del agradable ambiente reinante.

A todos mis compañeros y amigos del Departamento de Ingeniería Química (Rita, Celeste, Leti, Maria, Gema,Yoli, Rosana, Adrian, Janire, etc.) y en general a toda la gente fantástica que he tenido la suerte de conocer estos años, los que ya estaban cuando llegue, y los que han compartido conmigo mi andadura doctoral, y han hecho más agradable mi estancia en el Departamento. En especial, quiero agradecer a mis compañeras Celeste y Rita por su inestimable apoyo, sus ánimos en los momentos dificiles, las risas en las horas del café, y por todos los buenos momentos vividos desde que llegamos juntas al Departamento.

Y por último quisiera agradecer a mi familia y amigos, por el apoyo que me han dado desde siempre y sobre todo en los momentos difíciles.

ÍNDICE

LISTA DE FIGURAS

LISTA DE TABLAS

RESUMEN

El incremento de la contaminación de las aguas debido a actividades industriales, vertidos humanos, prácticas agrícolas y ganaderas, es un fenómeno ambiental de importancia. Las aguas residuales de coquería procedentes de la industria siderúrgica se caracterizan por su alto contenido en tiocianatos y fenoles. Estos contaminantes han de ser tratados antes de su vertido para cumplir con los límites establecidos por la legislación vigente.

Por otro lado, el elevado consumo de antibióticos tanto en veterinaria como en medicina humana está generando gran cantidad de contaminantes conocidos como contaminantes emergentes. Está demostrada la presencia de fármacos en las aguas residuales, así como su baja eliminación en los procesos convencionales de depuración de aguas. También, se han detectado muchos de estos compuestos en aguas subterráneas y superficiales. El principal problema de la presencia de estos compuestos en el medio ambiente es la aparición de cepas bacterianas resistentes a los antibióticos, y además producen efectos tóxicos sobre la fauna acuática.

La creciente necesidad de reutilizar el agua y de cumplir con una legislación cada vez más estricta en términos medioambientales, han hecho necesario el desarrollo de técnicas de tratamiento de aguas alternativas a los tratamientos convencionales existentes. Entre los distintos métodos de tratamientos de aguas, en el presente trabajo se ha elegido la operación de intercambio iónico para eliminar estos contaminantes de las aguas, por las ventajas que presenta frente a otras técnicas como bajo coste, selectividad, fácil regeneración y sencillez en diseño y operación.

En primer lugar, se ha estudiado la viabilidad del proceso de intercambio iónico para eliminar sulfamidas, debido a que se han detectado en elevada concentración en las aguas residuales. Así, se ha analizado la capacidad de retención de las sulfamidas sulfametoxazol (SMX) y sulfametazina (SMZ) en disoluciones sintéticas, empleando la resina Lewatit MP500. Se ha estudiado el equilibrio y la cinética del proceso de intercambio iónico en tanque agitado. Se han modelizado los resultados de equilibrio empleando isotermas de adsorción, y la cinética se ajustó al modelo de transferencia de masa a través de la película líquida y al modelo de difusión en poros. Se ha estudiado la

operación en columna, realizando sucesivos ciclos de carga y elución, y modelizado los datos experimentales ajustándolos a un modelo de lecho fijo.

De igual modo, se ha estudiado la competitividad en el proceso de adsorción empleando disoluciones de mezclas SMX y SMZ. Se han empleado varios modelos basados en la ecuación de Langmuir para describir la adsorción en el sistema binario. También, se ha analizado el proceso de intercambio iónico de SMX en disolución en presencia de sales para simular su comportamiento en aguas reales. Los datos experimentales se han ajustado a la ecuación de Langmuir para sistemas multicomponentes.

Asimismo, se ha estudiado la operación de intercambio iónico para eliminar tiocianato y fenol presentes en disoluciones acuosas y en aguas residuales industriales, empleando las resinas comerciales Lewatit MP500 y Lewatit M610. Se ha evaluado el equilibrio y la cinética del proceso en tanque agitado. Los datos de equilibrio se ajustaron a las isotermas Langmuir y Factor de Separación Constante, y la cinética del proceso se describió empleando el modelo de transferencia de masa a través de la película líquida y el modelo de difusión en poros. A su vez, se estudió la operación en columna. Se realizaron sucesivos ciclos de carga y elución, se determinó las capacidades de retención y la capacidad de recuperación del eluyente.

Finalmente, se han sintetizado polímeros de metacrilato mediante fotopolimerización en forma de partículas esféricas: se han caracterizado y estudiado su capacidad de adsorción de SMX en disolución acuosa. Con el polímero con el que se obtuvieron mejores capacidades de retención, se realizaron ensayos en tanque agitado y en columna empleando disoluciones sintéticas de SMX, SMZ y mezclas de ambos. Se determinaron los parámetros de equilibrio y cinética y se modelizó la operación en columna usando un modelo de lecho fijo. Además, se ha estudiado la capacidad del polímero sintetizado para retener tiocianato y fenol presentes en disoluciones acuosas en tanque agitado y en columna.

ABSTRACT

Increased water pollution due to industrial activities, dumping human, farming practices, is an important environmental phenomenon. Coke wastewater from the steel industry is characterized by its high content of phenols and thiocyanates. These contaminants must be treated before discharge to comply with the limits established by current legislation.

On the other hand, the high consumption of antibiotics in veterinary and human medicine are generating large amount of contaminants known as emerging contaminants. It is demonstrated the presence of drugs in wastewater and their low removal in conventional water treatment processes. Also, many of these compounds have been detected in groundwater and surface water. The main problems of the presence of these compounds in the environment is the emergence of antibiotic resistant bacterial strains and also produce toxic effects on aquatic organisms.

The growing need to reuse water and to comply with increasingly stringent legislation in environmental terms, have made it necessary development of water treatment techniques alternatives to existing conventional treatments.

Among the different water treatments existing methods, in this work we have chosen the ion exchange operation to remove these contaminants, which has the advantages over other techniques such as low cost, selectivity, easy regeneration and simplicity in design and operation.

Firstly, the feasibility of the ion exchange process to remove sulfonamides were studied due to they have been detected in high concentrations in wastewater. Thus, the retention capabilities of the sulfonamides sulfamethoxazole (SMX) and sulfamethazine (SMZ) were evaluated using synthetic solutions onto Lewatit MP500 resin. Equilibrium and kinetics of the ion exchange process was studied in batch. The equilibrium data were adjusted to isotherm, and kinetics data were modeled using the film mass transfer model through the liquid film and pore diffusion model. The column operation was studied, performing successive loading and elution cycles, and have been modeled using a fixed-bed model.

Similarly, the competition in the adsorption process was studied using mixtures solutions of SMX and SMZ. Several methods based on the Langmuir equation isotherm were used to correlate the binary adsorption data. In addition, the ion exchange process was analyzed using SMX in presence of salts to simulate real behavior in water. Multicomponent Langmuir model was used to describe the experimental data.

Likewise, the ion exchange operation was studied to remove thiocyanate and phenol present in aqueous solutions and in industrial wastewater, using the commercial resins Lewatit MP500 and Lewatit M610. Kinetics and equilibrium studies were carried out in batch. The equilibrium data were fit to the Langmuir and Constant Separation Factor isotherms, and kinetics of the process was described using the film mass transfer model through the liquid film and pore diffusion model. Furthermore, the column operation was evaluated. Successive loading and elution cycles were carried out in column, and the resin retention capacity and the regeneration capacity of the eluant were determined.

Finally, methacrylate polymer beads were synthesized by photopolymerization. They were characterized and its adsorption capacities were studied using SMX aqueous solutions. With the polymer which the highest retention capacity was obtained, tests were conducted in batch and in column using synthetic solutions of SMX, SMZ and mixtures of both compounds. The kinetics and equilibrium parameters were determined and the column operation was modeled using a fixed bed model. Also was studied the ability of the synthesized polymer to retain thiocyanate and phenol from synthetic aqueous solutions both in batch and column procedure.

1. INTRODUCCIÓN Y OBJETIVOS

1.1. INTRODUCCIÓN

Tanto para el hombre como para los seres vivos que habitan el planeta, el agua es una sustancia esencial para sus funciones vitales y para las actividades que rigen su vida. A pesar de que el agua cubre el 72% de la superficie de la Tierra, sólo el 0.7% de ésta se encuentra en forma de ríos y lagos, que es donde cuenta con las condiciones físicas y químicas más convenientes para su consumo en alimentación, higiene, y en las diversas actividades que el ser humano realiza como la agricultura o la industria [1]. La constante necesidad del hombre por el uso de este recurso natural ha traído como consecuencia que grandes masas de agua se contaminen, disminuyendo la cantidad de agua disponible. Los gobiernos de algunos países, principalmente de los más desarrollados, han comenzado a tener conciencia de la problemática existente y se han centrado en investigar diferentes técnicas de tratamiento de aguas para reducir los dañinos efectos que la contaminación ha ocasionado en este recurso. El objetivo de estos tratamientos es disminuir la cantidad de agentes contaminantes del agua dependiendo, no solo del tipo de contaminante, sino también, del uso que se hará del agua una vez que se haya sido tratada. En este trabajo nos centraremos en los contaminantes generados en las industrias siderúrgicas y en los denominados contaminantes emergentes.

Contaminantes emergentes. Fármacos

Los hábitos de consumo actuales en nuestra sociedad están generando una serie de residuos o microcontaminantes conocidos como contaminantes emergentes entre los que destacan fármacos, productos de higiene personal y detergentes [2].

Una característica común a todos ellos es que, si bien son introducidos en el medio ambiente a concentraciones no muy elevadas, lo hacen de manera regular y continua, de modo que concentraciones consideradas inicialmente inocuas pueden derivar en efectos negativos a largo plazo. De todos los contaminantes emergentes, los fármacos son los que probablemente hayan generado una mayor preocupación científica e impacto social en los últimos años debido principalmente a la cotidianeidad de su uso. Tras su administración, éstos son adsorbidos y metabolizados por el organismo y luego excretados junto con las aguas residuales. Algunas de estas sustancias no son degradadas en las depuradoras y llegan a las aguas superficiales junto con los vertidos

de los efluentes depurados [3, 4]. De la amplia variedad de fármacos existentes, los antibióticos son los que suscitan mayor interés tanto a nivel científico como social debido a que son los que se usan más habitualmente.

El uso indiscriminado de antibióticos tanto en salud humana como en la cría de animales de consumo, son los responsables directos del desarrollo de cepas bacterianas patógenas resistentes después de una exposición prolongada al antibiótico en cuestión, dificultando su uso en posteriores tratamientos, e indirectamente de la imposibilidad del tratamiento antimicrobiano para determinadas enfermedades infecciosas.

Dentro del grupo de los antibióticos, en este trabajo nos centraremos en las sulfamidas, y concretamente en el sulfametoxazol y la sulfametazina, ya que aparecen en elevadas concentraciones tanto en aguas residuales, efluentes de las estaciones depuradoras, aguas superficiales y subterráneas, y además son compuestos muy poco biodegradables. En estudios realizados en la Universidad de Santiago de Compostela se han detectado concentraciones en aguas residuales entre 0.6 y 6.6 µg/L de sulfametoxazol [5]. En Cataluña, se han detectado concentraciones de sulfametoxazol a la entrada de las estaciones depuradoras de aguas residuales (EDAR) de 590 ng/L y a la salida de 390 ng/L. En otras investigaciones han detectado concentraciones de hasta 1900 ng/L de sulfametoxazol y 220 ng/L de sulfametazina en aguas subterráneas [6, 7]. Como se puede observar, los sistemas convencionales de depuración de aguas no son eficaces eliminando estos compuestos, y debido a la existencia de una legislación medioambiental cada vez más rigurosa, es necesario desarrollar nuevos métodos de tratamiento alternativos.

Existe una amplia variedad de trabajos sobre eliminación de contaminantes emergentes mediante adsorción con carbón activo, procesos de oxidación avanzada, nanofiltración y osmosis inversa. A pesar de los buenos resultados obtenidos con algunos de los métodos como con los procesos de oxidación, también presentan algunas desventajas como el elevado coste y la generación de subproductos de reacción. Los procesos de adsorción tienen como ventajas que no dan lugar a subproductos y son más simples que otras técnicas en cuanto a diseño y operación. El adsorbente más empleado para la adsorción de contaminantes emergentes es el carbón activo, pero tiene el inconveniente de su elevado coste, además de la pérdida de eficacia tras su regeneración

mediante incineración. Por tanto, de ahí el interés por nuevas técnicas de eliminación de estos contaminantes.

Contaminantes de las industrias siderúrgicas

Los residuos generados en las plantas siderúrgicas en el proceso de obtención del coque, empleado para el funcionamiento de los altos hornos, se pueden dividir en tres grandes grupos: gaseosos (SO_2, CO, NOx), sólidos y líquidos. De todos ellos, las aguas de coquería y las procedentes del alto horno son las que contienen mayor cantidad de contaminantes. En concreto, el caudal de aguas residuales de coquería generado es del orden de 0.25-0.3 cm^3/Tm coque producido, denominación que incluyen a las aguas amoniacales, aguas de enfriamiento, condensados y efluentes de la recuperación de aceites ligeros.

Estas aguas residuales de coquería cuentan con una carga apreciable de toxicidad causada por compuestos tales como fenoles, cianuros, tiocianatos, amonio, sulfuros, cloruros así como pequeñas cantidades de hidrocarburos aromáticos y compuestos heterocíclicos nitrogenados. Presentan una elevada DQO, próxima a 4000 mg/L, siendo los principales tóxicos el tiocianato y el fenol, que se encuentran en concentraciones próximas a 400 mg/L tiocianato y entre 500-1000 mg/L fenol.

Los fenoles están considerados como compuestos muy tóxicos para el ser humano y para algunas formas de vida acuática. La ingestión de pequeñas cantidades de fenol puede provocar alteraciones hemáticas y disfunciones en el sistema nervioso, llegando a poder provocar la muerte del individuo con ingestiones de 1 gramo de fenol, y la muerte de peces cuando la concentración de fenol es superior a 3 ppm [8]. El tiocianato es considerado un compuesto muy tóxico para los peces, mientras que el riesgo para el medio acuático y terrestre está considerado como medio, llegando a ser letal para los mamíferos una concentración en sangre superior a 150 mg/L. Algunas de las características tóxicas del tiocianato son convulsiones, problemas de respiración y debilidad muscular para pequeñas exposiciones, hasta serios problemas de ansiedad y coordinación motriz por la ingesta de grandes cantidades [9].

Tras conocer los efectos dañinos que dichos compuestos provocan queda clara la necesidad de eliminarlos de las aguas residuales. Los fenoles pueden ser eliminados mediante tratamientos biológicos, procesos catalíticos, adsorción, membranas. El

método más común es el tratamiento biológico, pero en concentraciones altas, el fenol resulta tóxico para los microorganismos, inhibiendo su crecimiento. La adsorción con carbón activo es una técnica sencilla, sin embargo, sólo es útil para el tratamiento de aguas residuales con bajo contenido en fenoles, además del inconveniente que suponen los costes de su regeneración. En cuanto al tiocianato, hay varios trabajos sobre la eliminación de este contaminante mediante adsorción en carbón activo, cloración alcalina, membranas, oxidación y la técnica más extendida que es el tratamiento biológico. Cuando se encuentra en bajas concentraciones puede ser eliminado mediante procesos biológicos, pero a concentraciones altas resulta tóxico para los microorganismos, siendo inviable su tratamiento biológico para concentraciones superiores a 500 mg/L. Además, esta técnica requiere elevados tiempos de residencia, tanques de gran capacidad y microorganismos que son extremadamente sensibles a la temperatura y el pH.

Entre las posibles técnicas viables para la eliminación de las sulfamidas sulfametoxazol y sulfametazina, y del tiocianato y fenol procedentes de aguas residuales de coquería, en este trabajo se ha elegido el intercambio iónico con resinas, debido a que es una operación sencilla, barata y adecuada para usos a pequeña escala industrial. Además no produce contaminantes secundarios, es una técnica muy compacta, selectiva, versátil y de fácil regeneración del adsorbente. El intercambio iónico es uno de los métodos más usados para la eliminación de sustancias tóxicas de las aguas residuales municipales e industriales, pudiendo aplicarse a aguas residuales que contienen metales, aniones como haluros, sulfatos, nitratos, cianuros y compuestos orgánicos como ácidos carboxílicos, sulfónicos y fenoles. Las resinas de intercambio iónico se emplean sobre todo en el ablandamiento de aguas, operaciones hidrometalurgias y recuperación de iones durante la producción de productos farmacéuticos.

1.2. OBJETIVOS

El objetivo principal de este trabajo es determinar la viabilidad del proceso de intercambio iónico para eliminar dos tipos de contaminantes presentes en las aguas: tiocianatos y fenoles en las aguas residuales de coquería; contaminantes emergentes como las sulfamidas sulfametoxazol (SMX) y sulfametazina (SMZ) en aguas residuales,

superficiales y subterráneas, empleando tanto resinas comerciales como polímeros sintetizados en el propio laboratorio. En la siguiente figura se muestra un esquema del estudio llevado a cabo en este trabajo.

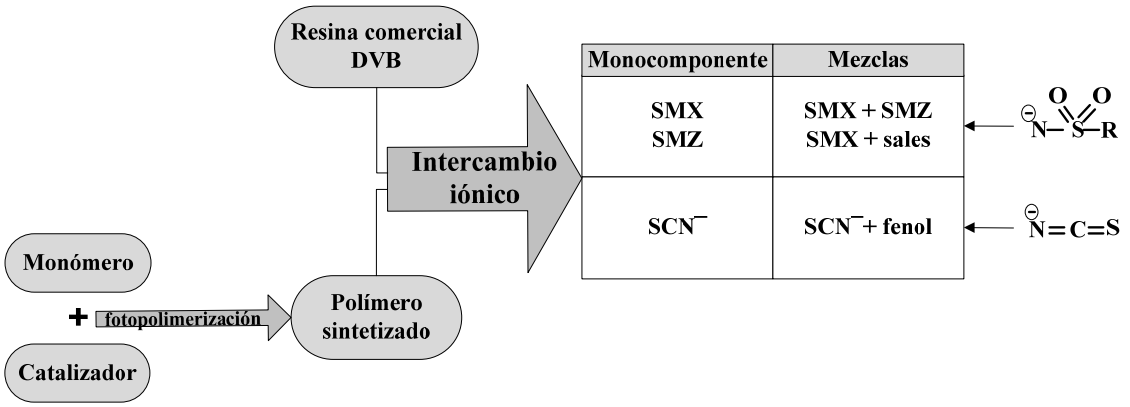

Figura 1. Esquema del estudio realizado

Específicamente, los objetivos desarrollados de detallan a continuación:

- ✓ Estudiar la viabilidad de la operación de intercambio iónico para eliminar SMX y SMZ presentes en disolución acuosa.
- ✓ Investigar la viabilidad de la operación de intercambio iónico para eliminar SMX en presencia de sales en soluciones acuosas.
- ✓ Analizar la competitividad entre SMX y SMZ en el proceso de intercambio iónico.
- ✓ Estudiar la viabilidad de la operación de intercambio iónico para eliminar tiocianato y fenol presentes en aguas residuales de coquería.
- ✓ Sintetizar y caracterizar resinas mediante fotopolimerización y estudiar su aplicabilidad para retener tiocianato, fenol, SMX y SMZ presentes en disoluciones acuosas.
- ✓ Modelizar los resultados obtenidos en el proceso de intercambio en los sistemas mono y multicomponentes.

El estudio se basará en la determinación de las capacidades de intercambio iónico en tanque agitado y modelización de los resultados de equilibrio y cinética obtenidos de cada sistema citado. Los datos experimentales de equilibrio se ajustarán a isotermas de adsorción para sistemas mono y multicomponentes y el estudio de la

cinética del proceso de intercambio iónico se realizará aplicando dos modelos: modelo de transferencia de masa a través de la película líquida y modelo de difusión en poros; determinando los parámetros de equilibrio y cinética. Así mismo, se estudiará la operación en columna, la capacidad de reutilización de las resinas, la capacidad de concentrar del eluyente y se simularán las curvas de ruptura obtenidas ajustándolas a un modelo de lecho fijo.

1.3. ESTRUCTURA DE LA MEMORIA

La actual memoria se presenta como un compendio de publicaciones que se enmarcan dentro del campo de tratamiento de aguas residuales. Cada una de las publicaciones consta de introducción, materiales y métodos, resultados y discusión. Dichas publicaciones están aceptadas o están siendo evaluadas por las revistas incluidas en el *Science Citation Index*. La estructura de la presente memoria se encuentra dividida en 7 capítulos.

En el **capítulo 1**, correspondiente a la introducción y objetivos de la memoria, se plantea la problemática actual derivada de la presencia de sulfamidas en el medio ambiente, así como la de tiocianatos y fenoles en las aguas residuales de coquería, exponiendo las causas reales que han motivado a la realización del presente trabajo.

En el **capítulo 2**, consideraciones teóricas, se desarrolla de forma más amplia los dos tipos de contaminantes en que se centra este trabajo (subapartado **2.1**), los fármacos como contaminantes emergentes y contaminantes de la industria siderúrgica. Dentro de éste subapartado se describen aspectos como la problemática de la presencia de fármacos en el medio ambiente, las vías de entrada y los efectos que provocan, y se desarrollan aspectos teóricos de las sulfamidas de estudio en cuestión, sulfametoxazol y sulfametazina. En cuanto a los contaminantes siderúrgicos, se describen los dos tipos de contaminantes en los que se centra este trabajo, tiocianato y fenol. A continuación se analizan los distintos tratamientos existentes para eliminar ambos contaminantes (subapartado **2.2**), centrándose este estudio en el uso de resinas de intercambio iónico que se desarrollará ampliamente en el subapartado **2.3**. Se explica la operación de intercambio iónico, modos de operación, equilibrio y cinética. En el subapartado **2.4** se exponen los materiales empleados como intercambiadores iónicos, se describe las diferentes técnicas de polimerización existentes, la formación de los copolímeros de

estireno-divinilbenceno y metacrilato, así como las técnicas de caracterización de los polímeros.

En el **capítulo 3**, metodología experimental, se describen las metodologías empleadas para la consecución de los resultados. Aunque la metodología específica de cada estudio realizado se detalla en su correspondiente publicación, en este capítulo se ha pretendido hacer hincapié en las técnicas comunes empleadas en la realización de los experimentos y en las técnicas analíticas usadas. Finalmente, se ha descrito el proceso de síntesis y caracterización de polímeros llevados a cabo en el laboratorio para la obtención de resinas posteriormente empleadas para la adsorción de los dos tipos de contaminantes en que se centra este trabajo.

El **capítulo 4**, correspondiente a la parte de resultados de la tesis, en el cual cada subapartado corresponde a cada uno de los artículos, bien publicados o en vista de serlo. Dichos trabajos son independientes entre sí, aunque todos tienen una base en común que es la eliminación de los contaminantes de las aguas (tiocianatos, fenoles y sulfamidas) mediante resinas de intercambio iónico (comerciales o sintetizadas en el laboratorio). En todas las publicaciones se ha estudiado el equilibrio y la cinética del proceso de intercambio iónico en tanque agitado, la operación en columna para simular la operación a escala industrial y se han modelizado los resultados.

En el subapartado **4.1** se presenta la publicación realizada centrada en el estudio de la operación de intercambio iónico para eliminar un tipo de sulfamida, el sulfametoxazol (SMX), presente en disolución acuosa empleando la resina comercial Lewatit MP500.

El subapartado **4.2** se muestra la publicación realizada con los resultados obtenidos en la eliminación de otro tipo de sulfamida, la sulfametazina (SMZ), empleando la resina comercial Lewatit MP500.

El subapartado **4.3** corresponde a la publicación realizada con los resultados obtenidos en la aplicación de la resina Lewatit MP500 para eliminar SMX presente en disolución acuosa en presencia de sales, para simular el comportamiento que tendría en aguas reales y analizar la competencia en el proceso de intercambio iónico.

En la publicación del subapartado **4.4** se exponen los resultados obtenidos empleando la resina comercial Lewatit MP500 y disoluciones mezclas de las sulfamidas SMX y SMZ, estudiando la competitividad entre ambos compuestos en el proceso de intercambio iónico.

El subapartado **4.5** corresponde a la publicación realizada basada en la eliminación de tiocianatos y fenoles presentes en las aguas residuales de coquería mediante dos tipos de resinas aniónicas comerciales, Lewatit MP500 y Lewatit M610.

En el subapartado **4.6**, se presenta la publicación realizada sobre la síntesis y caracterización de nuevas resinas y posterior uso para la eliminación de SMX en disolución acuosa, con los estudios de capacidad de retención, estudio y modelización del equilibrio y la cinética en tanque agitado, y estudio de la operación en columna.

El subapartado **4.7** corresponde a la publicación realizada con los resultados obtenidos empleando la resina sintetizada previamente, para eliminar SMZ en disolución acuosa y mezclas de SMX y SMZ en disoluciones acuosas. Finalmente, en esta sección de resultados, se expone en el subapartado **4.8** la publicación realizada empleando nuevamente la resina sintetizada para eliminar tiocianatos y fenoles presentes en disoluciones acuosas.

En el **capítulo 5** se exponen las conclusiones obtenidas en la presente memoria sobre los aspectos más importantes como capacidades de retención obtenidas, parámetros de equilibrio y cinética y reutilización de las resinas.

El **capítulo 6** está destinado a una bibliografía común a la memoria.

En la última parte de la memoria, bajo el título de **Anexos**, se recoge la difusión de la tesis doctoral y el informe del factor de impacto de las publicaciones.

2. CONSIDERACIONES TEÓRICAS

2.1. CONTAMINANTES

2.1.1. Los fármacos como contaminantes emergentes

Como ya se ha comentado en la introducción, de todos los contaminantes emergentes, los fármacos son los que más preocupan hoy en día debido a la cotidianidad en su uso. La **Tabla 1** muestra el consumo de antibióticos empleados en salud humana y en veterinaria en el 2011 en algunos países europeos y en Estados Unidos, pudiéndose observar como la mayor parte del consumo es en veterinaria. La **Figura 2** muestra como el 71% de los antibióticos usados en veterinaria son tetraciclinas, penicilinas y sulfamidas [10]. Las sulfamidas constituyen el tercer grupo más usado en veterinaria después de las tetraciclinas y penicilinas, y será en concreto en las sulfamidas en las que nos centremos en esta tesis.

Tabla 1. Consumo de antibióticos en medicina humana y veterinaria en 2011

	Humanos	Veterinaria
Francia	29.5 DDD*	912.8 ton**
Italia	28 DDD*	1826.3 ton**
España	19.5 DDD*	1671.9 ton**
Alemania	15 DDD*	1780.7 ton**
U.S.A	3628 ton***	13542 ton***

*Valores expresados en (DDD) dosis diaria definida por 1000 habitantes y por días Fuente: ESAC-Net (European Surveillance of Antimicrobial Consumption Network). **Fuente: European Medicines Agency. ***Fuente: U.S. FDA (Food and Drug Administration)

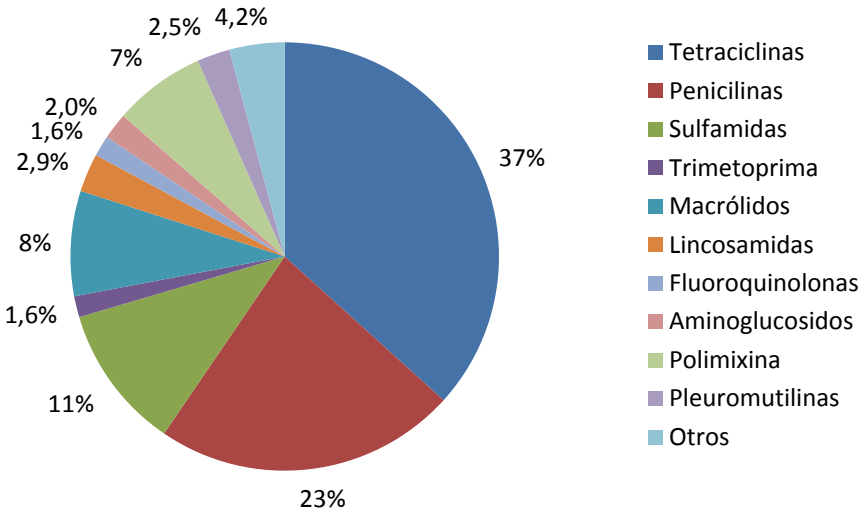

Figura 2. Distribución del consumo de antibióticos en veterinaria en Europa

Dentro de los fármacos, pueden considerarse los más representativos los siguientes grupos:

- Antiinflamatorios y analgésicos. Dentro de este grupo los compuestos más empleados son paracetamol, ácido acetilsalicílico, ibuprofeno y diclofenaco.
- Antidepresivos. Los más frecuentes son las benzodiacepinas.
- Antiepilépticos. El más común es la carbamazepina.
- Antilipemiantes. Los fármacos más frecuentes son los fibratos.
- β-bloqueantes. Los más utilizados son el atenodol, propanol y metoprolol.
- Antiulcerosos y antihistamínicos. Comúnmente se emplean la ranitidina y la famotidina, entre otros.
- Antibióticos. Entre los más importantes se encuentran las tetraciclinas, macrolitos, β-lactámicos, penicilinas, quinolonas, sulfamidas, fluoroquinonas, cloranfenicol y derivados imidazólicos.
- Otras sustancias: cocaína, barbitúricos, metadona, anfetaminas, opiáceos, heroína y otros narcóticos.

Un aspecto a destacar en los fármacos es que presentan una serie de características que los hace diferentes a los contaminantes químicos industriales convencionales:

- Están formados por moléculas grandes y químicamente complejas, de muy diferente peso molecular, estructuras, funcionalidad, forma, etc.
- Son moléculas polares y tienen más de un grupo ionizable.
- La persistencia en el medio ambiente es más de un año para fármacos como el sulfametoxazol y de varios años para el ácido clofíbrico.
- Después de su administración, las moléculas son adsorbidas, distribuidas y sujetas a reacciones metabólicas donde la estructura química de la molécula puede ser modificada.

2.1.1.1. Vías de entrada de los antibióticos al medioambiente

Tras la ingesta de antibióticos, una parte de ellos se transforman en el organismo, de modo que algunas de las especies originales y sus respectivos metabolitos son excretados en la orina y las heces en las aguas de desagüe (aguas

residuales urbanas) que llegan a las estaciones depuradoras de aguas residuales (EDAR). Su eliminación durante el tratamiento suele ser insuficiente para la mayoría de los fármacos, debido a que en los parámetros de control de las EDAR no se encuentra la determinación de ningún tipo de contaminante emergente, y los parámetros de control que utilizan como la DBO no son efectivos para estos compuestos. Por tanto, los efluentes de las EDAR se consideran una de las principales fuentes de vertido de estas sustancias en las zonas urbanas [11, 12, 13].

Por otro lado, la deposición de los lodos procedentes de las EDAR como fertilizantes en campos de cultivo constituye una importante vía de entrada de estos compuestos al medioambiente, ya que contienen fármacos que no han sido retenidos en los tratamientos biológicos. Una vez en el suelo, estos compuestos se infiltran en el terreno hasta los acuíferos o aguas superficiales al ser arrastrados por escorrentía [14, 15]. Otras vías de entrada son los efluentes de hospitales, los vertidos accidentales durante el proceso de fabricación, la eliminación de fármacos no usados o caducados a través de WCs, la filtración de fosas sépticas y otros sistemas de almacenaje de residuos [16, 17]. En las zonas rurales, los fármacos veterinarios usados en criaderos o cebaderos de ganadería intensiva llegan al medio ambiente por la deposición directa en el suelo de las heces y orina de los animales medicados, su almacenaje y posterior uso como estiércol en los campos de cultivo, pudiendo llegar a alcanzar los acuíferos por infiltración o aguas superficiales por escorrentía.

La **Figura 3** esquematiza las vías de entrada de los fármacos al medio ambiente [18]. Como se observa, algunos de estos fármacos no son eliminados completamente en las estaciones depuradoras de aguas residuales [19]. Los sistemas de tratamiento convencional, basados en el uso de microorganismos, resultan inadecuados para destruir de forma efectiva este tipo de compuestos orgánicos debido a su compleja estructura molecular y a las bajas concentraciones en las que se encuentran. En muchos casos el porcentaje eliminado es inferior al 10% [20, 21, 22].

Los fármacos encontrados con mayor frecuencia en los efluentes de las plantas de tratamiento son: antibióticos, antiácidos, antidepresivos, esteroides, analgésicos, anti-inflamatorios, β-bloqueantes, tranquilizantes y estimulantes. Estos fármacos terminan en las aguas superficiales y aguas subterráneas de muchos países. En la **Tabla 2** se recogen

las concentraciones detectadas en aguas superficiales por diferentes autores entre los años 1999 y 2004 [23, 7].

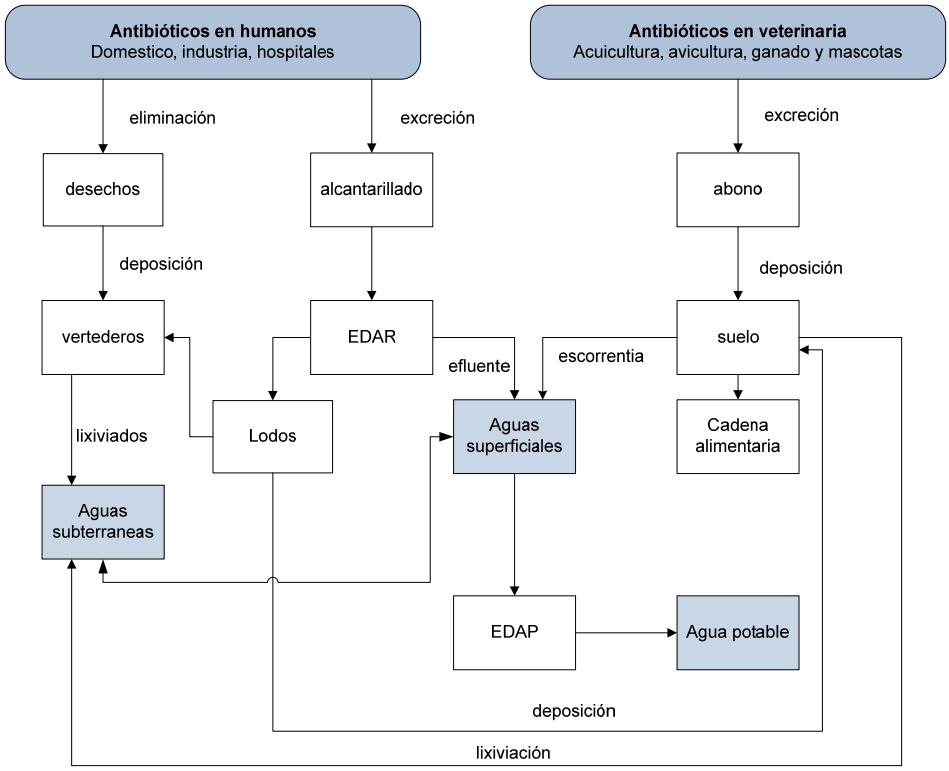

Figura 3. Vías de entrada de antibióticos humanos y veterinarios en el medio ambiente

Tabla 2. Concentraciones de fármacos detectadas en aguas superficiales

Tipo de fármaco	Sustancia detectada	Concentración máxima (ng/l)	Sustancia detectada	Concentración máxima (ng/l)
Antibióticos	Cloranfenicol	355	Sulfadimetoxina	60
	Clortetraciclina	690	**Sulfametazina**	220
	Ciprofloxacin	30	Sulfametizol	130
	Lincomicina	730	**Sulfametoxazol**	1900
	Norfloxacina	120	Tetraciclina	110
	Oxitetraciclina	340	Trimetroprim	710
	Roxitromincina	180	Tilosin	280
Antiácidos	Cimetidina	580	Ranitidina	10
Analgésicos	Codeína	1000	Indometacina	200
	Ácido acetilsalicílico	340	Ketoprofeno	120
	Carbamacepina	1100	Naproxeno	390
	Diclorofenac	1200	Fenazona	950
	Aminopirina	340		
Antiinflamatorios y antipiréticos	Ibuprofeno	3400	Paracetamol	10000
B-bloqueantes	Betaxolol	28	Metoprolol	2200
	Bisoprolol	2900	Propanolol	590
	Carazolol	110	Timolol	10
Antilipemiantes	Bezafibrato	3100	Gemfibrozil	510
Estimulantes	Cafeína	6000		

2.1.1.2. Efectos de los fármacos en el medio ambiente

Aunque hay pocos estudios sobre los efectos directos causados por la presencia de estas sustancias en el medio ambiente, se han detectado problemas en peces debido a la presencia de antidepresivos en las aguas superficiales, alteraciones en el comportamiento y fisiología de los insectos, inhibición en el crecimiento de plantas acuáticas y algas y desarrollo de bacterias resistentes [24]. Aunque a corto plazo parece que no se detectan efectos graves sobre la salud humana o el medio ambiente, sí resultan probables cambios en el medio ambiente y daños en el hombre a largo plazo, además de la proliferación de organismos resistentes a los antibióticos. En general, los seres humanos cada vez responden peor a los medicamentos y los agentes que producen enfermedades mutan con mayor facilidad, lo que supone un problema para la salud pública [25].

Normalmente los antibióticos más estudiados son los más persistentes en el medio acuático, entre los que destacan las sulfamidas, fluoroquinolonas y macrólidos [26]. Concretamente, los antibióticos de uso más común como el sulfametoxazol y la sulfametazina, en los que nos centraremos en esta tesis, pueden persistir en el medio ambiente más de un año ya que la hidrólisis de ellos a pH neutro es muy baja. En el agua potable las concentraciones encontradas son del orden de µg/L o ng/L, estando estos niveles muy por encima de sus dosis terapéuticas, lo que supone un riesgo para la salud humana [27, 28].

2.1.1.3. Las sulfamidas

Las sulfamidas son antibióticos bacteriostáticos que inhiben a bacterias como gram positivas, gram negativas y protozoos. Constituyen una familia de agentes antimicrobianos sintéticos, derivados de la sulfanilamida y utilizados en medicina humana en el tratamiento de infecciones urinarias, ojos y oídos, bronquitis crónicas, meningitis, neumonía y diarrea. Suelen aplicarse en combinación con la trimetoprima para potenciar su actividad antibiótica. También son utilizados en acuicultura y en ganadería para el tratamiento de especies destinadas al consumo humano. En la actualidad, las sulfamidas constituyen el tercer grupo de antibióticos más usados en veterinaria en la UE. Dentro de ellas, el sulfametoxazol y la sulfametazina son las más usadas en medicina humana y en veterinaria, respectivamente.

2.1.1.3.1. Propiedades físico-químicas de las sulfamidas

Todas las sulfamidas son compuestos sintéticos derivados de la sulfanilamida (para-aminobenceno sulfonamida) que fue la primera en descubrírsele actividad antimicrobiana. Poseen dos átomos de nitrógeno (N), el N4 amínico y el N1 amídico, y las distintas sulfamidas se diferencian entre sí en el radical (R) unido al grupo amino en N1(-2NHR) y a veces en el sustituyente del grupo amino en N4 (NH2). Casi todas las actuales sulfamidas derivan de sustituciones en el N1 ya que las realizadas en el N4 tienen generalmente menor actividad antibacteriana (**Figura 4**).

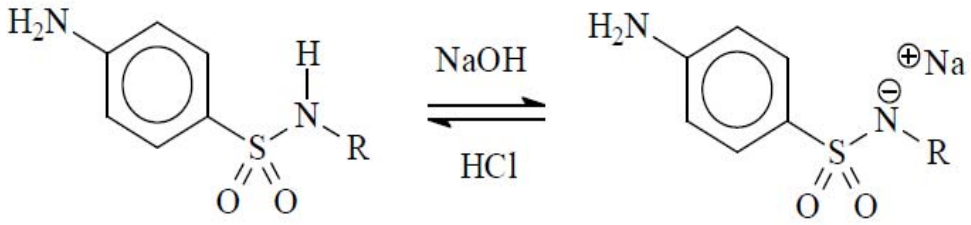

Figura 4. Carácter ácido del hidrógeno del grupo sulfanilamida N-sustituida

Las sustituciones en el grupo amino originan efectos variables en la actividad antibacteriana de la molécula. El grupo amido no es esencial en sí para la acción antimicrobiana, lo importante es que el azufre esté unido directamente al anillo de benceno. El grupo amino cuyo nitrógeno ha sido denominado N4 es esencial y suele sustituirse solamente por radicales que se transformen *in vivo* en un grupo amino libre. Si bien las diversas sustituciones químicas originan sulfamidas con características físicas, químicas y farmacocinéticas particulares, en general las propiedades antibacterianas son similares para todos los compuestos del grupo.

Químicamente son cristales blancos relativamente insolubles en agua, teniendo un amplio rango de valores de pK_a, son ácidos débiles y con diferentes pesos moleculares: sulfanilamida (172.2), sulfadiazina (250.3), sulfametoxazol (258.3) sulfametazina (278.3) y sulfadimetoxina (310.3).

El hidrógeno unido al nitrógeno del grupo sulfanilamida ($-SO_2NH-$) tiene carácter ácido por efecto del grupo sulfónico ($-SO_2-$), que es muy fuerte atrayendo electrones. Por lo tanto, en medio básico se forma la sal correspondiente,

solubilizándose en agua. Esta característica se utiliza en la prueba de Hinsberg para determinar si una amina es primaria, secundaria o terciaria.

Su solubilidad es mayor en los medios alcalinos que a pH neutros o ácidos y aumenta en medios con sales sódicas. En los líquidos biológicos con un pH menor que su pK_a predomina la forma no ionizada, siendo esta fracción la que difunde a través de las membranas celulares y penetra las barreras biológicas.

2.1.1.3.2. Sulfametoxazol y sulfametazina

El sulfametoxazol (SMX) es un antibiótico bacteriostático tipo sulfonamida, usado como parte de una combinación sinérgica con Trimetoprima en una relación 5:1 en el co-trimoxazol, también conocido por los nombres comerciales Bactrim, Septrin y Septra. Su actividad primaria es contra cepas susceptibles de Streptococcus, Staphylococcus aureus, Escherichia coli, Haemophilus y anaerobios orales, siendo su uso más frecuente el tratamiento de infecciones urinarias.

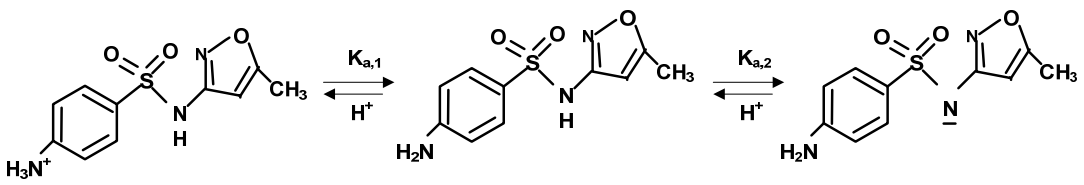

Figura 5. Estructura química de SMX y sus formas aniónicas y catiónicas

La Sulfametazina (SMZ) es un antimicrobiano empleado actualmente como quimioterapéutico en veterinaria, también perteneciente a la familia de las sulfamidas. Las características farmacocinéticas de la SMZ en rumiantes permiten su administración por distintas vías con una buena biodisponibilidad, una buena disposición tisular y una prolongada permanencia en el organismo que la hacen apta para el tratamiento de afecciones del aparato respiratorio, urinario, gastrointestinal y sistema nervioso central. En la **Tabla 3** se muestran las propiedades físico-químicas del SMX y SMZ.

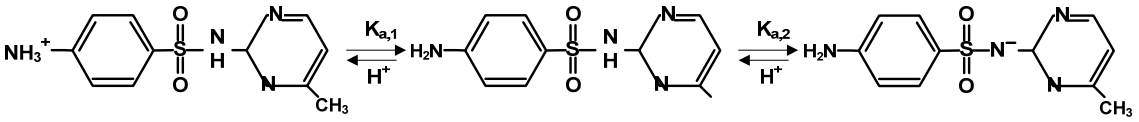

Figura 6. Estructura química de SMZ; y sus formas aniónicas y catiónicas

Tabla 3. Propiedades físico-químicas de SMX y SMZ [29]

Nombre	Sulfametoxazol (SMX)	Sulfametazina (SMZ)
Nombre sistemático	4-amino-N-(5-metilisoxazol-3-il)Bezcenosulfonamida	4-amino-N-(4,6-dietilpirimidinil-2-il) Benzenosulfonamida
Fórmula molecular	$C_{10}H_{11}N_3O_3S$	$C_{12}H_{14}N_4O_2S$
Peso molecular	253.28	278.33
Composición centesimal	C 47.42%, H 4.38%, N 16.59%, O 18.95%, S 12.66%	C 51.78%, H 5.07%, N 20.13%, O 11.50%, S 11.52%
Punto de fusión	171ºC	198.5ºC
pK_a	pK_a1= 1.6(amina aromática) pK_a2= 5.7(nitrógeno sulfonamida)	pK_a1= 2.65(amina aromática) pK_a2= 7.65(nitrógeno sulfonamida)
Solubilidad en agua	610 mg/L a 37ºC	1500 mg/L a 29º; 1920mg/L a 37ºC
Presión de vapor	$6.9x10^{-8}$ mmHg a 25º C	$8.6x10^{-9}$ mmHg a 25ºC
log K_{ow}	0.89	0.14
Cte. de Henry	$6.4x10^{-13}$ atm·m^3/mol	$3.05x10^{-13}$ atm·m^3/mol

Como ya se ha comentado previamente, estos dos compuestos son no biodegradables, y su persistencia en el medio ambiente es superior a un año, con los efectos dañinos que ello conlleva. Por tanto, de ahí la importancia de eliminar de este tipo de contaminantes.

El uso del cloro sigue siendo el tratamiento convencional de desinfección de agua potable más usado. El problema es que los productos farmacéuticos contienen aminas, que reacciona rápidamente para dar lugar a compuestos clorados. Por ejemplo, fármacos como es nuestro caso sulfametoxazol dan lugar a cloramidas como uno de los productos de oxidación. En el apartado 2.2 se exponen los distintos tratamientos existentes para eliminación de contaminantes de las aguas, haciendo un especial hincapié en la técnica de intercambio iónico (apartado 2.3), objeto de estudio en este trabajo y que se presenta como una alternativa eficaz y prometedora por su bajo coste y sencillez en operación, en comparación con los otros tratamientos alternativos existentes para la depuración de aguas que contienen contaminantes en baja concentración, pero que es necesario eliminar.

2.1.2. Contaminantes de la industria siderúrgica

2.1.2.1. Tiocianato en las aguas residuales

El tiocianato (SCN^-) es un ión poliatómico lineal y un buen ejemplo de pseudohaluro que se usa en varios procesos químicos, tales como producción de herbicidas e insecticidas, manufacturación de tiourea, procesos de fotoacabado, producción de tintes y fibra acrílica, y procesos de separación de metales y galvanizado. Las principales fuentes contaminantes de tiocianato se encuentran en las aguas residuales de procesos de gasificación de carbón y pirolisis, aunque también se desechan tiocianatos en procesos de extracción de oro y plata y en las industrias petroquímicas [30].

La formación del tiocianato en las aguas residuales de coquería se debe a la reacción del cianuro con compuestos de azufre. A su vez, el cianuro se forma por reacción del amoniaco con otros componentes del gas de coquización como C, CH_4, C_2H_4, C_2H_2 y/o CO a altas temperaturas. De hecho, no se ha observado la formación de cianuro en procesos en los que el carbón es sometido a temperaturas inferiores a 200ºC [31] y el amoniaco se forma a partir de los grupos amino o amino sustituidos presentes en la estructura del carbón. Estos grupos se liberan rápidamente durante el calentamiento del carbón. Se ha observado que la formación de amoniaco es superior si la gasificación se realiza en condiciones de hidrogenación que son las habitualmente empleadas en el proceso de coquización. Se estima que en un proceso de coquización se producen entre 3 y 4 kg de amoniaco por cada 1000 kg de carbón. Las principales vías de formación de tiocianato son debidas a la reacción del cianuro con polisulfuro o tiosulfato, como se muestra en la **Tabla 4**.

En la reacción 1, el sulfuro es oxidado a azufre formando polisulfuro que reacciona rápidamente con cianuro para dar tiocianato y sulfuro como ocurre en el caso que nos ocupa. En la reacción 2 el sulfuro es oxidado a sulfito, el cual reacciona con polisulfuro para producir tiosulfato, que reacciona con cianuro para dar tiocianato y sulfito. La **Figura 7** resume las dos vías principales de oxidación de sulfuro en aguas residuales de gasificación del carbón para dar SCN^-. El modelo incorpora las características esenciales de las reacciones 1 y 2.

Tabla 4. Principales vías de reacción para la formación de tiocianato en fase acuosa durante la gasificación del carbón [31]

1. Reacción de cianuro y polisulfuro	$2(NH_4)_2S + \frac{1}{2}O_2 + 2H^+ \overset{K_1}{\rightarrow} (NH_4)_2S_2 + H_2O + 2NH_4{}^+$ $(NH_4)_2S_2 + NH_4CN \overset{K_2}{\rightarrow} (NH_4)_2S + NH_4SCN$
2. Reacción del cianuro con tiosulfato	$2(NH_4)_2S + 3O_2 + 2H^+ \overset{K_1}{\rightarrow} (NH_4)_2SO_3$ $(NH_4)_2S_2 + (NH_4)_2SO_3 \overset{K_2}{\rightarrow} (NH_4)_2S_2O_3 + (NH_4)_2S$ $NH_4CN + (NH_4)_2SO_3 \overset{K_3}{\rightarrow} NH_4SCN + (NH_4)_2SO_3$

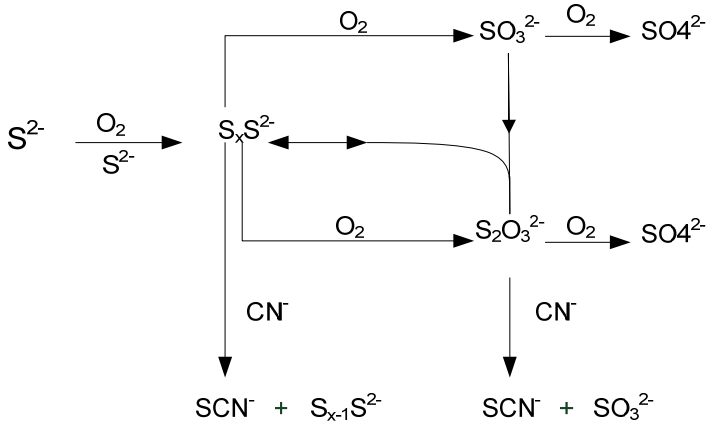

Figura 7. Vías de reacción de oxigenación del sulfuro para obtener tiocianato [31]

Según un trabajo realizado por Luthy [31], la velocidad de reacción del polisulfuro con cianuro es muy superior a la velocidad de reacción del cianuro con tiosulfato lo que indica que la reacción 1 es más importante. Los polisulfuros se forman fácilmente en ambientes acuosos que contengan azufre elemental, sulfuro de hidrogeno y amoniaco, como es el caso de las aguas que nos ocupan. Además, se ha observado que su formación se ve favorecida en las partes frías del sistema de conducción del gas de coque. Los polisulfuros se forman a través de sucesivas combinaciones secuenciales de átomos de azufre neutros con sulfuro. En medios acuosos neutros o básicos, las principales formas del ion polisulfuro son el tetra-y pentapolisulfuro (S_4^{2-}y S_5^{2-}). La rápida reacción de estos polisulfuros con cianuro para dar tiocianato explicaría las bajas concentraciones de cianuros detectadas en las aguas residuales de los condensados del gas de coquería.

Por otra parte, estudios cinéticos realizados sobre la oxigenación de sulfuro en disolución [32, 33] han mostrado que tanto la velocidad de reacción como los productos

obtenidos (polisulfuro o tiosulfato) dependen del pH, de la relación S^{2-}/O_2, y de la presencia de especies que puedan actuar como catalizadores (algunos iones metálicos y compuestos orgánicos) o inhibidores de la reacción. Las aguas amoniacales y de enfriamiento generadas en la gasificación del carbón presentan una concentración de sulfuros entre 0.005 y 0.02 M, lo que conduce a un relación S^{2-}/O_2 relativamente alta que en condiciones neutras o ligeramente alcalinas favorece la formación de polisulfuros. Sin embargo, Chen y Morris [32] encontraron que para pH superiores a 8.5 el principal producto de reacción era tiosulfato, independientemente de la relación sulfuro/oxígeno. En el caso que nos ocupa, las aguas residuales procedentes de los condensados del gas de coquería de una industria siderúrgica, el pH es próximo a 9, con lo cual es posible que se formen ambos compuestos. Dada la necesaria intervención del oxígeno en la formación del tiocianato, para limitar la oxidación del sulfuro y con ello controlar la formación de este contaminante, se debería, en la medida de lo posible, limitar el acceso del aire al gas de coquería.

El tiocianato formado en las aguas de coquería, además de suponer un serio problema para el tratamiento de las aguas que lo contienen, puede intervenir en la formación de depósitos y corrosión de los equipos y conducciones a través de las cuales se distribuye el gas de coque.

En cuanto a los métodos de degradación del tiocianato, hoy día se realiza principalmente por dos vías: por medio de microorganismos que son capaces de metabolizar y destruir este compuesto, o por medio de métodos químicos de oxidación. El principal problema de estas técnicas, es que el tiocianato puede eliminarse por medio de métodos biológicos en concentraciones entre 30-500 ppm, pero la presencia de otros contaminantes puede ralentizar la degradación como ocurre con la presencia de fenol en concentraciones superiores a 2000 ppm. Además en algunas aguas de coquería se han detectado concentraciones por encima de 1000 mg/L de tiocianato, por tanto el tratamiento biológico resulta inviable.

Respecto a los métodos de oxidación química, los más habituales son la cloración alcalina directa o la adición de hipoclorito. Pero este método aunque eficaz, presenta una serie de desventajas como la contaminación por cloruros y el uso de reactivos peligrosos y difíciles de manejar. De ahí que sean necesarios métodos alternativos respetuosos con las condiciones medioambientales para tratar aguas

contaminadas con tiocianatos. Como ya se ha comentado previamente, en este trabajo nos hemos decantado por el tratamiento mediante intercambio iónico que se explica en el apartado 2.3, dado las ventajas que presenta frente a otros tratamientos alternativos, como es bajo coste, efectividad, selectividad y sencillez en cuanto a diseño y operación.

2.1.2.2. Fenol en las aguas residuales

La presencia de fenol y sus derivados en efluentes industriales resulta especialmente indeseable por los efectos adversos que provocan; ya que a concentraciones muy inferiores a las tóxicas (ppb), ya comunican sabor y olor al pescado y al agua potable. En concentraciones altas, se manifiesta una elevada demanda química de oxigeno y toxicidad para la fauna acuática. Entre las fuentes más importantes de contaminación por fenol se pueden mencionar: plantas de coquización, refinerías de petróleo e industrias petroquímicas, industrias de plásticos, procesos de gasificación del carbón, estaño electrolítico y plantas farmacéuticas. Las concentraciones típicas de fenol y sus derivados en las aguas residuales industriales, se muestran en la **Tabla 5**.

Tabla 5. Concentraciones típicas de fenoles en efluentes industriales

Industrias	Concentración(mg/L)
Farmacéutica	1000
Obtención de benceno	50
Coquerías	1000 a 2000
Altos hornos	4000
Refinas de petróleo	2000 a 3000
Petroquímicas	50-700
Otras industrias	0.1 a 1600

La industria siderúrgica, conjuntamente con la petrolífera, son las mayores generadoras de residuos fenólicos. En la industria siderúrgica, las aguas de coquería y las del alto horno son las más tóxicas, ya que contienen gran cantidad de contaminantes, tales como sólidos en suspensión, fenoles, tiocianatos, amoniaco, sulfuros, cloruros, trazas de PAH's (Hidrocarburos Policíclicos Aromáticos) y compuestos heterocíclicos nitrogenados. En la **Tabla 6** se muestra la composición típica de este tipo de aguas.

Tabla 6. Características de las aguas de coquería [30]

Parámetro	Rango	Unidades
pH	8-10	-
Temperatura	40-70	ºC
Sólidos en suspensión	25-150	mg/L
DQO	3000-8000	mg/L
DBO5	2000-3000	mg/L
Fenol	500-1000	mg/L
N-NTK	5500-10000	mg/L
N-NH3	5000-10000	mg/L
CN^-	1-300	mg/L
SCN^-	1-400	mg/L
Sulfuros	50-3000	mg/L
Cloruros	100-350	mg/L
Hidrocarburos Aromáticos Policíclicos.	1-25	mg/L

La toxicidad de los fenoles en estos efluentes se debe tanto a su carácter nocivo como al elevado consumo de oxígeno durante su degradación. En concentraciones suficientes, puede llegar a agotar el oxígeno de la masa de agua receptora de estos efluentes, impidiendo la vida acuática [34]. El fenol y sus derivados son muy poco biodegradables, tienen un tiempo de vida media de descomposición de entre 2 y 72 días. Se consideran tóxicos para algunas formas de vida acuática en concentraciones superiores a 50 ppb, mientras que en seres humanos la ingestión de 1 gramo de fenol puede ser letal. Algunas de las principales características del fenol y sus derivados son las siguientes [35]:

- Extremada toxicidad: irritantes para los ojos, las membranas mucosas y la piel, causan convulsiones por simple adsorción, afectan al hígado, al sistema nervioso y a los riñones y su adsorción en la piel puede en algunos casos conducir a la muerte.
- Presentan una DBO elevada (2.4 mg O_2/mg fenol)
- Dan sabor y olor característicos y desagradables al agua.

Los fenoles clorados son productos intermedios en muchos procesos industriales. Su elevada toxicidad hace que sean designados como contaminantes prioritarios por la EPA (Environmental Protection Agency) [36]. En España, la concentración máxima admisible de fenoles en agua está regulada por la legislación de

aguas española y europea, situándose el valor máximo permitido entre 0.1 y 5 ppb, dependiendo de la clase de agua residual.

Existen varias técnicas disponibles para la eliminación del fenol como adsorción con carbón activo, resinas de intercambio iónico, WAO, SWAO, CWAO, AOPs, biológico, etc. La descripción de cada técnica se desarrolla en el apartado 2.2. La selección de la mejor técnica depende en especial de la concentración de fenol en la corriente, la presencia de otros contaminantes, así como los costes y la inversión necesaria. Como ya se ha comentado previamente, en este trabajo nos hemos centrado en empleo de resinas de intercambio iónico para eliminar estos compuestos de las aguas por las ventajas que presenta frente a otros procesos de depuración de aguas.

2.2. MÉTODOS DE TRATAMIENTO DE AGUAS RESIDUALES

Los procesos y tecnologías existentes en la actualidad para el tratamiento de aguas residuales son diversos y se clasifican frecuentemente en primarios, secundarios y terciarios. Los tratamientos primarios son aquellos destinados a la eliminación de sólidos suspendidos y grasas del agua residual. Los secundarios son los procesos biológicos cuyo objetivo es la remoción de la materia orgánica disuelta y los terciarios tienen como fin higienizar y adecuar el agua para el consumo urbano y aplicaciones industriales que requieran la máxima pureza del agua.

Los tratamientos terciarios a los que deben someterse los efluentes tienen que garantizar la eliminación del compuesto en el grado requerido por la legislación que regula el vertido del efluente. El nivel máximo admisible de contaminación puede conseguirse mediante la utilización de diversas técnicas tanto destructivas como no destructivas. En los métodos de tratamiento destructivos, el compuesto es transformado por oxidación, ya sea biológica, química o electroquímica, mientras que los métodos no destructivos permiten la recuperación del contaminante y su reutilización, como pueden ser los procesos de adsorción con carbón activo y resinas, procesos con membranas y la extracción con disolventes. A continuación se detallan algunos de los métodos de eliminación de contaminantes de las aguas residuales [37].

Incineración: consiste en la oxidación completa del residuo en fase gas y temperatura elevada. Es un método útil cuando se trata de pequeñas cantidades de aguas

con una concentración elevada de contaminantes oxidable. En caso contrario, los costes de operación asociados a la necesidad de utilizar un combustible auxiliar, se vuelven excesivos.

Oxidación química: es un método de depuración eficaz y ampliamente utilizado. Como oxidantes se emplean reactivos tipo peróxido de hidrógeno, ozono, dióxido de cloro y permanganato potásico. Se suelen utilizar como etapa final en el tratamiento de aguas residuales, cuando ya se ha llevado a cabo otros tratamientos. Suelen ser métodos bastante costosos debido a los reactivos y la energía requerida, por lo que sólo son aplicables cuando no hay otras posibilidades de eliminación. Presentan además las desventajas que pueden dan lugar a subproductos de reacción y se caracterizan por su baja selectividad.

Degradación biológica: Es uno de los tratamientos habituales en el caso de aguas residuales urbanas y en parte de las aguas industriales. Es aplicable a un amplio rango de concentraciones, pero presentan la desventaja de que muchos de los compuestos orgánicos presentes en las aguas residuales, sustancias tóxicas o recalcitrantes no pueden ser eliminados eficazmente por las bacterias.

Membranas: permiten la separación de contaminantes que se encuentran disueltos y en baja concentración y son procesos sencillos, sin embargo presentan las desventajas del elevado coste, no eliminan realmente el contaminante sino que lo concentran en otra fase, problemas de ensuciamiento de las membranas lo que conlleva la necesidad de otras sustancias para llevar a cabo la limpieza, ajustes de pH y ruido generado por los equipos necesarios para conseguir altas presiones.

Adsorción: consiste en la captación de partículas solubles en la superficie de un sólido. Los procesos de adsorción presentan las ventajas frente a otros métodos que no dan lugar a subproductos de reacción, sencillez en diseño y operación y son insensibles a sustancias tóxicas. El sólido universalmente utilizado en el tratamiento de aguas es el carbón activo, que ha sido empleado en el tratamiento de aguas para la eliminación de compuestos fenólicos en bajas concentraciones y la eliminación de contaminantes emergentes, pero su uso se ve restringido por los elevados costes. Además, el carbón activo una vez saturado, durante el proceso de regeneración en un horno se deteriora y

pierde capacidad de adsorción, por lo que es necesario reponer parte del mismo por carbón virgen en cada ciclo.

Dado que el coste es un parámetro importante a la hora de la elección del adsorbente, han surgido alternativas al carbón activo como zeolitas, arcillas (montmorillomita, bentonita) y los denominados adsorbentes de bajo costes, procedentes en su mayor parte de residuos sólidos orgánicos.

Intercambio iónico con resinas: se utilizan como adsorbentes resinas de intercambio iónico sintéticas con una elevada área superficial. Las resinas más empleadas son las de estructura basada en el polimetacrilato o poliestireno-divinilbenceno. Entre las ventajas del proceso destacan:

- Son equipos muy versátiles siempre que se trabaje con relativas bajas concentraciones
- Actualmente las resinas tienen altas capacidades de tratamiento, resultando compactas y económicas
- Son muy estables químicamente, de larga duración y fácil regeneración
- Facilidad de automatización y adaptación a situaciones específicas

El intercambio iónico es uno de los métodos más usados para la eliminación de sustancias tóxicas de las aguas residuales industriales. Se suele aplicar para la desmineralización y ablandamiento de aguas, así como para la retención de ciertos productos químicos, metales que están presentes como especies iónicas solubles, aniones no metálicos como haluros, sulfatos, nitratos, cianuros y compuestos orgánicos iónicos solubles en agua tales como ácidos carboxílicos, sulfónicos, algunos fenoles, aminas cuaternarias y alkisulfatos [38].

Por todas las ventajas que presenta la operación de intercambio iónico frente a los otros procesos descritos, como bajo coste, fácil regeneración, gran selectividad, y sencillez en diseño y operación; en este trabajo se ha elegido esta técnica para eliminar contaminantes como tiocianatos y fenoles procedentes de aguas residuales de coquería, y sulfamidas presentes en aguas residuales industriales, superficiales y subterráneas. A continuación se describe más detalladamente esta técnica.

2.3. INTERCAMBIO IÓNICO

El intercambio iónico es una reacción reversible, que tiene lugar cuando un ión de una disolución se intercambia por otro ión de igual signo que se encuentra unido a una partícula sólida inmóvil llamada intercambiador iónico. Una característica de los intercambiadores, también llamados resinas de intercambio es que su estructura permanece básicamente inalterada.

En la terminología habitualmente empleada [39], se denominan co-iones a los iones de la disolución cuya carga tiene el mismo signo que los grupos fijos del cambiador y contra-iones a los iones de la disolución de carga opuesta que son los pueden sufrir el intercambio, al contrario que los co-iones que no pueden, ya que la resina no permite la salida de los grupos iónicos fijos, y la entrada de co-iones haría que no se cumpliese la electroneutralidad. En función de la carga de los contra-iones la resina se denomina aniónica (intercambia aniones) o catiónica (intercambia cationes).

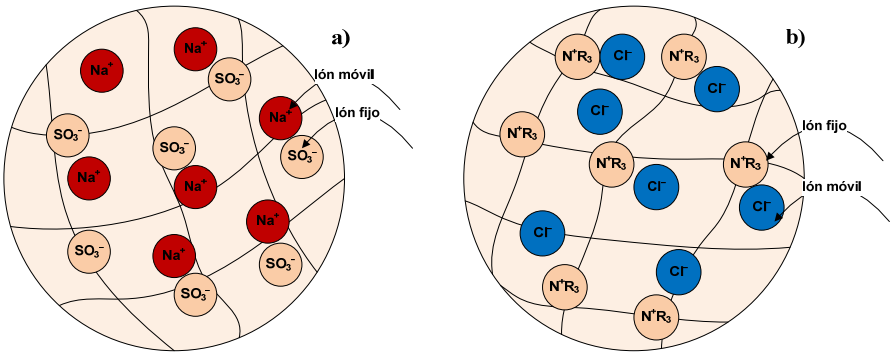

Figura 8. Representación esquemática de resina intercambiadoras de cationes (a) y aniones (b)

Actualmente las resinas orgánicas producidas sintéticamente son el adsorbente predominante en la industria. Cuando se ponen en contacto resina y disolución, los iones se reparten entre ambas fases hasta que se alcanza el equilibrio. Las resinas recuperan los iones de la disolución mediante el intercambio que tiene lugar en los poros (grupo funcional fijo), llegando a la saturación cuando se encuentran todos sus grupos funcionales cargados con el nuevo anión, alcanzando la capacidad máxima de intercambio. Esta capacidad es recuperable, mediante la etapa de elución o regeneración con otra disolución iónica fuerte.

Algunos de los parámetros característicos de las resinas son la capacidad de intercambio y la selectividad.

La *capacidad de intercambio* se define como la cantidad de iones que una resina puede intercambiar en determinadas condiciones experimentales y va a depender de la afinidad relativa del ión de intercambio por la resina. Se expresa en equivalentes por litro de resina o por gramo. Hay muchos factores que pueden afectar al proceso de intercambio iónico como son:

- Concentración y carga de los contaminantes
- La concentración de las especies iónicas presentes en el agua que pueden competir con la especie a recuperar
- La interferencia de especies inorgánicas u orgánicas
- La concentración de sólidos en suspensión o disueltos, aceites y grasas
- El pH de la disolución si el grupo activo tiene carácter ácido o básico
- La temperatura

La *selectividad* de una resina respecto a un par de iones presentes en una disolución se mide con el coeficiente de selectividad. Este parámetro depende de los siguientes factores:

- Naturaleza del grupo funcional, pues va a determinar el tipo de interacciones que se van a producir con los iones.
- Valencia del ión; el intercambiador prefiere los iones de valencia mayor y esta preferencia se acentúa cuanto menor es la concentración de la disolución. Para iones de la misma valencia la selectividad no depende de la concentración total de la disolución.
- Grado de solvatación de los iones; se prefiere el contra-ión que tenga menor volumen hidratado. La selectividad aumenta al aumentar el grado de reticulación de la resina y al disminuir la concentración total de la disolución.
- Polaridad del ión; será más selectiva para el ión que se una más frecuentemente con los grupos iónicos del intercambiador. Estas interacciones pueden ser del tipo par iónico, atracciones electrostáticas o interacciones de London.

- Tamaño de los contra-iones; el intercambiador es más efectivo para los iones de pequeño tamaño, pues los iones grandes no podrán introducirse en los poros de la resina por impedimentos estéricos.
- La naturaleza del esqueleto polimérico.

Otro aspecto de gran importancia en el estudio del intercambio iónico es la cinética. Como en todo sistema heterogéneo, el proceso tendrá lugar por etapas, siendo la más lenta la que determine la velocidad de intercambio: difusión en la capa líquida, difusión en la resina o reacción química. En condiciones habituales, la etapa controlante suele ser la difusión en la resina.

2.3.1. Equilibrio de intercambio iónico

El equilibrio de intercambio iónico se alcanza después de un contacto suficientemente prolongado entre un intercambiador iónico y una disolución que contiene un contra-ión que va a intercambiarse en el grupo fijo de la resina. Por tanto, se considera que el proceso tiene lugar entre dos iones cualquiera A y B, uno de los cuales, el B, se encuentra presaturando los grupos activos de la resina y el otro, el A, está en la disolución que se supone en contacto con ella. Este proceso se pude describir como la ecuación:

$$bA^{a+} + a\bar{B}^{b+} \leftrightarrow b\bar{A}^{a+} + aB^{b+} \tag{2.1}$$

donde la constante de equilibrio vendrá dada por:

$$K_B^A = \frac{q_A^b C_B^a}{C_A^b q_B^a} \tag{2.2}$$

donde *C* son las concentraciones de cada ion en la disolución y *q* las concentraciones en la resina de cada ion. Esta constante es conocida como coeficiente de selectividad, K_B^A.

Por otra parte, la preferencia de la resina por uno de los iones se expresa mediante el factor de separación α_A^B, que se define como:

$$\alpha_A^B = \frac{q_A C_B}{C_A q_B} \tag{2.3}$$

de modo que si el ion A es preferido por la resina, el valor de α_A^B será mayor que la unidad y si B es el preferido, será menor que la unidad. El factor de separación indica además la relación entre los coeficientes de distribución de los iones A y B, es decir, el cociente entre las concentraciones de cada ion en cada una de las fases.

El estudio del equilibrio de intercambio iónico puede hacerse desde distinto puntos de vista: químico (aplicando la ley de acción de masas), electroquímico (aplicando el modelo Donnan) y físico (aplicando las isotermas de equilibrio de adsorción. En este trabajo nos centraremos en el estudio del equilibrio de adsorción, debido a que los modelos químicos basados en razonamientos termodinámicos o electroquímicos dan lugar a modelos matemáticos muy complejos y de difícil aplicación en el diseño de equipos.

Para describir el equilibrio de intercambio se han desarrollado una serie de ecuaciones semiempíricas a las que se suelen ajustar los datos experimentales. Estas ecuaciones son las isotermas utilizadas habitualmente en adsorción y que muestran en muchos casos, ser adecuadas para el diseño de equipos debido a la semejanza entre los procesos de intercambio iónico y adsorción, y al hecho de que el intercambio iónico requiere de la adsorción previa de los iones en el intercambiador. En el estudio del equilibrio de adsorción debemos tener en cuenta si se trata de un sistema mono o multicomponente, es decir, en el caso de que haya más de una especie presente en la disolución hay que considerar si existe o no competencia entre ellas por los sitios activos de la resina. A continuación, se describen las isotermas de adsorción para sistemas mono y multicomponentes

2.3.1.1. Isotermas de adsorción para sistemas monocomponentes

Las isotermas de adsorción más conocidas y empleadas en intercambio iónico para sistemas de un solo componente son las de Langmuir, Freundlich y Factor de Separación Constante [40], que vienen dadas por las expresiones:

$$\text{Isoterma de Langmuir: } q_{e,i} = \frac{K_{eq} \cdot q_m \cdot C_{e,i}}{1 + K_{eq} \cdot C_{e,i}} \text{ ó } q_{e,i} = \frac{K_{L,i} \cdot C_{e,i}}{1 + a_L C_{e,i}} \qquad (2.4)$$

donde K_L es la constante de Langmuir e indica la adsorción del soluto, a_L se refiere a la energía de adsorción (L/mg) y $C_{e,i}$ es la concentración que queda en la disolución

después del proceso de adsorción una vez alcanzado el equilibrio. La capacidad máxima de saturación vendrá dada por $q_m = K_L/a_L$.

$$\text{Isoterma de Freundlich: } q_{e,i} = K_{eq} \cdot C_{e,i}{}^{b} \tag{2.5}$$

$$\text{Isoterma de Factor de Separación Constante: } q_{e,i} = \frac{K_{eq} \cdot q_t \cdot C_{e,i}}{C_t + (K_{eq} - 1) \cdot C_{e,i}} \tag{2.6}$$

donde C_t es la concentración total de iones en la disolución en equilibrio con q_t.

2.3.1.2. Isotermas de adsorción para sistemas multicomponentes

En el caso de sistemas multicomponentes, es decir con varios iones presentes en la disolución en contacto con la resina hay menos estudios realizados. Cuando hay varios iones presentes, puede aparecer el fenómeno de competencia por los sitios activos de la resina lo que implica fórmulas matemáticas bastante más complejas. Una de las alternativas es la utilización de isotermas conocidas para sistemas binarios y generalizarlas para sistemas multicomponentes. Una de las más empleadas es la ecuación de Langmuir extendida:

$$q_{e,i} = \frac{K_{L,i} \cdot C_{e,i}}{1 + \sum_{j=1}^{N} a_{L,i} \cdot C_{e,i}} \tag{2.7}$$

donde *i* es el número de compontes, $C_{e,i}$ es la concentración de equilibrio del componente *i* en la solución multicomponente, $q_{e,i}$ es la concentración de equilibrio alcanza por el componente *i* en la resina(mg/g) y $K_{L,i}$ y $a_{L,i}$ son los parámetros de Langmuir para cada componente.

Este modelo supone que la superficie del adsorbente es homogénea, que los diferentes solutos adsorbidos no interaccionan entre sí y que los sitios activos de la resina están igualmente disponibles para todos las especies. Estas consideraciones son ciertas cuando se trabaja en condiciones de bajas concentraciones y cuando no se tiene saturación total de la resina.

En el caso de que exista competición en el proceso de adsorción se desarrollaron otros modelos basados también en la isoterma de Langmuir extendida pero que introducen parámetros de corrección como es el caso de la ecuación de Jain y Snoeyink [41], el modelo P-factor desarrollado por McKay [42] y el modelo del factor constante de interacción η desarrollado por Schay [43].

Modelo de Jain y Snoeyink: $$q_{e,1} = \frac{(Q_{m1} - Q_{m2})a_{L1}C_{e1}}{1 + a_{L1}C_{e1}} + \frac{Q_{m2}a_{L1}C_{e1}}{1 + a_{L1}C_{e1} + a_{L2}C_{e2}} \quad (2.8)$$

$$q_{e,2} = \frac{Q_{m2}a_{L2}C_{e2}}{1 + a_{L1}C_{e1} + a_{L2}C_{e2}} \quad (2.9)$$

P-factor: $$q_{e,i} = \frac{1}{P_i}\frac{K_{L,i}C_{e,i\ multi}}{1 + a_{L,i}C_{e,i\ multi}} \quad (2.10)$$

$$\text{donde } P_i = \frac{(K_{L,i}/a_{L,i})_{monocomponente}}{(K_{L,i}/a_{L,i})_{multicomponente}} \quad (2.11)$$

Factor η: $$q_{e,i} = \frac{K_{L,i}\left(C_{e,i}/\eta_{L,i}\right)}{1 + \sum_{j=1}^{N} a_{L,j}\left(C_{e,j}/\eta_{L,j}\right)} \quad (2.12)$$

2.3.1.3. Principales variables que influyen en el equilibrio

Influencia del pH: el pH es una variable fundamental en el estudio del intercambio iónico con resinas ácido o base débil. Así, una resina ácido débil a un pH ácido será incapaz de reaccionar, ya que todos sus grupos se encontrarán protonados.

Influencia de la temperatura: la adsorción se ve desfavorecida con el aumento de temperatura.

Influencia de la fuerza iónica: cuanto mayor sea la diferencia de concentración entre la resina y la disolución, mayor será la presión osmótica y mayor por tanto el hinchamiento. En estas condiciones, la resina preferirá al ión que tenga el mayor volumen hidratado y que permita una mayor relajación de la matriz resina. Por tanto, podemos actuar sobre la selectividad de la resina, modificando adecuadamente las concentraciones relativas de los contra-iones en disolución y haciendo que se capte preferentemente un ión u otro.

2.3.2. Cinética de intercambio iónico

El intercambio iónico es esencialmente una redistribución de los contra-iones, *A*, que están en el grupo fijo de la resina y los iones, *B*, presentes en una disolución, por difusión [39]. Las etapas que están presentes en el proceso de intercambio iónico son:

- Difusión de los iones a través de la capa de fluido que rodea la partícula (película líquida).
- Difusión de los iones en el interior de los poros de la resina.
- Intercambio de iones en los sitios activos del sólido, reacción de "intercambio químico".

La difusión de los contra-iones está sujeta a la restricción de electroneutralidad, como los iones de la especie *A* se mueven hacia la disolución, una cantidad estequiométrica de la especie *B* lo hará hacia el interior de la resina para que haya un equilibrio de cargas en los grupos iónicos fijos. Por tanto, la difusión de los iones es la base de la teoría cinética de intercambio iónico [44].

2.3.2.1. Etapa controlante de la cinética

De las tres etapas que tienen lugar sucesivamente en el intercambio iónico, es muy importante conocer cuál es la etapa más lenta, ya que esta etapa generará una resistencia mayor que las demás etapas y es considerada la etapa controlante de la velocidad del proceso.

Uno de los primeros autores en estudiar la cinética de los procesos de intercambio iónico fue Boyd, este autor concluyó que sólo las etapas de difusión pueden ser controlantes, ya que la etapa de fijación en los grupos activos de la resina es muy rápida [45]. Este autor también fue el primero en aplicar el concepto de "capa límite" establecido por Nernst [46] que supone la existencia de una película estancada de líquido bien diferenciada de la masa por una superficie límite. El grosor de la película Nernst está relacionado con el número adimensional Sherwood de acuerdo a la ecuación:

$$\delta = \frac{2 \cdot r_0}{Sh} \tag{2.13}$$

Tanto la difusión en el interior de la partícula como en la película líquida pueden ser controlantes e incluso en algunos casos las dos intervienen en la velocidad del proceso. Si controla la difusión en el interior de la partícula, en este caso la difusión en la película líquida es mucho más rápida que la difusión en la partícula, es decir solo existe un perfil de concentraciones en el interior de la partícula. Si controla la difusión

en la película líquida, la difusión en el interior de la partícula es mucho más rápida que en la película y los gradientes de concentración están presentes sólo en ésta fase.

Por lo general, la cinética de los procesos de intercambio iónico suele estar controlada por la difusión en el interior de la partícula. Sólo se encuentra que el proceso está controlado por la difusión en la película si el intercambiador posee una elevada concentración de grupos fijos, una baja reticulación y las partículas tienen un diámetro muy pequeño, con disoluciones muy diluidas y con insuficiente agitación [39].

La naturaleza de la etapa controlante se puede predecir usando un criterio cuantitativo que ha sido desarrollado por Helfferich [39], que tiene en cuenta el efecto de las siguientes variables: capacidad de intercambio iónico, concentración de la disolución, tamaño de partícula, espesor de la película líquida, coeficiente de difusión y el factor de separación. La expresión es la siguiente:

$$\frac{q_T D_p \delta}{C_T D^{\infty} R_0}\left(5 + 2\alpha_{A/B}\right) \ll 1; \text{ control por difusión en los poros} \qquad (2.14)$$

$$\frac{q_T D_p \delta}{C_T D^{\infty} R_0}\left(5 + 2\alpha_{A/B}\right) \gg 1; \text{ control por transferencia en la película} \qquad (2.15)$$

donde q_T es la concentración máxima de iones fijados en la resina, C_T es la concentración de la disolución, D_p es el coeficiente de difusión en los poros, D^{∞} es el coeficiente de difusión molecular, δ es el espesor de la película líquida, R_0 es el radio de la partícula y $\alpha_{A/B}$ es el factor de separación.

2.3.3.2. Modelos cinéticos

Los procesos de difusión se describen a partir de la primera ley de Fick:

$$J_i = -D \cdot grad\ C_i \qquad (2.16)$$

donde el flujo es proporcional al gradiente de concentración, el coeficiente de difusión es constante y no hay procesos simultáneos que interfieran, pero no es del todo real generalizar todos los procesos a esta situación tan simple. Este es el caso de la operación de intercambio iónico donde la primera ley de Fick puede usarse, pero deben de tenerse en cuenta los siguientes factores.

En el intercambio iónico, la matriz ocupa una fracción sustancial de volumen en el medio y obstruye la difusión y por tanto, la predicción de las velocidades de difusión. La teoría cinética de intercambio iónico desvía esta dificultad considerando el intercambiador iónico (resina, es decir, poros más matriz) como una fase cuasi-homogénea, sin tener en cuenta las heterogeneidades con respecto de la estructura geométrica y se aplica la ecuación de Fick a esta fase sólida. La velocidad de intercambio iónico dependerá por tanto del tamaño y forma de las partículas, pero en un tratamiento teórico se suele asumir que todas las partículas son esféricas y de tamaño uniforme. Un tratamiento riguroso en el que se tendrían en cuenta irregularidad de forma y tamaño de las partículas sería muy difícil, por tanto, se asume una aproximación para estos casos y se supone partículas esféricas para estimar la velocidad de los procesos, asumiendo una relación empírica del tamaño de las partículas de material a esferas equivalentes.

Todo modelo cinético pretenderá ajustar los datos experimentales concentración-tiempo a unas ecuaciones genéricas y que a la vez sean fáciles de manejar, por ello, los más empleados son los modelos basados en la ley de Fick: modelo de transferencia de masa a través de la película líquida y modelo de difusión en poros. Estos modelos han sido ampliamente desarrollados en el apartado de resultados en cada publicación, pero a continuación se resumen brevemente.

Modelo de transferencia de masa a través de la película líquida. En este modelo se supone que la capacidad de retención del compuesto en la resina está limitada por la superficie externa de la partícula. Las ecuaciones que describen este modelo son:

$$\frac{dq_i}{dt} = K_f a_p (C_i - C^*) \tag{2.17}$$

$$V_L C_i + V_r q_i = V_L C_0 \tag{2.18}$$

$$q_i(t) = C_0 (V_L/V_r)\left(1 - \frac{C^*}{C_0}\right)\left(1 - \exp\left(\frac{-K\,t}{V_L/V_r}\right)\right) \tag{2.19}$$

donde q_i es la concentración de la especie i en la resina a tiempo t, K_f es el coeficiente de transferencia de masa a través de la película líquida (cm/s), C* es la concentración de equilibrio en la superficie de la partícula, a_p es el área superficial específica, V_L es el

volumen de líquido, V_R es el volumen de resina, C_0 es la concentración inicial de la disolución y K es la constante aparente de transferencia de masa, $K = K_f \cdot a_p$.

Modelo de difusión en poros. Este modelo considera a la resina como un material poroso. Las ecuaciones que lo describen son:

$$\frac{\partial q_i(R,t)}{\partial t} = \frac{\partial q_{ei}(R,t)}{\partial t} + \varepsilon_i \frac{\partial C_{pi}(R,t)}{\partial t} = \frac{1}{R^2}\left[\frac{\partial}{\partial R} R^2 \varepsilon_i D_p \frac{\partial C_{pi}(R,t)}{\partial t}\right] \quad (2.20)$$

$$\varepsilon_i V(C_{iT} - C_i(t) = (1-\varepsilon_i) V \overline{q_{ei} + \varepsilon_i C_{pi}(t)} \quad (2.21)$$

$$\overline{q_{ei} + \varepsilon_i C_{pi}}(t) = \frac{3}{R_0{}^3} \int_0^R R^2 \left(q_{ei} + \varepsilon_i C_{pi}\right)(R,t) dR \quad (2.22)$$

Condiciones iniciales y de contorno:

$$Cpi\,(R,0) = 0 \quad (2.23)$$

$$\text{En } R = 0 \rightarrow \left.\frac{\partial C_{pi}\,(R,t)}{\partial R}\right|_{R=0} = \left.\frac{\partial q_i\,(R,t)}{\partial R}\right|_{R=0} \quad (2.24)$$

$$\text{En la interfase} \rightarrow (R = R0) \rightarrow C_{pi}(R0,t) = C_i\,(t) \quad (2.25)$$

donde q_{ei} es la concentración de la especie *i* en los poros, C_{pi} es la concentración de la especie *i* en la disolución en el interior de los poros, ε_i es la porosidad de la resina, D_p es la difusividad en los poros, C_{iT} es la concentración inicial de la especie *i* en la disolución, V es el volumen de disolución, R es al coordenada radial y R_0 el radio de la partícula.

En estos modelos se supone geometría esférica para la fase sólida y se establecen condiciones iníciales y de contorno para obtener los coeficientes de difusión en la película líquida (K_f) y en el interior de la partícula (D_p), que serán diferentes.

En este trabajo se llevó a cabo el estudio de la cinética en tanque agitado aplicando estos dos modelos, se determinaron los parámetros K_f y D_p, y se dedujo la etapa controlante aplicando la ecuación de Helfferich, como se mostrará en la sección de resultados.

2.3.3. Modos de operación

Los modos de operación en intercambio iónico son tres: operación discontinua en tanque agitado, operación semicontinua en columna y operación en continuo en columna. En todos ellos se lleva a cabo tres pasos básicos de operación: acondicionamiento, carga y elución.

En la **etapa de acondicionamiento** la resina comercial se pone en contacto con una disolución que contiene los iones A, estos iones quedan retenidos en el grupo iónico fijo neutralizando la carga de éste. Cuando la resina está saturada de estos iones queda preparada para llevarse a cabo el proceso de carga.

En la **etapa de carga** la disolución que contiene el contra-ión B se pone en contacto con la resina acondicionada con iones del mismo signo que B. Este ión B tendrá más preferencia por los grupos fijos que el ión A y se producirá el intercambio iónico reteniendo de la disolución los contra-iones B hasta que la resina está saturada.

En la **etapa de elución**, el ión B se retira de los sitios activos de la resina, ya que es desplazado por otro ión C que tiene mayor afinidad por los mismos. El proceso es similar al de la carga, la única diferencia es que la concentración de los iones C en la solución de elución es superior a la de la carga en iones B, de este modo se lleva a cabo un proceso de concentración del ión recuperado B.

2.3.3.1. Operación discontinua en tanque agitado

En los procesos industriales no es muy común llevar a cabo el intercambio iónico en tanque agitado debido a problemas y dificultades que se producen en este tipo de operación. Pero si es factible su uso a escala de laboratorio para hacer estudios de equilibrio y cinética de los procesos de intercambio iónico.

El modo de operación es cíclico y cada ciclo consta de las tres etapas anteriormente mencionadas. Los equipos tienen un diseño similar al de otros equipos de contacto líquido-sólido, la resina se encuentra en suspensión con el líquido y se lleva a cabo una agitación para favorecer el contacto. Sin embargo, el diseño sólo es factible para disoluciones sin contenido en sólidos, para poder llevar a cabo la separación de la resina de la disolución de forma sencilla en cada etapa del proceso.

2.3.3.2. Operación semicontinua en columna

Esta operación es la que se emplea más a menudo en los procesos de intercambio iónico. El intercambiador se coloca en el interior de la columna vertical, a través de la cual fluye la disolución a tratar. El proceso global consta de varias etapas que se describen a continuación:

Empaquetamiento de la columna. Consiste en introducir el intercambiador en el interior de la columna evitando la formación de bolsas de aire entre sus partículas para así obtener un lecho uniforme. Esta operación se realiza habitualmente lavando el intercambiador con agua destilada, que además resulta útil para eliminar posibles impurezas y el fenómeno de swelling. Este fenómeno se basa en el hinchamiento del polímero debido a que el disolvente penetra en los poros de la estructura polimérica, ensanchándolos y abriendo la estructura. A simple vista, se observa un aumento del volumen que ocupa la resina. El swelling puede causar graves problemas si tiene lugar una vez el intercambiador se encuentra confinado en la columna y no se ha dejado suficiente espacio para alojarlo una vez se ha incrementado su volumen.

Acondicionamiento del intercambiador. Muchas resinas comerciales se venden en una forma iónica que puede no ser adecuada para el tratamiento que se desea realizar. Por ejemplo, una resina básica fuerte que tenga como contra-ión un grupo OH^- y que, por necesidades del proceso, sea deseable tener un ión Cl^-. En la etapa de acondicionamiento se procede a cambiar el contra-ión de la resina poniéndola en contacto con una disolución concentrada del ion que se desea tener. Una vez se ha conseguido este objetivo y la resina está en la forma iónica deseada, debe eliminarse el exceso de esta disolución lavando la resina con agua destilada.

Etapa de carga. En esta etapa tiene lugar el intercambio de iones entre la disolución a tratar y el intercambiador. La disolución a tratar se introduce en la columna y fluye gradualmente a través del intercambiador. Las condiciones de operación (velocidad de flujo, pH de la disolución, etc.) dependerán del tipo de intercambiador utilizado, y es importante optimizarlas para obtener un buen rendimiento en cuanto a la capacidad y selectividad.

Cuando el intercambiador comienza a estar saturado con los iones de la disolución que entra, se observa un aumento de la concentración de dichos iones en la

disolución que sale de la columna. Esta descarga de iones se conoce como *breakthrough* o curva de ruptura, e indica que el tratamiento de la disolución por el intercambiador ya no está siendo efectivo. Una vez la concentración de estos iones en la disolución de salida iguala a la de la concentración de entrada, el intercambiador ha agotado toda su capacidad de intercambio en las condiciones de operación.

Etapa de regeneración. Esta etapa consiste en devolver el intercambiador saturado a su forma iónica inicial, empleando una disolución concentrada en el ion originalmente asociado al intercambiador. Esta etapa es importante en el proceso de intercambio iónico ya que el buen funcionamiento del intercambiador en sucesivos procesos de carga depende de una regeneración eficiente. Para obtener el máximo rendimiento de esta etapa es importante optimizar parámetros como la concentración y volumen de disolución regenerante así como la velocidad de flujo.

En los procesos de intercambio iónico en columna se puede trabajar de dos modos:

- Las disoluciones de carga y de regeneración se introducen siempre por la parte superior de la columna (**Figura 9 a**).
- El regenerante se introduce en dirección opuesta a la disolución de carga, es decir, por la parte inferior de la columna. Este proceso se denomina, proceso en contracorriente (**Figura 9 b**).

El procedimiento más habitual es el primero, ya que supone un equipamiento más barato que el segundo. No obstante, este modo de operación utiliza el regenerante menos eficientemente que el proceso en contracorriente. En éste, al pasar el regenerante de abajo a arriba, se fluidiza el lecho de intercambiador, de manera que se aumenta la superficie de contacto, la regeneración es más rápida y se necesita menos volumen de regenerante.

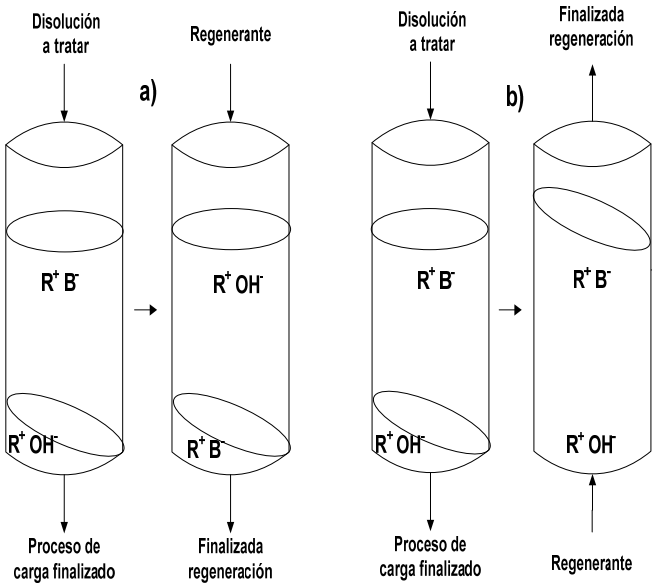

Figura 9. Proceso de intercambio iónico en columna: **a)** regeneración por la parte superior de la columna; **b)** regeneración por la parte inferior de la columna

2.3.3.3. Operación en continuo

En la mayoría de los procesos industriales se trabaja en continuo y por tanto, los efluentes que hay que tratar por intercambio iónico también van a ser continuos, es decir, el proceso de carga se lleva a cabo ininterrumpidamente. Para ello, es necesario que haya una circulación de la resina a través del equipo y ésta es transvasada de la columna de carga a la de elución, para que las columnas de carga y elución no paren de trabajar. El uso de lechos móviles de resina permite esta operación continua, cuya ventaja principal es la de obtener grandes eficacias de separación. Cabe destacar que la mayor parte de los procesos descritos como continuos, son en realidad semicontinuos, en los que la resina está quieta durante un tiempo en las columnas de carga y regeneración, y el movimiento es sólo para el transvase entre ellas. Sin embargo, dado que ambos periodos suelen ser bastante cortos, los sistemas se pueden considerar en su conjunto continuos. Dentro de los equipos continuos cabe destacar los equipo de lecho fijo y los de lecho fluidizado [47].

Equipos de lecho fijo. Han sido desarrollados tanto en régimen de corrientes paralelas como en contracorriente. De entre ellos destacan:

- El contador de Higgs: es el de mayor aplicación industrial, formado por dos columnas unidas en sus extremos superior e inferior por las que circula la resina,

y en el que, a diferentes puntos, se irá poniendo en contacto con el agua a tratar, el regenerante y el agua de lavado.

- El sistema Arion, empleado en la recuperación de amonio y nitrato en la industria de fertilizantes nitrogenados, cuya principal característica es un sistema de drenaje en torno a la columna de regeneración.
- El sistema Asahi, que consta de tres columnas (una de carga, otra de regeneración y una tercera de lavado), y en las que los modos de carga y transvase están sincronizados para las tres columnas.
- El sistema Kontimat, muy similar al Asahi.
- El sistema Permutit y Avco, este último realmente continuo.

Equipos de lecho fluidizado. Permite el tratamiento de disoluciones con sólidos suspendidos. Pueden clasificarse en procesos en una única etapa y en procesos de varias etapas o lechos fluidizados en serie, separados por platos perforados, siendo estos últimos los más comunes y entre ellos cabe destacar:

- El sistema NIMCIX; costa de dos columnas divididas en varias etapas por platos perforados, que periódicamente son cargadas por la parte superior con resina procedente de la otra columna.
- El contador Himsley, de funcionamiento análogo al anterior, pero con diferencias en el diseño de los platos y de las columnas.
- El sistema Fluicon, realmente continuo, formado por dos columnas, una de carga y otra de regeneración y lavado y en la que tanto la disolución como la resina están en continuo movimiento (**Figura 10**).

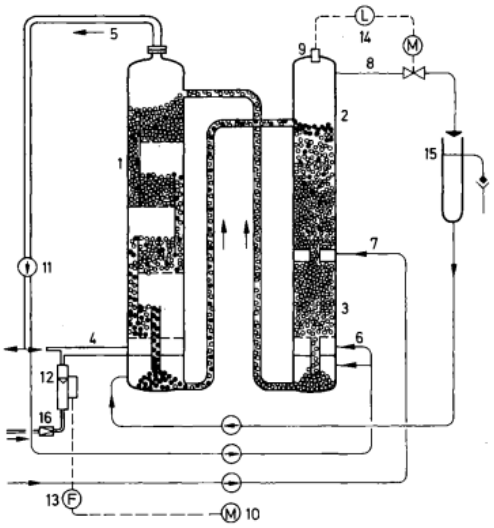

1. Columna de carga
2. Columna de regeneración
3. Columna de lavado
4. Alimentación
5. Agua tratada
6. Agua de lavado
7. Efluente de regeneración

Figura 10. Sistema Fluicon: sistema en continuo de intercambio iónico [48]

Todos los equipos descritos, tanto los de lecho fijo como de lecho fluidizado, tienen importantes ventajas respecto a los equipos de operación cíclica. Las más importantes son:

- Las instalaciones suelen ser menores y más compactas, por tanto disminución de los costes de las instalaciones.
- La calidad del efluente obtenida es constante.
- La cantidad de resina necesaria es menor (aproximadamente la mitad).
- Las caídas de presión son menores.

2.4. MATERIALES DE INTERCAMBIO IÓNICO

2.4.1. Tipos de intercambiadores iónicos

Los intercambiadores iónicos forman un grupo de materiales muy heterogéneo cuya característica común es que contienen una carga eléctrica fija capaz de enlazar a iones de carga opuesta. Se clasifican en dos grandes grupos: intercambiadores orgánicos e intercambiadores inorgánicos. Ambos grupos incluyen materiales sintéticos y naturales.

Los intercambiadores inorgánicos más importantes naturales o sintéticos son las zeolitas, aluminosilicatos cristalinos con la propiedad de intercambiar cationes. Las naturales poseen una estructura relativamente abierta con canales y cavidades comunicadas dentro de la red, mientras que las sintéticas tienen una estructura cristalina regular, rígida y bastante cerrada. En ambos casos parecen no mostrar buenas propiedades intercambiadoras, aunque son muy eficaces como tamices moleculares porque sólo adsorben moléculas pequeñas.

Los intercambiadores orgánicos más importantes son las resinas sintéticas, ya que son los materiales más habituales en las aplicaciones de intercambio iónico en la industria, por ello será en las que nos centremos. Son compuestos que poseen una estructura general basada en una red orgánica tridimensional (matriz polimérica) donde se soportan las cargas eléctricas (grupos iónicos funcionales fijos) y unos iones móviles que neutralizan esas cargas fijas y que serán quienes sufran el intercambio.

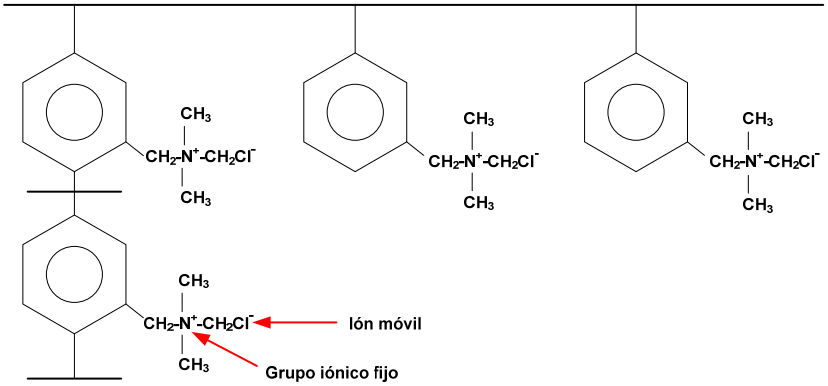

Figura 11. Resina de intercambio iónico básica fuerte. Matriz de estireno-divinilbenceno

Entre las resinas orgánicas sintéticas destacan las basadas en la estructura de estireno-divinilbenceno (**Figura 11**) debido a su buena resistencia química y física, y estabilidad en todo el rango de pH y a la temperatura, de ahí que sean las resinas comerciales más empleadas. También están empezando a ser muy usadas las resinas basadas en copolímeros de metacrilato debido a las ventajas que presentan como alta selectividad, efectividad, estabilidad tanto en condiciones ácidas como básicas, y además son fácilmente funcionalizables.

2.4.2. Técnicas de polimerización de resinas orgánicas

El desarrollo de las resinas orgánicas comenzó con la síntesis de las mismas mediante polimerización por condensación (fenol-formaldehido), y posteriormente, se sintetizaron mediante polimerización por adición.

Los elementos básicos para realizar una polimerización son el monómero (o mezcla de monómeros) y un agente iniciador, que puede ser temperatura, radiación o un agente químico. Además, según las características que se quiera dar al producto final también se le puede añadir un agente porogénico. Existen diferentes técnicas de llevar a cabo la polimerización por adición, y la elección de una u otra dependerá del objetivo de la polimerización y de las sustancias a polimerizar. Las distintas técnicas se describen a continuación:

2.4.2.1. Polimerización en bloque

La polimerización en bloque o "bulk" es el sistema más simple. Tan solo requiere la presencia de un iniciador de la polimerización en concentraciones muy bajas y usualmente se descompone durante el proceso, por lo que se obtendrá un polímero de alta pureza. Esta técnica se suele aplicar a polímeros de etileno, estireno y metilmetacrilato. El producto así sintetizado formará un monolito que puede ser utilizado como tal o molido para su utilización en forma de partículas.

2.4.2.2. Polimerización en solución

El monómero y el iniciador se disuelven en un solvente miscible en todas las proporciones con el monómero. Hay dos tipos:

- Homogénea: el polímero resultante es soluble en el disolvente, sucede en el caso de acetatos de nitrilo, acrilonitrilos y ésteres de ácido acrílico.
- Heterogénea: el polímero es insoluble, por lo que al formarse se produce una precipitación. Es aplicable al acetato de vinilo y al cloruro de vinilo. Esta técnica tiene una serie de ventajas y desventajas:
  - Ventajas: el solvente actúa de diluyente, ayuda en la disipación del calor de polimerización y reduce la viscosidad, y el control térmico es más fácil que en bloque.

- Desventajas: pueden ocurrir enlaces con moléculas del disolvente que afectan a la pureza del producto, la extracción final del disolvente es más complicada y puede producirse contaminación ambiental al desechar el disolvente.

2.4.2.3. Polimerización en suspensión

Se trata de una polimerización en fase heterogénea desde el principio. Esta técnica combina las ventajas de la polimerización en bloque y en solución, y se emplea en la producción de polímeros de vinilo. Se basa en la dispersión de la mezcla de polimerización en una masa grande de un solvente no miscible (medio de suspensión) mediante agitación. Para monómeros no solubles en agua, ésta se usa invariablemente como medio de suspensión.

El tamaño de las gotas de monómero dentro de la fase acuosa por lo general se encuentra en el rango de 0.1 mm a 5 mm y se necesita una agitación continua para evitar la agregación de las mismas. Para ayudar a la formación de las fases de suele utilizar una baja concentración de polímeros solubles en agua (polivinil alcohol, polivilipirrolidona) como estabilizantes de la suspensión, ya que en las etapas medias de la conversión las gotas tienden a agruparse cuando las bolas del polímero se vuelven pegajosas. Una vez terminado el proceso de polimerización, el polímero aparece en forma de pequeñas bolitas precipitadas en el fondo del recipiente. Posteriormente, el polímero tiene que ser lavado para purificarlo.

2.4.2.4. Polimerización en emulsión

La polimerización se realiza en fase acuosa, y se requiere un iniciador soluble en agua y muchos más estabilizantes que en la polimerización en suspensión. Además, se requiere un emulsificador, un regulador de la tensión superficial, una solución tampón para regular el pH y un regulador de longitud de cadena. La principal ventaja es que se puede conseguir un alto grado de polimerización a temperatura ambiente.

2.4.3. Formación de copolímeros de estireno-divinilbenceno

El proceso de polimerización ocurre en dos fases, formación de la matriz polimérica y posterior funcionalización [39]:

a) Formación de la matriz polimérica. Se forma por reacción entre el estireno y el divinilbenceno por medio de una polimerización por adición como se observa en la **Figura 12** y se suele llevar a cabo mediante polimerización por suspensión. El estireno y el divinilbenceno que son insolubles en agua, se mezclan mediante un agitador a una velocidad que rompe la mezcla en pequeñas esferas. Estas esferas a medida que transcurre la reacción se endurecen formando perlas esféricas, que es en la forma en la que se suelen presentar estas resinas. En este punto el copolímero no está funcionalizado.

El grado de reticulación confiere a la resina estabilidad y resistencia mecánica, así como insolubilidad. Se puede ajustar variando el contenido de divinilbenceno (agente reticulante) en la mezcla de reacción. El contenido nominal de DVB (divinilbenceno) se usa para indicar el grado de entrecruzamiento, refiriéndose a los moles por ciento de DVB puro en la mezcla de polimerización. En esta polimerización, la incorporación de una molécula con dos grupos insaturados (DVB) da lugar a la formación de una unión entre dos cadenas.

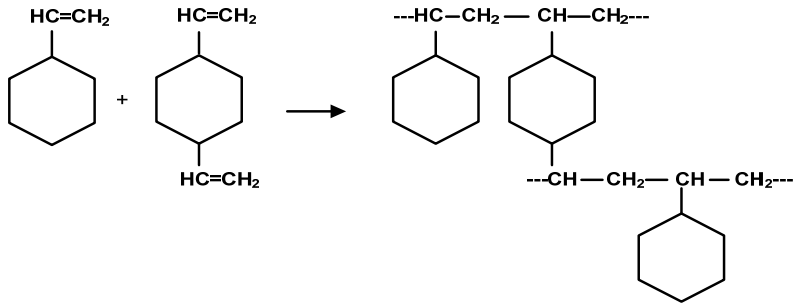

Figura 12. Reacción de polimerización por adicción de estireno-divinilbenceno [49]

b) Funcionalización. Hay dos formas de llevar a cabo la funcionalización de una resina de intercambio iónico, es decir la fijación del grupo iónico intercambiador dentro de la estructura de la resina (matriz):

- Incorporar el grupo funcional durante la polimerización, por ejemplo empleando monómeros ya funcionariados, que contienen los grupos iónicos.
- Llevando a cabo primero el proceso de polimerización y después introducir los grupos funcionales sobre la matriz polimérica mediante las reacciones químicas oportunas como sulfonación o cloro-aminación. Los grupos iónicos más comunes que se introducen en la matriz son:

- Ácido sulfónico para producir una resina catiónica fuerte
- Ácido carboxílico para producir una resina catiónica débil
- Amonio cuaternario para producir una resina aniónica fuerte
- Aminas primarias, secundarias o terciarias para producir resinas aniónicas débiles.

2.4.4. Formación de copolímeros de metacrilato

Los polímeros de metacrilato pueden ser sintetizados por varios mecanismos. La técnica más común es la polimerización por radicales libres ya que se forman a partir de monómeros que contienen dobles enlaces C=C. Ésta se puede realizar de manera homogénea (bloque o en solución), o de manera heterogénea (suspensión o emulsión). La polimerización por radicales libres es una reacción rápida que consta de las etapas de reacción en cadena características: iniciación, propagación y terminación.

En la etapa inicial o de iniciación se necesita el concurso de una molécula capaz de generar radicales, conocidos como iniciadores. Los iniciadores son compuestos muy reactivos que tienen algún enlace fácil de romper por la acción de la luz o calor, por lo tanto, son activados mediante radiación o cambios de temperatura, convirtiéndose en un radical o en un grupo iniciador cargado con carga positiva o negativa. Entre los iniciadores más usados destacan 2',2'-azobisisobutironitrilo (AIBN) y 1,1'-azobis(ciclohexano carbonitrilo) (ACCN), y su forma de actuar tiene lugar formando radicales libres que luego se adicionan al monómero permitiendo que tenga lugar la fase de propagación de la cadena.

La activación del doble enlace en la polimerización por radicales libres puede realizarse no sólo mediante iniciadores químicos, que es el caso más frecuente, sino también por la acción del calor (activación térmica) necesitándose temperaturas elevadas o de determinadas radiaciones (fotoquímica o radioquímica).

Uno de los derivados de metacrilato más usados es el metacrilato de metilo, que puede ser usado solo o acompañado de otro compuesto que una las cadenas principales (crosslinker) como el propio metacrilato de metilo, el divinilbenceno, estireno, etc., siempre que contengan el mismo grupo vinilo que posibilita la polimerización.

Figura 13. Polimerización polimetacrilato de metilo

Para regular el tamaño de los poros obtenidos es preciso incorporar un agente reticulante y un disolvente porogénico. El tamaño de los poros depende de los siguientes factores: % de agente reticulante, % de porogénico, tipo de porogénico y temperatura de reacción. Los dos primeros afectan a la composición y propiedades mecánicas del polímero mientras que los dos últimos afectan más a los poros y son más efectivos. Hay tres tipos de agentes porogénicos: disolventes que solvatan las cadenas de polímeros, no solventes y polímeros lineales.

En el presente trabajo se sintetizaron copolímeros de metacrilato empleando como monómero 2-dietilaminoetil metacrilato (DEAEM) y como crosslinker etilenglicol dimetacrilato (EGDMA) dando lugar al copolímero (DEAEM-co-EGDMA). La ventaja de usar polímeros de metacrilato con bases aminas, es que debido a la presencia de grupos amino en los monómeros se elimina la etapa de aminofuncionalización, necesaria para introducir el grupo amino en el polímero. Los monómeros de metacrilato con base aminada son ampliamente utilizados en la síntesis de membranas poliméricas y en soportes cromatográficos empleados en retención de proteínas [50] y purificación de aguas residuales.

2.4.5. Clasificación de las resinas orgánicas: funcionalidad y estructura de red

Las resinas orgánicas sintéticas las podemos clasificar según su funcionalidad y estructura de red.

Las resinas según su *funcionalidad* se clasifican en dos grupos: resinas catiónicas que intercambian cationes y resinas aniónicas que intercambian aniones. Dentro de ellas distinguimos entre:

Resinas catiónicas de ácido fuerte. Se producen por sulfonación del polímero con ácido sulfúrico, el grupo funcional es el ácido sulfónico ($-SO_3H$) que es altamente ionizable, intercambian iones positivos (cationes). Estas resinas pueden operar a cualquier pH.

Resinas catiónicas de ácido débil. El grupo funcional es el ácido carboxílico (COOH) presente en uno de los componentes del copolímero, principalmente el ácido acrílico o metacrilato. Son resinas altamente eficientes y no son funcionales a pH ácidos. Estas resinas fijan los cationes de calcio, magnesio, sodio y potasio de los bicarbonatos y liberan ácido carbónico. Los cationes unidos a los aniones sulfatos, cloruros y nitratos no son intercambiadores [51].

Resinas aniónicas de base fuerte. Se obtienen a partir de la reacción de copolímeros de estireno-divinilbenceno clorometilados con aminas terciarias. El grupo funcional es una sal de amonio cuaternario (NH_4^+). Intercambian iones negativos y necesitan una gran cantidad de regenerante, normalmente sosa.

Resinas aniónicas débiles. Resinas funcionalizadas con grupos de amina primaria (NH_2), secundaria ($-NHR$) y terciaria ($-NR_2$). Suelen aplicarse a la adsorción de ácidos fuertes con buena capacidad pero su cinética es lenta. Se trata de una resina muy eficiente, requiere menos sosa para su regeneración, pero no se puede utilizar a pH altos, puede sufrir problemas de oxidación o ensuciamiento, deben de ser usadas en aguas con niveles elevados de sulfatos o cloruros, fijan los aniones de los ácidos fuertes como sulfatos, cloruros, nitratos, pero no los aniones débiles del ácido carbónico (H_2CO_3), ni del ácido silícico (H_2SiO_3) [51].

Las resinas según su *estructura de red* se pueden clasificar en: microporosas o tipo gel, y en macroporosas o macroreticulares [52].

Las primeras resinas en desarrollarse fueron las **resinas tipo gel**, que son un polielectrolito con enlaces C-C uniendo las cadenas hidrocarbonadas dentro de una estructura macromolecular. En estas resinas el fenómeno swelling es muy importante. El proceso de swelling favorece la permeabilidad de iones en la matriz de la resina y mejora la accesibilidad a los grupos funcionales. Como inconveniente, el aumento del tamaño de la resina puede dar problemas de exceso de presión si la resina está

empaquetada en una columna y también, que la resina sufra procesos de hinchado y deshinchado puede, con el tiempo, afectar a la estabilidad mecánica del polímero.

Por ejemplo, una resina con baja proporción de divinilbenceno se hinchará mucho en disolución acuosa, abriendo ampliamente su estructura, lo cual permitirá la difusión de iones de gran tamaño.

Posteriormente a estas resinas se desarrollaron las **resinas macroporosas**, cuya característica principal es que su tamaño de poro medio es superior a las primeras. Su composición es parecida a las resinas de tipo gel, la diferencia es que éstas se obtienen por una técnica de polimerización en la que se utiliza un disolvente en el que el monómero se disuelve muy bien, pero que en el polímero no es soluble. Al formarse el polímero esta sustancia va quedando encerrada en la red y posteriormente al eliminarse se forman huecos en las zonas que antes estaban ocupadas por el disolvente. En la **Tabla 7** se muestra un resumen de las resinas comerciales más utilizadas:

Tabla 7. Resinas comerciales más utilizadas en los procesos de intercambio iónico

Denominación	Características	Matriz	Estructura	Grupo funcional	Nombre comercial
DOWEX 50 W	Catiónica fuerte	Poliestireno	Geliforme	Sulfónico	Dowex
IR-120	Catiónica fuerte	Poliestireno	Geliforme	Sulfónico	Amberlite
S 100	Catiónica fuerte	Poliestireno	Geliforme	Sulfónico	Lewatit
CNP 80	Catiónica fuerte	Poliestireno	Macroporosa	Carboxílico	Lewatit
DOWEX 1	Aniónica fuerte	Poliestireno	Geliforme	Trimetil-bencilamonio	Dowex
IRA-400	Aniónica fuerte	Poliestireno	Geliforme	Amina cuaternaria	Amberlite
MP 500	Aniónica fuerte	Poliestireno	Macroporosa	Amina cuaternaria	Lewatit
MP 64	Aniónica fuerte	Poliestireno	Macroporosa	Amina terciaria	Lewatit
TP 207	Quelatante	Poliestireno	Macroporosa	Iminodiacetato	Lewatit

2.4.6. Aplicaciones de los intercambiadores en la industria

Además de su aplicación en el tratamiento de aguas, la tecnología de intercambio iónico se aplica a distintos procesos dentro de la industria como purificación, catálisis, recuperación de metales valiosos, etc. A continuación, se describen brevemente estas áreas de aplicación de las resinas [52]:

- **Tratamiento de aguas.** Se emplean en la eliminación de la dureza del agua, la alcalinidad, eliminación del ion amonio, desionización del agua.
- **Tratamiento de residuos nucleares.** Se aplican en el tratamiento de efluentes contaminados con elementos radioactivos y en la purificación del agua de refrigeración del núcleo.
- **Aplicaciones en la industria alimentaria.** Para desmineralizar líquidos azucarados y jarabes, controlar la acidez, olor, color, sabor y contenido en sal del alimento y también para aislar o purificar un aditivo o un componente del alimento.
- **Aplicaciones en la industria farmacéutica.** Se utilizan en la recuperación y purificación de diversos productos como antibióticos, vitaminas, enzimas, proteínas.
- **Catálisis.** Se aplican como catalizadores heterogéneos en reacciones químicas como hidrólisis, esterificación, formación de amidas, condensaciones, etc.
- **Agricultura.** Se emplean en la absorción de nutrientes por parte de las plantas, para retener la humedad del suelo y para elevar el pH en suelos ácidos.
- **Hidrometalurgia.** Se usan en la recuperación y concentración de metales valiosos como cobre, uranio y cromo, oro, platino y plata. También en el tratamiento de efluentes procedentes de la industria de refinado de metales.

2.4.7. Caracterización físico-química de los polímeros

Las propiedades cromatográficas de cualquier fase estacionaria dependen de ciertas propiedades físicas tales como la cantidad de superficie disponible, tipo de porosidad, resistencia mecánica y posibilidades de convención del fluido a través de los poros de las misma, entre otras [53].

2.4.7.1. Análisis de la distribución granulométrica

Se trata de uno de los métodos más modernos utilizados para la determinación de la distribución del tamaño de partículas sólidas, y se basa en la difracción de la radiación laser. La difracción es el fenómeno que se presenta cuando la luz, en su recorrido, se encuentra con obstáculos que impiden el paso de una porción del frente de ondas. Así cuando la luz incide sobre una partícula, se produce cuatro efectos:

difracción sobre el contorno, reflexión sobre la superficie, refracción y adsorción por parte de la partícula.

El resultado de la medida hecha con estos equipos suele venir expresado en términos de esferas equivalentes, d_v= D(4,3) que es la medida del tamaño de la distribución de todas las partículas basado en el volumen de la esfera, y D(3,2) que es el diámetro de la esfera de área superficial equivalente.

2.4.7.2. Análisis térmico

Las técnicas de análisis térmico permiten medir una propiedad de una sustancia o de sus productos de reacción, estando la muestra sometida a un programa controlado de temperatura. Cuando se calienta una sustancia se producen cambios físicos como cambios de fase, o químicos como consecuencia de la descomposición o reacción de la sustancia.

Termogravimetría (TG). El análisis termogravimétrico (TG) se basa en la determinación de manera continua de la variación de masa de una sustancia sometida a tratamiento térmico. La información que se va a obtener de la curva termogravimétrica es muy variada: estabilidad térmica, composición de la muestra, determinación de volátiles y cenizas, destilación y evaporación de líquidos, etc.

Termogravimetría derivada (DTG). Representa la variación de masa respecto al tiempo (dm/dt) frente a la temperatura o al tiempo. Por tanto, las curvas DTG son la derivada de las curvas TG. La curva que se obtiene presenta una serie de máximos y mínimos. Los puntos de inflexión en la curva TG se corresponden con los mínimos en la curva DTG. La curva DTG permite identificar la temperatura a la cual la velocidad de pérdida de masa es máxima.

2.4.7.3. Adsorción-desorción de nitrógeno a 77K

Una de las técnicas más utilizadas para la caracterización textural de los sólidos es la basada en la adsorción física de gases. Las técnicas de adsorción de gases se basan en la determinación de la cantidad de gas necesario para formar una monocapa sobre la superficie del sólido. Esta se expresa en número de moléculas, y conociendo el área media ocupada por una molécula, es posible determinar el área superficial específica del adsorbente.

Atendiendo a la clasificación de la IUPAC de los poros según su tamaño, se consideran microporos aquellos que tienen un diámetro menor de 2 nm, mesoporos los que tienen un diámetro comprendido entre 2 y 50 nm y macroporos aquellos con diámetro superior a 50 nm.

Medida del área superficial. La determinación de la superficie específica de un sólido se lleva a cabo utilizando el método BET. La ecuación BET es:

$$\frac{p}{n^a(p^0 - p)} = \frac{1}{n_m^a C} + \frac{(C-1)}{n_m^a C} \cdot \frac{p}{p^0} \qquad (2.26)$$

donde n^a es la cantidad adsorbida a la presión relativa p/p^0, n^a_m es la capacidad de monocapa del adsorbente y C es una constante que depende de la forma de la isoterma. El rango de linealidad está limitado por debajo de $p/p^0 \approx 0.3$

Análisis de la mesoporosidad. La fisisorción sobre un sólido mesoporoso tiene lugar en dos fases: en la primera parte se forma una monocapa sobre la superficie del sólido y posteriormente, al aumentar la presión del gas, una multicapa. En la segunda fase, se produce el fenómeno de condensación capilar llenándose los poros. En estas condiciones, al tener lugar la desorción y vaciarse los capilares, las moléculas de adsorbato se separan del interior del líquido y como consecuencia, la superficie es curva y la presión a la que tiene lugar la desorción es diferente, y menor, que aquella a la que ocurre la adsorción. Por tanto, la isoterma de desorción no coincide con la adsorción, presentándose un fenómeno de histéresis.

2.4.7.4. Análisis de la macroporosidad. Porosimetría por intrusión de mercurio

La porosimetría de mercurio es una técnica universalmente empleada en la caracterización textural de materiales con tamaño de poro intermedio o grande. Se fundamenta en la falta de espontaneidad que muestran los líquidos que "no mojan" la superficie de los sólidos, como es el caso del mercurio, que penetra en el interior de los conductos.

En un típico experimento de porosimetría, el material objeto de análisis, tras ser sometido a vacío para evacuar todo el espacio poroso, se sumerge en mercurio. A continuación se va aumentando secuencialmente la presión externa del sistema y

midiendo el volumen de mercurio que se introduce en los poros del sólido. El análisis matemático de los datos experimentales permite obtener ciertos parámetros característicos del sólido, como son el porcentaje de porosidad, radio de los poros más abundantes, densidad aparente, etc.

2.4.7.5. Microscopía electrónica de barrido (SEM)

Esta técnica permite examinar la superficie microscopía de sólidos mediante la medida de un parámetro característico de la superficie, durante el barrido de ésta por un haz muy fino de electrones. El parámetro medido suele ser el coeficiente de emisión electrónica secundaria. Por lo tanto, el microscopio electrónico de barrido consiste en un sistema que permite crear y desviar un haz de electrones, así como medir la variación del parámetro escogido durante el barrido. Permite obtener imágenes de gran calidad proporcionando información acerca de la forma y dimensiones de las partículas que constituyen el sólido, así como de la forma y distribución de los poros y cavidades.

Todas estas técnicas han sido usadas en este trabajo para caracterizar los polímeros sintetizados en el laboratorio y cuyos resultados se mostrarán en la sección de resultados.

3. MATERIALES Y MÉTODOS

3.1. MATERIALES

3.1.1. Resinas comerciales

En los ensayos realizados con aguas residuales de coquería se emplearon dos tipos de resinas comerciales: Lewatit MP500 y Lewatit M610. La primera es una resina aniónica fuerte tipo macroporosa; la segunda es una resina aniónica fuerte tipo gel, y ambas resinas son fabricadas por Lanxess.

En los ensayos realizados con las sulfamidas se empleó la resina Lewatit MP500. Las características de ambas resinas se muestran en la **Tabla 8.**

Tabla 8. Características de las resinas Lewatit MP500 y Lewatit M610

Resinas	**Lewatit MP500**	**Lewatit M610**
Forma de suministro	Cl^-	Cl^-
Grupo funcional	Amina cuaternaria tipo I	Amina ternaria tipo II
Matriz	Poliestireno reticulado	Poliestireno reticulado
Estructura	Macroporosa	Gel
Granulometría >90% (mm)	0.47(±0.06)	0.6(±0.05)
Densidad húmeda(g/mL)	1.06	1.1
Contenido en agua (%)	62	45-60
Capacidad total (eq /L)	1.1	1.25
Estabilidad a T (ºC)	-20/100	1/70
Estabilidad en margen de pH	0/14	0/14
Estabilidad al almacenaje (años)	2	2
Estabilidad al almacenaje en T (ºC)	-20/40	1/40

3.1.2. Disoluciones

En las etapas de carga de las resinas Lewatit MP500 y M610 con tiocianatos y fenoles se emplearon las siguientes disoluciones:

- Disoluciones sintéticas de tiocianato, preparadas a partir de KSCN fabricado por Panreac.
- Disoluciones mezclas de tiocianato + fenol, preparadas a partir de KSCN y fenol≥ 99% fabricado por Sigma, Aldrich.
- Aguas residuales procedentes de los condensados del gas de coquería de la industria siderúrgica, proporcionados por Arcelor Mittal. Éstas fueron filtradas previamente por su alto contenido en sólidos.

En cuanto a los ensayos realizados con sulfamidas y la resina Lewatit MP500, se emplearon diferentes concentraciones de las siguientes disoluciones:

- Disoluciones sintéticas de sulfametoxazol (pureza>98 % w/w, Sigma, Aldrich)
- Disoluciones sintéticas de sulfametazina (pureza>99 % w/w, Sigma, Aldrich)
- Disoluciones mezclas de sulfametoxazol y sulfametazina
- Disoluciones mezclas de sulfametoxazol y sales (cloruro, sulfato y nitrato) preparadas a partir de K_2SO_4 (pureza ≥99% w/w), $NaNO_3$ (pureza ≥99% w/w) y NaCl (pureza ≥99% w/w) fabricadas por Sigma-Aldrich. La concentración de sales fue fijada en 250 mg/L Cl^-, 250 mg/L SO_4^{2-} y 50 mg/L NO_3^- debido a que son los valores máximos admitidos en aguas para consumo humano por la organización mundial de la salud (OMS).

En las etapas de acondicionamiento se empleó una disolución de NaOH 1M, y en las etapas de elución se empleó en todos los casos una disolución de NaOH 0.5M, preparadas a partir de NaOH (Sigma, Aldrich).

3.2. METODOLOGÍA EXPERIMENTAL

La metodología de trabajo empleada en los ensayos realizados en tanque agitado consta de dos etapas: acondicionamiento de la resina y carga de la misma; y en columna consta de tres etapas: acondicionamiento, carga y elución de la resina. Todos los ensayos se llevaron a cabo a temperatura ambiente. A continuación se explica el protocolo seguido en cada caso.

3.2.1. Ensayos en tanque agitado

En todos los ensayos realizados en tanque agitado se siguió el mismo procedimiento experimental que se describe a continuación:

1. **Acondicionamiento de la resina**

Las resinas Lewatit MP500 y M610 suministradas por el fabricante tienen grupos funcionales cargados de cloruro, por tanto, se deben acondicionar previamente antes de su uso. Las resinas se acondicionaron con una disolución de NaOH 1M. En este proceso, los grupos cloruro de la resina son intercambiados por grupos OH^- mediante la

puesta en contacto con la disolución de sosa. Esta etapa de contacto se realiza 2 veces, durante un periodo de 20 minutos cada uno. Posteriormente, la resina se separa de la disolución por decantación y se lava dos veces con agua destilada durante 5 minutos. Finalmente se separa la resina del agua por decantación.

2. Etapa de carga

Dentro de esta etapa se realizan varios estudios que se describen a continuación:

- Elección de la relación L/S (mL disolución/gramos de resina) adecuada.

Se pone en contacto una disolución del compuesto de estudio en cada caso con la resina, manteniendo fijo el volumen de disolución y variando la masa de resina. La agitación empleada fue de 300 rpm en todos los ensayos y se llevaron a cabo en matraces Erlenmeyers de 500 mL. El mecanismo empleado para proporcionar la agitación es un agitador magnético IKA RCT standard. Las resina fue cargada con disoluciones de tiocianato, fenol, mezclas de tiocianato + fenol, SMX, SMZ, mezclas de SMX + SMZ y mezclas de SMX + sales, en concentraciones que se indican en cada capítulo de resultados.

A lo largo del experimento se fueron tomando muestras (2 mL) con la micropipeta, a intervalos de tiempo suficientes durante la operación (entre 1 y 5 minutos). El experimento se llevó a cabo durante dos horas, tiempo suficiente para que se alcanzase el equilibrio. Para la elección de la relación L/S óptima, se elije aquella en la que representando capacidades de retención frente a las respectivas relaciones L/S, se obtiene un máximo en la capacidad de adsorción.

- Estudio de la capacidad de adsorción

Una vez obtenida la relación L/S adecuada, se realizaron ensayos para ver como varían las capacidades de adsorción con la concentración inicial. Para ello se empleó la relación L/S obtenida como adecuada, y se fue variando la concentración inicial del compuesto de estudio. De nuevo se fueron tomando muestras con el tiempo durante dos horas para ver como varía la concentración a lo largo del ensayo hasta que se alcanza el equilibrio. A partir de estos datos, se llevó a cabo el estudio del equilibrio y la cinética del proceso, modelizando los resultados obtenidos, tal como se describe en la sección de resultados dentro de cada artículo.

En la **Figura 14** se muestra un esquema del proceso de intercambio llevado a cabo en tanque agitado.

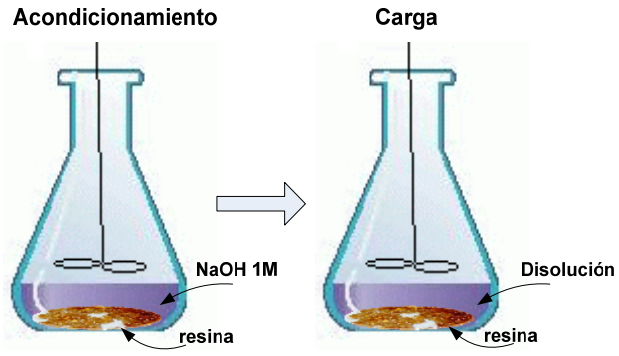

Figura 14. Procedimiento experimental en tanque agitado: acondicionamiento y carga

3.2.2. Ensayos en columna

En este apartado se llevaron a cabo experimentos de carga y elución en columna a temperatura ambiente, empleando una columna cromatográfica Vantage-L32x250 (32 mm de diámetro y 250 mm de altura regulable) de la marca Millipore en los ensayos con aguas residuales que contenían tiocianato y fenol. La columna se empacó con la resina (Lewatit MP500 y Lewatit M610), y se acondicionó con una disolución de NaOH 1M con flujo descendente, durante 20 minutos aproximadamente para reemplazar los grupos Cl^- por grupos OH^-. A continuación, se lavó la resina con agua destilada durante 15 minutos.

La carga de la columna se lleva a cabo con flujo descendente, regulándolo para los distintos ensayos realizados. Las resinas Lewatit MP500 y M610 se cargaron con disoluciones sintéticas de tiocianato, mezclas de tiocianato y fenol, y con aguas residuales industriales.

En el caso de los ensayos con sulfamidas, se llevaron a cabo empleando la resina Lewatit MP500 y una columna cromatográfica Vantage-L11x250. El proceso se realizó de la misma forma, y en este caso la resina se cargó con disoluciones sintéticas de sulfametozaxol, sulfametazina, mezclas de ambas sulfamidas y disoluciones mezclas de sulfametoxazol y sales (cloruros, sulfatos y nitratos).

Para seguir la evolución del proceso de carga con el tiempo, se fueron tomando muestras cada 5-10 minutos a la salida de la columna. El proceso se llevó a cabo hasta

que se saturó la resina, esto es que la concentración a la salida de la columna era la misma que la concentración de la muestra inicial, obteniéndose la curva de ruptura.

La última etapa correspondiente a la elución, se realizó con flujo descendente empleando una disolución de NaOH 0.5M, tomando de nuevo muestras con el tiempo y analizándolas para seguir la evolución de la concentración a lo largo de la etapa. El proceso se llevó a cabo hasta que la concentración a la salida de la columna era prácticamente nula.

En la **Figura 15** se representa el esquema del procedimiento experimental empleado en columna, con las tres etapas de acondicionamiento, carga y elución, y en la **Figura 16** se muestra el dispositivo experimental en cuestión.

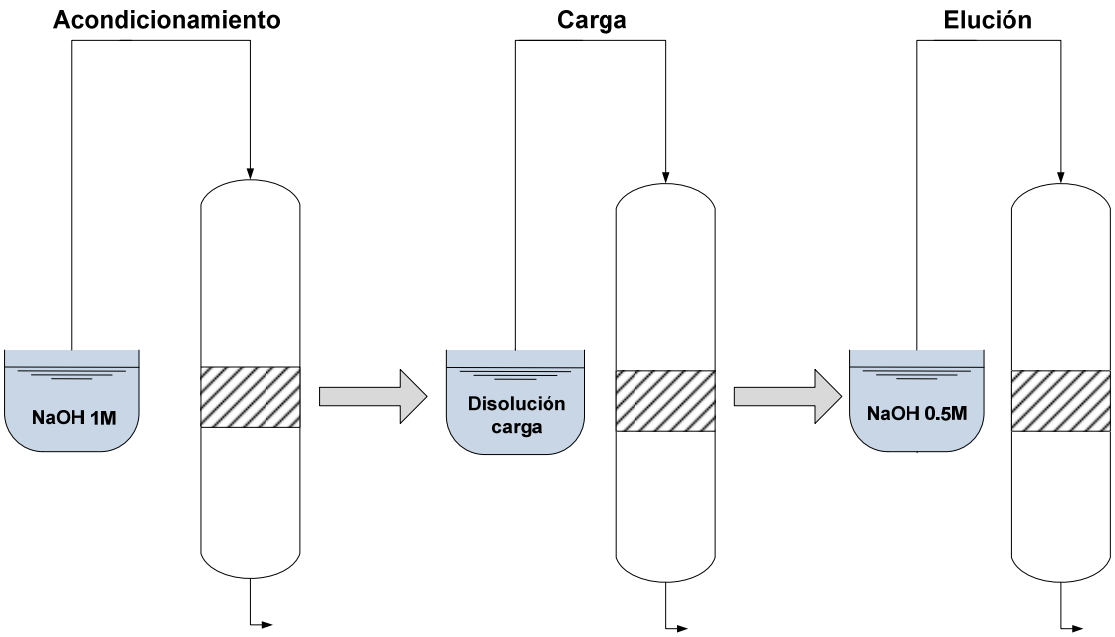

Figura 15. Procedimiento experimental en columna: acondicionamiento, carga y elución

Figura 16. Montaje llevado a cabo en columna para la realización de los experimentos

3.3. METODOS ANALÍTICOS

En todos los ensayos, el seguimiento de la concentración de los experimentos se realizó midiendo la concentración de cada compuesto en la disolución.

El tiocianato y fenol fueron analizados siguiendo el protocolo extraído del libro "Métodos normalizados para el análisis de aguas potables y residuales" [54].

El análisis del tiocianato se realizó por espectrofotometría mediante el método del complejo de hierro (Fe^{3+}); mediante un espectrofotómetro UV/Vis THERMO SCIENTIC, a una longitud de onda de 460 nm. La curva de calibrado del tiocianato se obtuvo por la medida espectrofotométrica de 6 disoluciones patrón de tiocianato de concentraciones 5, 7.5, 10, 12, 15, 17 y 20 ppm, preparadas a partir de una disolución de tiocianato de 1000 ppm de la marca Panreac. Las muestras se diluyen para llevar a cabo la medida.

El análisis del fenol se realizó también por espectrofotometría mediante el método de la 4-aminoantipirina, a una longitud de onda de 510 nm. La curva de

calibrado del fenol se obtuvo por la medida espectrofotométrica de 6 disoluciones patrón de fenol de concentraciones 1, 2, 3, 4, 5, 10 y 20 ppm a partir de una disolución de fenol de 1000 ppm de la marca Sigma. Las muestras se diluyen para llevar a cabo la medida.

Se midió el pH a lo largo de los ensayos mediante un electrodo selectivo en un pH metro Basic 20 CRISON para ver su evolución con el tiempo.

El análisis de las sulfamidas sulfametoxazol y sulfametazina se llevó a cabo mediante cromatografía líquida de alta resolución (HPLC). Se empleó un cromatógrafo Agilent (modelo serie 1200, California, Estados Unidos) de detección UV (**Figura 17**), y una columna C_{18} de fase reversa, Mediterranean Sea_{18}, 5 µm x 25 cm x 46 cm de Teknokroma. La adquisición y análisis de datos fue realizada son el software Agilent ChemStation. Previamente al análisis, las muestras fueron filtradas con filtros de PVDF de 0.45 µm. La fase móvil empleada fue una mezcla de dos disoluciones: disolución de 0.1% de ácido trifluoroacético (TFA) en metanol (eluyente A) y disolución de 0.1% de TFA en agua milli-Q (eluyente B). En los análisis realizados para un solo compuesto, el método fue isocrático (60% eluyente A y 40% eluyente B), y en los ensayos de mezclas de sulfamidas se empleó un gradiente binario (desde 30% A hasta 95% B). Se empleo una longitud de onda de 270 nm y un flujo de 0.7 mL/min. Los tiempos de análisis fueron 10 y 12 minutos dependiendo de si los análisis eran de un solo compuesto o de mezclas, y los tiempo de retención fueron 4.9 min para el SMX y 5.2 min para el SMZ en el método isocrático; y 8.9 min para el SMX y 9.2 para el SMZ en mezclas empleando gradiente binario.

En el caso de los ensayos de SMX con sales, el seguimiento de la concentración de las sales cloruro, sulfato y nitrato se realizó mediante un IC (Ion Cromatograph) DIONEX 120. La fase móvil empleada fue una mezcla de Na_2CO_3 y $NaHCO_3$ (4.5 mM CO_3^{2-} y 0.8 mM HCO_3^-). Los tiempos de retención fueron 2.58 min para Cl^-, 4.33 min para NO_3^- and 10.33 min para SO_4^{2-}.

El seguimiento de la concentración de tiocianato y fenol en disoluciones sintéticas se realizó en algunos ensayos empleando HPLC. En este caso la fase móvil estaba formada por dos disoluciones: acetonitrilo (eluyente A) y un disolución al 0.4% de H_2PO_4 en agua milli-Q (eluyente B). Se empleó un gradiente binario (30% eluyente

A hasta 95% eluyente B), un flujo de 0.7 mL/min, un tiempo de análisis 12 min y una longitud de onda de 210 nm. Los tiempos de retención fueron de 5 min para el tiocianato y de 8.8 min para el fenol.

Figura 17. Cromatógrafo de líquidos de alta eficacia (HPLC) empleado en las determinaciones analíticas

3.4. SÍNTESIS DE POLÍMEROS

3.4.1. Fotopolimerización de polímeros de metacrilato

De los diferentes métodos existentes para polimerizar, en este trabajo se eligió sintetizar polímeros mediante suspensión debido a que se obtienen polímeros en forma de esferas, los cuales son más fáciles de emplear en los ensayos en columna, pues se evitan los problemas de caídas de presión existentes con las partículas que se obtienen al polimerizar en bloque. Además, hoy en día, en la mayoría de las investigaciones se sintetizan los polímeros en forma de partículas esféricas.

Como ya se ha comentado en el apartado de consideraciones teóricas, en la polimerización mediante suspensión intervienen dos fases, una fase orgánica en la que se disuelven los monómeros, y una fase acuosa que contiene el agente estabilizante de la suspensión. A su vez, el iniciador debe ser activado, bien mediante calor o mediante radiación UV. En este trabajo, la síntesis se llevó a cabo mediante fotopolimerización en un reactor UV (UV Laboratory Reactor System 2, Peschl-Ultraviolet). Se emplearon

polímeros de metacrilato con base aminada debido a que se evita la etapa de amino funcionalización como ya se ha comentado en el apartado de consideraciones teóricas. El procedimiento es el siguiente:

En el reactor se introduce la fase acuosa que contiene el agente estabilizante, en este caso al 1% de Polivinilpirrolidona (PVP). A continuación, se introduce la fase orgánica que contiene el monómero 2-dietilaminoetil metacrilato (DEAEM), el agente entrecruzante (crosslinker) etilenglicol dimetacrilato (EGDMA), el disolvente acetonitrilo, el agente porogénico polietilenglicol (PEG) de 1 kDa o ciclohexanol, y el iniciador 1,1'-azobisciclohexanocarbonitrilo (ACCN). La proporción de fase acuosa y fase orgánica fue 1:3. En la **Figura 18** se muestra la estructura química de DEAEM y EGDMA.

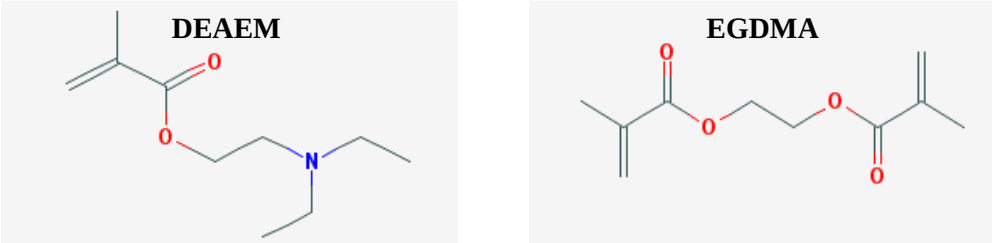

Figura 18. Estructura química de DEAEM y EGDMA [29]

La **Tabla 9** muestra la composición de los polímeros sintetizados, que difieren en el agente porogénico empleado. La elección tanto de los monómeros de partida como de la proporción monómero:agente entrecruzante (DEAEM:EGDMA) 40:60 (% mol) fue basándose en un trabajo previo del grupo de investigación realizado sobre síntesis de polímeros de metacrilato para la retención de proteínas, ya que con esta proporción es con la que se obtuvo mejores resultados [50]. El tiempo de reacción empleado fue de 3 horas y agitación de 900 rpm. La polimerización se llevó a cabo con refrigeración externa para controlar la temperatura y mantenerla constante durante todo el proceso en 30ºC. La proporción de disolvente empleada se calculó como el 50% de la masa total del polímero formado, mientras que el iniciador representa el 1% del total de la masa de polímero. Los polímeros obtenidos se denominaron A (que contiene como agente porogénico ciclohexanol) y B (que contiene como agente porogénico PEG 1 kDa).

Tabla 9. Composición polímeros

Fase acuosa	1% PVP (3.45g de PVP)	
Fase orgánica	Polímeros	
	A	B
DEAEM: EGDMA (mol %)	40:60	40:60
EGDMA(g)	32	32
DEAEM(g)	20	20
ACN(g)	52	52
ACCN (g)	1.040	1.040
Ciclohexanol (mL)	20	---
PEG 1kDa (g)	---	2
Proporción fases orgánica: acuosa	1:3	1:3

Una vez finalizada la polimerización, las partículas de polímero obtenidas se lavan con agua sucesivas veces para eliminar el exceso de agente porogénico. Posteriormente, se centrifugan y se ponen a secar en una estufa durante toda la noche a 60ºC.

En la **Figura 19** se muestra el reactor empleado en la polimerización, UV-Laboratory Reactor System 2 (Peschl-Ultraviolet). Éste reactor utiliza una intensidad de 0.163 W/cm^3 y la lámpara tiene una potencia de 150 W.

Figura 19. Reactor UV empleado para la síntesis de polímeros

3.4.2. Caracterización de los polímeros

Los polímeros obtenidos se caracterizaron mediante las técnicas descritas en el apartado de consideraciones teóricas.

Distribución del tamaño de partículas. La distribución del tamaño de partículas de midió mediante un granulómetro láser Mastersizer S long bench (Malvern Instruments LTd., UK), que posee una lente de 300 RF capaz de medir tamaños de partículas entre 0.05 y 900 μm (**Figura 20**). Con este ensayo se obtuvo datos como la distribución de las partículas basado en el volumen d_v= D (4,3) y el diámetro de la esfera superficial equivalente D (3,2).

Figura 20. Mastersizer empleado en la determinación de la distribución del tamaño de las partículas

Análisis térmico. Se estudió el comportamiento térmico de los polímeros sintetizados mediante el equipo Mettler SDTA851e con una termobalanza Mettler 4000 (TG 50). La muestra (40-50 mg) se calentó bajo nitrógeno con una velocidad de calentamiento de 10ºC/min desde 25º hasta 1000ºC.

Adsorción-desorción de nitrógeno a 77K. Las resinas fueron previamente desgasificadas a vacío a 130ºC. Las isotermas de adsorción-desorción de nitrógeno a 77K se obtuvieron utilizando la técnica volumétrica con el equipo Micromeritics ASAP 2020 (**Figura 21**).

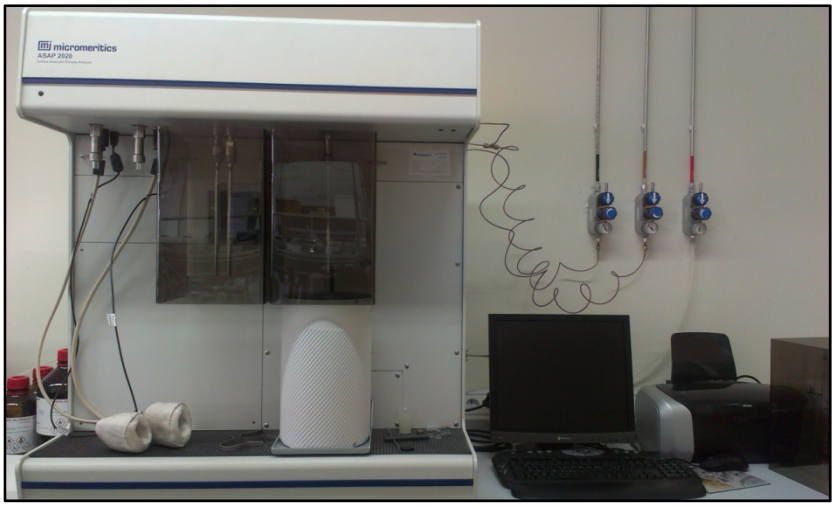

Figura 21. Equipo empleado en la adsorción-desorción de nitrógeno (ASAP 2020)

Porosimetría de intrusión de mercurio. Las medidas realizadas en el presente trabajo se efectuaron con el porosímetro Micromeritics Autopore IV, que opera en un rango de presiones entre 0.1 y 200 MPa, lo que permite medir radios de poros de hasta 0.004 μm (**Figura 22**).

Figura 22. Porosímetro de intrusión de mercurio

Microscopía electrónica de barrido. Se realizaron microfotografías de los materiales con un microscopio electrónico Jeol 6610 que opera a 20 kV. La muestra se colocó en un trozo de metal con cinta adhesiva conductora de doble cara y se revistió con una película delgada de oro utilizando un equipo Balzers SCD 004.

3.4.3. Capacidad de retención de los polímeros sintetizados

Se probó la capacidad para retener SMX de los polímeros sintetizados. Para ello se partió de una disolución acuosa de SMX de concentración 100 mg/L y se puso en contacto 1 gramo de cada resina sintetizada, previamente acondicionada siguiendo el mismo procedimiento que se describió para las resinas comerciales. Se realizaron dos ensayos empleando las relaciones liquido/sólido (mL disolución/g resina) 50 y 200 con ambas resina. El tiempo de contacto fue de dos horas, suficiente para que se alcanzase el equilibrio.

Con la resina con la que se obtuvo mejor capacidad de retención, en este caso la fabricada con agente porogénico ciclohexanol (resina A), se llevó a cabo los mismos estudios realizados previamente con la resina comercial Lewatit MP500, es decir, primeramente se realizaron experimentos en tanque agitado para determinar la relación liquido/sólido (L/S) adecuada. Posteriormente, con ésta relación L/S, se estudió la variación de la capacidad de retención con la concentración inicial. Para ello se puso en contacto 0.5 gramos de resina previamente acondicionada con 400 mL de disolución de SMX de distinta concentración inicial. El tiempo de contacto fue de 2 horas en todos los ensayos, y se tomó muestras (2 mL) a diferentes tiempos (entre 1 y 5 minutos) para seguir la evolución de la concentración con el tiempo.

Se llevó a cabo la operación en columna empleando la columna Vantage-L11x250, siguiendo el procedimiento descrito anteriormente con la resina comercial. Se empacó la columna con la resina A y se acondicionó con una disolución de NaOH 1M, durante 20 minutos con un flujo descendente de 6 mL/min. A continuación, se lavó con agua destilada durante 5 minutos. Posteriormente, se llevó a cabo la etapa de carga de la resina empleando disoluciones de SMX. Las concentraciones empleadas se muestran en la sección de resultados de la publicación en cuestión. Se fueron tomando muestras a intervalos de tiempo (entre 5 y 10 minutos) a la salida de la columna para seguir la evolución del proceso.

Una vez saturada la resina, se lavó con agua. A continuación, se realizó la etapa de elución empleando una disolución de NaOH 0.5 M con un flujo descendente de 5 mL/min, tomando muestras con el tiempo.

Se probó también la capacidad de la resina A para retener SMZ, y SMZ mezclado con SMX en disoluciones acuosas, siguiendo el procedimiento descrito para el SMX en las etapas de acondicionamiento, carga y elución. Las concentraciones empleadas de SMZ y de mezclas de SMX+SMZ se indican en la sección de resultados.

Finalmente, se probó la capacidad de la resina A para retener tiocianato y fenol presentes en disoluciones acuosas en tanque agitado y en columna. Se llevaron a cabo experimentos en tanque agitado en los cuales se puso en contacto 0.5 gramos de resina previamente acondicionada con 100 mL de una disolución de SCN^- de concentración 100 mg/L, a diferentes pH (3, 8 y 11). Los experimentos se llevaron a cabo en matraces Erlenmeyer de 250 mL, con una velocidad de agitación de 300 rpm. El tiempo de contacto fue de 2 horas y se fueron tomando muestras a intervalos de tiempo (entre 5 y 10 minutos) para seguir la evolución del proceso.

Se estudió el efecto de la concentración inicial. Para ello se puso en contacto 0.5 gramos de resina previamente acondicionada con 100 mL de disolución de SCN^- a diferentes concentraciones iniciales, todas ellas ajustadas al pH con el que se obtuvo mayor capacidad de retención.

Se llevaron a cabo de igual modo ensayos con disoluciones sintéticas mezclas de tiocianato y fenol en igual proporción a distintas concentraciones iniciales, empleando 0.5 gramos de resina y 100 mL de estas disoluciones mezclas. El tiempo de contacto fue de 2 horas, y la velocidad de agitación 300 rpm. Se tomaron muestras a intervalos de tiempo (cada 5 ó 10 minutos). El análisis de las concentraciones de tiocianato y fenol se realizó mediante HPLC tal como se describió en el apartado de métodos analíticos.

Se llevó a cabo la operación en columna, empleando la columna Vantage-L11x250. La columna se empacó con la resina A y se acondicionó tal como se ha descrito previamente. A continuación, se llevó a cabo la etapa de carga empleando disoluciones sintéticas de SCN^-, fenol y mezclas de SCN^- y fenol en igual proporción, con un flujo descendente de 6 mL/min. Se tomaron muestras a intervalos de tiempo (entre 5 y 10 minutos) hasta que se saturó la resina. Posteriormente, se llevó a cabo la

elución empleando una disolución de NaOH 0.5M con un flujo descendente de 5 mL/min, tomando muestras a intervalos de tiempo (entre 1 y 5 minutos) y analizándolas en el HPLC. La operación se realizó hasta que no se detectó concentración del compuesto a la salida de la columna.

4. RESULTADOS

4.1. ELIMINACIÓN DE SULFAMETOXAZOL EN DISOLUCION ACUOSA MEDIANTE INTERCAMBIO IÓNICO EMPLEANDO UNA RESINA ANIÓNICA FUERTE EN LECHO FIJO

En este subapartado se recoge los resultados obtenidos de la eliminación de sulfametoxazol en disoluciones sintéticas empleando una resina aniónica comercial.

Como ya se ha comentado en consideraciones teóricas en el apartado de 2.1., se han detectado antibióticos en los efluentes de las plantas de tratamiento de aguas residuales, aguas subterráneas y superficiales, debido a que estos contaminantes son no biodegradables y no se pueden eliminar mediante los métodos convencionales de depuración de aguas, con los efectos dañinos que su presencia conlleva para el medio ambiente. En el artículo que a continuación se presenta, se ha estudiado la eliminación de sulfametoxazol presente en soluciones acuosas empleando una resina de intercambio aniónica, Lewatit MP500. Se ha estudiado el equilibrio y la cinética del proceso en tanque agitado y se han determinado la capacidad de retención y los parámetros de equilibrio y cinética. Asimismo, se ha estudiado la operación en columna, realizando varios ciclos de carga y elución para estudiar la pérdida de efectividad de la resina tras varios ciclos, analizar la capacidad del eluyente para regenerar la resina y se han modelizado las curvas de ruptura obtenidas.

Artículo: Sulfamethoxazole removal from synthetic solutions by ion exchange using a strong anionic resin in fixed bed

Situación: artículo publicado en *Solvent Extraction and Ion Exchange* (Taylor & Francis)

Referencia:

López, A.M.; Rendueles, M.; Díaz. M. Sulfamethoxazole removal from synthetic solutions by ion exchange using a strong anionic resin in fixed bed. *Solvent Extraction and Ion Exchange*, 31:763-781, 2013

Solvent Extraction and Ion Exchange, 31: 763–781, 2013

ISSN: 0736-6299 print / 1532-2262 online
DOI: 10.1080/07366299.2013.810961

Taylor & Francis
Taylor & Francis Group

SULFAMETHOXAZOLE REMOVAL FROM SYNTHETIC SOLUTIONS BY ION EXCHANGE USING A STRONG ANIONIC RESIN IN FIXED BED

Ana María López Fernández, Manuel Rendueles, and Mario Díaz

Department of Chemical Engineering and Environment Technology, University of Oviedo, Oviedo, Spain

Numerous antibiotics like sulfonamides have been found in effluents from drug manufacturers due to the fact that these pollutants cannot be removed completely in STPs. Removal of pharmaceuticals by adsorption and ion exchange comprise some of the most promising techniques due to their low cost, easy regeneration, and selective removal of pollutants. This article studies the removal of sulfamethoxazole (SMX), a common antibiotic that prevents the formation of dihydrofolic acid and which is the most frequently detected as sulfonamide in municipal sewage. The SMX retention capacity of an anionic ion exchange resin, Lewatit MP-500 (Lanxess Chemical), was initially determined. Equilibrium and kinetics were studied and equilibrium constants and diffusivity values were obtained using different models. Load and elution breakthrough curves were plotted to evaluate ion exchange operation in a fixed bed column. In the elution step, 100% SMX was recovered in all cycles and could be concentrated up to nine times, thus facilitating the treatment of this compound. Load and elution breakthrough curves were simulated using a fixed bed model in which axial dispersion was considered the parameter model fit. A good correlation between experimental results and the numerical solution of the fixed bed model demonstrates the validity of the model.

Keywords: ***ion exchange, sulfamethoxazole, synthetic solutions, fixed bed model***

INTRODUCTION

In the last fifteen years, scientists have paid growing attention to pharmaceuticals as new emerging pollutants. The most important ways that drug are introduced into the environment are through waste effluents from manufacturing processes in which numerous pharmaceuticals were found at concentrations of up to micrograms per liter, excreta, disposal of unused or expired drug products, and accidental spills during manufacturing or distribution.[1] The presence of pharmaceuticals in the environment originates from the fact that these pollutants cannot be completely removed at sewage treatments plants (STPs) and hence persist in the environment. In general, total removal rates of pharmaceuticals at STPs are currently 40-60%. Some of the most representative pharmaceuticals found in STPs are antibiotics, anti-inflammatories, antiepileptics, and tranquilizers. Incomplete

Address correspondence to Manuel Rendueles, Department of Chemical Engineering and Environment Technology, University of Oviedo, C/Julian Claveria 8, Oviedo 33006, Spain. E-mail: mrenduel@uniovi.es

removal of certain pharmaceuticals, such as clofibric acid, was also observed at drinking water treatment plants (DWTP).[2, 3] Furthermore, the adverse effects of pharmaceuticals at the μgL^{-1} level on living organisms have recently been confirmed. Pharmaceuticals such as sulfonamide and tetracycline are the most widely used in aquaculture and in the livestock farming industry. Although some of these antibiotics are completely metabolized to inactive compounds, most of them are excreted in urine, feces, and manure as parent compounds or active metabolites. As a result, sulfonamides and tetracycline are detected in sewage, agricultural wastewater, surface water, and in the influent and treated water of drinking water treatment plants.[4, 5] There is hence a need to optimize and improve the current technologies used at STPs and DWTPs for removing pharmaceutical residues, especially for treating pharmaceutical industrial wastewater and purifying surface water at DWTPs.[6, 7, 8] Waste treatment methods such as adsorption, biodegradation, chemical oxidation, incineration, and solvent extraction have been studied to remove these toxic organic compounds. Among these methods, adsorption has been widely used as an effective method for the removal of organic contaminants from wastewater.[9, 10, 11, 12] Although activated carbon has a high capacity for adsorbing toxic organic substances, especially hydrophobic compounds, and can be easily modified by chemical treatment to increase its adsorption capacity, it also has several drawbacks. Powdered activated carbon is hard to separate from an aquatic system when it becomes exhausted or the effluents reach the legal discharge limit. Furthermore, inefficient removal of pharmaceuticals, which are either electrically charged or hydrophilic, has been observed. The regeneration of exhausted activated carbon by chemical and thermal procedures is also expensive and leads to loss of the adsorbent.

The adsorption of a common antibiotic drug, Sulfamethoxazole (SMX), an antibacterial sulfonamide widely used to treat urinary tract infections, and an anti-parasite drug, metronidazole (MN), on activated carbon (AC) from aqueous solutions was studied at different pH, adsorbent concentration, and temperatures by Çalişkan and Göktürk.[12] These authors found that the increase in pH of the solutions caused a decrease in adsorption of SMX and MN on AC. The adsorption of SMX on an alumina-surface interface at room temperature was investigated by Bajpai.[13] Adsorption is pH-dependent and found to increase with increasing pH of the medium. Adsorption also decreases with increasing temperature of the adsorption medium. SMX is the most frequently detected sulfonamide in municipal sewage.

Polymeric resins are becoming more common in wastewater treatment due to their low costs, easy regeneration with chemical solutions (both acid and alkali) under ambient conditions, and selectivity compared to activated carbon. Activated carbon sorbs most organic chemical indiscriminately, making it difficult to recover certain organic chemical selectively for reuse.[14] Belter et al.[15] patented an ion exchange process that used a weak-base anion exchange resin to adsorb streptomycin, which could subsequently be eluted with a dilute acid solution. In a later study in 1983, Belter[16] once again used ion exchange to remove and recover antibiotics from pharmaceutical wastewater.

Removal of antibiotics using MIEX, a macroporous strong base magnetic ion exchange resin was studied by Choi et al.[4] As most antibiotics are present in ionic form and have *pka* values near neutral pH, the afore-mentioned authors found that SAs and TAs were removed by MIEX. Ion exchange on a strong-acid cation resin (Dowex 50W-50xAx400) and a strong-base anion resin (Dowex 1x4-400) was evaluated in the removal of seven common antibiotics at water treatment plants by Adams et al.:[5] carbadox, sulfachlorpyridazine, sulfadimethoxine, sulfamerazine, sulfamethazine, sulfathiazole, and trimethoprim. Anion exchange experiments employing a strong base anion exchange

resin were only slightly more effective. Vergili[17] studied the adsorption of carbamazepine, propyphenazone, and sulfamethoxazole using a polymer resin, Lewatit VP OC 1163.

More recently, Ardelean et al. studied the adsorption of p-Nitrophenol from water on a functionalized polymer, P1n, and a commercial resin, Amberlite XAD-4,[18] while Grimmett[19] studied the removal of sulfamethazine by four Purolite hypercrosslinked adsorbents (MN152, MN250, PD400, and PAD600) in aquatic systems.

The aim of the present study was to investigate the feasibility of ion exchange treatment of effluents from pharmaceutical plants. Lewatit MP500, a macroporous strong anionic resin was selected as adsorbent because the ion exchange process is less dependent on pH when using a strong resin compared to a weak one, as was proved in previous assays. Assays were carried out to determine the capacity of the afore-mentioned resin to retain SMX from synthetic solutions prepared in distilled water. Equilibrium and kinetics were studied in order to characterize the operation, determining their parameters in batch experiments. The adsorption equilibrium constants were determined using Langmuir and Constant Separation Factor isotherms. The kinetics was analyzed using two models: a film mass transfer model and the pore diffusion model. Finally, several operational load and elution cycles were performed in a fixed bed column using synthetic solutions of SMX to evaluate the behavior of the resin in an industrial operation. The breakthrough curves of the load and elution steps were fitted using a fixed-bed adsorption model. The adsorption of SMX on Lewatit MP500 resin was studied, considering only one compound, without competing with other organic and inorganic compounds that are present in actual effluents. This approximation allows the performance of the ion exchange resin to be studied as regards SMX retention.

MATERIALS AND METHODS

Materials

Sulfamethoxazole (SMX) (purity $>$ 98% w/w) and sulfamethoxazole (standard analytical grade) were purchased from Sigma-Aldrich. Methanol (HPLC grade) was used for liquid chromatography and ultra-pure water was prepared in a Milli-Q purification system. All other chemicals were obtained from Sigma-Aldrich. The filters used for filtration were obtained from Millipore (0.45 μm PVDF for the samples) and Whatman (0.22 μm PTFE for the mobile phase). Stock solutions were prepared by dissolving the pharmaceutical in distilled water. All experiments were carried out at the pH values of pharmaceuticals in water solutions (pH = 5.0-5.5).

A commercial organic polymeric resin (Lewatit MP500) manufactured by Lanxess was used as adsorbent. The strong base resin Lewatit MP500 has a quaternary amine (macroporous type I) and crosslinked polystyrene matrix. The main properties of the resin is shown in Table 1.

Analytical Methods

Sulfamethoxazole was determined in the samples using HPLC (Waters 2690) and a column (Mediterranean Sea_{18}, 5 μm × 25 cm × 46 cm, plus a reverse-phase column from Waters) equipped with a UV detector. Prior to HPCL analysis, the samples were treated using 0.45 μm PVDF filters. The mobile phase consisted of methanol (eluent A) and water (eluent B). The method was isocratic (60% of eluent A and 40% of eluent B). Analysis was

Table 1 Characteristics of Lewatit MP500.

General description	
Ion form	Cl^-
Functional group	Quaternary amine (type I)
Matrix	Cross-linked polystyrene
Polymer Structure	Macroporous
Bead side >90% (mm)	0.47(±0.06)
Density (g/mL)	1.06
Total capacity (min.eq /L)	1.1

performed at a flow rate of 1 mL/min. The wavelength used for detection was 254 nm and the retention time for SMX was 3.9 min.

Adsorption Studies

Batch Experiments. Batch experiments were carried out at room temperature in cylindrical stirred tanks employing a stirring rate of 300 rpm. Initially, the ionic form of the wet resin was Cl^-. Subsequently, in order to condition it, the resin was contacted with a solution of NaOH 1 M with an L/S ratio (volume of liquid (mL)/ mass of wet resin (g)) = 20, 2 times, 20 minutes each time, to substitute the Cl^- groups by $OH^®$ groups. Next, the resin was washed with distilled water twice for 5 minutes each time with an L/S ratio = 50, and then separated from the solution.

The resin was subsequently contacted with the loading synthetic solutions of SMX prepared in distilled water. Thus, the OH^- groups of the resin were exchanged for SMX groups. The L/S ratio was adjusted by maintaining the volume of solution (300 mL) and varying the amount of wet resin. The contact time was 100 minutes in all tests, this time being considered sufficient to reach operative equilibrium. The volume of the samples extracted from the tank each time was 2 mL, which did not substantially change the volume of the solution. The concentration of SMX ions in the resin was determined by mass balance, calculating the difference between the initial and final quantity of charged ions in the solution. This batch operation allows the equilibrium and kinetics constants to be determined without any hydrodynamic effect that could be present in a fixed bed operation.

Column Experiments. Continuous flow adsorption experiments were carried out in a glass column with an internal diameter of 1.1 cm. Columns were prepared by packing them with 1.3 grams of wet resin, (bed height 2 cm). Solutions were pumped through the column by a peristaltic pump (Masterflex) in down-flow mode.

To condition the wet resin in the fixed bed, a solution of NaOH 1M was pumped through the column for 20 minutes at a flow rate of 11 mL/min. Distilled water was then fed through the column at a flow rate of 11 mL/min for 15 minutes to wash the resin.

The load stage using synthetic solutions of SMX prepared in distilled water was carried out at a down-flow rate of 11 mL/min. Effluent samples were collected (4 mL approximately) at specified time intervals (5-10 minutes) and measured by HPLC to monitor the evolution of SMX concentration with time. The breakthrough curve was plotted until the SMX concentration at the outlet of the column effluent reached the initial concentration of the solution feed. After adsorption, distilled water was fed through the column to wash the resin, thus removing any unabsorbed SMX ions on the adsorbent surface or entrapped between adsorbent particles.

After loading, the elution stage was carried out by pumping a solution of NaOH 0.5 M through the column at a flow-rate 11 mL/min. The effluent samples were collected at the outlet of the column every 5-10 minutes to monitor the evolution of the concentration with time. The elution curve was plotted until no SMX concentration was detected at the outlet of the column.

Five load/elution cycles were performed using concentrations of 200, 300, and 400 mg/L SMX for the load step and NaOH 0.5 M as eluent. All load steps were carried out in down-flow mode. In the elution steps, the first three cycles were carried out in down-flow mode and the fourth and fifth cycles were carried out in up-flow mode in order to compare the influence of the flow direction on the recovery of SMX in this stage.

RESULTS AND DISCUSSION

Batch Equilibrium Study

In order to evaluate the behavior of the MP500 resin under different L/S ratios (volume of liquid (mL)/mass of wet resin (g)) (600, 800, 1000, 1200, 1500, and 1800), several runs were carried out to obtain the appropriate L/S ratio. In these trials, different amounts of resins were loaded with 300 mL of the SMX synthetic solution with a concentration of 100 mg/L, monitoring SMX concentration with time until reaching equilibrium. The results show that with L/S = 1500 it was possible to achieve the equilibrium concentration (37.4 mg/L SMX) and total operational capacity (110 mg SMX/mL wet resin) in 100 minutes. This L/S ratio was accordingly chosen as the value for all subsequent tests.

Several runs were carried out to obtain the capacities of the resin. The MP500 resin was contacted with different SMX solution concentrations (50, 75, 150, 200, and 250 mg/L SMX) with a L/S ratio (volume of liquid (mL)/mass of wet resin (g)) of 1500, determined in the afore-mentioned assays as suitable for calculating the retention capacity of the resin. The results show that equilibrium was reached in all cases in approximately 100 minutes, obtaining adsorption capacities of 58 mg/mL wet resin and an equilibrium concentration of 21.3 mg SMX/L in the assay using an initial concentration of 50 mg SMX/L, and an adsorption capacity of 183 mg/mL wet resin and an equilibrium concentration of 156 mg SMX/L in the assay using an initial concentration of 250 mg SMX/L.

The process was modeled assuming a sorption process, seeing as the rate-controlling step of ion exchange is usually the diffusion of the counter anions rather than the "chemical" exchange reaction at the fixed ionic groups. This means that the ion-exchange process is essentially a diffusion phenomenon.[22] Although reaction rate constants maybe defined formally, in their physical interpretation, they have little in common with the rate constants of actual chemical reactions.

In this case, the resin is loaded with OH^- groups after conditioning. Thus, when it is put in contact with the SMX synthetic solutions, the equilibrium reaction is:

$$R - OH + SMX \leftrightarrow R - SMX + OH^-$$

Two different models, Langmuir and Separation Factor isotherms, were used to define the relationship between the load capacity and the solution concentration. The equation of the Langmuir isotherm is:

$$q_i = \frac{K_{eq} \cdot q_t \cdot C_i}{1 + K_{eq} \cdot C_i} \quad (1)$$

where K_{eq} is the equilibrium constant, q_t is the maximum capacity of the resin (mg SMX/mL wet resin), C_i is the solution concentration of species i (mg SMX/L), and q_i the concentration of species i in the resin (mg SMX/mL wet resin). For the Constant Separation Factor isotherm, the equation is:

$$q_i = \frac{K_{eq} \cdot q_t \cdot C_i}{C_T + (K_{eq} - 1) \cdot C_i} \tag{2}$$

where C_T is the minimum SMX equilibrium concentration in the solution with a saturated resin (mg SMX/L), and the other parameters in the equation have the same meaning as in the Langmuir isotherm. The equilibrium constants and the maximum adsorption capacity were obtained accordingly. A comparison of experimental results with the predicted values using the Langmuir and the CSF isotherms are shown in Fig. 1. It can be seen that the Langmuir and CSF isotherms show a good correlation between the experimental results and predicted values. The different isotherm parameters obtained are presented in Table 2.

Batch Kinetics Study. The process of adsorption was monitored from the initial time to equilibrium time with all solutions. After 100 minutes, the solution concentration of SMX does not change substantially, so operational equilibrium can be assumed. The ion exchange operation was taken from the loading experiments conducted in a stirred tank with synthetic solutions with initial concentrations of 50, 75, 150, 200, and 250 mg/L SMX. The concentration profiles of SMX can be studied using film mass transfer and pore diffusion kinetic models to determine the mass transfer mechanisms.[20–21]

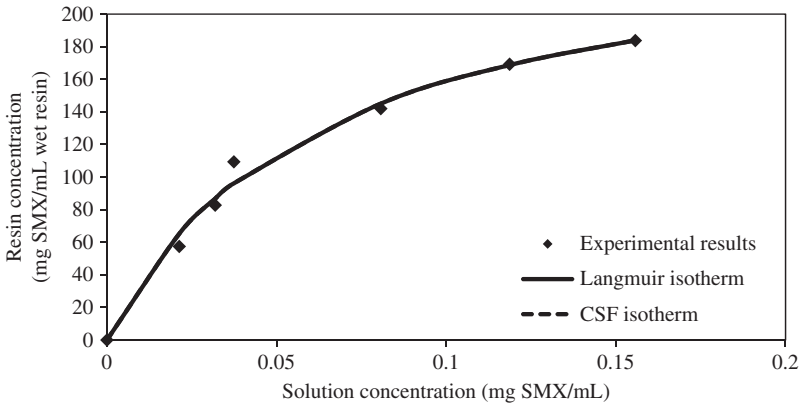

Figure 1 Equilibrium adsorption data and fitting curves of adsorption of SMX from synthetic solution onto Lewatit MP500 resin, by two isotherms models Langmuir and Constant Separation Factor.

Table 2 Isotherm parameters obtained in batch trials.

	Langmuir Isotherm	FSC Isotherm
K_{eq}	15.84	6.34
q_t (mg SMX/mL resin)	258.5	217.7
C_T (mg SMX/mL solution)	–	0.337

Film Mass Transfer Model. In this model, the retention of SMX is assumed to be limited by the external surface of the particle.[22] The model can be described by the following equations:

$$\frac{dq_i}{dt} = K_f a_p \left(C_i - C^*\right) \tag{3}$$

where q_i is the concentration of specie i in the resin at time t (mg/mL wet resin), K_f is the mass transfer coefficient in the fluid phase (cm/s), C^* is the equilibrium SMX concentration in the solution (mg SMX/mL), and a_p is the specific surface area, that is, the total surface area per unit of volume (cm^{-1}). $K_f a_p$ can be considered as K, the mass transfer apparent constant.

$$V_L C_i + V_r q_i = V_L C_O \tag{4}$$

where V_L is the volume of liquid, V_r is the volume of wet resin, and C_o is the initial SMX concentration in solution. Integrating Eq. (3) in Eq. (4), we obtain the following equation:

$$q_i\,(t) = C_0\,(V_L/V_t)\left(1 - \frac{C^*}{C_0}\right)\left(1 - \exp\left(\frac{-Kt}{V_L/V_t}\right)\right) \tag{5}$$

The mass transfer constant, K, can be determined by regression using the experimental data, fitting these to Eq. (3). The anion exchange beads are of constant size with a spherical geometry; therefore, $K_f = K/\ a_p$. A comparison of the experimental results for the SMX concentration and the theoretical values obtained with (4) and (5) will thus give the parameters values for all the experiments. A comparison of experimental and theoretical results for the kinetics of synthetic solutions of SMX can be seen in Fig. 2. The values obtained for the mass transfer constant are presented in Table 3. As can be appreciated, there is negligible variation in the kinetic parameters with concentration, although the Kf/K ratio is constant. The kinetic parameters are higher for higher concentrations. This could be due to the concentration gradient between the surface of the resin and the solution,

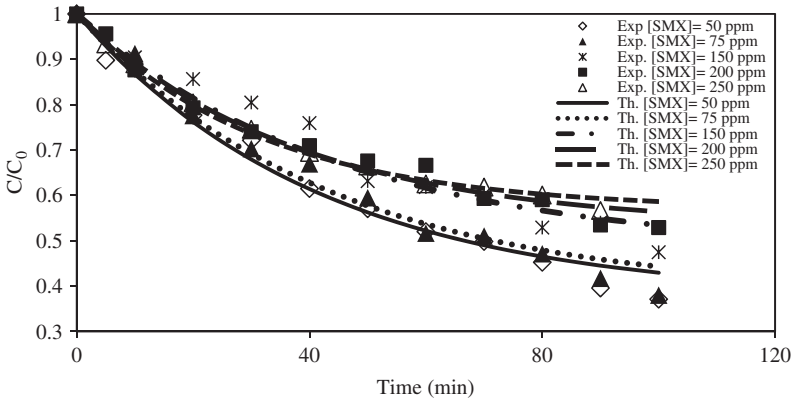

Figure 2 Fitting of kinetics data using the film mass transfer model for the adsorption of SMX synthetic solution with different concentrations (50-250 mg SMX/L) onto Lewatit MP500 resin.

Table 3 Mass Transfer Constant, calculated by the film mass transfer model for synthetic solutions of SMX.

Experiments	K (min^{-1})	K_f (cm/s)
Synthetic solution, $C_{0\,SMX} = 50$ mg/L	0.0230	$3.0{\cdot}10^{-6}$
Synthetic solution, $C_{0\,SMX} = 75$ mg/L	0.0229	$3.0{\cdot}10^{-6}$
Synthetic solution, $C_{0\,SMX} = 150$ mg/L	0.0234	$3.1{\cdot}10^{-6}$
Synthetic solution, $C_{0\,SMX} = 200$ mg/L	0.0261	$3.4{\cdot}10^{-6}$
Synthetic solution, $C_{0\,SMX} = 250$ mg/L	0.0315	$4.1{\cdot}10^{-6}$

which enhances the kinetics of the process. For modeling purposes, these parameters were considered constant for each concentration.

Pore Diffusion Model. This model[23] considers the resin to be a porous matrix. The model is described by the following equations:

- Mass balance inside the particle:

$$\frac{\partial q_i\,(R,t)}{\partial t} = \frac{\partial q_{ei}\,(R,t)}{\partial t} + \varepsilon_i \frac{\partial C_{pi}\,(R,t)}{\partial t} = \frac{1}{R^2}\left[\frac{\partial}{\partial R} R^2 \varepsilon_i D_p \frac{\partial C_{pi}\,(R,t)}{\partial t}\right] \tag{7}$$

  where q_{ei} is the pore concentration of specie i, C_{pi} is the pore solution concentration of specie i, ε_i is the resin porosity, and D_p is the pore diffusivity.
- Mass balance in the bulk solution:

$$\varepsilon_i V\left(C_{iT} - C_i\,(t) = (1-\varepsilon_i)\,\overline{V q_{ei} + \varepsilon_i C_{pi}\,(t)}\right. \tag{8}$$

  where C_{iT} is the initial concentration of species i in solution, and V is the volume of solution.
- Average concentration in particle:

$$\overline{q_{ei} + \varepsilon_i C_{pi}}\,(t) = \frac{3}{R_0^3}\int_0^R R^2\left(q_{ei} + \varepsilon_i C_{pi}\right)(R,t)\,dR \tag{9}$$

  where R is the radial coordinate, and R_0 is the particle radius.

  The initial and boundary conditions needed to solve the systems are:
- Initial conditions:

$$\mathrm{C_{pi}\,(R,0) = 0} \tag{10}$$

- Boundary conditions:

$$\mathrm{In\ R = 0} \rightarrow \left.\frac{\partial C_{pi}\,(R,t)}{\partial R}\right|_{R=0} = \left.\frac{\partial q_i\,(R.t)}{\partial R}\right|_{R=0} \tag{11}$$

$$\mathrm{At\ the\ interphase\ (R = R_0) \rightarrow C_{pi}\,(R_0, t) = Ci(t)} \tag{12}$$

A FORTRAN subroutine, PDECOL,[24] was used to solve these equations. The subroutine uses the orthogonal collocation on finite elements method to solve the system of non-linear differential equations. The diffusivity values obtained are given in Table 4.

Table 4 Pore diffusivities calculated by the pore diffusion model for synthetic solution of SMX.

Experiments	$D_p(cm^2/s)$
$[SMX]_0 = 50$ mg/L	$2.8 \cdot 10^{-10}$
$[SMX]_0 = 75$ mg/L	$2.8 \cdot 10^{-10}$
$[SMX]_0 = 150$ mg/L	$1.9 \cdot 10^{-10}$
$[SMX]_0 = 200$ mg/L	$2.5 \cdot 10^{-10}$
$[SMX]_0 = 250$ mg/L	$2.5 \cdot 10^{-10}$

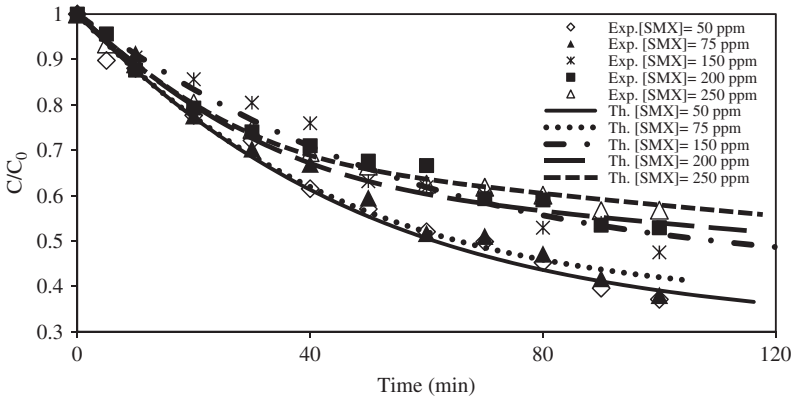

Figure 3 Fitting of kinetics data using the pore diffusion model for the adsorption of SMX synthetic solution with different concentrations (50-250 mg SMX/L) onto Lewatit MP500 resin.

As can be seen, the values of the coefficient of diffusivity are similar, presenting the same order of magnitude in all assays.

Figure 3 shows the fitting of the experimental results to this model with diffusivity values from Table 4 for all the assays. The good agreement between experimental data and the theoretical prediction shows the goodness of the model.

Rate-Controlling Step

A method proposed by Helfferich[22] was used to identify the rate-controlling step (diffusion inside the solid particles or diffusion in the film surrounding the particles) of the ion exchange process. This model constitutes a theoretical method to predict the rate-controlling step and reflects the effect of the ion exchange capacity, solution concentration, particle diameter, film thickness, film mass transfer coefficient, pore diffusivity (D_p), and separation constant parameter. The criteria are based on the following expression:

$$\frac{q_T D_p \delta}{C_T D^{\infty} R_0} \left(5 + 2\alpha_{A/B}\right) \tag{12}$$

When the obtained value of this factor is below 1, particle diffusion control exists. Otherwise, if the value is above 1, film diffusion control can be deduced. In this expression, Δ is the thickness of the film, which can be calculated as

$$\delta = \frac{2R_0}{Sh} \tag{13}$$

Sh being the Sherwood number.

$$Sh = \frac{K_f d_p}{D} \tag{14}$$

where $q_{T,}$ is the maximum capacity adsorption of the resin, and C_T, is the minimum equilibrium concentration in the solution with a saturated resin obtained in CFS isotherm. K_f is the mass transfer coefficient in cm/s and can be calculated from the mass transfer model. $K_f = K/a_p$, where a_p is the specific of the spherical particles, $a_p = 3/R_0$. D^∞ is the diffusivity coefficient in the film,[25] and $\alpha_{A/B}$ is the separation factor defined as the relationship between the distribution coefficients of the two ions. This can be calculated as $\alpha_{A/B}=\overline{C_A}C_B/C_A\overline{C_B}$, where C_i is the concentration of species i in the solution, and $\overline{C_i}$ is the concentration of species i in the resin. One way of calculating this parameter is to approximate it to the amount of SMX adsorbed (initial concentration in the resin minus equilibrium concentration) divided by the equilibrium concentration of SMX. The manufacturer's parameters for the resin[22] can be seen in Table 5 along with the previously calculated values.

The Sherwood number and the film thickness were obtained using the values in Tables 2, 3, 4, and 5. Once all the parameters are known, they can then be introduced in Eq. (12). The value of Helfferich's factor is higher than 1 in all cases. Therefore, the diffusion through the film around the spheres is the rate-controlling step, even though diffusion inside the solid particles was expected to be the rate-controlling step due to the high stirring speed (300 rpm).

Table 5 Manufacturer's parameters for the resin and data calculated by theoretical models.

R_0(cm)	ε_i	ρ(g/cm^3)	a_p (cm^{-1})	D^∞ (cm^2/s)[22]
0.024	0.34	1.06	128	$1.08\cdot10^{-5}$
Calculated data in equilibrium for synthetic solutions of SMX				
q_T (mg SMX/mL)	C_T (mg SMX/mL)	K_{eq}	Essays	$\alpha_{\frac{A}{B}}$[22]
217.7	0.337	6.34	$[SMX]_0 = 50$ mg/L	1.7
			$[SMX]_0 = 75$ mg/L	1.6
			$[SMX]_0 = 150$ mg/L	1.1
			$[SMX]_0 = 200$ mg/L	0.9
			$[SMX]_0 = 250$ mg/L	0.8

Fixed Bed Operation

Breakthrough Curves from the Load and Elution Stages. After studying the equilibrium and kinetics of the process, tests were conducted in a fixed bed column using synthetic solutions of SMX at concentrations of 200, 300, and 400 mg/L to obtain the corresponding breakthrough curves. To determine the suitable flow rate in load and elution steps, previous assays were carried out modifying the flow, finding that 11 mL/min was adequate to reach the saturation of the resin. Furthermore, this flow falls within the range of flow recommended in the specifications of the resin and is similar to that used by other authors such as Çalişkan and Göktürk [12] in assays in a fixed bed column to remove SMX using a similar amount of adsorbent in the column.

Operation in a fixed bed column was initially tested using a synthetic solution of 200 mg/L SMX. The breakthrough curve for the load step shows dispersive results, with no increase or pronounced jump in concentration being observed over time. Complete saturation of the column (with a resin volume of 1.3 mL) was achieved in 300 minutes (around 2286 bed volumes). The retention of the resin packed in the column was calculated by numerical integration of the area under the breakthrough curves of the load stage. The operative capacity found in the bed was 206 mg SMX/mL wet resin.

Resin life is one of the key parameters for determining the kind of resin to be applied in industrial production. After adsorption, the resin was regenerated with NaOH 0.5 M at a flow rate of 11 mL/min. The elution curve presents a high elution peak in the first minutes of the elution step, reaching a concentration of 1900 mg/L and then diminishing quickly to achieve complete elution in 180 minutes (1500 bed volume). The good capacity of the MP500 resin to concentrate the solute has thus been proved, which is very interesting for reducing the sulfonamides present in wastewater from drug manufacturers. In order to evaluate the effectiveness of the elution, a mass balance to SMX was carried out, integrating the area under the elution curve. The SMX ion mass eluted was thus determined and compared with the loaded ions, obtained from the load curve. One hundred per cent of the SMX retained was recovered in 180 minutes.

After this first stage of loading and elution steps, four more cycles were carried to study the behavior of the resin after several cycles, using concentrations of 300 mg SMX/L in the third and fourth cycles and 400 mg SMX/L in the second and fifth cycles.

As in the first stage, the breakthrough curves of the load steps showed a dispersive shape, with no increase or pronounced jump in concentration over time, detecting SMX at the outlet of the column from the first minutes and reaching the initial sample concentration in 180 minutes. The retention capacity of the resin was 246.4 mg SMX/mL wet resin and 260 mg SMX/mL wet resin in each one of the two cycles using an initial concentration of 400 mg/L; and 209 and 200 mg SMX/mL wet resin in the other two cycles using an initial concentration of 300 mg/L. The resin was then regenerated with a solution of NaOH 0.5M at a flow rate of 11 mL/min in down-flow mode in the second and third cycles and up-flow mode in the fourth and fifth cycles, obtaining a negligible concentration of SMX at the outlet of the column in 180 minutes and recovering 100% of SMX in all cycles. Hence, the direction of flow does not affect the amount of SMX recovered. Contrary to the typical behavior of organic compounds that are only partially eluted, total elution was obtained in the present study.

The breakthrough curves for the load and elution steps of all cycles are presented in Figs. 4 and 5, respectively. The retention capacity of the resin in the successive stages of loading can be seen in Table 6. After five cycles of load and elution, the results show that

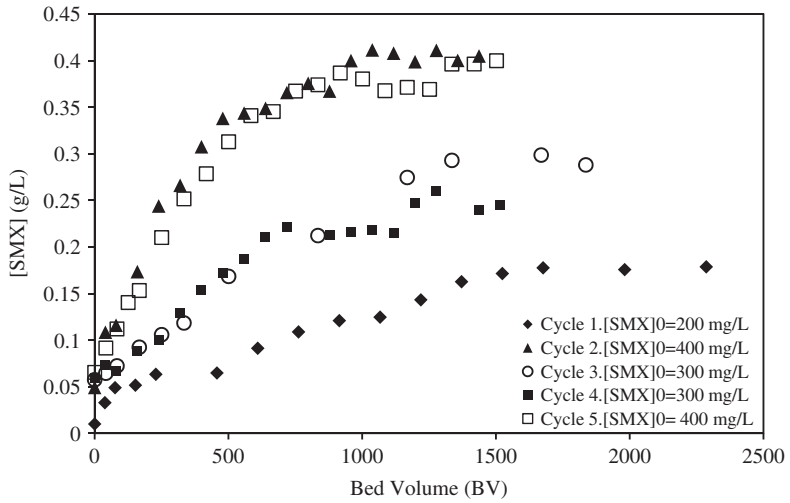

Figure 4 Breakthrough curves for the sorption of SMX from synthetic solutions prepared in distilled water, onto Lewatit MP500 resin. (Conditions: flow rate: 11 mL/min, volume resin: 1.3 mL, Z = 3 cm).

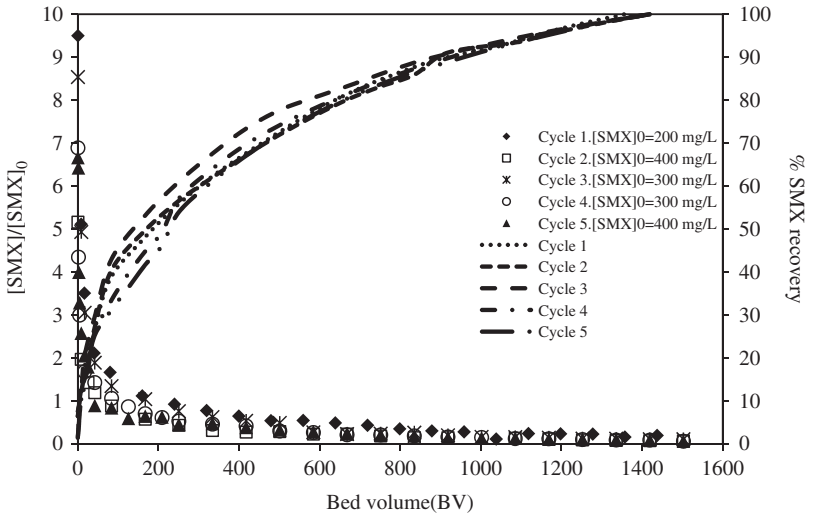

Figure 5 Breakthrough curves for the elution step of SMX from synthetic solutions prepared in distilled water, onto the resin Lewatit MP500. (Conditions: flow rate: 11 mL/min, volume resin: 1.3 mL, Z = 3 cm). In main axis is represented the evolution of SMX concentration and in secondary axis is represented the evolution of the recovery ratio of SMX as a function of stripping solution.

the resin is a very effective adsorbent for the removal of SMX. The retention capacity of the resin does not decrease with successive cycles, recovering 100% SMX in all cases, and concentrating the SMX after elution: nearly 9 times after elution in the first cycles, and 7 times in the last two cycles, as can be seen in Fig. 5, thus permitting easier treatment of this compound.

Table 6 Total capacity from load breakthrough curves, volume resin = 1.3 mL, flow rate = 11 mL/min.

Cycles	$[SMX]_0$	Capacity (mg SMX/ mL resin)
1	200 mg/L	206
2	400 mg/L	246.4
3	300 mg/L	209
4	300 mg/L	200.4
5	400 mg/L	260.5

Fixed Bed Model

The analysis of the fixed bed experiments in the cases of the load and elution curves was carried out considering a model developed by Costa[26] and used by Fernandez et al.[28] This model was used to simulate the load and elution breakthrough curves in a laboratory column. The model takes into account equilibrium and kinetic aspects, axial dispersion in the column, and no film transfer resistance.

The basic equations of the proposed model in this case are:

- General balance of the solute in the bed:

$$D_{ax}\frac{\partial^2 C_i(z,t)}{\partial z^2} - u_i\frac{\partial C_i(z,t)}{\partial z} = \frac{\partial C_i(z,t)}{\partial t} + \frac{(1-\varepsilon_l)}{\varepsilon_l}\left(\frac{\partial \bar{q}_i(z,t)}{\partial t} + \frac{\partial \bar{C}_{pi}(z,t)}{\partial t}\right) \quad (15)$$

$$\text{where } \bar{q}_i(z,t) = \frac{\int_0^R R^2 q_i(z,r,t)\,dR}{\int_0^R R^2 dR} \quad (16)$$

D_{ax} is axial dispersion parameter (cm^2/s), C_i is the solution concentration of species i (g/L), ε_l is the bed porosity, $\bar{q}_i$ is the average particle concentration of species i (g/L wet resin), t is the time (min), and z is the spatial coordinate (cm).

- Mass balance of the solute inside the particles:

$$\frac{\partial q_i(z,R,t)}{\partial t} + \varepsilon_i\frac{\partial C_{pi}(z,R,t)}{\partial R} = \frac{1}{R^2}\frac{\partial}{\partial R}\left[R^2\varepsilon_i D_p\frac{\partial C_{pi}(z,R,t)}{\partial R}\right] \quad (17)$$

where ε_i is the wet resin porosity; q_i is the particle concentration of species i (g/L wet resin); D_p is the pore diffusivity (cm^2/s), and R is the radial coordinate (cm).

- Initial and boundary conditions in the load step
  - Initial conditions:

$$\text{at } t = 0, C_i(z,t) \text{ and } C_{pi}(z,t) \text{ depend on washing } (z > 0) \quad (18)$$

$C_{pi}(z,t) = 0$, because there are no ions inside the pores or in the column, the SMX not retained in the active sites of the resin was removed in the washing step.

where C_i is the solution concentration of species i (g/L) and C_{pi} is the pore solution concentration of species i in batch runs or the feed solution concentration of species i in column runs (g/L).

- Boundary conditions:
- inside the particle:

$$\left.\frac{\partial C_{pi}(z,R,t)}{\partial R}\right|_{R=0} = \left.\frac{\partial q_i(z,R,t)}{\partial R}\right|_{R=0} = 0 \tag{19}$$

$$\text{in R} = \text{R}_0 \quad \frac{\partial q_i(z,,R,t)}{\partial t} + \varepsilon_i \frac{\partial C_{pi}(z,R,t)}{\partial t} = \frac{3}{R_0} k_l \left[C_i(z,t) - \bar{C}_{pi}(z,R,t)\right] \tag{20}$$

where R_0 is the particle radius (cm)

- in the column:

$$z = 0; C_i = C_{iT}; Z = L; \frac{\partial C_i(z,t)}{\partial z} = 0 \tag{21}$$

where L is the length of the column (cm)

In the elution step, the equations of the balance of solute inside the particles and in the column are the same, the main difference being the initial and boundary conditions that may be employed in the elution step.

- Boundary conditions in the elution step:
- In the solution,

$$Z = 0; C_i = C_{iT} \tag{22}$$

$$Z = L; \quad \frac{\partial C_i(z,t)}{\partial z} = 0 \tag{23}$$

- Inside the particles,

$$\text{R} = 0 \quad \left.\frac{\partial C_{pi}(z,R,t)}{\partial R}\right|_{R=0} = \left.\frac{\partial q_i(z,R,t)}{\partial R}\right|_{R=0} = 0 \tag{24}$$

$$\text{R} = \text{R}_0 \quad \frac{\partial q_i(z,R,t)}{\partial t} + \varepsilon_i \frac{\partial C_{pi}(z,R,t)}{\partial t} = \frac{3}{R_0} k_l \left[C_i(z,t) - \bar{C}_{pi}(z,R,t)\right] \tag{25}$$

- Initial conditions in the elution step:

$$\text{t} = 0; \text{C}_\text{i}(\text{z},\text{t}) \text{ depend on washing } (\text{z} = 0) \tag{26}$$

$$\text{t} = 0; \text{C}_\text{pi}(\text{z},\text{t}) \text{ depend on washing } (\text{z} > 0) \tag{27}$$

To solve the fixed bed model, parameters such as bed porosity, particle porosity, equilibrium constants, diffusivities in pores, and the capacity of the resin must be known. Equilibrium data and diffusivity values were determined for the system in previous batch experiments. Bed porosity was calculated in previous studies[28] and particle porosity is a parameter of the resin specifications. The axial dispersion parameter was not available for the laboratory column, so it was considered the parameter model fit.

A FORTRAN subroutine, PDECOL,[24] was used to solve the differential equation system proposed for the fixed bed model; this subroutine uses the method of orthogonal

collocation on finite elements to solve the system of non-linear differential equations. PDECOL can only solve one spatial and the temporal independent variables. In the fixed bed model, there are two spatial independent variables: the radial coordinate in the particle and the axial coordinate in the bed.

A simplification proposed by Morbidelli[29, 30, 31] may be used which considers a constant profile concentration inside the particles. With this simplification, the particles mass transfer coefficient can be calculated using a correlation proposed by Glueckauf.[32] When the film mass transfer coefficient in the model is given by $k_l = \varepsilon_i k_i$, the Glueckauf correlation is then $k_i = 5D_p/R_0$. With this simplification, it is not necessary to solve the radial particle coordinate, as the particle concentration is considered an average and hence the resulting system has only one spatial and one temporal independent variable. Equation (21) shows the simplification inside the particle for a linear driving force with the mass transfer coefficient. Hence, the film mass transfer coefficient is substituted by the expression of the Glueckauf correlation.

$$\frac{\partial \bar{q}_i\,(z,R,t)}{\partial t} + \frac{\varepsilon_i \bar{C}_{pi}\,(z,R,t)}{\partial t} = \frac{3}{R_0} k_l \left(C_i\,(z,t) - \bar{C}_{pi}\,(z,t)\right) \tag{28}$$

where $\bar{q}_i$ is the average particle concentration of species i (g/L wet resin), ε_i is the resin porosity, $\bar{C}_{pi}$ is the pore solution concentration of species i (g/L), k_l is the mass transfer coefficient (cm/s), and R_0 is the particle radius (cm).

The theoretical model including all these simplifications would thus be:

- Conservation of the mass of the solute in the solution:

$$\frac{1}{Pe}\frac{\partial^2 x_i\,(z^*,\theta_{st})}{\partial z^{*2}} - \frac{\partial x_i\,(z^*,\theta_{st})}{\partial z^*} = \frac{\partial x_i\,(z^*,\theta_{st})}{\partial \theta_{st}} + \frac{15\varepsilon_i\,(1-\varepsilon_l)\,N_D}{\varepsilon_l}\left[x_i\left(z^*,\theta_{st}\right) - x_{pi(z^*,\theta_{st})}\right] \tag{29}$$

- Conservation of the mass of the solute inside the particles:

$$\frac{\partial x_{pi}\,(z^*,\theta_{st})}{\partial \theta_{st}} = \frac{15\varepsilon_i N_{Di}}{\varepsilon_i + \frac{K_i q_{Ti}/C_{Ti}}{(1+(K_i-1)x_{Pi}(z^*,\theta_{st}))^2}}\left[x_i\left(z^*,\theta_{st}\right) + x_{pi(z^*,\theta_{st})}\right]$$

obtained by the relationship:

$$\frac{\partial q_i}{\partial t} = \frac{\partial q_i}{\partial C_i}\frac{\partial C_i}{\partial t} \tag{30}$$

In which $\partial q_i/\partial C_i$ was obtained by differentiating the equilibrium isotherm.

- Boundary conditions in the solution

$$z^* = 0 \quad x_i\,(z^*,\theta_{st}) = x_{Ti} \tag{31}$$

$$z^* = L \quad \frac{\partial x_i(z^*,\theta_{st})}{\partial z^*} = 0 \tag{32}$$

- Initial conditions:

$$\theta_{st} = 0 \quad \partial x_i\,(z^*, \theta_{st}) = x_{Ti} \text{ en } \quad z^* = 0 \tag{33}$$

$$\theta_{st} = 0 \quad x_i\,(z^*, \theta_{st}) \quad \text{depends on washing} \quad \forall z^* > 0 \tag{34}$$

The spatial coordinate in the column is normalized by L, the length of the column, and time by the stoichiometric time, t_{st}, which is the time for the resin to become completely saturated. N_D is the number of intraparticle mass transfer units ($N_D = \tau D_p/R_0$), with $\tau = L/u_i$, special time. *Pe* is the Peclet number, $Pe = u_i L/D_{AX}$.

The values of the differnt parameters used in this study are shown in Table 7. The axial dispersion calculated as a fitting parameter was between 2-9 cm^2/s in the load steps in down-flow mode and between 50-67 cm^2/s in the elution steps in up-flow mode. Some differences were found in the values of axial dispersion, D_{ax}, in the load step due to the experimental conditions, which presented certain difficulties in maintaining the flow rate constant at 11 mL/min. The experimental and theoretical load and elution breakthrough curves are shown in Figs. 6 and 7, respectively. A good correlation can be seen between

Table 7 Fixed bed operating parameters.

Flow rate (ml/min)	11
Bed Porosity (ε_l)	0.5
Particle Porosity (ε_i)	0.34
Equilibrium Constant SMX ($K_{eq\text{-}CSF}$)	6.34
Equilibrium Constant OH^-	0.16
Diffusivity in pores (cm^2/s)	$1.0{\cdot}10^{-7}$–$4.0{\cdot}10^{-7}$
Bed Height (cm)	3
Retention Capacity of SMX (g SMX/L wet resin)	206–260

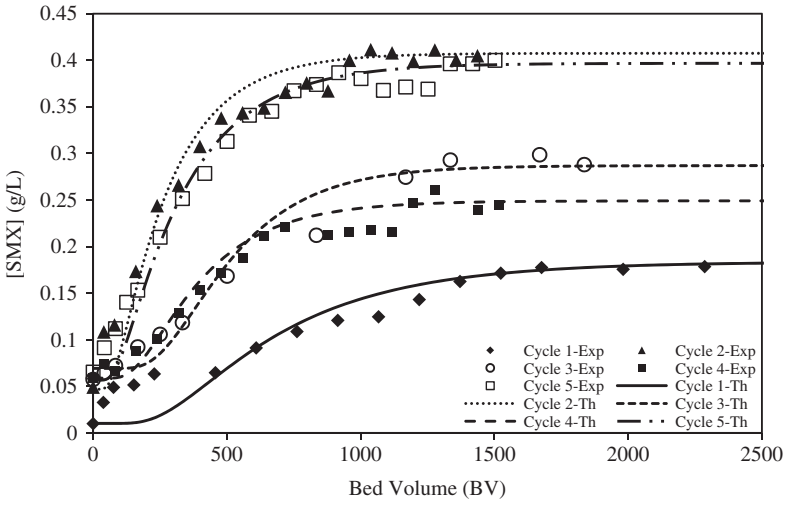

Figure 6 Experimental and theoretical load breakthrough curves for SMX from synthetic solutions, onto resin Lewatit MP500 in a fixed bed column. Conditions: initial concentrations: cycle1= 200 mg/L; cycle 2= 400 mg/L; cycle 3= 300 mg/L; cycle 4= 300 mg/L; cycle 5 = 400 mg/L; flow rate = 11 mL/min, volume resin: 1.3 mL, Z = 3 cm).

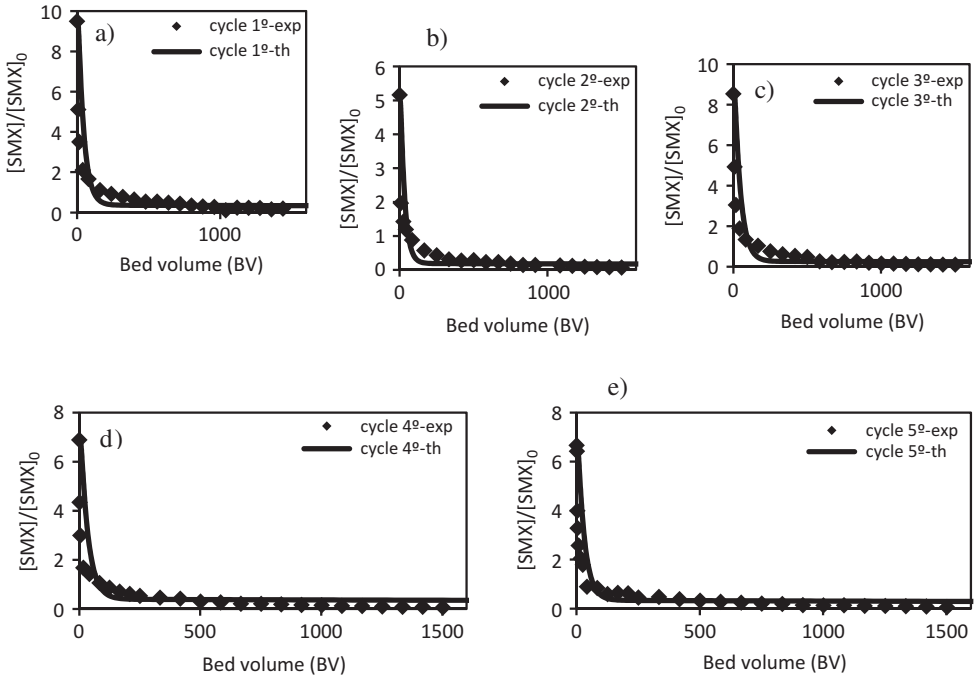

Figure 7 Experimental and theoretical elution curves for SMX from synthetic solutions, using NaOH 0.5 M as eluant in a fixed bed column. Conditions: (a) $[SMX]_0 = 200$ mg/L; b) $[SMX]_0 = 400$ mg/L; c) $[SMX]_0 = 300$ mg/L; d) $[SMX]_0 = 300$ mg/L; e) $[SMX]_0 = 400$ mg/L; flow rate = 11 ml/min, volume resin: 1.3 mL, Z = 3 cm).

experimental results and the numerical solution of the fixed bed model for the load and elution stages, thus demonstrating the validity of the model.

CONCLUSIONS

The removal of SMX from aqueous synthetic solutions using a strong anionic resin (Lewatit MP500) was carried out successfully. Batch experiments were conducted using synthetic solutions of 50-250 mg/L SMX with an L/S ratio = 1500 ((volume of liquid (mL)/ mass of resin (g)) determined in previous assays as suitable to calculate the retention capacity of the resins. The results show that this resin has a high SMX removal capacity. To study the adsorption equilibrium, experimental data were fitted to Langmuir and Constant Separation Factor isotherms, obtaining the equilibrium constants and the maximum adsorption capacity.

In order to determine the rate-controlling step of the process, the mass transfer coefficient and the intraparticle diffusivity were obtained from experimental data. The film mass transfer model was used to calculate the mass transfer constant, obtaining values between $3.1 \cdot 10^{-6}$ and $4.1 \cdot 10^{-6}$ cm/s. The pore diffusion model was also tested to fit the kinetic data, obtaining diffusivity values between $2.5 \cdot 10^{-10}$ and $3.1 \cdot 10^{-10}$ cm^2/s. The Helfferich method to predict the rate-controlling step showed that the adsorption of SMX onto Lewatit MP500 resin is controlled by mass transfer through the liquid film.

Successive cycles of loading and elution in a column setup were performed with synthetic solutions of SMX, using Lewatit MP500 resin and a solution of NaOH 0.5 M as eluent. The retention capacities of the resin and the ability of the eluent were evaluated. The shape of the breakthrough curves obtained is appropriate to verify the viability of the ion exchange operation to remove SMX present in effluents from the STPs of pharmaceutical manufacturers. Furthermore, NaOH was found to be a good eluent as it provides a good elution peak, completely eluting SMX in all cycles and concentrating SMX nearly 9 times after elution in the first cycles and 7 times in the last two cycles, thus permitting easier final treatment of this compound. Fixed bed operation was simulated using a proposed model that takes into account axial dispersion, equilibrium and kinetic parameters for the system under study. The numerical solution of the model shows good agreement between experimental data and the predicted values for the load and elution curves.

It is of interest to consider the presence of other ionic species that compete for the active groups of the resin in order to see the effect on SMX retention in the presence of other ions in the ion exchange resin when working with actual wastewaters. Previous assays have shown a slight reduction in the capacity of the resin to retain SMX in the presence of chloride, sulfate, and nitrate.

In conclusion, taking into account the equilibrium, kinetics, and fixed bed results reported in this article, it can be concluded that Lewatit MP500 resin is effective for removing SMX present in effluents from STPs.

REFERENCES

1. Díaz-Cruz, M. S.; López de Alda, M.J.; Barceló, D. Environmental behavior and analysis of veterinary and human drugs in soils, sediments and sludge. Trends Anal. Chem. **2003**, *22*(6), 340–352.
2. Ternes, T. A.; Meisenheimer, M., McDowell, D.; Sacher, F.; Brauch, H. J.; Haist-Gulde, B.; Preus, G.; Wilme, U.; Zulei, Seibert, N. Removal of pharmaceuticals during drinking water treatment. Environ. Sci. Technol. **2002**, *36*, 3855–3863.
3. Westerhoff, P.; Yoon, Y.; Snuder, S.; Wert, E. Fate of endocrine-disruptor, pharmaceutical, and personal care product chemicals during simulated drinking water treatment processes. Environ. Sci. Technol. **2005**, *39*, 6649–6663.
4. Choi, K-J.; Son, H-J.; Jim, S-H. Ionic treatment for removal of sulfonamide and tetracycline classes of antibiotic. Science Total Environ. **2007**, *387*, 247–256.
5. Adams, C.; ASCE, M.; Wang, Y.; Loftin, K.; Meyer, M. Removal of antibiotics from surface and distilled water in conventional water treatment processes. J. Environ Eng. **2002**, *128*, 253–260.
6. Le-Minh, N., Khan, S. J., Drewes, J. E., Stuetz, R. M. Fate of antibiotics during municipal water recycling treatment processes. Water Research **2010**, *44*, 4295–4323.
7. Carballa, M.; Omil, F.; Lema, J.M.; Llompart, M.; García, C.; Rodriguez, I.; Gómez, M.; Ternes, T. Behaviour of pharmaceuticals and personal care products in a sewage treatment plant of northwest Spain. Water Sci.Technol. **2005**, *52*(8), 29–35.
8. Gros, M.; Petrovic, M.; Ginebrada, A.; Barceló, D. Removal of pharmaceuticals during wastewater treatment and environment risk assessment using hazard indexes. Environ. International **2010**, *36*, 15–26.
9. Xuan Bui, T.; Choi, H. Adsorptive removal of selected pharmaceutical by mesoporous silica SBA-15. J. Hazardous Materials **2009**, *168*, 602–608.
10. Drillia, P.; Dokianakis, S. N.; Fountoulakis, M. S.; Kornaros, M.; Stamatelatou, K.; Lyberatos, G. On the occasional biodegradation of pharmaceuticals in the activated sludge process: The sample of the antibiotic sulfamethoxazole. J. Hazard. Materials **2005**, *122*, 259–265.

11. Vieno, N. M.; Harkki, H.; Tuhkanen, T.; Kronberg, L. Occurrence of pharmaceuticals plant. Environ. Sci. Technol. **2007**, *41*, 5077–5084.
12. Çalişkan, E.; Göktürk, S. Adsorption characteristics of sulfamethoxazole and metronidazole on activated carbon. Separ. Sci. Technol. **2010**, *45*, 244–255.
13. Bajpai, A. K.; Rajpoot, M. Adsorption behavior of sulfamethoxazole onto an alumina-solution interface. Bull. Chem. Soc. Jpn. **1996**, *69*, 521–527.
14. Xu, Z.; Zhang, Q.; Fang, H. Applications of porous resin sorbents in industrial wastewater treatment and resource recovery. Critical Rev. Environ. Sci. Technol. **2003**, *33*(4), 363–389.
15. Belter, P.A. *Ion Exchange Recovery of Antibiotics: Principles of Biotechnology*; Pergamon Press: New York; Vol. 2, pp 473–480.
16. Belter, P. A.; Cunningham, F.L.; Chen, J. W. Development of a recovery process for novobiocin. Biotechnol. Bioeng. **1973**, *15*, 533–549.
17. Vergili, I.; Barlas, H. Removal of selected pharmaceutical compounds from water by an organic polymer resin. J Sci. Indus. Res. **2009**, *68*, 417–425.
18. Ardelean, R. Davidescu, C.M. and Popa, A. Adsorption of p-nitrophenol from water on polymeric adsorbents. Chem Bull. "Politehnica" Univ. Timisoara. **2010**, *55*(69), 132–135.
19. Grimmett, M. E. Removal of sulfamethazine by hypercrosslinked adsorbents in aquatic systems. J Environ. Qual. **2013**, *42*, 2–9.
20. Boyd, G. E.; Adamson, A. W.; Myers, L. S. The exchange adsorption from aqueous solutions by organic zeolites. II. Kinetics. J. Am. Chem. Soc. **1947**, *69*, 2836–2848.
21. Boyd, G. E.; Schubert, J.; Adamson, A. W. The exchange adsorption of ions from aqueous solutions by organic zeolites. I. Ion-exchange equilibria. J. Am. Chem. Soc. **1947**, *69*(11), 2818–2829.
22. Helfferich, F. *Ion Exchange*; McGraw-Hill: New York; 1962.
23. Rodrigues, A. E.; Tondeur, D. *Percolation Processes: Theory and Applications*; NATO ASI Series; 1981, pp 31–81.
24. Madsen, N. K.; Sincovec, R. F. Algorithm 540: PDECOL, General Collocation Software for Partial Differential Equations [D3]. ACM Transactions on Mathematical Software (TOMS). **1979**, *3*, 326–351.
25. Seader, J.D.; Henley, E.J. *Separation Process Principles*, 2nd ed.; 2006.
26. Costa, C.; Rodrigues, A.E. Design of cyclic fixed-bed adsorption processes. Part I: Phenol adsorption on polymeric adsorbents. AICheE J. **1985**, *31*(10), 1654–1654.
27. Fernández, A.; Rendueles, M.; Rodrigues; Díaz, M. Co-ion behavior at high concentration cationic ion exchange. Ind. Eng. Chem. Res. **1994**, *33*, 2789–2794.
28. Torre, M.; Bachiller, D.; Fernández, P.; Rendueles, M.; Diaz, M. Cyanide recovery from gold extraction process waste effluents by ion exchange ii. modelling of the fixed bed operation. Solvent Extr. Ion Exch. **2006**. *24*(1), 81–97.
29. Santacesaria, E.; Morbidelli, M.; Danise, P.; Mercenari, M.; Carra, S. Separation of xylenes in Y-zeolites. 1. Determination of the adsorption equilibrium parameters, selectivities and mass transfer coefficients through finite baths experiments. Ind. Eng. Chem. Process Des. Dev. **1982**, *21*, 440–445.
30. Santacesaria, E.; Morbidelli, M.; Danise, P.; Mercenari, M.; Carra, S. Separation of xylenes on Y-zeolites. 2. Breakthrough curves and their interpretation. Ind. Eng. Chem. Process Des. Dev. **1982**, *21*, 446–451.
31. Carra, S.; Santacesaria, E.; Morbidelli, M.; Storti, G.; Gelosa, D. Separation of xylenes on Y-zeolites. 3. Pulse curves and their interpretation. Ind. Chem. Eng. Process Des. Der. **1982**, *21*, 451–457.
32. Glueckauf, E. Theory of chromatography. Part 10.—Formulæ for diffusion into spheres and their application to chromatography. *Trans. Faraday Soc*. **1955**, *51*, 1540–1551.

4.2. RETENCIÓN DE SULFAMETAZINA EN DISOLUCIÓN ACUOSA MEDIANTE INTERCAMBIO IÓNICO EMPLEANDO UNA RESINA ANIÓNICA FUERTE EN COLUMNA DE LECHO FIJO

En este subapartado se recogen los resultados obtenidos de la eliminación de sulfametazina mediante intercambio iónico con una resina aniónica comercial.

Como ya se ha comentado anteriormente, es evidente la presencia de antibióticos en las aguas subterráneas y superficiales procedentes en una gran parte de las actividades ganaderas. En este trabajo se plantea el intercambio iónico como una alternativa para eliminar este tipo de contaminantes de las aguas de forma eficaz, sencilla y económica. En el artículo que se presenta a continuación se ha estudiado la eliminación de sulfametazina en disoluciones acuosas empleando una resina aniónica, Lewatit MP500. Se ha estudiado el equilibrio y la cinética del proceso de intercambio iónico en tanque agitado, y se han determinado los parámetros de equilibrio y cinética. A su vez, se ha estudiado la operación en columna llevando a cabo sucesivos ciclos de carga y elución, y se han modelizado los resultados obtenidos.

Artículo: Sulfamethazine retention from water solutions by ion exchange with a strong anionic resin in fixed bed.

Situación: artículo aceptado en *Separation Science and Technology* (Taylor & Francis). Manuscript ID LSST-2013-7165

SULFAMETHAZINE RETENTION FROM WATER SOLUTIONS BY ION EXCHANGE WITH A STRONG ANIONIC RESIN IN FIXED BED

Ana María López Fernández, Manuel Rendueles* and Mario Díaz

Department of Chemical Engineering and Environment Technology, University of Oviedo, Oviedo, Spain

ABSTRACT

Veterinary antibiotics such as sulfonamides were detected in the environment from animal excreta that end up in manure which is applied as a fertilizer and can contaminate soil, and consequently surface and groundwater through run off or leaching. The contaminated surface waters can enter in the drinking water treatment plants (DWTPs) which are not designed to remove highly polar micropollutants like antibiotics. Removal of pharmaceuticals by adsorption and ion exchange constitutes a promising technique for its low cost, easy regeneration and selective removal of pollutants. This work studies the removal of sulfamethazine (SMZ), a common antibiotic used for therapeutic purposes. The SMZ retention capacity of an anionic ion exchange resin, Lewatit MP500 (Lanxess Chemical), was determined. Equilibrium and kinetics were studied and equilibrium constants and diffusivity values were obtained using different models. Load and elution breakthrough curves were plotted to evaluate ion exchange operation in a fixed bed column. In the elution step, 100% SMZ was recovered in all cycles and could be concentrated up to twelve times, thus facilitating its final treatment or removal. Load and elution breakthrough curves were simulated using a fixed bed model in which axial dispersion was considered the parameter model fit. The good correlation between experimental results and the numerical solution of the fixed bed model demonstrated the validity of the model.

Keywords: Ion exchange, sulfamethazine, fixed bed operation

INTRODUCTION

The presence of pharmaceuticals, namely antibiotics, in the ecosystem has been known for almost 30 years. In recent years, however, the use of antibiotics in veterinary and human medicine has become widespread (annual consumption of 100000-200000 tons) (1) thereby increasing the possibility of water contamination with such compounds. Table 1 provides some data on the consumption of antibiotics in human and veterinary medicine in 2011 in different European Union countries and U.S. Human and veterinary antibiotics have been detected in different matrices. The introduction of these compounds into the environment via anthropogenic sources can constitute a potential risk for aquatic and terrestrial organisms. Although only present at vestigial levels, antibiotics may cause resistance in bacterial populations and lead to these pharmaceuticals becoming ineffective in the treatment of several diseases in the near future. These contaminants are continually discharged into the natural environment by a diversity of input sources. Among these, animal excreta constitute the major source of environmental contamination by drugs, with most of the drugs used in veterinary medicine ending up in manure. When spread on fields as a fertilizer, manure can contaminate surface and groundwater through run off or leaching. Ultimately, contaminated surface waters can reach drinking water treatment plants (DWTPs) (2), which are also unprepared to remove these compounds, and pass into water distribution systems. Another important source of contamination is the direct release of veterinary antibiotics through their application in aquaculture. Improper disposal of unused/expired drugs, waste effluents from the manufacturing

process or accidental spills during manufacturing or distribution can also be considered significant sources of contamination.

Table 1. Consumption of antibiotics in human and veterinary medicine

	Human*	Veterinary **
France	29.5	912.8 ton
Italy	28	1826.3 ton
Spain	19.5	1671.9 ton
Germany	15	1780.7 ton
U.S.***	3628 ton	13542 ton

*Values expressed in Defined Daily Doses (DDD) per 1000 inhabitants and per days. Data source: ESAC-Net (European Surveillance of Antimicrobial Consumption Network)

**Data source: European Medicines Agency. ***Data source: U.S. FDA (Food and Drug Administration)

Antibiotics are normally detected in the higher µg/L range in hospital effluents, the lower µg/L range in municipal wastewater, and the ng/L range in surface, sea and groundwater(3). The presence of these residues has also been reported in vegetables and cereals such as carrots, lettuces, green onions, cabbages, cucumbers and corn (4-7). To date, although legal limits have been established for antibiotics in food (4-1500 µg/kg for milk and 25-6000 µg/kg for other foodstuffs of animal origin (European Union, 1990), there is no legislation regarding environmental matrices.

Conventional wastewater treatment plants (WWTPs) were designed without consideration of antibiotics removal in wastewater. Many previous studies have shown that while some antibiotics may be eliminated in WWTPs, some may be hard to be removed in this process, and can therefore reach the aquatic environment (2). A solution that is both practical and economical is required to reduce the daily amounts of antibiotics discharged into the environment. A wide range of chemical and physical methods for the removal of organic compounds can be employed; chemical oxidation, biodegradation, adsorption, liquid extraction and membranes techniques. The choice of method will depend on the pollutant concentration in the effluent and the cost of the process. An overview of the research papers published in international journals between 2000 and 2010 in this area can be found in Homen and Santos (8).

Biological processes, filtration and coagulation-flocculation-sedimentation are the most widely used techniques in conventional wastewater treatment plants (9-12) However, the low efficiencies of these methodologies with respect to a number of emergent contaminants in addition to the fact that they sometimes cannot be implemented led to the development of new alternatives some years ago. Oxidation processes such as chlorination have been used to disinfect drinking water treatment plants containing pharmaceuticals before the application of a biological treatment (13). Advanced oxidation processes comprise oxidative methods that may be applied to fluctuating compositions (14,15). However, these processes are limited by mass transfer issues, are extremely pH-dependent, require a greater amount of oxidant to treat the same pollutant load, very costly equipment and a high energy supply. Although Fenton and photo-Fenton processes are both applicable to matrices with low COD concentrations, waters with high concentrations of ions such as seawater cannot be treated by these (16,17). Membrane processes such as reverse osmosis, nano- and ultrafiltration can effectively reduce high levels of dissolved salts, but present limitations in the removal of organic compounds (9,18), and are sensitive process to temperature and organic material in water matrices.

Removal of antibiotics by adsorption constitutes one of the most promising techniques used to remove organic contaminants. This technique has the advantage of removing analytes instead of producing potentially more dangerous metabolites (19,20). The most commonly used adsorbents are granular activated carbons, although they have the drawbacks of being very

costly and difficult to regenerate (normally requiring incineration) (21). Therefore, there is growing interest in finding alternative low-cost adsorbents. Polymeric resins are becoming more widely used in wastewater treatment due to their low cost, easy regeneration and selective removal of pollutants. Adams (9) and Choi (22) studied the use of a polymeric resin for the removal of sulfonamides and tetracyclines, obtaining high removal efficiencies (90% for sulfonamides and >80% for tetracyclines).

One of the main antibiotics used in the swine industry is sulfamethazine, a commonly used sulfonamide drug (23). Sulfamethazine (SMZ) is used for therapeutic purposes, to treat infections, and as a growth promoter (24-26). Studies conducted in 1988 by the National Center for Toxicological Research indicated that sulfamethazine is carcinogenic and that thyroid tumors developed in rats and mice after receiving 2.4-4.8 mg/L of sulfamethazine in their diet over 2 years. Therefore, the interest for removing this compound from contaminated water.

The chemical structure of sulfamethazine (SMZ) and its dissociated form is presented in Figure 1. SMZ present two pKa; $pK_{a,1}$= 2.65 and $pK_{a,2}$= 7.65 (25). SMZ at pH of aqueous solutions (pH= 6.5 approximately) is presented slightly in anionic form.

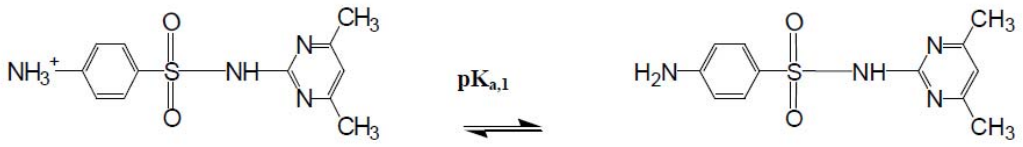

Cationic form

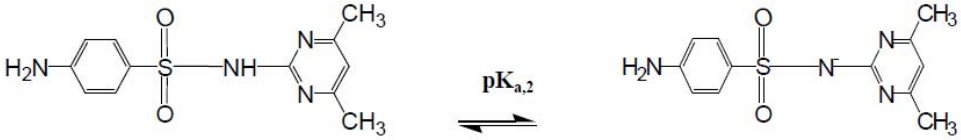

Anionic form

Figure 1. Chemical structure of sulfamethazine and its anionic and cationic forms (28)

The reactions that take placed during the loading step using an anionic resin, which initially presents Cl^- groups, and after conditioning with NaOH is charged with OH^- is given next:

$$R - OH^- + SMZ^- \leftrightarrow R - SMZ^- + OH^-$$

The aim of the present study was to investigate the feasibility of ion exchange treatment of effluents from drug manufacturers containing SMZ. Lewatit MP500, a macroporous strong anionic resin was tested to determine its capacity to retain SMZ from synthetic solutions. Equilibrium and kinetics were studied in order to characterize the operation. The adsorption equilibrium constants were determined using Langmuir and Constant Separation Factor isotherms. The kinetics of the process was analyzed using two models: a film mass transfer model and the pore diffusion model. Finally, several load and elution cycles were performed in a fixed bed column to evaluate the behavior of the resin in an industrial operation. The breakthrough curves of the load and elution steps were fitted using a fixed-bed adsorption model.

MATERIALS AND METHODS

Materials

Sulfamethazine (purity ≥99% w/w) was purchased from Sigma-Aldrich. The chemical properties of sulfamethazine are: molecular formule: $C_{12}H_{14}N_4O_2S$; melting point: 197ºC; molecular weight: 278.33 g/mol; dissociation constants: pKa_1= 2.65 (aromatic amine) and pKa_2= 7.65 (sulfonate nitrogen) (25); octanol/water partition coefficient: log K_{ow}= 0.14; solubility in water: $1.5 \cdot 10^3$ mg/L (29ºC) and $1.92 \cdot 10^3$ mg/L (37ºC), solubility increases with increasing pH; from Hazardous Substances Data Bank (HSBD).

Methanol (HPLC grade) was used for liquid chromatography and ultra pure water was prepared in a Milli-Q purification system. All other chemicals were obtained from Sigma-Aldrich. The filters used for filtration were obtained from Millipore (0.45 µm PVDF for samples) and Whatman (0.22 µm PTFE for the mobile phase). Stock solutions were prepared by dissolving the pharmaceutical in distilled water. Experiments were carried out at pH values of pharmaceuticals in aqueous solutions: pH= 6.5 approximately.

A commercial organic polymeric resin (Lewatit MP500) manufactured by Lanxess was used as the adsorbent. The strong base resin Lewatit MP500 has a quaternary amine (macroporous type I) and a crosslinked polystyrene matrix. The main properties of the resin are shown in Table 2.

Table 2. Characteristics of Lewatit MP500

General description	
Ion form	Cl^-
Functional group	Quaternary amine (type I)
Matrix	Crosslinked polystyrene
Polymer structure	Macroporous
Bead size >90% (mm)	0.47(±0.06)
Density (g/mL)	1.06
Total capacity (min. eq /L)	1.1

Analytical methods

Determination of sulfamethazine in the samples was performed using HPLC (Agilent 1200) and a column (mediterranea sea18, 5µm x 25 cm x 46 cm, plus a reverse-phase column from Waters) combined with UV detection. Prior to HPLC analysis, the samples were treated using 0.45 µm PVDF filters to ensure that the samples would be free of other compounds that might interfere in the analysis. The mobile phase consisted of methanol (eluent A) and water (eluent B). The method was isocratic (60% of eluent A and 40% of eluent B). Analysis was performed at a flow rate of 0.7 mL/min. The wavelength used for detection was 270 nm and the retention time was 5.2 min.

Experimental Method

Batch Experiments. Runs were carried out at room temperature in cylindrical stirred tanks operating at an agitation rate of 300 rpm. Initially, the ionic form of wet resin was Cl^-, therefore, the conditioning of the resin was carried out by contacting it with a solution of NaOH 1 M with an L/S ratio (volume of liquid (mL)/ mass of resin (g)) = 20, 2 times, 20 minutes each time, for exchange Cl^- groups for OH^-. The resin was then washed with distilled water twice for 5 minutes each time with an L/S ratio = 50 and subsequently separated from the solution.

The resin was then contacted with the loading solution. The L/S ratio was adjusted by maintaining the volume of solution (300 mL) and varying the amount of wet resin. Contact time was 100 minutes in all tests, this time being considered sufficient to reach operating

equilibrium. The volume of the samples extracted from the tank each time was 2 mL, which did not substantially change the volume of the solution. The concentration of SMZ ions in the resin was determined by mass balance, calculating the difference between the initial and final quantity of charged ions in the solution.

Column Experiments. Continuous flow adsorption experiments were carried out in a glass column with an internal diameter of 1.1 cm and a total tube length of 25 cm. Columns were prepared by packing each one with 1.3 grams of wet resin. Solutions were pumped through the column by means of a peristaltic pump (Masterflex) in down-flow mode.

Conditioning of the resin in the fixed bed was carried out with a solution of NaOH 1 M. This solution was pumped through the column for 20 minutes at a flow rate of 11 mL/min. Distilled water was then fed through the column at a flow rate of 11 mL/min, for 15 minutes to wash the resin.

Three load stages were carried out using synthetic solutions of 200, 300 and 400 mg/L SMZ at a down-flow rate of 5.6-7.5 ml/min. The effluent samples were collected (4 mL approximately) at specific times intervals (5-10 minutes) and analyzed by HPLC to monitor the evolution of SMZ concentration with time. The breakthrough curve was plotted until the SMZ concentration at the column effluent outlet reached the initial concentration of the feed solution. After adsorption, distilled water was fed through the column to remove any unabsorbed SMZ ions on the adsorbent surface or entrapped between adsorbent particles.

After each loading, the elution step was carried out by pumping a solution of NaOH 0.5 M through the column at a down-flow-rate of between 5-7.2 mL/min. The effluent samples were collected at the column outlet every 5-10 minutes to monitor the evolution of the concentration with time. The elution curve was plotted until the concentration of SMZ at the column outlet was less than 1 mg/L.

RESULTS AND DISCUSSION

Batch equilibrium study

In order to evaluate the behavior of the MP500 resin under different L/S ratios (600, 800, 1000, 1200, 1500 and 1800 mL solution/g wet resin)), several runs were carried out to obtain the most appropriate ratio. Different amounts of wet resin were loaded with 300 mL of the SMZ synthetic solution at a concentration of 100 mg/L, plotting the SMZ concentration over time to monitor the process until reaching equilibrium. A mass balance was used to determine the equilibrium compositions of the resin and the solution phase with respect to chloride. Results show that, with an L/S ratio = 1000, it was possible to reach the equilibrium concentration (28.1 mg SMZ/L) and total operational capacity (80.7 mg SMZ/mL resin). This L/S ratio was accordingly chosen as the value for all the following tests.

Several runs were carried out to obtain the capacities of the resin. The MP500 resin was contacted with different SMZ solution concentrations (30, 50, 100, 150, 200 and 250 mg/L SMZ) with an L/S ratio (volume of liquid (mL)/mass of wet resin (g)) = 1000, determined in previous assays as the most suitable for calculating the resin's retention capacity. Results show that equilibrium is reached in all cases in approximately 100 minutes. Table 3 shows the equilibrium concentration and the adsorption capacities obtained at different initial concentrations. Increasing initial SMZ concentration in the solution causes increasing in the SMZ adsorption capacity of the resin to remain constant when the maximum adsorption capacity is reached.

Table 3. Equilibrium concentrations (C_e) and adsorption capacities (q_e exp) obtained in batch experiments at different SMZ initial concentrations (C_0). Conditions: mass wet resin: 0.5g, volume solution: 500 ml, stirring rate: 300 rpm. Calculated values using the Langmuir and CSF isotherms.

C_0 (mg SMZ/L)	C_e (mg /L)	q_e(exp) (mg /g)	q_e(cal. Langmuir) (mg /g)	q_e(cal. CSF) (mg /g)
30	6.2	25.2	23.1	22.4
50	11.8	40.1	37.0	36.1
100	39.8	59.6	69.4	68.8
150	70.2	82.7	82.6	82.4
200	105.3	96.9	90.1	90.1
250	157.1	93.9	95.7	96.1
		RMSE	**χ^2(mg/g)**	**$\mathcal{E}$ (%)**
	Langmuir	5.12	2.4	6.9
	CSF	5.14	2.6	7.7

RMSE= root mean square error; χ2= Chi square analysis, Ɛ= average percentage error

Two different models, Langmuir and Constant Separation Factor isotherms, were used to define the relationship between the load capacity and the solution concentration. The equation of the Langmuir isotherm is:

$$q_e = \frac{K_L \cdot C_e}{1 + a_L \cdot C_e} \quad (1)$$

where K_L indicates the solute adsorptivity, a_L is related to the energy of adsorption and C_e is the residue SMZ ions concentration remain after adsorption (mg/L). A linear transform method (LTFM) was used to find the Langmuir constant. The Langmuir constant K_L (L/g) and a_L (L/mg) can be determined from a linearized form of Langmuir equation Eq. (1) represented by Eq. (2)

$$\frac{C_e}{q_e} = \frac{a_L}{K_L} C_e + \frac{1}{K_L} \quad (2)$$

The monolayer saturation capacity Q_0 for the Langmuir isotherm (mg/g resin) was calculated as k_L/aL. The liner correlation coefficient for the Langmuir isotherm was 0.995. For the Constant Separation Factor isotherm, the equation is:

$$q_i = \frac{K_{eq} \cdot q_t \cdot C_i}{C_T + (K_{eq} - 1) \cdot C_i} \quad (3)$$

where C_t is the minimum SMZ equilibrium concentration in the solution with a saturated resin (mg/L). Keq is the equilibrium constant and qt is the maximum capacity adsorption of the resin (mg/g resin). The equilibrium constants and the maximum absorption capacity were subsequently obtained using Statgraphics program. The correlation coefficient was 0.981. The different isotherm parameters obtained are given in Table 4. The experimental data and the predicted values for the Langmuir and CFS isotherms are shown in Table 3. A comparison of the experimental results to the predicted values using the Langmuir and CSF isotherms is shown in Figure 2. To quantify the agreement between the model predictions and experimental data were used the root-mean-square error (RMSE):

$$RMSE: \sqrt{\frac{\sum_{i=1}^{n}(q_i^{exp} - q_i^{model})^2}{n}} \quad (4)$$

Where *n* is the number of data points: i=1…n. The develop equilibrium equations also were evaluated using Chi-square analysis (29) and non linear regression analysis. Eq. (5) shows how to calculate χ^2. The advantage of the Chi-square analysis is that all equilibrium equations can be compared at the same abscissa and ordinate. Is the data predicted by the model were similar to experimental data; χ^2 (mg/g) would be small and viceversa.

$$\chi^2 = \sum_{i=1}^{N} \frac{\left(q_{eq,exp} - q_{eq,cal}\right)^2}{q_{eq,cal}} \quad (5)$$

$q_{eq,cal}$ is the equilibrium capacity obtained from a model mg/g; $q_{eq,exp}$ the equilibrium capacity obtained from experiments (mg/g) and N number measurements.

Eq. (6) shows the average percentage error (Ɛ) used in the non-linear regression analysis (30). The error between the experimental data and the predicted data were calculated using Eq. (6).

$$\varepsilon(\%) = \frac{\sum_{i=1}^{N}\left|\left(q_{eq,exp} - q_{eq,cal}\right)/q_{eq,exp}\right|}{N} x\ 100 \quad (6)$$

Table 3 presents the values of the RMSE, χ^2 and $\mathcal{E}(\%)$ for both isotherms. Both isotherms showed a good fit between experimental results and predicted values, and the values of RMSE were similar for both isotherms. Comparing the values of the correlation coefficient, χ^2 and Ɛ (%) the Langmuir isotherms was better to predict and correlate the experimental data.

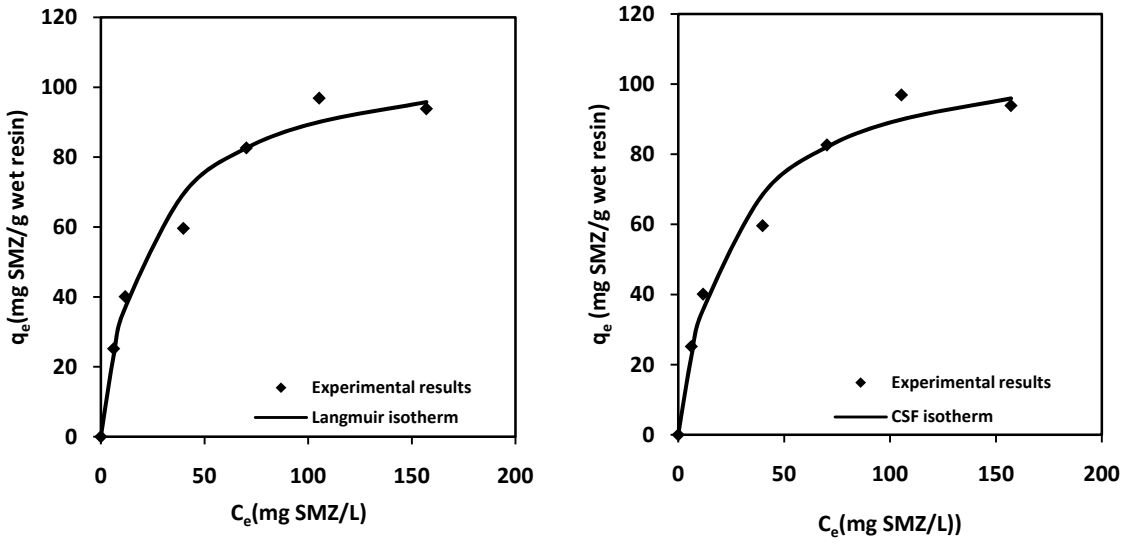

Figure 2. Equilibrium adsorption data and fitting curves of adsorption of SMZ from synthetic solution onto Lewatit MP500 resin; by two isotherms models Langmuir and Constant Separation

Table 4. Isotherm parameters obtained in batch

Langmuir Sorption isotherm constants		CSF isotherm constants	
K_L(L/g)	4.74	K_{eq}	45.84
a_L (L/mg)	0.043	C_T (mg /mL)	1.1
Q_0 (mg SMZ/g wet resin)	110	q_t (mg SMZ/g wet resin)	109
R^2	0.995	R^2	0.981

Batch kinetics study

Kinetics experiments were carried out in batch assays with an L/S ratio = 1000 (mL solution/g wet resin) monitoring the SMZ concentration over time from the initial time to equilibrium with all solutions. After 100 minutes, the solution concentration of SMZ does not change substantially, so operational equilibrium can be assumed. The experiments were conducted in stirred tank using synthetic solutions with initial concentrations of 50, 100, 150, 200 and 250 mg/L SMZ.

The process was modeled assuming sorption process, seeing as the rate-controlling step of ion exchange is usually the diffusion on the counter ions rather than the chemical reaction at the fixed ionic groups. This means that the ion exchange process is essentially a diffusion phenomenon (27).

The concentration profiles of SMZ can be modeled using two diffusion models: the film mass transfer model and the pore diffusion kinetics model to determine the mass transfer mechanisms (31,32).

Film Mass Transfer Model. In this model, the retention of SMZ is assumed to be limited by the external surface of the particle (27). The model can be described by the following equations:

$$\frac{dq_i}{dt} = K_f a_p (C_i - C^*) \tag{7}$$

where q_i is the concentration of specie i in the resin at time t; K_f is the mass transfer coefficient in the fluid phase (cm/s); $C^*$is the equilibrium SMZ concentration in the solution; and a_p is the specific surface area, i.e. the total surface area per unit of volume. $K_f a_p$ can be considered as K, the mass transfer apparent constant.

$$V_L C_i + V_r q_i = V_L C_0 \tag{8}$$

where V_L is the volume of liquid; V_r is the volume of wet resin; and C_o is the initial SMZ concentration in solution. By integrating Eq. 7 and introducing Eq. 8, the following equation is obtained:

$$q_i(t) = C_0 (V_L/V_r)\left(1 - \frac{C^*}{C_0}\right)\left(1 - \exp\left(\frac{-K\,t}{V_L/V_r}\right)\right) \tag{9}$$

The mass transfer constant, K, can be determined by regression using the experimental data, fitting these to Eq. 7. The anion exchange beads are of constant size with a spherical geometry; therefore, K_f = K/ a_p. Comparison of the experimental results for the SMZ concentration and the theoretical values obtained with Eqs. (8) and (9) will then give the goodness of fit of the obtained value for all the experiments. A comparison of experimental and theoretical results for the kinetics of synthetic solutions of SMZ can be seen in Figure 3. The values obtained for the mass transfer constant are given in Table 5, with the respective

correlation coefficient (R^2). To quantify the agreement between the model predicted and experimental observations the RMSE (root mean square error) were used, defined as:

$$RMSE: \sqrt{\frac{\sum_{j=1}^{n}(C_i^{exp} - C_i^{model})^2}{n}} \quad (10)$$

where C_i^{exp} (mg/L) is the experimental equilibrium concentration and C_i^{model} (mg/L) is the equilibrium concentration obtained by calculated from the model. The correlation coefficients obtained were >0.9 in all experiments and the RMSE calculated with Eq. 10 were minimal, <0.027, so the film mass transfer model predicts well the SMZ kinetics adsorption onto resin.

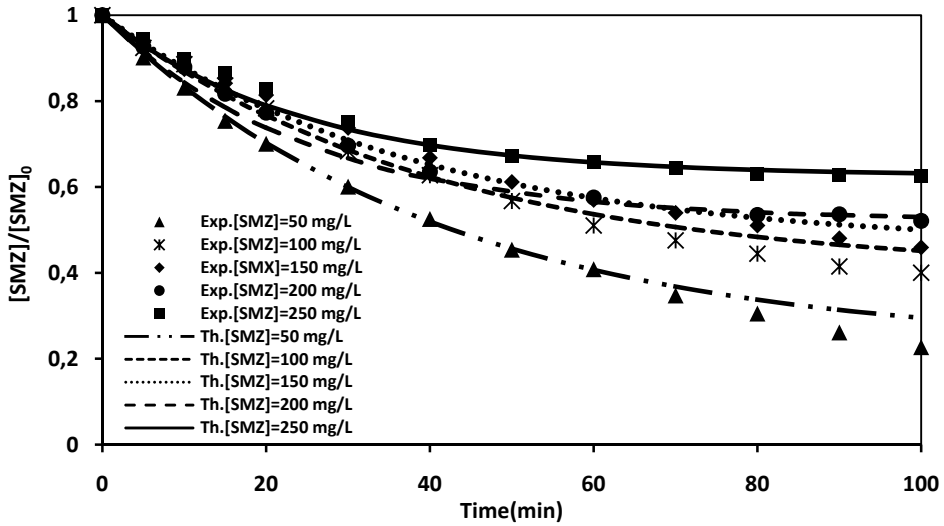

Figure 3. Fitting of kinetic data using the film mass transfer model for the adsorption of SMZ synthetic solution with different concentrations (50-250 mg SMX/L) onto Lewatit MP500 resin.

Table 5. Mass Transfer Constant calculated by film mass transfer model; using synthetic solutions of SMZ

Experiments	K (min^{-1})	K_f (cm/s)	R^2	RMSE*
Synthetic solution, $C_{0\ SMZ}$= 50 mg/L	0.0243	3.2E-06	0.999	0.026
Synthetic solution, $C_{0\ SMZ}$= 100 mg/L	0.0247	3.2E-06	0.994	0.027
Synthetic solution, $C_{0\ SMZ}$= 150 mg/L	0.025	3.3E-06	0.989	0.020
Synthetic solution, $C_{0\ SMZ}$= 200 mg/L	0.0348	4.5E-06	0.973	0.021
Synthetic solution, $C_{0\ SMZ}$= 250 mg/L	0.0413	5.4E-06	0.993	0.018

*RMSE= root mean square error

Pore Diffusion Model. This model (33) considers the resin to be a porous matrix. The model is described by the following equations:

- Mass balance inside the particle:

$$\frac{\partial q_i(R,t)}{\partial t} = \frac{\partial q_{ei}(R,t)}{\partial t} + \varepsilon_i \frac{\partial C_{pi}(R,t)}{\partial t} = \frac{1}{R^2}\left[\frac{\partial}{\partial R} R^2 \varepsilon_i D_p \frac{\partial C_{pi}(R,t)}{\partial t}\right] \quad (11)$$

where q_{ei} is the pore concentration of specie i; C_{pi} is the pore solution concentration of specie i; ε_i is the resin porosity; and D_p is the pore diffusivity.

- Mass balance in the bulk solution:

$$\varepsilon_i V(C_{iT} - C_i(t) = (1 - \varepsilon_i) V \overline{q_{ei} + \varepsilon_i C_{pi}(t)} \quad (12)$$

where C_{iT} is the initial concentration of species i in solution; and V is the volume of solution.

- Average concentration in particle:

$$\overline{q_{ei} + \varepsilon_i C_{pi}}(t) = \frac{3}{R_0^3} \int_0^R R^2 \left(q_{ei} + \varepsilon_i C_{pi}\right)(R,t)dR \quad (13)$$

where R is the radial coordinate; and R_0 is the radius of particle.

The initial and boundary conditions needed to solve the systems are:

- Initial conditions:

$$C_{pi}(R, 0) = 0 \quad (14)$$

- Boundary conditions:

$$\text{In } R = 0 \rightarrow \left.\frac{\partial C_{pi}(R,t)}{\partial R}\right|_{R=0} = \left.\frac{\partial q_i(R,t)}{\partial R}\right|_{R=0} \quad (15)$$

$$\text{At the interphase, } (R = R_0) \rightarrow C_{pi}(R_0, t) = C_i(t) \quad (16)$$

A FORTRAN subroutine, PDECOL (34), was used to solve these equations. The subroutine uses the orthogonal finite element method to solve the system of non-linear differential equations. The diffusivity values obtained are given in Table 6 with the RMSE calculated with Eq. (10).

Table 6. Pore diffusivities calculated by the pore diffusion model using synthetic solutions of SMZ

Experiments	$D_p(cm^2/s)$	RMSE*
$[SMZ]_0$= 50 mg/L	$3.6 \cdot 10^{-10}$	0.021
$[SMZ]_0$= 100 mg/L	$2.5 \cdot 10^{-10}$	0.011
$[SMZ]_0$= 150 mg/L	$2.2 \cdot 10^{-10}$	0.019
$[SMZ]_0$= 200 mg/L	$2.8 \cdot 10^{-10}$	0.022
$[SMZ]_0$= 250 mg/L	$2.1 \cdot 10^{-10}$	0.009

*RMSE= root mean square error

Figure 4 shows the fit of the experimental results to this model with the diffusivity values in Table 6 for all the assays. The values of RMSE in all experiments were <0.022%, so the good agreement between experimental data and the theoretical prediction shows the goodness of fit of the model.

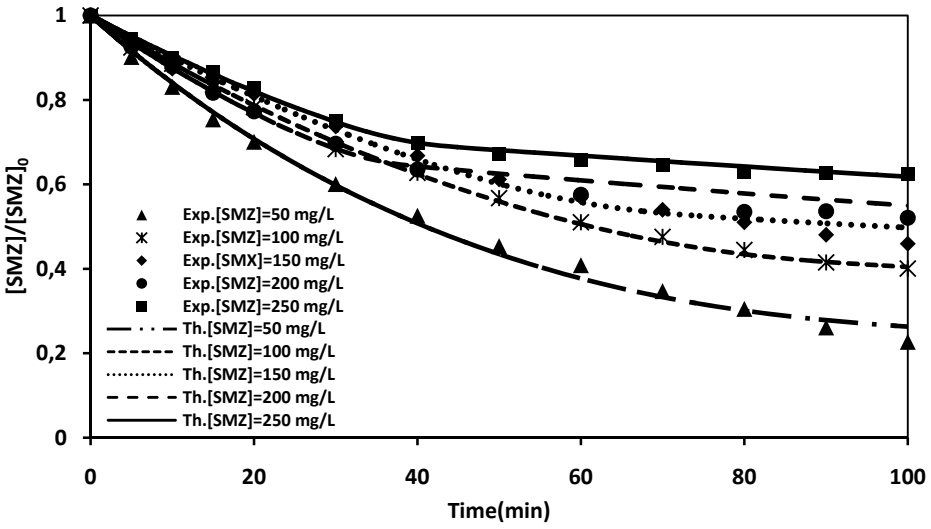

Figure 4. Fitting of kinetic data using the pore diffusion model for the adsorption of SMZ synthetic solution with different concentrations (50-250 mg SMX/L) onto Lewatit MP500 resin.

Rate-Controlling Step. A method proposed by Helfferich (27) was used to identify the rate-controlling step (diffusion inside the solid particles or diffusion in the film surrounding the particles) of the ion exchange process. This model constitutes a method for theoretically predicting the rate-controlling step which reflects the effect of the ion exchange capacity solution concentration, particle diameter, film thickness, film mass transfer coefficient, pore diffusivity (D_p), and separation constant parameter. The criteria are based on the following expression:

$$\frac{q_T D_p \delta}{C_T D^{\infty} R_0}\left(5 + 2\alpha_{A/B}\right) \tag{17}$$

When the obtained value of this factor is below 1, particle diffusion control exists. Otherwise, film diffusion control can be deduced if the value is above 1. In this expression, δ is the thickness of the film, which can be calculated as:

$$\delta = \frac{2R_0}{Sh} \tag{18}$$

Sh being the Sherwood number.

$$Sh = \frac{K_f d_p}{D_{pe}} \tag{19}$$

K_f being the mass transfer coefficient in cm/s, which can be calculated from the mass transfer model. $K_f = K/a_p$, where a_p is the specific surface area of the spherical particles, $a_p = 3/R_0$; d_p is the particle diameter, D_{pe} is the effective pore diffusivity calculated as Reid (35).

$$D_{pe} = \frac{\varepsilon_i D^{\infty}}{\tau} \tag{20}$$

where D^{∞} is the diffusivity coefficient in the film of SMZ in water, τ is the tortuosity of the adsorbent and ε_i its porosity. The molecular diffusivity of SMZ in water was estimated by the Wilke-Chang correlation (36), expressed in cm/s:

$$D^{\infty} = 7.4x10^{-8}\frac{(øM_B)^{1/2}\,T}{\mu_B V_A^{0.6}} \quad (21)$$

The molar volume for SMZ is V_A= 189.8 cm^3/mol. Wilke and Chang recommended that ø be chosen 2.6. If the solvent is water, the viscosity of water μ_B in the temperature of range of this work is 1.0 cp. $\alpha_{A/B}$ is the separation factor; defined as the relation of distribution coefficients of both ions that can be calculated as $\alpha_{A/B} = \overline{C_A}\,C_B\,/C_A\,\overline{C_B}$, where C_i is the concentration of specie i in the solution and $\overline{C_i}$ is the concentration of specie i in the resin. A way of calculate this parameter is approaching it to the amount of SMZ adsorbed (initial concentration in the resin minus equilibrium concentration) between equilibrium concentration of SMZ. The manufacturer's parameters of the resin (27) as well as the previously calculated values can be seen in Table 7.

Table 7. Manufacturer's parameters of the resin and calculated data from theoretical models for Helfferich method to determine the rate-controlling step

Resin parameters					
R_0(cm)	ε_i	ρ(g/cm^3)	τ	a_p(cm^{-1})	D^{∞}(cm^2/s)
0.024	0.34	1.06	5	128	$1.02\cdot10^{-5}$
Calculated data in equilibrium using synthetic solutions of SMZ					
q_T (mg SMX/mL resin)	C_T (mg SMX/mL)	K_{eq}		Essays, $[SMZ]_0$	$\alpha_{A/B}^{[27]}$
115	1.1	45.84		50mg/L	3.4
				100mg/L	1.5
				150mg/L	1.2
				200mg/L	1.9
				250mg/L	0.6

The Sherwood number and the film thickness were obtained using the values in Table 5,Table 6 andTable 7.

Table *7*. Once all parameters are known, they can then be introduced in Eq. (17). The value of Helfferich's factor is less than 1 (between 0.07 and 0.4) in all cases. Therefore, particle diffusion is the rate-controlling step, like it was expected due to the high agitation speed employed (300 rpm).

Fixed Bed Operation

Breakthrough Curves from Load and Elution Steps. After studying equilibrium and kinetics, tests were conducted in fixed fed columns using synthetic solutions of SMZ at concentrations of 200, 300 and 400 mg/L to obtain the breakthrough curves.

Initially, fixed bed column operation was tested using a synthetic solution of 200 mg/L SMZ and a flow rate of 7 mL/min. The breakthrough curve of the load step shows a certain dispersive curve, with no pronounced jump in SMZ concentration with time. As can be seen in Figure 5a, complete saturation of the column (with a resin volume of 1.3 mL) was achieved in 250 minutes (bed volume= 1400)

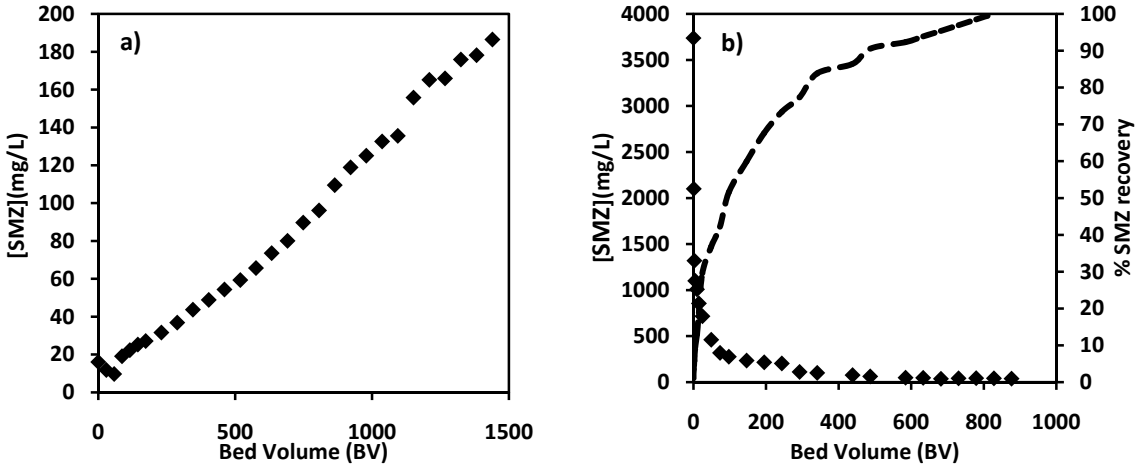

Figure 5. **a)** Breakthrough curve for the sorption of SMZ in 1st cycle onto Lewatit MP500 resin. Conditions: $[SMZ]_0$= 200 mg/L; flow rate= 7 mL/min, volume resin= 1.3 mL. **b)** Breakthrough curve of 1st elution cycle using NaOH 0.5M as eluant, flow rate= 6.0 mL/min

Retention of the resin packed in the column was calculated by numerical integration of the area under the breakthrough curves of the load step. The bed was found to have a total capacity of 136 mg SMZ/mL resin.

Resin life is one of the key parameters for determining the kind of resin to be used in industrial production. After adsorption, the resin was regenerated with NaOH 0.5 M. As can be observed in Figure 5b, the elution curve presents a high elution peak in the first minutes of the elution step, reaching a concentration of 3740 mg/L and rapidly diminishing to achieve complete elution in 180 minutes (Bed Volume= 877). The good capacity of the MP500 resin to concentrate the solute has thus been proved, which is very interesting from the point of view of reducing the sulfonamides present in wastewater from drug manufacturers.

In order to evaluate the effectiveness of the elution process, a mass balance to SMZ was carried out, integrating the area under the elution curve. The eluted SMZ ion mass was accordingly determined and compared with that of the loaded ions, obtained from the load curve. All the retained SMZ was recovered in 180 minutes.

After this first stage of column loading and elution, two cycles were carried out using concentrations of 300 and 400 mg/L SMZ to study the operation of the resin.

In the second cycle, the resin was loaded with a solution of 300 mg/L SMZ. As in the first stage, the results of the breakthrough curve were dispersive, there is no increase or pronounced jump in concentration over time, reaching a concentration of 215 mg/L in 250 minutes (Bed Volume= 1528) at a flow rate of 7.5 mL/min. The retention capacity of the resin was 197.1 mg/mL resin. The resin was then regenerated with a solution of NaOH 0.5 M at a down-flow rate of 7.2 ml/min, reaching a concentration of 4070 mg/L in the first minutes and decreasing to 58 mg/L SMZ at 180 minutes (Bed Volume= 1050) and negligible at 240 minutes (Bed Volume=1400), with 100% recovery of SMZ. The load and elution curves of this cycle are shown in Figure 6 a-b, respectively.

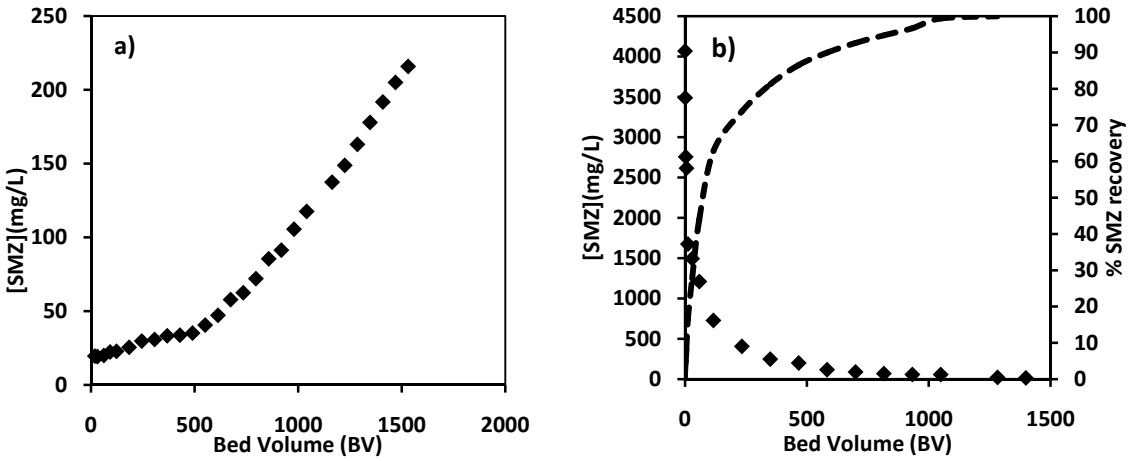

Figure 6. **a)** Breakthrough curve for the sorption of SMZ in 2nd cycle onto Lewatit MP500. Conditions: $[SMZ]_0$= 300 mg/L; flow rate= 7.5 mL/min, volume resin= 1.3 mL. **b)** Breakthrough curve of 2nd elution cycle using NaOH 0.5M as eluant, flow rate= 6.0 mL/min

In the third cycle, the resin was loaded with a solution of 400 mg/L SMZ at a flow rate of 5.6 ml/min. Unlike in the two previous cycles, the breakthrough curve obtained in this cycle showed a compact profile, although SMZ was detected at the column outlet from the first minutes on, though at a very low concentration. There was a jump in the concentration at 60 minutes (Bed Volume= 275), reaching a concentration of 360 mg/L in 330 minutes (Bed Volume= 1515). The retention capacity was 296 mg/mL resin. In the elution step operating at a down-flow rate of 5 ml/min, a concentration of 4800 mg/L was obtained in the first minutes, reaching a concentration of less than 70 mg/L at 180 minutes (Bed Volume= 720) and negligible at 300 minutes (Bed Volume=1225). Therefore, complete elution of the retained SMZ was achieved in 300 minutes. The load and elution curves of this third cycle can be seen in Figure 7 a-b, respectively.

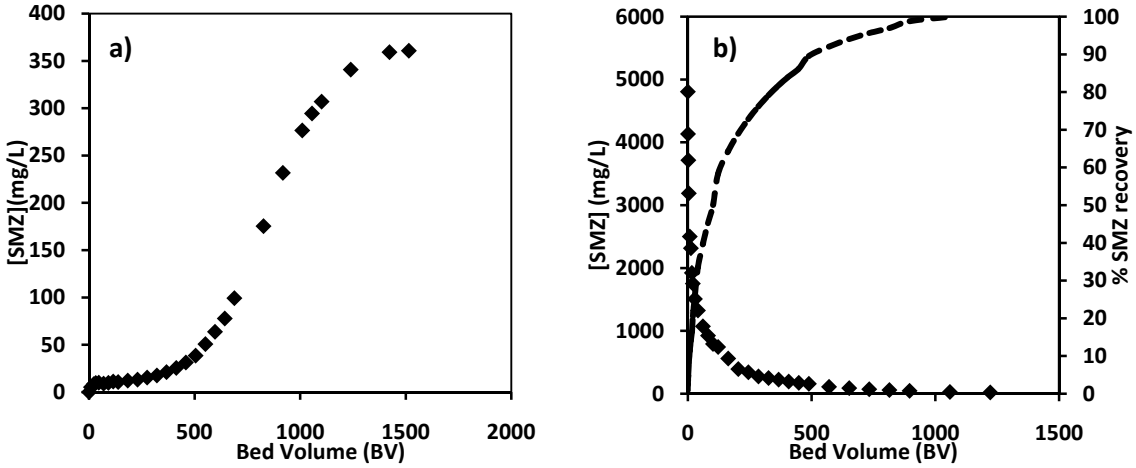

Figure 7. **a)** Breakthrough curve for the sorption of SMZ in 3th cycle onto Lewatit MP500. Conditions: $[SMZ]_0$= 400 mg/L; flow rate= 5.6 mL/min, volume resin= 1.3 mL. **b)** Breakthrough curve of 3th elution cycle using NaOH 0.5M as eluant, flow rate= 5.0 mL/min

Fixed Bed Model

In the case of the load and elution curves, analysis of the fixed bed experiments was carried out considering a model developed by Costa (37) and employed by Fernandez et al.

(38,39). This model was used to simulate the load and elution breakthrough curves in a laboratory column. The model takes into account aspects relating to equilibrium and kinetics, axial dispersion in the column and no film transfer resistance. The developed model can be seen in López et al. (40).

To solve the fixed bed model, parameters such as bed porosity, particle porosity, equilibrium constants, diffusivities in the pores and the capacity of the resin must be known. All these parameters were determined for the system in previous batch experiments. The equations of the proposed model in this case are:

- Conservation of the mass of solute in the solution:

$$\frac{1}{Pe}\frac{\partial^2 x_i(z^*,\theta_{st})}{\partial z^{*2}} - \frac{\partial x_i(z^*,\theta_{st})}{\partial z^*} = \frac{\partial x_i(z^*,\theta_{st})}{\partial \theta_{st}} + \frac{15\varepsilon_i(1-\varepsilon_l)N_D}{\varepsilon_l}\left[x_i(z^*,\theta_{st}) - x_{pi(z^*,\theta_{st})}\right] \quad (22)$$

- Conservation of the mass of solute inside the particles:

$$\frac{\partial x_{pi}(z^*,\theta_{st})}{\partial \theta_{st}} = \frac{\frac{15\varepsilon_i N_{Di}}{K_i\, {}^{q_{Ti}}/_{C_{Ti}}}}{\varepsilon_i + \frac{}{\left(1+(K_i-1)x_{Pi}(z^*,\theta_{st})\right)^2}}\left[x_i(z^*,\theta_{st}) + x_{pi(z^*,\theta_{st})}\right] \quad (23)$$

obtained by the relationship:

$$\frac{\partial q_i}{\partial t} = \frac{\partial q_i}{\partial C_i}\frac{\partial C_i}{\partial t} \quad (24)$$

In which $\partial q_i/\partial C_i$ was obtained by differentiating the equilibrium isotherm.

- Boundary conditions in the solution

$$z^* = 0 \qquad x_i(z^*,\theta_{st}) = x_{Ti} \quad (25)$$

$$z^* = L \qquad \frac{\partial x_i(z^*,\theta_{st})}{\partial z^*} = 0 \quad (26)$$

- Initial conditions:

$$\theta_{st}=0 \quad \partial x_i(z^*,\theta_{st}) = x_{Ti} \text{ en } z^*=0 \quad (27)$$

$$\theta_{st}=0 \quad x_i(z^*,\theta_{st}) \text{ depends on washing } \forall z^*>0 \quad (28)$$

The spatial coordinate inside the column is normalized by L, the length of the column, and time by the stoichiometric time, t_{st}, i.e. the time for the resin to become completely saturated. N_D is the number of intraparticle mass transfer units ($N_D = \tau D_p/R_0$), with $\tau = L/u_i$, special time. *Pe* is the Peclet number $Pe = u_i L/D_{AX}$. The axial dispersion parameter was not available for the laboratory column, so it was considered the sole parameter model fit. A FORTRAN subroutine, PDECOL (34), was used to solve the differential equation system proposed for the fixed bed model.

The values of the different parameters employed in this study are shown in Table 8. The axial dispersion calculated as a fitting parameter in the three load steps was around 0.6 cm^2/s; and 60 cm^2/s in all the elution steps. The experimental and theoretical load and elution breakthrough curves for the three cycles are shown in Figure 8 and Figure 9, respectively. A good fit can be appreciated between experiment results and the numerical solution of the fixed bed model for the load and elution steps, thus demonstrating the validity of the model.

Table 8. Fixed bed operational parameters of the studied system

Bed Porosity	0.5
Particle Porosity	0.34
Equilibrium Constant SMZ	45.8
Equilibrium Constant OH^-	0.02
Diffusivity in the pores (cm^2/s)	$9.0 \cdot 10^{-8}$-$1.8 \cdot 10^{-7}$
Bed Height (cm)	3
Retention Capacity of SMZ (g SMZ/L wet resin)	136-296

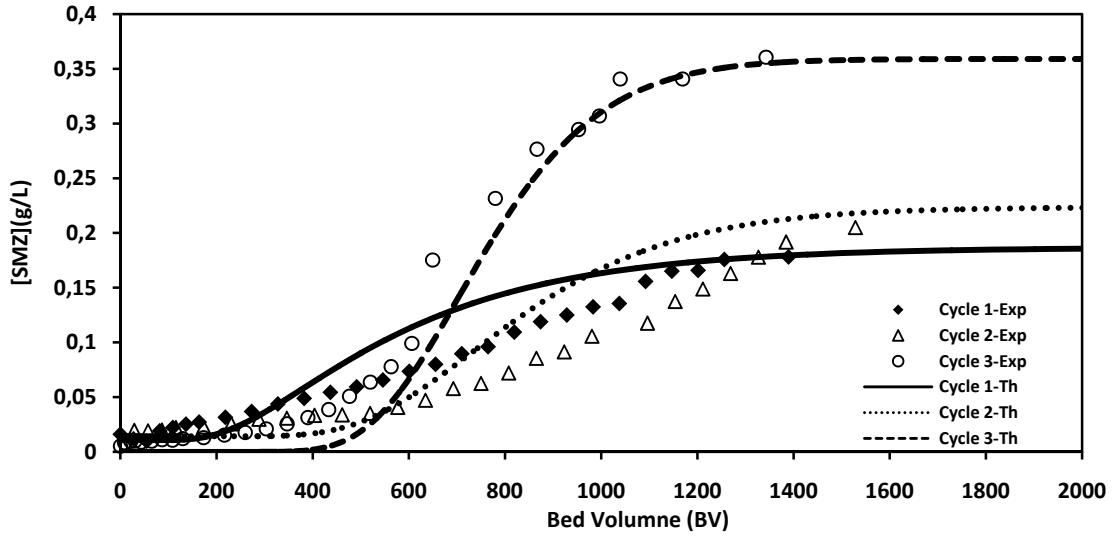

Figure 8. Experimental and theoretical load curves for the sorption of SMZ from synthetic solutions, in a fixed bed column. Conditions: cycle 1 $[SMZ]_0$= 200 mg/L, flow rate= 7 ml/min; cycle 2 $[SMZ]_0$= 300 mg/L, flow rate= 7.5 ml/min; cycle 3 $[SMZ]_0$= 400 mg/L, flow rate= 5.6 ml/min; volume resin= 1.3 mL.

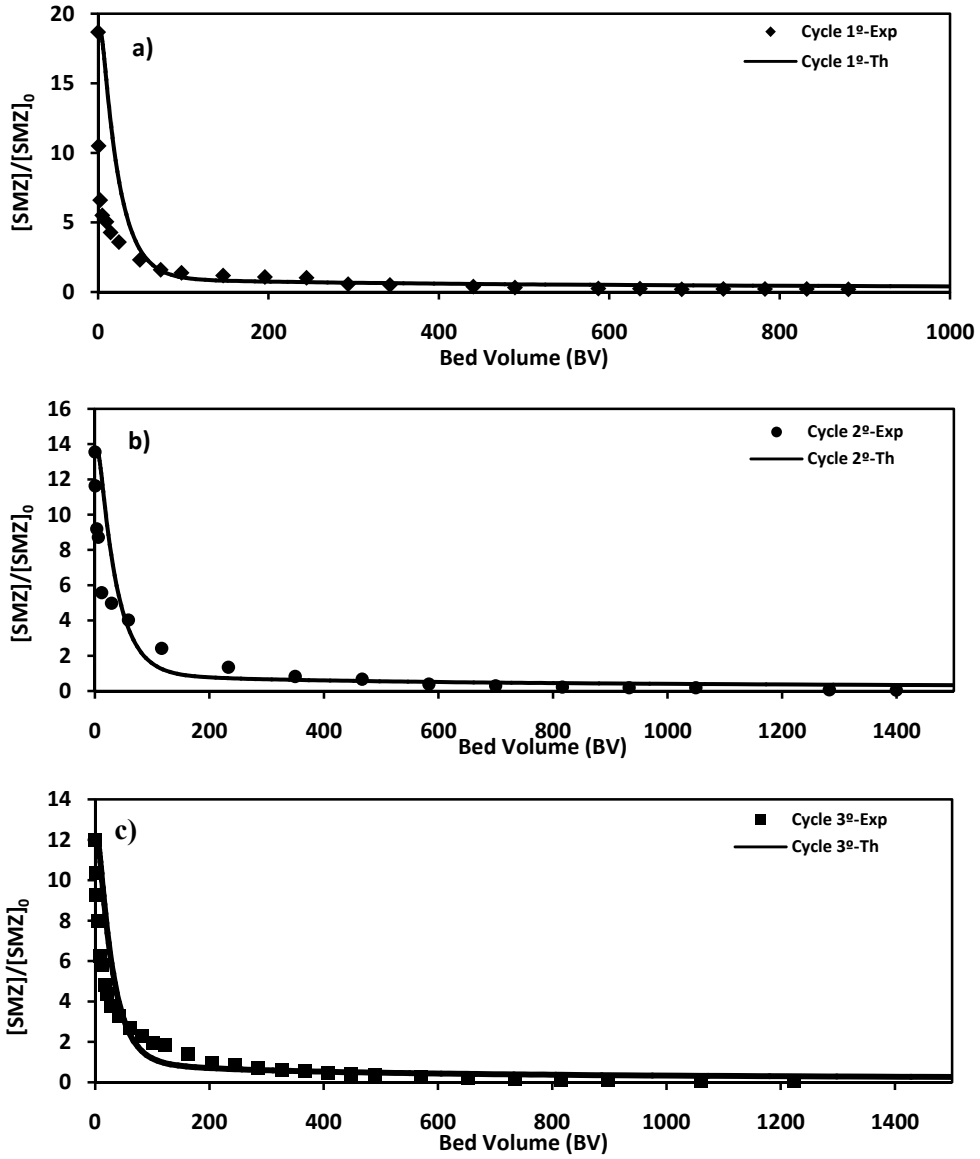

Figure 9. Experimental and theoretical elution curves for SMZ using NaOH 0.5 M in a fixed bed column. Conditions: **a)** $[SMZ]_0$= 200 mg/L, flow rate= 6 mL/min; **b)** $[SMZ]_0$= 300 mg/L, flow rate= 6 mL/min; **c)** $[SMZ]_0$= 400 mg/L; flow rate= 5 mL/min; volume resin=1.3 mL

CONCLUSIONS

The removal of SMZ from aqueous solutions using a strong anionic resin (Lewatit MP500) was satisfactorily carried out. Batch experiments were conducted using synthetic solutions of 30-250 mg/L SMZ with an L/S ratio = 1000 (volume of liquid/mass of wet resin (g)) determined in previous assays as the most suitable to calculate the retention capacity of the resin. The results show the high adsorption capacity of the resin for removing SMZ from synthetic solutions. To study the adsorption equilibrium, the experimental data were fitted to Langmuir and Constant Separation Factor isotherms, obtaining the equilibrium constants and the maximum adsorption capacity. The estimated Langmuir equilibrium constant were K_L=4.74, a_L= 0.043, and the maximum adsorption capacity Q_0= 110 mg/g wet resin.

Kinetic adsorption was studied using the film mass transfer model and the pore diffusion model, obtaining the mass transfer coefficient ($3.2 \cdot 10^{-6}$ - $5.4 \cdot 10^{-6}$ cm/s) and the diffusivity values ($2.1 \cdot 10^{-10}$ - $3.8 \cdot 10^{-10}$ cm^2/s). The Helfferich method to predict the rate

controlling step showed that the adsorption of SMZ onto the Lewatit MP500 resin is controlled by particle diffusion as was expected due to the high agitation speed employed.

Three load and elution cycles were performed in columns with synthetic solutions of 200, 300 and 400 mg/L, using 1.3 g of the Lewatit MP500 resin and a solution of NaOH 0.5M as eluent. The retention capacities of the resin were evaluated. The repeatability of the operation was tested following three sequential load-elution cycles with good results and stable operability. The SMZ was eluted completely using NaOH 0.5 M in all cycles. It was possible to concentrate more than twelve times the initial concentration of the SMZ in the effluent in all cycles, thus facilitating the treatment of this compound. Fixed bed operation was simulated using fixed bed model that takes into account axial dispersion, equilibrium and kinetic parameters for the system under study. The numerical solution of the model shows good fit between experimental data and predicted values for the load and elution curves, thus demonstrating the validity of the model. Taking into account the equilibrium, kinetic and fixed bed results reported in this paper, it may be concluded that the Lewatit MP500 resin is effective in removing SMZ present in effluents from Sewage Treatment Plants (STPs).

ACKNOWLEDGES

Financial support of Ana María López from FICYT “Severo Ochoa Programme” grant (Gobierno del Principado de Asturias) are gratefully acknowledged.

REFERENCES

1. Kümmerer K. Significance of antibiotics in the environment (2003). J. *Antimicrob Chemother, 52:* 5-7.
2. Xu, W.; Zhang, G.; Zou, S.C.; Li, X.D.; Liu, Y. C. (2007) Determination of selected antibiotics in the Victoria Harbour and the Pearl River, South China using high-performance liquid chromatography-electrospray ionization tamdem mass spectrometry. *Environ. Pollut.*, *145*: 672-679.
3. Kümmerer, K. (2009) Antibiotics in the aquatic environment- a review-Part I. *Chemosphere*, *75*: 417-434.
4. Kumar, K.; Gupta, S.C.; Baidoo, S.K.; Chander, Y.; Rosen, C.J. (2005) Antibiotic uptake by plants from soil fertilized with animal manure. *J. Environ. Qual.*, *34*: 2082-2085.
5. Boxall, A.B.A.; Johnson, P.; Smith, E.J.; Sinclair, C.J.; Stutt, E.; Levy, L.S. (2006) Uptake of veterinary medicines from soils into plants. *J. Agric. Food Chem.*, *54*: 2288-2297.
6. Grote, M.; Schwake-Anduschus, C.; Michel, R.; Stevens, H.; Heyser, W.; Langenkämper, G.; Betsche, T.; Freitag, M. (2007) Incorporation of veterinary antibiotics into crops from manured soil. *FAL Agric. Res.*, *57*: 25-32.
7. Dolliver, H. A.; Kumar, K.; Gupta, S.C. (2007) Sulfamethazine uptake by plants from manure-amended soil. *J. Environment. Qual.*, *36*: 1224-1230.
8. Homen, V. and Santos, L. (2011) Degradation and removal methods of antibiotics from aqueous matrices-A review. *Journal of Environment Management*, *92*: 2304-2347.
9. Adams, C.; ASCE, M.; Wang, Y.; Loftin, K.; Meyer, M. (2002) Removal of antibiotics from surface and distilled water in conventional water treatment processes. *J. Environ. Eng.*, *128*: 253-260.
10. Göbel, A.; McArdell, C.S.; Joss, A.; Siegrist, H.; Giger, W. (2007) Fate of sulfonamides, macrolides and trimethoprim in different wastewater treatment technologies. *Sci. Total Environ.*, *372*: 361-371.
11. Stackelberg, P.E.; Gibs, J.; Furlong, E.T.; Meyer, M.T.; Zaugg, S.D.; Lippincott, R.L. (2007) Efficiency of conventional drinking water treatment processes in removal of pharmaceuticals and other organic compounds. *Sci. Total Environ., 377*: 255-272.
12. Vieno, N.M.; Hrkki, H.; Tuhkanen, T.; Kronberg, L. (2007) Occurrence of pharmaceuticals in river water and their elimination in a pilot scale drinking water treatment plant. *Environ. Sci. Technol.*, *41*: 5077-5084.
13. Acero, J.L.; Benitez, F.J.; Real, F.J.; Roldan, G. (2007) Kinetics of aqueous chlorination of some pharmaceuticals and their elimination from water matrices. Water Res., *44*; 4158-4170.
14. Andreozzi, R.; Canterino, M.; Marotta, R.; Paxeus, N. (2005) Antibiotic removal from wastewaters: the ozonation of amoxicillin. *J. Hazard. Mater.*, *122*: 243-250.
15. Balcioğlu L.A.; Ötker, M. (2003) Treatment of pharmaceutical wastewater containing antibiotics by O_3/H_2O_2 processes. *Chemosphere*, *50*: 85-95.

16. Trovó, A.G; Nogueira, R.F.P.; Agüera, A.; Sirtori, C.; Fernández-Alba, A.R. (2009) Photodegradation of sulfamethoxazole in various aqueous media: persistence, toxicity and photoproducts assessment. *Chemosphere*, *77*: 1292-1298.
17. Pérez-Moya, M.; Graells, M.; Castells, G.; Amigó, J.; Ortega, E.; Buhigas, G.; Pérez, L.M.; Mansilla, H.D. (2010) Characterization of the degradation performance of the sulfamethazine antibiotic by Photo-Fenton process. *Water Res.*, *44*: 2533-2540.
18. Li, S.-Z.; X.-Y.; Wang, D.-Z. (2004) Membrane (RO-UF) filtration for antibiotic wastewater treatment and recovery of antibiotics. *Sep. Purif. Technol.*, *34*: 109-114.
19. Putra, E.K.; Pranowo, R.; Sunarso, J.; Indraswati, N.; Ismadji, S. (2009) Performance of activated carbon and bentonite for adsorption of amoxicillin from wastewater: mechanism, isotherms and kinetics. *Water Res.*, *43*: 2419-2430.
20. Rivera-Utrilla, J.; Prados-Joya, G.; Sánchez Polo, M.; Ferro Garcia, M.A.; Bautista-Toledo, I. (2009) Removal of nitroimidazole antibiotics from aqueous solution by adsorption/bioadsorption on activated carbon. *J. Hazard. Mater.*, *170*: 298-305.
21. Crisafully, R.; Milhome, M.A.L.; Cavalcante, R.M.; Silveira, E.R.; De Keukeleire, D.; Nascimiento, R.F. (2008) Removal of some polycyclic aromatic hydrocarbons from petrochemical wastewater using low-cost adsorbent of natural origin. *Bioresour. Technol*., *99*: 4515-4519.
22. Choi, K.; -J.; Son, H.-J.; Kim, S.-H. (2007) Ionic treatment for removal of sulphonamide and tetracycline classes of antibiotic. *Sci. Total Environ.*, *387*: 247-256.
23. Huang, C.H.; Renew, J.E.; Smeby, K.L.; Pinkston, K.E.; Sedlak, D.L. (2001) Assessment of potential antibiotic contaminants in water and preliminary occurrence analysis. Water Resour., *120*: 30-40.
24. Bajpai, A.K.; Rajpoot, M.; Mishra, D.D. (2000) Studies on the correlation between structure and adsorption of sulfonamide compounds. *Colloid. Surface*, *168* (3): 193-205.
25. Tolls, J. (2001) Sorption of veterinary pharmaceuticals in soils: a review. *Environ. Sci. Technol*., *35*: 3397-3406.
26. Grant , G.A.; Frison, S.L.; Sporns, P. (2003) A sensitive method for detection of sulfamethazine and N4-acetylsulfamethazine residues in environmental samples using solid phase inmunoextraction coupled with MALDI-TOF MS. *J. Agric. Food Chem.*, *51*: 5367-5375.
27. Helfferich, F. (1962) *Ion Exchange*. McGraw-Hill: New York.
28. Lertpaitoonpan, W. (2008) Sorption, degradation and transport of Sulfamethazine in soils and manure-amended soils. Iowa State University, Ames, Iowa.
29. Yuh, SH. (2004) Selection of optimum sorption isotherm. *Carbon. 42*: 2113-2130.
30. Aksu Z.; Tunç, O. (2004) Application of biosorption for penicillin G removal comparison with activated carbon. *Process Biochem., 40*: 831-847.
31. Boyd, G. E.; Adamson, A. W.; Myers, L. S. (1947) The exchange adsorption from aqueous solutions by organic zeolites. II. Kinetics. *Journal of the American Chemical Society*, *69*: 2836-2848.
32. Boyd, G. E.; Schubert, J.; Adamson, A. W. (1947) The exchange adsorption of ions from aqueous solutions by organic zeolites. I. Ion-exchange Equilibria. *Journal of the American Chemical Society.*, *69*(11): 2818-2829.
33. Rodrigues, A. E.; Tondeur, D. (1981) *Percolation Processes: Theory and Applications*. NATO ASI Series: 31-81.
34. Madsen, N. K.; Sincovec, R. F. (1979) *ACM Transactions on Mathematical Software (TOMS)*, *3*: 326-351
35. Reid, R.C., Praustniz, J.M., Poling, B.E. (1988) *The properties of Gases and Liquids.* McGraw-Hill, New York.
36. Wilke, C.R., Chang, P. (1955) Correlation of diffusion coefficients in dilute solutions. *AIChE J., 1* (2): 264-270.
37. Costa, C. Rodrigues, A. (1985) Design of cyclic fixed-bed adsorption processes. Part I: Phenol adsorption on polymeric adsorbents. *AIChE Journal, 31 (10)*: 1645-1654.
38. Fernández, A. Rodrigues, A.E. Díaz, M. (1994) Modelling of Na/K Exchange in Fixed Beds with Highly Concentrated Feed. *Chem. Eng. J., 54***:** 17-22.
39. Fernández, A. Rendueles, M. Rodrigues, Díaz, M. (1994) Co-ion behavior at high concentration cationic ion exchange. *Ind. Eng. Chem. Res., 33* (11): 2789-2794.
40. López, A.M.; Rendueles, M.; Díaz, M. (2013) Sulfamethoxazole removal from synthetic solutions by ion exchange using a strong anionic resin in fixed bed. *Solvent Extraction and Ion Exchange, 31*:763-781.

4.3. COMPETICIÓN DE SULFAMETOXAZOL CON SALES EN EL PROCESO DE INTERCAMBIO IÓNICO

En este trabajo se ha descrito el proceso de intercambio iónico de sulfametoxazol en presencia de sales para estudiar la competencia que existe entre ellos por los sitios activos de la resina.

En el artículo que se presenta a continuación, se ha querido simular el comportamiento que tendría el sulfametoxazol en aguas reales donde habitualmente se encuentra mezclado con sales como sulfatos, nitratos, cloruros, etc. Se han elegido como concentraciones de sales para los experimentos 250 mg/L cloruros, 250 mg/L sulfatos y 50 mg/L nitratos, debido a que son los valores máximos permisibles por la OMS para aguas potables. Se ha descrito el equilibrio empleando isotermas para sistemas multicomponentes y se han determinado los parámetros cinéticos. Se estudió también la operación en columna empleando disoluciones sintéticas mezclas de sulfametoxazol con sales, para ver cómo sería su comportamiento en un proceso industrial, cómo varía la capacidad de retención de sulfametoxazol en presencia de sales y ver la efectividad del eluyente para regenerar la resina. También se modelizaron las curvas de ruptura obtenidas empleando un modelo de lecho fijo.

En este artículo también se ha estudiado el equilibrio y la cinética del proceso de intercambio iónico de sulfato, nitrato y cloruro en sistemas individuales, y se han determinado las constantes de equilibrio y cinéticas.

Artículo: Competition of salts with sulfamethoxazole in an anionic ion exchange process

Situación: artículo bajo revisión en *Industrial & Engineering Chemistry Research* (Manuscript ie-2014-001899)

COMPETITION OF SALTS WITH SULFAMETHOXAZOLE IN AN ANIONIC ION EXCHANGE PROCESS

Ana María López Fernández, Manuel Rendueles* and Mario Díaz

Department of Chemical Engineering and Environment Technology, University of Oviedo, Oviedo, Spain

Abstract

Sulfomethoxazole is an emergent contaminant in waters. It is an antibiotic for humans and animals that is difficult to biodegrade in drinking water and sewage treatment plants. As the most frequent sulfonamide, its treatment and removal is difficult. In its anionic form, it can be retained by ion exchange, although competition with other ions, especially salts present in natural and treated water, needs to be taken into consideration due to competition between the anions for the active sites of the resin. This paper studies the removal of sulfamethoxazole (SMX) from low saline waters. Lewatit MP500 ion exchange resin was used to remove SMX in synthetic solutions in the presence of chloride, sulfate and nitrate salts. Multicomponent system solutions containing a fixed concentration of salts and different concentrations of SMX were tested in batch experiments. Adsorption equilibrium constants were determined using Langmuir and Constant Separation Factor isotherms, and the Extended Langmuir isotherm for multicomponent systems. Kinetics was analyzed using the film mass transfer and the pore diffusion models. Finally, two operational load and elution cycles were carried out in a fixed bed column using synthetic solutions of SMX and salts to obtain the corresponding breakthrough curves. Results show that the ion exchange resin is able to retain SMX despite the high competition of the other anions for the active sites of the resin.

Keywords: ion exchange, pharmaceutical contaminants, isotherms, kinetics, fixed bed operation

1. Introduction

The presence of antibiotics in the ecosystem has been known for almost 30 years. In recent years, the use of antibiotics in veterinary and human medicine has become widespread, with the ensuing increase in water contamination by these compounds. Human and veterinary antibiotics are detected in different matrices. These contaminants are continually discharged into the natural environment by a diversity of input sources (households, industries, hospitals, aquaculture, livestock, poultry and pets). Most wastewater treatment plants (WWTPs) are not designed to remove highly polar micropollutants like antibiotics[1,2]. They may therefore be transported to surface waters and reach groundwater after leaching. Ultimately, contaminated surface waters can enter drinking water treatment plants (DWTPs), which are likewise not equipped to remove these compounds, which eventually reach the water distribution system. Practical, economical solutions must therefore be developed to reduce the daily amounts of antibiotics discharged into the environment.

A wide range of chemical and physical methodologies can be employed for the removal of organic compounds. Different methods may be chosen depending on the concentration of the pollutant in the effluent and the cost of the process[3]. The treatment options typically considered for the removal of emerging contaminants include adsorption[4], Advanced Oxidation Processes (AOPs)[5-8], Nanofiltration (NF), and Reverse Osmosis (RO) membranes[9]. However, the shortcomings of most of these methods include high investment and maintenance costs, secondary pollution (generation of toxic sludge, etc.) and complicated procedures involved in

the treatment. On the other hand, physicochemical treatments such as coagulation/flocculation processes[10,11] have generally been found to be unable to remove Endocrine Disrupting Compounds and Personal Care Products (PPCPs). Although AOPs can be effective in the removal of emerging compounds, these processes can lead to the formation of oxidation intermediates that are as yet mostly unknown.

Adsorption processes do not add undesirable by-products and have been found to be better than other techniques for wastewater in terms of simplicity of design and operation, and insensitivity of toxic substances[12]. Among several materials used as adsorbents, Activated Carbons (ACs) have been used for to remove different types of emerging compounds in general, although their use is sometimes restricted due to their high cost[13,14]. Moreover, when AC has been exhausted, it can be regenerated for further use, although the regeneration process results in a loss of carbon and the regenerated product may have a slightly lower adsorption capacity compared to the virgin activated carbon. Interest in alternative adsorbents has subsequently grown with the aim of finding new low-cost adsorbents[15,16].

Polymer resins are becoming more common in wastewater treatment due to their low cost, easy regeneration and selective removal of pollutants. Adams[17] and Choi[18] studied the use of polymeric resin for the removal of sulfonamides and tetracyclines. They obtained high removal efficiencies (90% for sulfonamides and >80% for tetracyclines). Vergili[19] studied the adsorption of carbamazepine, propyphenazone and sulfamethoxazole using a polymeric resin, Lewatit VP OC 1163. This resin showed a large adsorption capacity for pharmaceuticals with low solubility.

Sulfamethoxazole (SMX) is a common antibacterial antibiotic sulfonamide that is widely used to treat urinary tract infections in humans and animals. It prevents the formation of dihydrofolic acid, a compound that bacteria must be able to produce in order to survive. It is also the most frequently detected sulfonamide in municipal sewage.

The aim of this study was to investigate the feasibility of ion exchange treatment of low saline natural waters contaminated with sulfamethoxazole (SMX) in the presence of chloride, nitrate and sulfate salts. Lewatit MP500, a macroporous strong anionic resin was tested to determine its capacity to retain SMX in the presence of these salts, comparing the results with those previously obtained for SMX in single solutions. Equilibrium and kinetics were studied in order to characterize the operation. The adsorption equilibrium constants were determined using Langmuir and Constant Separation Factor isotherms for single component systems, and the extended Langmuir isotherm for the multicomponent system. The kinetics was analyzed using two models: a film mass transfer model and the pore diffusion model. Finally, several load and elution cycles were performed in a fixed bed column to evaluate the behavior of the resin in an industrial operation. The breakthrough curves of the load and elution steps were fitted using a fixed-bed adsorption model.

2. Materials and methods

2.1. Materials

Sulfamethoxazole (purity>98 % w/w), K_2SO_4 (purity ≥99% w/w), $NaNO_3$ (purity ≥99% w/w), and NaCl (purity ≥99% w/w) were purchased from Sigma-Aldrich. The chemical properties of sulfamethoxazole are: molecular formula: $C_{10}H_{11}N_3O_3S$; melting point: 171 ºC, molecular weight: 253.28 g/mol; dissociation constants: pKa_1= 1.6(aromatic amine) and pKa_2= 5.7(sulfonate nitrogen); octanol/water partition coefficient: log K_{ow}= 0.89; and solubility in water: 610 mg/L at 37 ºC; from Hazardous Substances Data Bank (HSDB).

All chemicals were purchased from Sigma-Aldrich, methanol (HPLC grade) was used for liquid chromatography and ultra pure water was prepared in a Milli-Q purification system. The filters used for filtration were obtained from Millipore (0.45 µm pore PVDF for samples) and Whatman (0.22 µm pore PTFE for the mobile phase). Experiments were carried out at pH values of aqueous solutions of between 5.0 and 5.5.

A commercial organic polymeric resin (Lewatit MP500) manufactured by Lanxess was used as adsorbent. The strong base resin Lewatit MP500 has a quaternary amine (macroporous type I) and a crosslinked polystyrene matrix. The main properties of the resin are shown in Table 1.

Table 1. Characteristics of Lewatit MP500

General description	
Ion form	Cl^-
Functional group	Quaternary amine (type I)
Polymer Structure	Macroporous
Bead side >90% (mm)	0.47(±0.06)
Density (g/mL)	1.06
Total capacity (min.eq /L)	1.1

2.2. Analytical methods

Determination of sulfamethoxazole in the samples was performed using HPLC (Agilent 1200) and a column (mediterranea sea18, 5µm x 25 cm x 46 cm, plus a reverse-phase column from Waters) combined with UV detection. Prior to HPCL analysis, the samples were treated using 0.45 µm PVDF filters to ensure that they were free of other compounds that might interfere in the analysis. The mobile phase consisted of eluent A (methanol) and eluent B (water). The method was isocratic (60% of eluent A and 40% of eluent B). Analysis was performed at a flow rate of 0.7 mL/min. The wavelength used for detection was 270 nm and the retention time was 4.9 min. The column compartment temperature was 40 ºC. Injection volume: 20 µL. Analysis was performed at a flow rate of 0.7 mL/min.

The determination of salts (chloride, nitrate and sulfate) was performed using an Ion Chromatograph (DIONEX 120). The mobile phase was a mixture of Na_2CO_3 and $NaHCO_3$(4.5 mM CO_3^{2-} and 0.8 mM HCO_3^-). The retention times were 2.58 min for Cl^-, 4.33 min for NO_3^-, and 10.33 min for SO_4^{2-}.

2.3. Experimental Method

Batch Experiments. Runs were carried out at room temperature in cylindrical stirred tanks operating at a stirring rate of 300 rpm. Initially, as the ionic form of the wet resin was Cl^-, the conditioning was carried out by contacting the resin with a solution of NaOH 1 M with an L/S ratio (volume of liquid (mL)/ mass of wet resin (g)) = 20, 2 times, 20 minutes each time, to exchange the Cl^- groups by OH^- groups. The resin was then washed with distilled water twice for 5 minutes each time with an L/S ratio = 50 and subsequently separated from the solution.

The resin was then contacted with the loading solution containing 250 mg/L SO_4^{2-}, 250 mg/L Cl^-, 50 mg/L NO_3^- and different concentrations of SMX (between 62 and 124 mg/L) using an L/S ratio (mL solution/g)= 150, 200 and 250. The concentration of salts was chosen in line with permissible limits for drinking water quality set by national legislation and WHO (World Health Organization).

Experiments were also carried out using single components of salts (chloride, sulfate and nitrate). The experiments using SMX alone were carried out in a previous study[20]. The present experiments were carried out using an L/S ratio (mL solution/g wet resin) = 1000 and the following initial concentration of salts: $[NO_3^-]_0$= 50-125 mg/L; $[SO_4^{2-}]_0$= 50-300 mg/L and $[Cl^-]_0$= 50-350 mg/L.

The contact time employed in the experiments was 120, the time considered sufficient to reach operative equilibrium. The volume of the samples extracted from the tank each time was 2 mL, which did not substantially change the volume of the solution. The concentration of SMX, chloride, sulfate and nitrate ions in the resin were determined by mass balance, calculating the difference between the initial and final amount of charged ions in the solution.

Column Experiments. Continuous flow adsorption experiments were carried out in a glass column with an internal diameter of 1.1 cm and a total tube length of 25 cm. Column was prepared by packing with 2 grams (1.9 mL) of wet resin. Solutions were pumped through the column by a peristaltic pump (Masterflex) in down-flow mode.

To condition the resin in the fixed bed, a solution of NaOH 1M was pumped through the column for 20 minutes at a flow rate of 11 mL/min. Distilled water was then fed through the column at a flow rate of 11 mL/min for 15 minutes to wash the resin.

Two load stages using synthetic solutions containing 125 mg/L SMX, 250 mg/L Cl^-, 250 mg/L SO_4^{2-} and 50 mg/L NO_3^- in the first stage and 90 mg/L SMX and the same concentration of salts in the second stage were carried out at a down-flow rate of 11 mL/min and 10.5 mL/min, respectively. Effluent samples (4 mL approximately) were collected at specified times intervals (5-10 minutes) and measured by HPLC and IC to monitor the evolution of SMX and salt concentrations over time. The breakthrough curve was plotted until the concentration at the outlet of the column effluent reached the initial concentration of the feed solution. After adsorption, distilled water was fed through the column to remove any unabsorbed ions on the adsorbent surface or entrapped between adsorbent particles.

After each loading, an elution step was carried out by pumping a solution of NaOH 0.5M through the column at a down-flow-rate of 10 mL/min and 9 mL/min, respectively. Effluent samples were collected at the outlet of the column every 5-10 minutes to monitor the evolution of the concentration over time. The elution curve was plotted until no concentrations were detected at the column outlet.

3. Results and discussion

3.1. Batch equilibrium study

In order to evaluate the capacity of the MP500 resin to retain SMX in the presence of salts, several runs were carried out using different L/S ratios (volume of liquid (mL)/mass of wet resin (g))= 150, 200 and 250 and synthetic solutions of SMX + salts (chloride + sulfate + nitrate) with a fixed concentrations of salts, 250 mg/L Cl^-, 250 g/L SO_4^{2-}, 50 mg/L NO_3^-, and different concentrations of SMX, between 62 and 124 mg/L SMX. The concentrations of each compound were monitored over time until reaching equilibrium. Equilibrium concentrations were obtained within 100 minutes. A mass balance was used to determine the equilibrium compositions of each anion in the resin and in the solution phase. The equilibrium concentrations obtained and their respective adsorption capacities are shown in Table 2. As the resin was initially charged with ions Cl^-, the evolution of the Cl^- concentrations was not monitored in the ion exchange process.

Table 2. Comparison of experimental data and calculated values from the extended Langmuir model for a multicomponent system containing SMX in different initial concentrations (C_0) and a fixed amount of salts (50 mg/L NO_3^-, 250 mg/L SO_4^{2-} and 250 mg/L Cl^-)

L/S	C_0 (g/L)	$C_{e,i\text{-experimental}}$ (g/L)			$q_{e,i\text{-experimental}}$ (g/L resin)			$q_{e,i\text{-calculated}}$ (g/L resin)		
	SMX	SMX	NO_3^-	SO_4^{2-}	SMX	NO_3^-	SO_4^{2-}	SMX	NO_3^-	SO_4^{2-}
150	0.062	0.034	0.012	0.05466	4.5	5.1	31	4.6	4.7	32.1
200	0.092	0.0589	0.0166	0.07	7.2	7.1	34.9	7.6	5.8	36.5
200	0.124	0.0844	0.0171	0.078	8.4	7.3	36.5	10.4	5.6	38.3
250	0.124	0.0920	0.021	0.097	9.0	8.3	40.6	10.9	6.2	43.1
		SMX	NO_3^-	SO_4^{2-}						
R^2		0.997	0.9912	0.999						
χ^2(g/L resin)		0.74	1.53	0.33						
Ɛ(%)		13.3	18.5	4.8						
RMSE		1.402	1.504	1.815						
E_i		0.106	0.156	0.009						

χ^2= Chi-square analysis; RMSE=root-mean-square error; Ɛ(%)=average percentage error; E_i= objective function (dimensionless)

Two different models, the Langmuir and Constant Separation Factor isotherms, were used to define the relationship between the resin load capacity and the equilibrium solution concentration of salts in single systems and in SMX together with salt mixtures, without considering the presence of the other salts in solution, i.e., considering no competition between the anions in the ion exchange process. Comparison of these results with those obtained in a previous study[20] on SMX in a single system allows the determination of the loss in capacity of the resin to remove SMX due to the presence of salts in the aqueous solution.

The Langmuir sorption isotherm is the best known and the most widely used isotherm for modelling the sorption of a solute from a liquid solution:

$$q_{e,i} = \frac{K_{eq} \cdot q_T \cdot C_{e,i}}{1 + K_{eq} \cdot C_{e,i}} \quad (1)$$

where K_{eq} is the equilibrium constant(L/g), q_T is the maximum adsorption capacity of the resin (g/L resin), $C_{e,i}$ is the equilibrium solution concentration of species i (g/L), and $q_{e,i}$ is the amount of specie i adsorbed by the resin at equilibrium (g/L resin).

The equation for the Constant Separation Factor isotherm is:

$$q_{e,i} = \frac{K_{eq} \cdot q_T \cdot C_{e,i}}{C_T + (K_{eq} - 1) \cdot C_{e,i}} \quad (2)$$

where C_T (g/L) is the minimum equilibrium concentration in the solution with a saturated resin. The equilibrium constants and the maximum absorption capacity were obtained using the Statgraphic program. Figures 1 and 2 compare the experimental results with the values predicted by the Langmuir and the CSF isotherms for SMX in mixtures considering no competition between each substance, and for each salt individually. It can be seen that the Langmuir and CSF isotherms show a good correlation between the experimental results and predicted values.

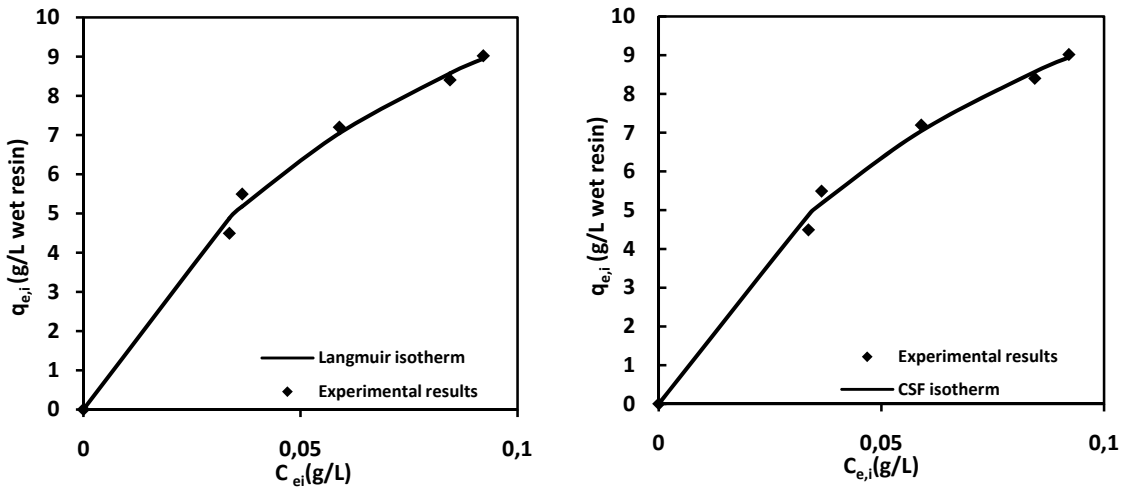

Figure 1. Comparison of experimental data with predicted values from the Langmuir and Constant Separation Factor isotherms for SMX in mixtures with salts (nitrate, sulfate, and chloride) considering no competition between them.

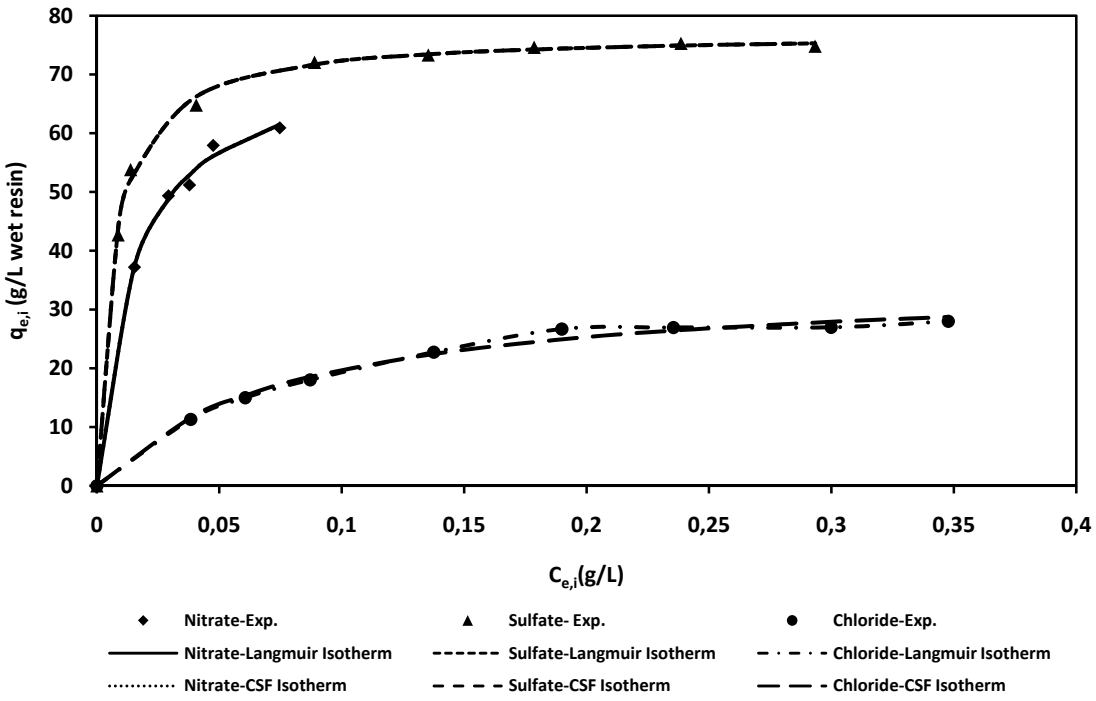

Figure 2. Comparison of experimental data with predicted values from the Langmuir and Constant Separation Factor isotherms for nitrate, sulfate and chloride in a single component system.

The different isotherm parameters obtained for SMX in mixtures using the Langmuir isotherm were: $K_{eq\text{-}Lang}$= 11.8 L/g and $q_{T\text{-}Lang}$= 17.2 g SMX/L wet resin, with a correlation coefficient R^2= 0.994; and for the CSF isotherm: $K_{eq\ CSF}$= 9.1, $q_{T\text{-}CSF}$= 15.3 g SMX/L wet resin, $C_{T\text{-}CSF}$= 0.69 g SMX/L, with a correlation coefficient R^2= 0.999. The parameters obtained for SMX, NO_3^-, SO_4^{2-} and Cl^- in single component systems are summarized in Table 3.

Table 3. Isotherm parameters obtained in a single system

	Langmuir						Constant Separation Factor						
	K_{eq} (L/g)	q_T (g/L resin)	R^2	χ^2	Ɛ(%)	E_i	K_{eq}	q_T (g/L resin)	C_T	R^2	χ^2	Ɛ(%)	E_i
SMX[20]	15.8	258	0.9897	2.99	5.52	0.036	6.34	218	0.34	0.9897	2.99	6.72	0.036
NO_3^-	66.7	73.8	0.9973	0.12	1.76	0.002	48.7	72.3	0.72	0.9973	0.12	1.76	0.002
SO_4^{2-}	151.6	76.9	0.9986	0.13	1.28	0.002	68.5	75.8	0.44	0.9986	0.13	1.28	0.002
Cl^-	12.7	35.2	0.9925	0.22	2.94	0.008	23.3	33.7	1.7	0.9925	0.22	2.96	0.008

χ^2= Chi-square analysis (g/L resin); Ɛ(%)=average percentage error; E_i= objective function (dimensionless)

To quantify the agreement between the model predictions and experimental data, the proposed equilibrium equations were evaluated using Chi-square analysis[21] and non-linear regression analysis. Eq. (3) shows how to calculate χ^2. The advantage of Chi-square analysis is that all equilibrium equations can be compared on the same abscissa and ordinate. If the data predicted by the model is similar to experimental data, χ^2 (g/L resin) will be small, and vice versa.

$$\chi^2 = \sum_{i=1}^{N} \frac{\left(q_{eq,exp} - q_{eq,cal}\right)^2}{q_{eq,cal}} \tag{3}$$

where $q_{(eq,cal)}$ is the equilibrium capacity obtained from a model (g/L resin), $q_{(eq,exp)}$ is the equilibrium capacity obtained from experiments (g/L resin), and N is the number of measurements.

Eq. (4) shows the average percentage error (Ɛ) used in the non-linear regression analysis[22]. The errors between experimental data and predicted data were calculated using Eq. (4)

$$\varepsilon(\%) = \frac{\sum_{i=1}^{N} \left|\left(q_{eq,exp} - q_{eq,cal}\right)/q_{eq,exp}\right|}{N} x\ 100 \tag{4}$$

In addition, to quantify the agreement between the model predictions and the experimental data observations, an objective function relating the experimental and the predicted component uptake may be defined as[23]:

$$E_i = \sum_{j=1}^{Q} \left(\frac{q_i^{exp} - q_i^{model}}{q_i^{exp}} \right)^2 \tag{5}$$

where Q if the number of data points: j=1…Q, and q_i^{exp} and q_i^{model} are the experimental and the predicted sorption capacities.

The error function values obtained for SMX in mixtures for the Langmuir isotherm were: χ^2= 0.057, $\mathcal{E}$= 2.82%, and E_i= 0.0044; and for the CSF isotherm: χ^2= 0.057, $\mathcal{E}$= 3.85%, and E_i= 0.0115. Although both isotherms describe the adsorption process well, the Langmuir isotherm showed slightly better results when comparing the error functions. In the case of salts in a single component system, Table 3 presents the values of the objective functions (E_i), the values of χ^2 and the values of the average percentage errors ($\mathcal{E}$) for both isotherms. After evaluating the error functions, both isotherms are seen to describe the equilibrium adsorption process of each salt in single system well, as similar results were obtained.

On the other hand, when comparing the capacity to adsorb SMX alone or in mixtures, it can be seen that the maximum adsorption capacity for SMX decreases considerably from 258 g

SMX/L wet resin to 17.2 g SMX/L wet resin in mixtures. A reduction in the capacity to adsorb SMX means that the presence of salts in the solution interferes in the adsorption process. Hence, competitive adsorption using the Extended Multicomponent Langmuir isotherm, Eq. (6), was used to model the experimental data.

$$q_{e,i} = \frac{K_{eq,i} \cdot q_T \cdot C_{e,i}}{1 + \sum K_{eq,i} \cdot C_{e,i}} \quad (6)$$

where $q_{e,i}$ is the amount of solutes sorbed per unit of sorbent at equilibrium concentrations, $C_{e,i}$ (g/L), q_T is the maximum sorption capacities of the solutes (g/L resin), and $K_{eq,i}$ (L/g) is the equilibrium constant of each solute. This Langmuir equation is a simple extension of the single-component Langmuir isotherm to account for multicomponent sorption. This model assumes: i) a homogeneous surface with respect to the energy of adsorption, ii) no interaction between adsorbed species, and iii) all adsorption sites are equally available to all adsorbed species. The model comprises four parameters: q_T, $K_{eq\ SMX}$, $K_{eq\ NO3^-}$ and $K_{eq\ SO4^{2-}}$. The computer program Scientific was used to evaluate these parameters. The values obtained were: $K_{eq\ SMX}$= 1.4 L/g SMX, $K_{eq\ NO3^-}$= 6 L/g NO_3^-, $K_{eq\ SO4^{2-}}$= 9 L/g SO_4^{2-} and q_T= 105 g SMX/L wet resin, with a correlation coefficient R^2= 0.999. Comparison between experimental data and the values predicted by the extended Langmuir equation for a multicomponent system of SMX with salts is shown in Table 2, as well as the error functions, Chi-square analysis, average percentage error (Ɛ) and objective function (E_i). The experimental data and predicted values obtained for this system are given in Figure 3. The higher value of the $K_{eq,i}$ parameter for SO_4^{2-} than for NO_3^- and SMX implies that Lewatit MP500 has a higher affinity for SO_4^{2-} than for NO_3^- or SMX.

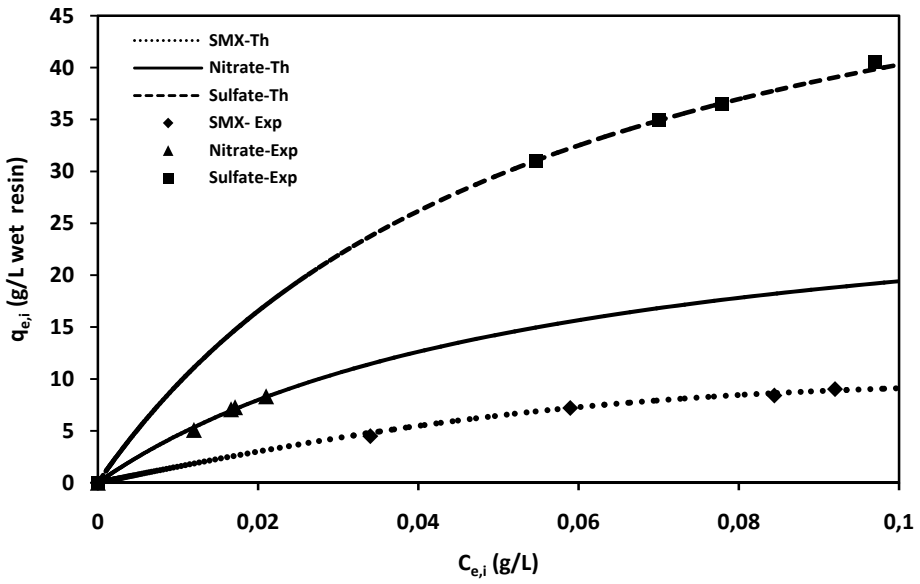

Figure 3. Comparison of experimental data with the values predicted by the Extended Langmuir isotherm for a multicomponent system.

3.2. Batch kinetics study

Kinetics experiments were carried out in batch mode with mixtures of SMX and salts in a multicomponent system monitoring SMX, nitrate, sulfate and chloride concentrations over time from the initial time to equilibrium time for all solutions, and also with salts in a single component system.

3.2.1. Multicomponent system

In the SMX + salts assays, the solution concentration of SMX does not change substantially after 100 minutes, so operational equilibrium may be assumed. The experiments were conducted in a stirred tank using synthetic solutions with initial concentrations of 62, 92 and 124 mg SMX/L and fixed concentrations of 250 mg/L SO_4^{2-}, 250 mg/L Cl^- and 50 mg/L NO_3^-.

The process was modeled assuming a sorption process, seeing as the rate controlling step in ion exchange is usually the diffusion of the counter anions rather than the chemical exchange reaction at the fixed ions groups. This means that the ion-exchange process is essentially a diffusion phenomenon. The concentration profiles of SMX in mixtures can be modeled using two diffusion models, the film mass transfer model and the pore diffusion kinetics model, to determine the mass transfer mechanisms involved[24,25].

Film Mass Transfer Model. In this model, SMX retention is assumed to be limited by the external surface of the particle[26]. The behavior of this model may be described by the following equations:

$$\frac{dq_i}{dt} = K_f a_p (C_i - C^*) \tag{7}$$

where q_i is the concentration of specie i in the resin at time t, K_f is the mass transfer coefficient in the fluid phase (cm/s), $C^*$is the equilibrium concentration in the solution (mg SMX/mL), and a_p is the specific surface area, i.e., the total surface area per unit of volume (cm^{-1}). $K_f a_p$ may be considered to be equal to K, the apparent mass transfer coefficient.

$$V_L C_i + V_r q_i = V_L C_0 \tag{8}$$

where V_L is the volume of liquid, V_r is the volume of resin and C_o is the initial concentration in solution. Integrating Eq. (7) and introducing Eq. (8), the following equation is obtained:

$$q_i(t) = C_0 (V_L/V_r)\left(1 - \frac{C^*}{C_0}\right)\left(1 - \exp\left(\frac{-K\,t}{V_L/V_r}\right)\right) \tag{9}$$

The mass transfer coefficient, K, may be determined by regression using the experimental data, fitting these to Eq. (7). The anion exchange beads are of constant size with a spherical geometry; therefore $K_f = K/a_p$. Comparison of the experimental results for SMX concentration and the theoretical values obtained using (8) and (9) will thus give the goodness of the obtained value for all the experiments. Comparison of experimental and theoretical results for the kinetics of synthetic solutions can be seen in Figure 4. The value obtained for the mass transfer coefficient was $5.5 \cdot 10^{-6}$ cm/s, with a correlation coefficient R^2>0.95 and an average percentage error, $\mathcal{E}$ (%), calculated as in Eq.(10), of between 1.4% and 3.6% in all assays.

$$\varepsilon(\%) = \frac{\sum_{i=1}^{N} \left| (C_{i,exp} - C_{i,cal})/C_{i,exp} \right|}{N} x\ 100 \tag{10}$$

On comparing the value obtained for SMX in mixtures with the results obtained in single assays ($K_{f\,SMX} = 3.4 \cdot 10^{-6}$ cm/s [20]), they are seen to be of the same order of magnitude.

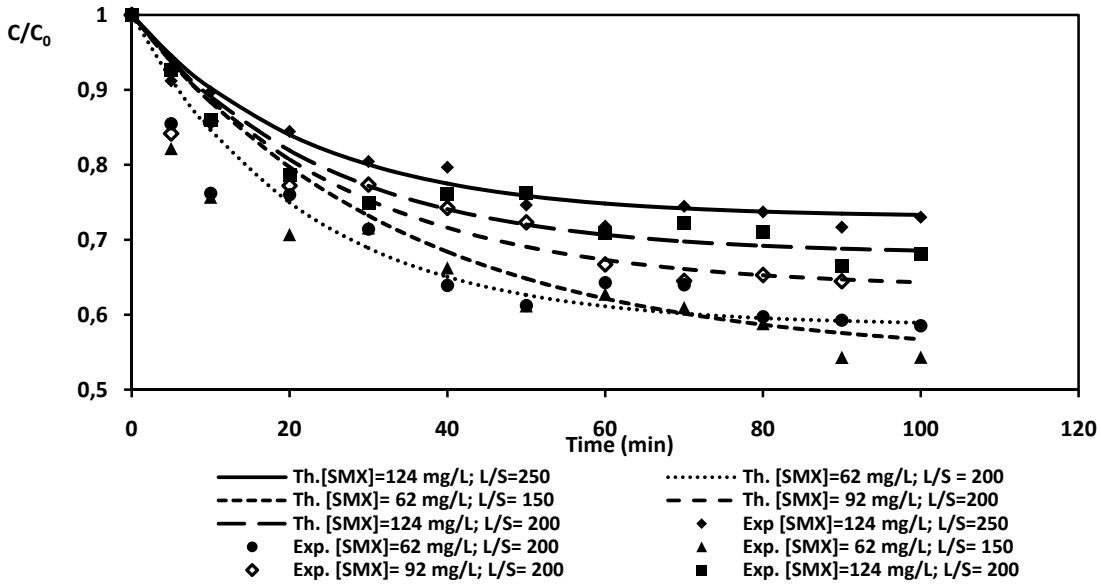

Figure 4. Fitting of kinetics data using the film mass transfer model for the adsorption of a synthetic solution of SMX at different concentrations (62-124 mg SMX/L) and concentrations of salts (250 mg/L SO_4^{2-}, 250 mg/L Cl^-, 50 mg/L NO_3^-) onto Lewatit MP500 resin.

Pore Diffusion Model. This model[27] considers the resin to be a porous matrix. The model is described by the following equations:

- Mass balance inside the particle:

$$\frac{\partial q_i(R,t)}{\partial t} = \frac{\partial q_{ei}(R,t)}{\partial t} + \varepsilon_i \frac{\partial C_{pi}(R,t)}{\partial t} = \frac{1}{R^2}\left[\frac{\partial}{\partial R} R^2 \varepsilon_i D_p \frac{\partial C_{pi}(R,t)}{\partial t}\right] \qquad (11)$$

where q_{ei} is the pore concentration of specie *i*, C_{pi} is the pore solution concentration of specie *i*, ε_i is the resin porosity, and D_p is the pore diffusivity.

- Mass balance in the bulk solution:

$$\varepsilon_i V(C_{iT} - C_i(t) = (1-\varepsilon_i)V\overline{q_{ei} + \varepsilon_i C_{pi}(t)} \qquad (12)$$

where C_{iT} is the initial concentration of species *i* in solution, and V is the volume of solution.

- Average concentration in the particle:

$$\overline{q_{ei} + \varepsilon_i C_{pi}}(t) = \frac{3}{R_0^3}\int_0^R R^2 \left(q_{ei} + \varepsilon_i C_{pi}\right)(R,t)dR \qquad (13)$$

where R is the radial coordinate and R_0 is the particle radius.

The initial and boundary conditions needed to solve the systems are:

- Initial conditions:

$$C_{pi}(R,0) = 0 \tag{14}$$

- Boundary conditions:

$$\text{In R} = 0 \rightarrow \left.\frac{\partial C_{pi}(R,t)}{\partial R}\right|_{R=0} = \left.\frac{\partial q_i(R,t)}{\partial R}\right|_{R=0} \tag{15}$$

$$\text{At the interphase } (R=R_0) \rightarrow C_{pi}(R_o,t) = C_i(t) \tag{16}$$

A FORTRAN subroutine, PDECOL[28], was used to solve these equations. The subroutine uses the method of orthogonal collocation on finite elements to solve the system of non-linear differential equations. The diffusivity value obtained was $1.3 \cdot 10^{-8}$ cm^2/s and the average percentage error calculated as in Eq.(10) was between 1.6% and 3.3%. Figure 5 shows the fit of the experimental results to this model for all the assays. The good agreement between experimental data and the theoretical prediction shows the goodness of the model. Comparing the value obtained in these assays with the value obtained in single assays of SMX ($D_{p\ SMX\ alone}$ = $2.6 \cdot 10^{-10}$ cm^2/s[20]), the diffusivity value for SMX in mixtures are higher.

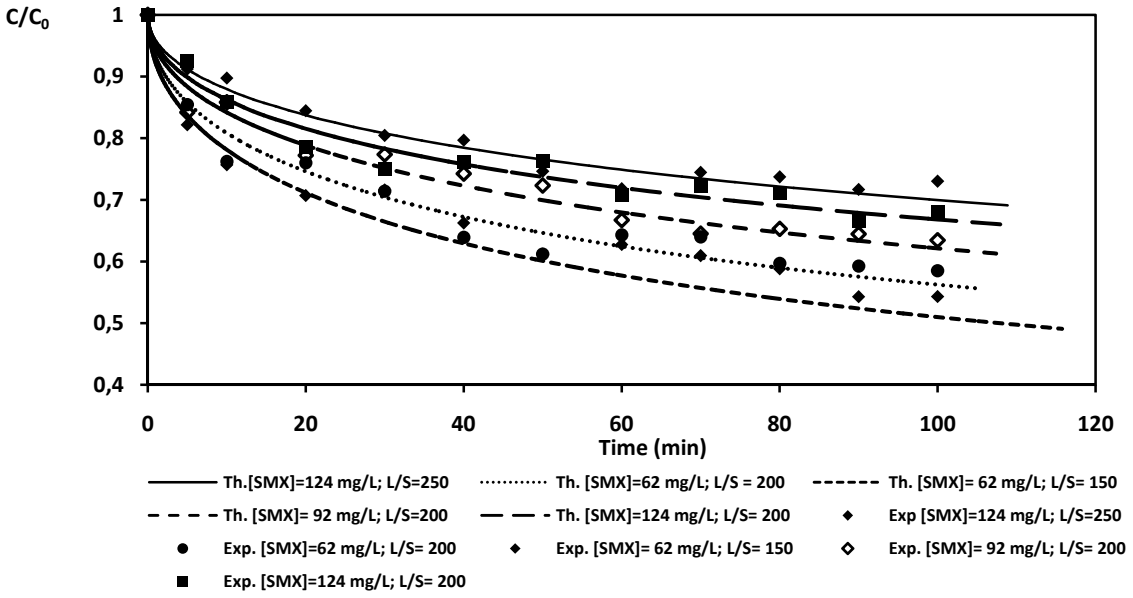

Figure 5. Fitting of kinetics data using the pore diffusion model for the adsorption of a synthetic solution of SMX at different concentrations (62-124 mg SMX/L) and concentrations of salts (250 mg/L SO_4^{2-}, 250 mg/L Cl^-, 50 mg/L NO_3^-) onto Lewatit MP500 resin.

Rate controlling step. A method proposed by Helfferich[26] was used to identify the rate-controlling step (diffusion inside the solid particles or diffusion in the film surrounding the particles) of the ion exchange process. This model constitutes a method for theoretically predicting the rate-controlling step that reflects the effect of the ion exchange capacity, solution concentration, particle diameter, film thickness, film mass transfer coefficient, pore diffusivity (D_p), and separation constant parameter. The criteria are based on the following expression:

$$\frac{q_T D_p \delta}{C_T D^{\infty} R_0}\left(5 + 2\alpha_{A/B}\right) \tag{17}$$

When the value of this factor is below 1, particle diffusion control exists. Otherwise, film diffusion control can be deduced if the value is above 1. In this expression, δ is the thickness of the film, which can be calculated as:

$$\delta = \frac{2R_0}{Sh} \tag{18}$$

Sh being the Sherwood number.

$$Sh = \frac{K_f d_p}{D_{pe}} \tag{19}$$

where K_f is the mass transfer coefficient in cm/s, which can be calculated from the mass transfer model. $K_f = K/a_p$, where a_p is the specific surface area of the spherical particles, $a_p = 3/R_0$, d_p is the particle diameter, and D_{pe} is the effective pore diffusivity calculated as in Reid[29].

$$D_{pe} = \frac{\varepsilon_i D^{\infty}}{\tau} \tag{20}$$

where D^{∞} is the diffusivity coefficient in the film of SMX in water, τ is the tortuosity of the adsorbent, and ε_i its porosity. The molecular diffusivity of SMX in water was estimated by the Wilke-Chang correlation[30], expressed in cm^2/s:

$$D^{\infty} = 7.4x10^{-8} \frac{(øM_B)^{1/2}\, T}{\mu_B V_A^{0.6}} \tag{21}$$

The molar volume for SMX is VA= 173.1 cm3/mol. Wilke and Chang recommended a value of 2.6 for ø. If the solvent is water, the viscosity of water, μB, in the temperature of range of this study is 1.0 cp. MB is the molecular weight of the solvent (g/mol), and T the absolute temperature, T=293 K. The value of molecular diffusivity obtained was D∞= 1.08·10-5 cm2/s. $\alpha_{A/B}$ is the separation factor, defined as the ratio of distribution coefficients of both ions, which can be calculated as $\alpha_{A/B} = \overline{C_A}\, C_B / C_A\, \overline{C_B}$, where C_i is the concentration of specie i in the solution, and $\overline{C_i}$ is the concentration of specie i in the resin. One way of calculating this parameter is to approximate it to the amount of adsorbed SMX (initial concentration in the resin minus equilibrium concentration) divided by the equilibrium concentration of SMX. The αA/B values for SMX in mixtures ranged between 0.4 and 0.8 in all trials.

The manufacturer's parameters for the resin are: density, ρ= 1.06 g/cm3; tortuosity, τ=5; particle radius, R0 = 0.024 cm; specific surface area, ap= 128 cm-1; and particle porosity, Ɛi= 0.34. The values of qT= 15.31 g/L resin and cT= 0.69 g/L were calculated previously from the CSF isotherm, while the value of pore diffusivity calculated from the pore diffusion model was Dp= 1.3·10-8 cm2/s.

Once all parameters are known, they can then be introduced in Eq. (17). The value of Helfferich's factor is less than 1 (between 0.8 and 0.9) in all cases. Therefore, particle diffusion is the rate-controlling step, as was expected due to the high stirring speed employed (300 rpm).

3.2.2. Salts in a single component system

The chloride, nitrate and sulfate adsorption processes were monitored from the initial time to equilibrium time for all solutions. The ion exchange operation was taken from the loading experiments conducted in stirred tanks with synthetic solutions of chloride, sulfate and nitrate salts. In the case of SMX, the results have been reported in a previous paper[20]. The concentration profiles of chloride, sulfate and nitrate salts can be studied using the film mass transfer and pore diffusion kinetics model to determine the mass transfer mechanisms as described above in Section *3.2.1*.

The values obtained for the mass transfer coefficient for each component were: $K_{f\text{-}chloride}= 2.6\cdot10^{-5}$ cm/s, $K_{f\text{-}sulfate}= 9.3\cdot10^{-6}$ cm/s, and $K_{f\text{-}nitrate}= 6.3\cdot10^{-6}$ cm/s, with the following correlations coefficients: $R^2_{nitrate}>0.99$, $R^2_{sulfate}>0.99$, and $R^2_{chloride}>0.95$. A comparison of experimental data and theoretical results for the kinetics of synthetic chloride, sulfate and nitrate solutions can be seen in Figure 6. The values of the average percentage error, $\mathcal{E}(\%)$, calculated as in Eq.(10) were: $\mathcal{E}(\%)$= 0.7-1.7 for nitrate, $\mathcal{E}(\%)$= 0.5-3.2 for sulfate, and $\mathcal{E}(\%)$= 0.4-1.5 for chloride. These results show a good correlation between experimental results and the values predicted by the model.

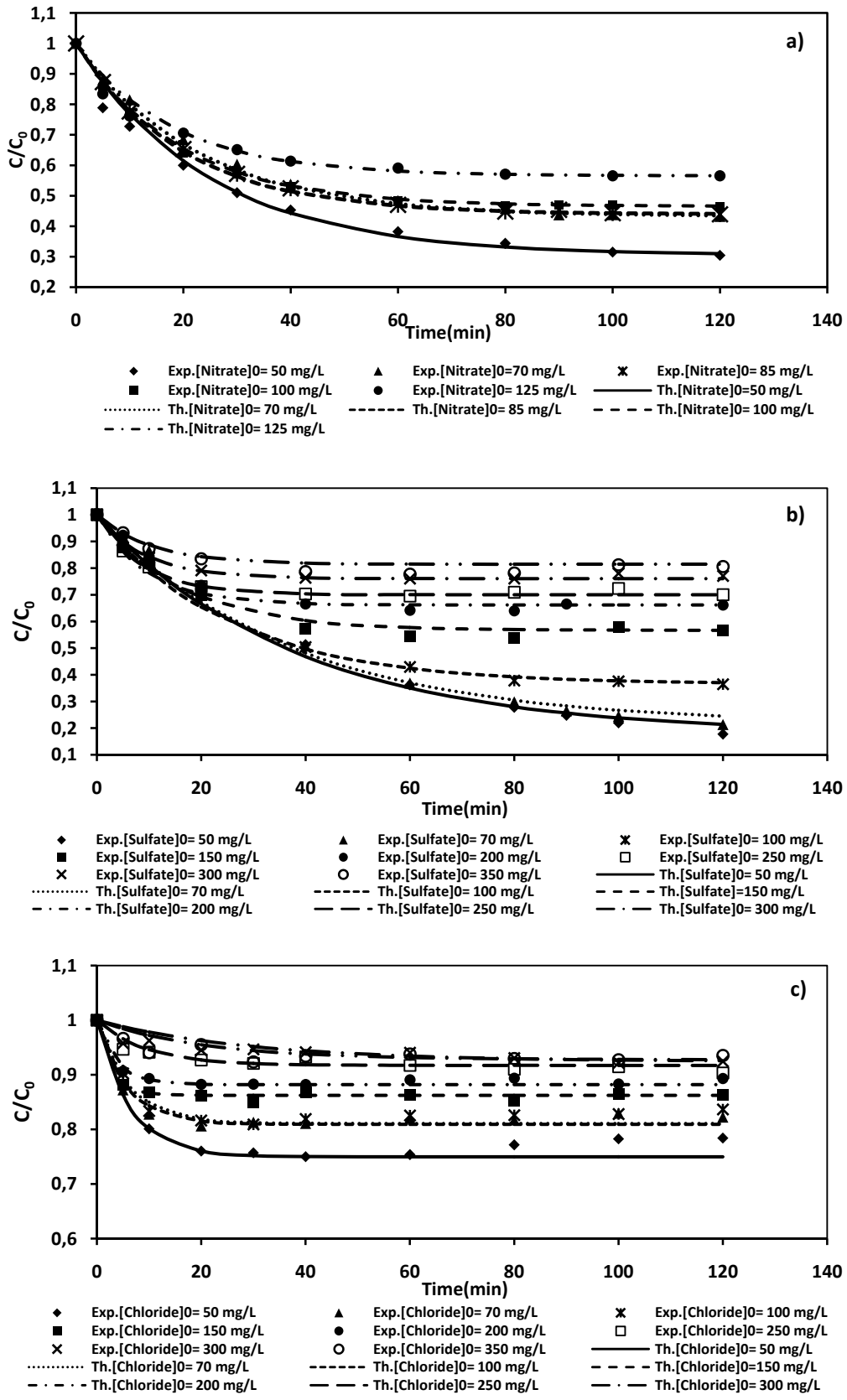

Figure 6. Fitting of kinetics data using the film mass transfer model for the adsorption of nitrate **(a)**, sulfate **(b)** and chloride **(c)** in synthetic solutions at different concentrations.

The diffusivity values obtained from the pore diffusion kinetics model for each component were: $D_{p\text{-}chloride}= 3.9\cdot10^{-8}$ cm^2/s, $D_{p\text{-}sulfate}= 2.7\cdot10^{-8}$ cm^2/s, and $D_{p\text{-}nitrate}= 2.3\cdot10^{-8}$ cm^2/s. The average percentage error values obtained from Eq.(10) were: $\mathcal{E}(\%)$= 3.3-5.3 for nitrate, $\mathcal{E}(\%)$= 1.3-6.8 for sulfate, and $\mathcal{E}(\%)$= 0.6-1.9 for chloride. Figure 7 shows a comparison of experimental data and the values predicted by the pore diffusion model for each component, obtaining a good correlation between both sets of values.

The rate-controlling step was calculated as described previously. The values of the separation factor, $\alpha_{A/B}$, for chloride, sulfate and nitrate salts in single assays were 0.3, 4.6, and 2.3, respectively. The molar volume values were: $V_{A\text{-}chloride}$= 27.1 cm^3/mol, $V_{A\text{-}sulfate}$= 65.5 cm^3/mol and $V_{A\text{-}nitrate}$= 37.6 cm^3/mol. The molecular diffusivities obtained were: $D^{\infty}_{chloride}= 1.92\cdot10^{-5}$ cm^2/s, $D^{\infty}_{sulfate}= 3.27\cdot10^{-5}$ cm^2/s and $D^{\infty}_{nitrate}= 2.68\cdot10^{-5}$ cm^2/s. The value of Helfferich's factor is less than 1 in the case of chloride; therefore, particle diffusion is the rate-controlling step, as was expected due to the high stirring speed employed (300 rpm). In the case of the nitrate and sulfate salts, the values of Helfferich's factor were 10 and 20, respectively, which means film diffusion is the rate controlling step, contrary to what was expected.

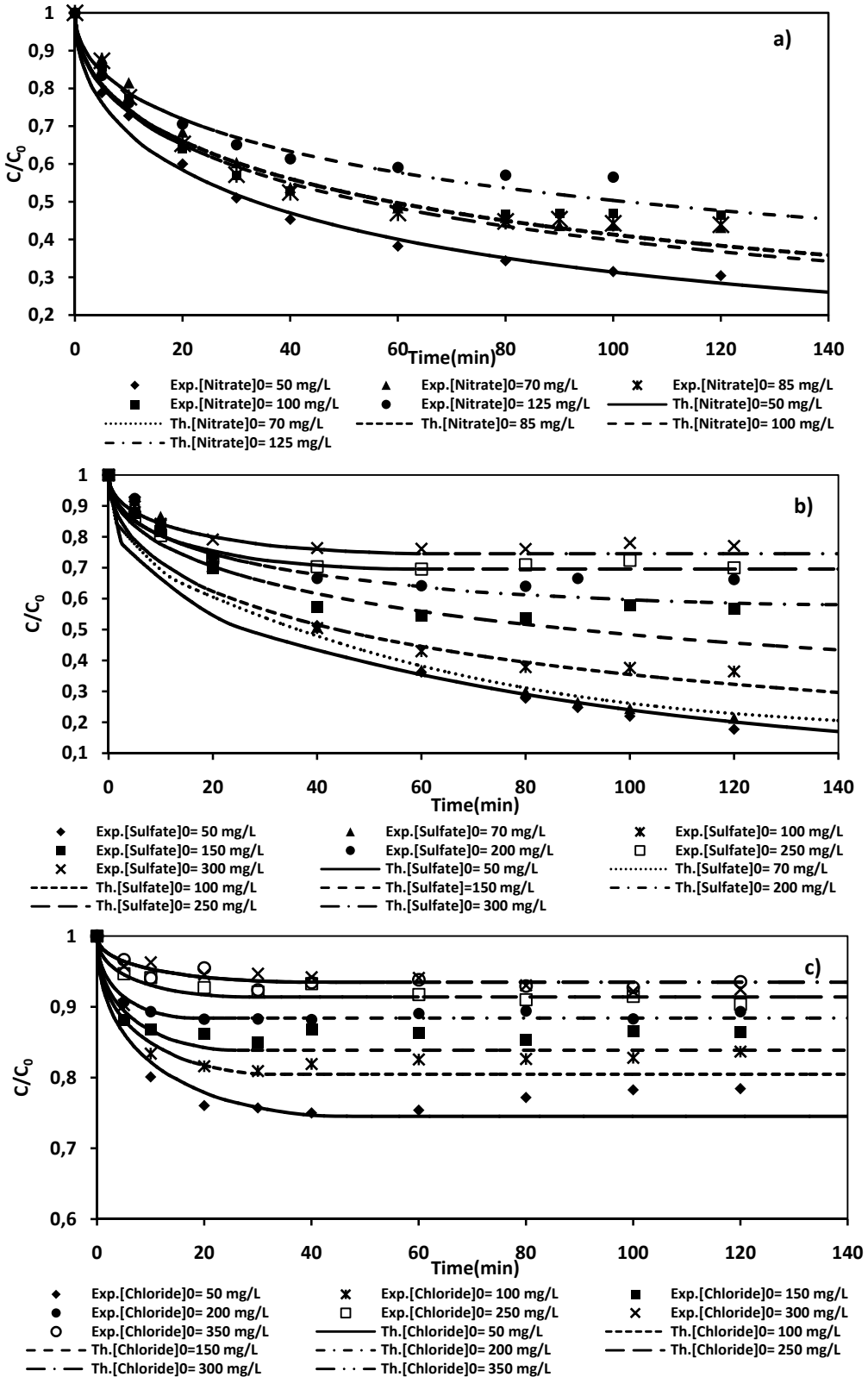

Figure 7. Fitting of kinetics data using the pore diffusion model for the adsorption of nitrate **(a)**, sulfate **(b)** and chloride **(c)** in synthetic solutions at different concentrations.

3.3. Fixed Bed Operation

Breakthrough Curves for the Load and Elution Steps. After studying the equilibrium and kinetics of the process, tests were conducted in a fixed bed column using synthetic solutions of SMX + salts in concentrations of 125 and 90 mg SMX/L and a fixed concentration of salts of 250 mg/L Cl^- + 250 mg/L SO_4^{2-} + 50 mg/L NO_3^- to obtain the corresponding breakthrough curves.

Operation in a fixed bed column was initially tested using a synthetic solution of 125 mg/L SMX + salts in the aforementioned concentrations, a volume of resin of 1.9 mL and a flow rate of 11 mL/min for 180 minutes. The amount of resin and the flow rate in load and elution steps was the same as those used in previous assays using SMX alone found to be adequate to achieve saturation of the resin.

The breakthrough curves for the load step show scattered results for all compounds, with no pronounced jump in concentration being observed over time. Concentrations of all compounds were detected from the first minutes of operation onwards, equilibrium subsequently being achieved for all anions in 60 minutes. SMX reached its equilibrium concentration in 5 minutes and Cl^- in 30 minutes, while NO_3^- and SO_4^{2-} did so in 60 minutes. The retention capacity of the resin packed in the column was calculated by numerical integration of the area below the breakthrough curves of the load step. The operational capacity of the bed was found to be: 5 mg SMX/mL wet resin, 15 mg NO_3^-/mL wet resin, 42 mg Cl^-/mL wet resin and 50 mg SO_4^{2-}/mL wet resin.

Resin life is one of the key parameters for determining the kind of resin to be applied in industrial production. After adsorption, the resin was regenerated with NaOH 0.5 M at a flow rate of 10 mL/min for 60 minutes. The concentration at the outlet of the column was negligible for all compounds within 20 minutes, recovering 100% of SMX, sulfate and nitrate in the elution step. Sulfate presented a high elution peak in the first minutes of operation, reaching a concentration of 1143 mg/L, approximately 4 times the initial concentration. In the case of SMX and nitrate, similar concentrations to their respective initial concentrations were obtained in the first minutes. This agrees with the results obtained in the load step, in which the resin showed a higher capacity of adsorption for the sulfate salt than for SMX and the nitrate salt. Therefore, the resin has more capacity to adsorb and concentrate sulfate than the other compounds. The breakthrough curves for the load and elution steps are shown in Figure 8a-b.

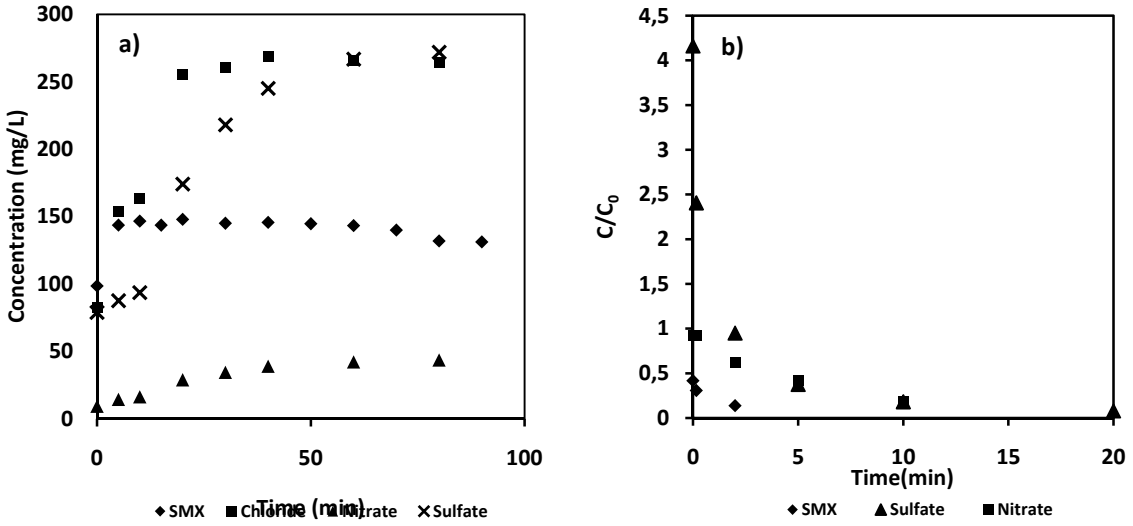

Figure 8. Breakthrough curves for the sorption of SMX, chloride, sulfate and nitrate from synthetic solutions prepared in distilled water (a), and elution using NaOH 0.5M (b) onto Lewatit MP500. Conditions: $[SMX]_0$= 125 mg/L, $[SO_4^{2-}]_0$= 250 mg/L, $[Cl^-]$= 250 mg/L, $[NO_3^-]_0$=50 mg/L; flow rate load= 11 ml/min, flow rate elution= 10 mL/min, volume resin= 1.9 mL (Z=3 cm).

After this first cycle of load and elution steps in a column setup, another cycle was carried out using a concentration of 90 mg/L SMX + salts in concentrations of 250 mg/L sulfate, 250 mg/L chloride and 50 mg/L nitrate to study the behavior of the resin, operating at a flow rate of 10.5 mL/min for 180 minutes. As in the previous cycle, concentrations were detected at the outlet of the column from the first minutes of operation onwards. SMX reached the concentration of initial sample in 20 minutes, subsequently remaining constant until the end of the operation. The sulfate salt showed a breakthrough point at 10 minutes, increasing quickly until saturation of the resin in 70 minutes. The chloride salt showed a jump in concentration at 10 minutes, increasing quickly until 340 mg/L in 20 minutes, hence above its initial concentration in the sample. It then decreased to 250 mg/L, subsequently remaining constant until the end of operation. This means that the chloride front was displaced by the sulfate within the fixed bed and hence a chloride elution peak was observed ahead of the sulfate front. The nitrate salt was detected at the outlet of the column after 15 minutes of operation, increasing progressively until nearly reaching its initial concentration in 70 minutes, subsequently remaining constant until the end of operation. The operational capacity of the bed was found to be: 4 mg SMX /mL wet resin, 7 mg NO_3^-/mL wet resin, 49 mg Cl^-/mL wet resin and 57 mg SO_4^{2-}/mL wet resin.

The resin was then regenerated using a solution of NaOH 0.5M at a down-flow rate of 9 mL/min for 60 minutes. As in the previous cycle, a high elution peak was detected in the case of the sulfate salt, reaching a concentration of 2656 mg/L (9.5 times the initial concentration). It then decreased rapidly, being completely removed in 20 minutes. Nitrate reached a concentration of 115 mg/L (2.6 times its initial concentration), also being completely removed in 20 minutes. In the case of SMX, no peak was detected in the first minutes of operation seeing as the concentration decreased very quickly, less than 10 mg SMX/L being detected at the outlet from the first minutes of operation, obtaining complete removal in 10 minutes. As in the other cycle, 100% of all compounds were recovered. The breakthrough curves for the load and elution steps of the second cycle are shown in Figure 9a-b.

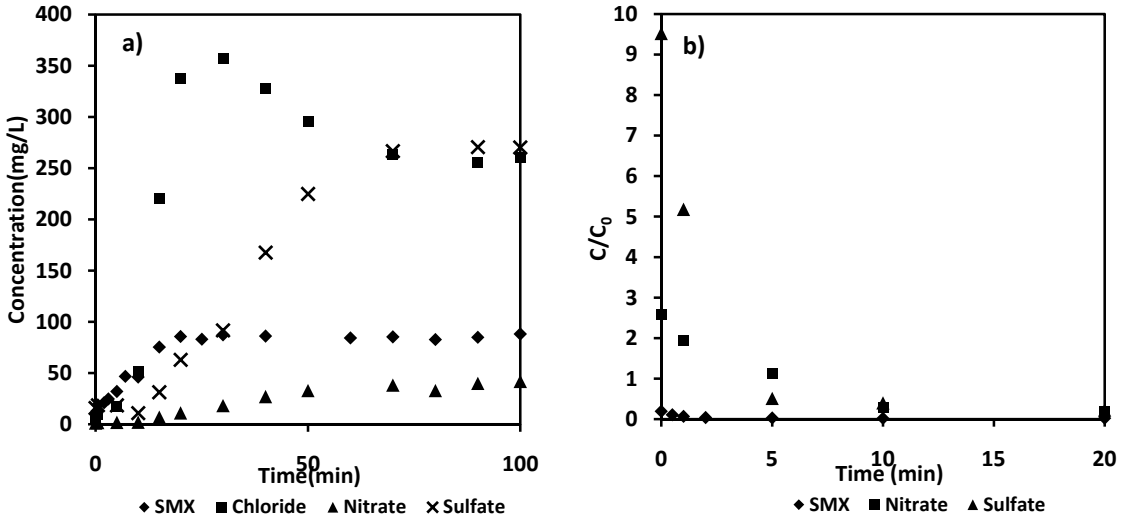

Figure 9. Breakthrough curves for the sorption (a) of SMX, chloride, sulfate and nitrate from synthetic solutions prepared in distilled water, and elution (b) using NaOH 0.5M, onto Lewatit MP500. Conditions: $[SMX]_0$= 90 mg/L, $[SO_4^{2-}]_0$= 250 mg/L, $[Cl^-]$= 250 mg/L, $[NO_3^-]_0$=50 mg/L; flow rate load= 10.5 ml/min, flow rate elution= 9 mL/min, volume resin= 1.9 mL; Z=3 cm.

Comparing these results with those obtained in single assays of SMX in a fixed bed column, a high decrease in the capacity to adsorb SMX can be observed. In single assays employing an initial concentration of 200 mg SMX/L and a flow rate of 11 ml/min, an adsorption capacity of 194 mg SMX/mL wet resin[20] was obtained. Now, using 125 mg SMX/L in mixtures, an adsorption capacity of 5 mg SMX/mL wet resin was obtained. This means that the presence of salts in solution affects the resin's capacity to adsorb SMX. The resin showed more affinity for sulfate and chloride salts than for SMX.

3.4. Fixed Bed Model

In the cases of the load and elution curves, analysis of the fixed bed experiments was carried out considering a model developed by Costa[31] and used by Fernandez et al.[32,33]. This model was used to simulate the load and elution breakthrough curves in a laboratory column. The model takes into account aspects of equilibrium and kinetics, axial dispersion in the column and no film transfer resistance. The developed model can be seen in López et al.[20].

Parameters such as bed porosity, particle porosity, equilibrium constants, diffusivities in the pores and the capacity of the resin must be known to solve the fixed bed model. All these parameters were determined for the system in previous batch experiments. The equations of the proposed model in this case are:

- Conservation of the mass of solute in the solution:

$$\frac{1}{Pe}\frac{\partial^2 x_i(z^*,\theta_{st})}{\partial z^{*2}} - \frac{\partial x_i(z^*,\theta_{st})}{\partial z^*} = \frac{\partial x_i(z^*,\theta_{st})}{\partial \theta_{st}} + \frac{15\varepsilon_i(1-\varepsilon_l)N_D}{\varepsilon_l}\left[x_i(z^*,\theta_{st}) - x_{pi(z^*,\theta_{st})}\right] \quad (22)$$

- Conservation of the mass of solute inside the particles:

$$\frac{\partial x_{pi}(z^*,\theta_{st})}{\partial \theta_{st}} = \frac{15\varepsilon_i N_{Di}}{\varepsilon_i + \frac{K_i\, q_{Ti}/_{C_{Ti}}}{\left(1+(K_i-1)x_{Pi}(z^*,\theta_{st})\right)^2}} \left[x_i(z^*,\theta_{st}) + x_{pi(z^*,\theta_{st})}\right] \quad (23)$$

Obtained via the relationship:

$$\frac{\partial q_i}{\partial t} = \frac{\partial q_i}{\partial C_i}\frac{\partial C_i}{\partial t} \quad (24)$$

In which $\partial q_i/\partial C_i$ was obtained by differentiating the equilibrium isotherm.

- Boundary conditions in the solution

$$z^* = 0 \qquad x_i(z^*,\theta_{st}) = x_{Ti} \quad (25)$$

$$z^* = L \qquad \frac{\partial x_i(z^*,\theta_{st})}{\partial z^*} = 0 \quad (26)$$

- Initial conditions:

$$\theta_{st}=0 \quad \partial x_i(z^*,\theta_{st}) = x_{Ti} \text{ en } z^*=0 \quad (27)$$

$$\theta_{st}=0 \quad x_i(z^*,\theta_{st}) \text{ depends on washing } \forall z^*>0 \quad (28)$$

The spatial coordinate inside the column is normalized by L, the length of the column, and time by the stoichiometric time, t_{st}, i.e. the time for the resin to become completely saturated. N_D is the number of intraparticle mass transfer units ($N_D = \tau D_p/R_0$), with $\tau = L/u_i$, special time. *Pe* is the Peclet number, $Pe = u_i L/D_{AX}$. The axial dispersion parameter was not available for the laboratory column, so it was considered the sole parameter model fit. A FORTRAN subroutine, PDECOL[28], was used to solve the proposed differential equation system for the fixed bed model.

The values of the different parameters used in this study and the axial dispersion calculated as a fitting parameter in the load and elution steps for chloride, sulfate, nitrate and SMX are shown in Table 4. The experimental and theoretical breakthrough curves for the load and elution steps obtained in the first cycle are shown in Figures 10 and 11, respectively. A good correlation can be observed between experimental results and the numerical solution of the fixed bed model for the load and elution steps, thus showing the validity of the model.

Table 4. Fixed bed operating parameters

	SO_4^{2-}	Cl^-	NO_3^-	SMX
$K_{eq\text{-}CSF}$	68.54	23.35	48.72	3.30
Diffusivity in pores (cm^2/s)	$2.7\cdot10^{-8}$	$3.9\cdot10^{-8}$	$2.3\cdot10^{-8}$	$1.3\cdot10^{-8}$
D_{AX} (cm^2/s) load	12	16	12	5
D_{AX} (cm^2/s) elution	90	---	60	90
Retention Capacity (mg/mL resin) 1st cycle	50	42	15	5
Retention Capacity (mg/mL resin) 2nd cycle	57	49	7.2	4
Flow (ml/min)	11			
Bed Porosity (ε_l)	0.5			
Particle Porosity	0.34			
Bed Height (cm)	3			

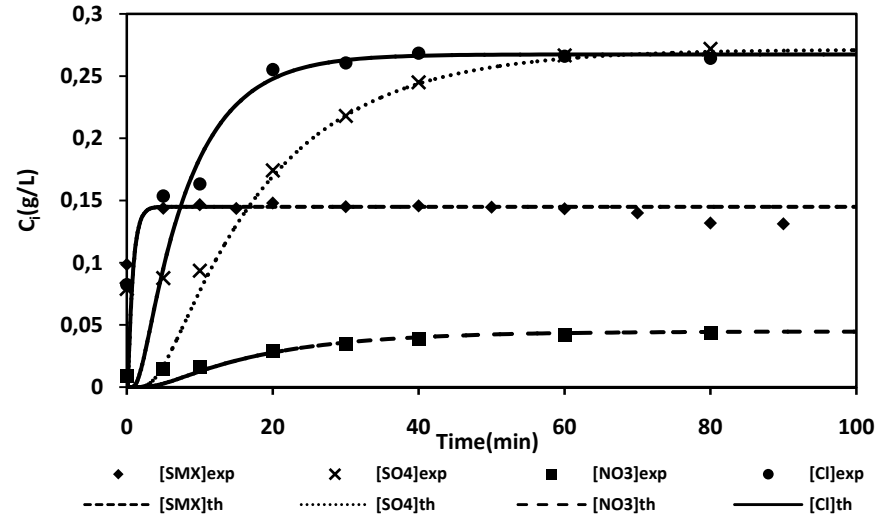

Figure 10. Experimental and theoretical load breakthrough curves for SMX, chloride, sulfate and nitrate from synthetic solutions prepared in distilled water, onto Lewatit MP500. Conditions: [SMX]0= 125 mg/L, [SO42-]0= 250 mg/L, [Cl^-]= 250 mg/L, [$NO3^-$]0=50 mg/L; flow rate= 11 ml/min; volume resin= 1.9 mL (Z=3 cm).

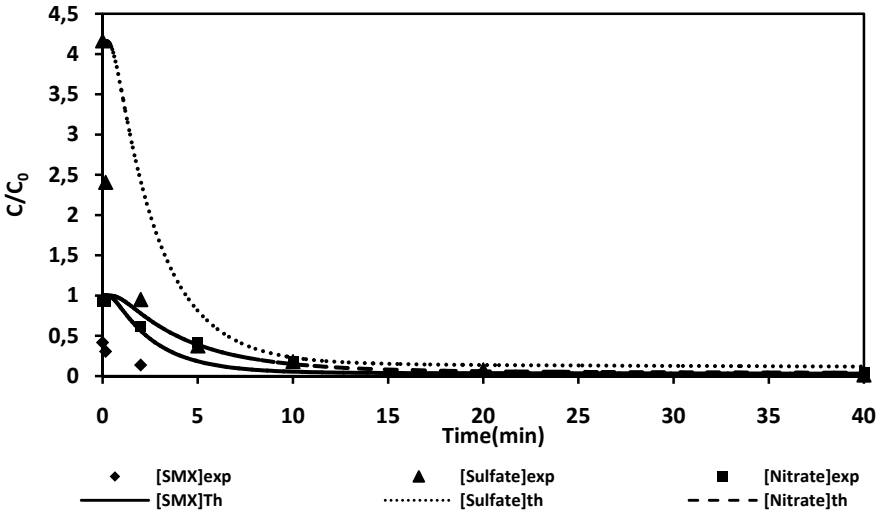

Figure 11. Experimental and theoretical elution curves for SMX, sulfate and nitrate from synthetic solutions using NaOH 0.5 M as eluent in a fixed bed onto Lewatit MP500. Conditions: $[SMX]_0$= 125 mg/L, $[SO_4^{2-}]_0$= 250 mg/L, [Cl^-]= 250 mg/L, $[NO_3^-]_0$=50 mg/L; flow rate= 10 ml/min, volume resin= 1.9 mL (Z=3 cm).

4. Conclusions

The removal of SMX in the presence of salts (sulfate, nitrate and chloride) using a strong anionic resin (Lewatit MP500) was carried out successfully. Batch experiments were conducted using synthetic solutions of SMX (C_0= 62-124 mg/L) and a fixed concentration of salts (250 mg Cl^-/L, 250 mg SO_4^{2-}/L and 50 mg NO_3^-/L) with an L/S ratio (volume of liquid(mL)/mass of wet resin(g))= 150-250. Experiments with salts in a single component system were also carried out in batch mode, using synthetic solutions of nitrate (C_0=50-125 mg/L), sulfate (C_0= 50-300 mg/L) and chloride (C_0=50-350 mg/L) salts, respectively, with an L/S ratio= 1000, the highest adsorption capacity being obtained for the sulfate. The adsorption

process in mixtures was relatively fast, with equilibrium being established in 100 minutes. To study the equilibrium of the process, the experimental data were fitted to Langmuir and Constant Separation isotherms, and to the Extended Langmuir isotherm for a multicomponent system. The results showed that there was competition between components in the adsorption process in mixtures. The equilibrium constants for the Extended Langmuir isotherm were: $K_{eq\ SMX}$= 1.4 L/g SMX, $K_{eq\ Nitrate}$= 6 L/g NO_3^-, and $K_{eq\ Sulfate}$= 9 L/g SO_4^{2-}, with a maximum adsorption capacity, q_T= 105 g SMX/L wet resin. In the case of salts in a single component system, the results were: $K_{eq\text{-}Lang.\ Sulfate}$=151.6 L/g SO_4^{2-}, $q_{T\ sulfate}$= 76.9 g SO_4^{2-}/L wet resin; $K_{eq\text{-}Lang\ Nitrate}$= 66.7 L/g NO_3^-, $q_{T\ Nitrate}$= 73.8 g NO_3^-/L wet resin and $K_{eq\text{-}Lang.\ Chloride}$=12.7 L/g Cl^-, $q_{T\ Chloride}$=35.2 g Cl^-/L wet resin. Hence, the resin presents more affinity for the sulfate than for the other salts. The kinetics of adsorption of SMX in mixtures was studied using the film mass transfer model and the pore diffusion model, obtaining the mass transfer coefficient (K_f), and the intraparticle diffusivity (D_p) from experimental data. The values obtained were: $K_{f\ SMX}$ = $5.5 \cdot 10^{-6}$ cm/s and $D_{p\ SMX}$= $1.3 \cdot 10^{-8}$ cm^2/s. In the case of salts in a single system, the mass transfer coefficient and the pore diffusivity values were also obtained.

Load and elution cycles in a fixed bed column were carried with synthetic solution mixtures of SMX and salts, using Lewatit MP500 resin and a solution of NaOH 0.5 M as the eluent. The retention capacity of the resin and the ability of the eluent were evaluated. The breakthrough curves showed that the resin was able to adsorb SMX despite the presence of salts. Furthermore, NaOH was found to be a good eluent because it allows the concentrating of sulfate and nitrate salts, thereby enabling simple treatment of these compounds, at the same time as recovering 100% of SMX, sulfate and nitrate in all the elution steps. Fixed bed operation was simulated using a proposed model that takes into account axial dispersion, equilibrium and kinetic parameters for the system under study. The numerical solution shows a good agreement between experimental data and the predicted values for the load and elution curves.

Acknowledgements

Author Ana María López acknowledges a PhD fellowship from the Severo Ochoa Programme (Gobierno Regional del Principado de Asturias, Spain)

References

1. Xu, W.; Zhang, G.; Zou, S.C.; Li, X.D.; Liu, Y.C. Determination of selected antibiotics in the Victoria Harbour and the Pearl River, South China using high-performance liquid chromatography-electrospray ionization tandem mass spectrometry. *Environ. Pollut.* **2007,** *145*, 672-679.
2. Silvia Díaz-Cruz, M.; López de Alda, M.J.; Barceló, D. Environmental behavior and analysis of veterinary and human drugs in soils, sediments and sludge, *Trends in Analytical Chemistry*, **2003**, *22* (6), 340-351.
3. Homen, V. and Santos, L. Degradation and removal methods of antibiotics from aqueous matrices-A review. *Journal of Environment Management* **2011**, *92*, 2304-2347.
4. Grassi, M.; Kaykioglu, G.; Belgiorno, V.; Lofrano, G. Removal of Emerging Contaminants from Water and Wastewater by Adsorption Process. In *Emerging Compounds Removal from Wastewater;* G. Lofrano (ed.), SpringBriefs in Green Chemistry for Sustainability, 2012; pp. 15-37.
5. Andreozzi, R.; Canterino, M.; Marotta, R.; Paxeus, N. Antibiotic removal from wastewaters: the ozonation of amoxicillin. *J. Hazard. Mater.* **2005,** *122*, 243-250.
6. Balcioğlu, L.A.; Ötker, M. Treatment of pharmaceutical wastewater containing antibiotics by O_3/H_2O_2 processes. *Chemosphere* **2003,** *50*, 85-95.
7. Trovó, A.G.; Nogueira, R.F.P.; Agüera, A.; Sirtori, C.; Fernández-Alba, A.R. Photodegradation of sulfamethoxazole in various aqueous media: persistence, toxicity and photoproducts assessment, Chemosphere **2009,** *77*, 1292-1298.
8. Pérez-Moya, M.; Graells, M.; Castells, G.; Amigó, J.; Ortega, E.; Buhigas, G.; Pérez, L.M.; Mansilla, H.D. Characterization of the degradation performance of the sulfamethazine antibiotic by Photo-Fenton process, *Water Res*. **2010,** *44*, 2533-2540.
9. Li, S.Z.; Li, X.-Y.; Wang, D.-Z. Membrane (RO-UF) filtration for antibiotic wastewater treatment and recovery of antibiotics. *Sep. Purif. Technol*. **2004,** *34* (1-3), 109-114.

10. Vieno, N.M.; Härkki, H.; Tuhkanen, T.; Kronberg. L. Occurrence of pharmaceuticals in river water and their elimination in a pilot-scale drinking water treatment plant. *Environ. Sci. Technol*. **2007,** *41*, 5077-5084.
11. Stackelberg, P.E.; Gibs, J.; Furlong, E.T.; Meyer, M.T.; Zaugg, S.D.; Lippincott, R.L. Efficiency of conventional drinking water treatment processes in removal of pharmaceuticals and other organic compounds. *Sci. Total Environ*. **2007,** *377,* 255-272.
12. Tong, D.S.; Zhou, C.H.; Lu, Y.; Yu, H.; Zhang, G.F.; Yu. W.H. Adsorption of acid red dye on octadecyl trimetilammonium montmorillonite, *Appl. Clay Sci*. **2010,** *50*, 427-431.
13. Putra, E.K.; Pranowo, R.; Sunarso, J.; Indraswati, N.; Ismadji. S. Performance of activated carbon and bentonite for adsorption of amoxicillin from wastewater: mechanism, isotherms and kinetics. *Water Res*. **2009,** *43*, 2419-2430.
14. Rivera-Utrilla, J.; Prados-Joya, G.; Sánchez Polo, M.; Ferro Garcia, M.A.; Bautista-Toledo, I. Removal of nitroimidazole antibiotics from aqueous solution by adsorption/bioadsorption on activated carbon. *J. Hazard. Mater*. **2009,** *170*, 298-305.
15. Gupta, V.K.; Carrott, P.J.M.; Ribeiro Carrott, M.M.L.; Sushas, T.L. Low cost adsorbents: growing approach to wastewater treatment- a review, Crit. Rev. *Env. Sci. Technol*. **2009,** *39*, 783-842.
16. Crisafully, R.; Milhome, M.A.L.; Cavalcante, R.M.; Silveira, E.R.; De Keukeleire, D.; Nascimiento, R.F. Removal of some polycyclic aromatic hydrocarbons from petrochemical wastewater using low-cost adsorbent of natural origin. *Bioresour. Technol.* **2008**, *99*, 4515-4519.
17. Adams, C.; ASCE, M.; Wang, Y.; Loftin, K.; Meyer, M. Removal of antibiotics from surface and distilled water in conventional water treatment processes, *J. Environ. Eng.* **2002**, *128,* 253-260.
18. Choi, K.-J.; Son, H.-J.; Kim, S.-H. Ionic treatment for removal of sulphonamide and tetracycline classes of antibiotic. *Sci. Total Environ.* **2007,** *387*, 247-256.
19. Vergili, I.; Barlas, H. Removal of selected pharmaceutical compounds from water by an organic polymer resin. *Journal of Scientific & Industrial Research* **2009,** *68*, 417-425.
20. López, A.M.; Rendueles, M.; Díaz, M. Sulfamethoxazole removal from synthetic solutions by ion Exchange using a strong anionic resin in fixed bed. *Solvent Extraction and Ion exchange* **2013**, *31*, 763-781.
21. Yuh, SH. Selection of optimum sorption isotherm. *Carbon* **2004**, *42*, 2113-1230.
22. Aksu, Z.; Tunç, O. Application of biosorption for penicillin G removal comparison with activated carbon. *Process Biochem.* **2004**, *40*, 831-847.
23. Shallcross, M.; Herrmann, C.C.; McCoy, B.J. An improved model for the prediction of multicomponent ion exchange equilibria. *Chem. Eng. Sci.* **1988**, *43*, 279-288.
24. Boyd, G.E.; Adamson, A.W.; Myers, L.S. The exchange adsorption from aqueous solutions by organic zeolites. II. Kinetics. *Journal of the American Chemical Society* **1947,** *69*, 2836-2848.
25. Boyd, G.E.; Schubert, J.; Adamson, A.W. The exchange adsorption of ions from aqueous solutions by organic zeolites. I. Ion-exchange Equilibria. *Journal of the American Chemical Society,* **1947,** *69* (11), 2818-2829.
26. Helfferich, F. *Ion Exchange*; McGraw-Hill, New York, 1962.
27. Rodrigues, A.E., Tondeur, D. *Percolation Processes: Theory and Applications*, NATO ASI Series, 1981, pp. 31-81.
28. Madsen, N.K. Sincovec. R.F. Algorithm 540: PDECOL, General Collocation Software for Partial Differential Equations [D3]. *ACM Transactions on Mathematical Software (TOMS)* **1979**, *5* (3), 326-351.
29. Reid, R.C., Praustniz, J.M., Poling, B.E. (1988) *The properties of Gases and Liquids*. McGraw-Hill, New York.
30. Wilke, C.R., Chang, P. (1955) Correlation of diffusion coefficients in dilute solutions. *AIChE J., 1* (2): 264-270.
31. Costa, C. Rodrigues, A. Design of cyclic fixed-bed adsorption processes. Part I: Phenol adsorption on polymeric adsorbents, *AIChE Journal* **1985,** *31*(10), 1645-1654.
32. Fernández, A. Rodrigues, A.E. Díaz, M. Modelling of Na/K Exchange in Fixed Beds with Highly Concentrated Feed. *Chem. Eng. J.* **1994,** *54*, 17-22.
33. Fernández, A.; Rendueles, M.; Rodrigues, A. Díaz, M. Co-ion behavior at high concentration cationic ion exchange. *Ind. Eng. Chem. Res.* **1994,** *33* (11), 2789-2794.

4.4. RETENCIÓN COMPETITIVA ENTRE SULFAMETOXAZOL Y SULFAMETAZINA SOBRE RESINA DE INTERCAMBIO IÓNICO ANIÓNICA FUERTE

En este subapartado se recogen los resultados obtenidos en el proceso de intercambio iónico de mezclas sintéticas de sulfametoxazol y sulfametazina empleando una resina aniónica fuerte.

En la publicación que se presenta a continuación se ha pretendido describir la competencia existente en el proceso de intercambio iónico entre dos sulfamidas, sulfametoxazol y sulfametazina, que generalmente aparecerán juntas en las aguas, empleando una resina aniónica fuerte, Lewatit MP500, y poder comparar los resultados con los obtenidos con cada sulfamida en sistemas individuales. Se ha estudiado el equilibrio y la cinética del proceso en tanque agitado. Se han determinado los parámetros de equilibrio y cinéticos, ajustando los datos experimentales a isotermas de adsorción para sistemas binarios, y se ha determinado la constante cinética de difusividad en poros. Asimismo, se ha estudiado la operación en columna con mezclas de ambas sulfamidas, para ver como varían las capacidades de retención respecto al sistema individual y comprobar la efectividad del eluyente en la regeneración de la resina. A su vez, de modelizó la operación en columna empleando un modelo de lecho fijo.

Artículo: Competitive retention of sulfamethoxazole (SMX) and sulfamethazine (SMZ) in a strong anionic ion exchange resin

Situación: artículo bajo revisión en *Solvent Extraction and Ion Exchange* (Manuscript N14-16)

COMPETITIVE RETENTION OF SULFAMETHOXAZOLE (SMX) AND SULFAMETHAZINE (SMZ) IN A STRONG ANIONIC ION EXCHANGE RESIN

Ana María López Fernández, Manuel Rendueles* and Mario Díaz

Department of Chemical Engineering and Environmental Technology, University of Oviedo, Oviedo, Spain

ABSTRACT

Numerous antibiotics such as sulfonamides have been found in effluents from drug manufacturers. Removal of pharmaceuticals by adsorption and ion exchange comprise some of the most promising techniques for the retention of these compounds from wastewaters due to their low cost, easy regeneration and selective removal of pollutants. This paper studies the removal of sulfamethoxazole (SMX) and sulfamethazine (SMZ), the most common sulfonamide antibiotics detected in municipal sewage. Lewatit MP500 (Lanxess Chemical) ion exchange resin was used to remove SMX and SMZ present in solutions. Batch experiments were carried out in cylindrical stirred tanks. Binary system solutions of equal mass concentration were prepared containing 30-250 mg/L of each compound, SMX and SMZ, and tested with an L/S ratio (mL solution/g resin) = 1000 obtained in previous experiments. Equilibrium and kinetics were studied in order to characterize the operation. The adsorption equilibrium constants for SMX and SMZ were determined using a modified extended Langmuir model for multicomponent equilibrium sorption. Kinetics was analyzed using pore diffusion model. Finally, several loading and elution cycles were carried out in fixed bed to obtain the breakthrough curves, comparing the experimental data to predicted values from a fixed bed model.

Keywords: ion exchange, pharmaceutical contaminants, isotherms, kinetics, fixed bed operation

1. Introduction

The use of antibiotics in veterinary and human medicine has become widespread in recent years (annual consumption of 100 000-200 000 tons) [1], consequently increasing the likelihood of water contamination with such compounds. Human and veterinary antibiotics have been detected in sewage, agricultural wastewater, surface water, and the influent to and treated water from drinking water treatment [2, 3]. The chief ways that drugs are introduced into the environment are via waste effluents from manufacturing processes, excreta, disposal of unused or expired drug products, and accidental spills during manufacturing or distribution. Among these, animal excreta are the major source of environmental contamination by drugs, as most of the drug used in veterinary medicine ends up in manure. When dispersed on fields as a fertilizer, manure can contaminate soil and hence surface water and groundwater through run-off or leaching. Human antibiotics are likewise introduced into the environment through excretion (urine and feces), ending up at wastewater treatment plants (WWTPs). Most WWTPs are not designed to remove highly polar micropollutants like antibiotics [4]. These may consequently be transported to surface waters and reach groundwater after leaching. Eventually, contaminated surface waters can enter drinking water treatment plants (DWTPs), which are also not equipped to remove these compounds, which mean that they end up in the water distribution system.

Another important source of contamination is the direct release of veterinary antibiotics through their application in aquaculture. Waste effluents from the manufacturing process or accidental spills during manufacturing can also be considered significant sources of

contamination [5, 6]. Antibiotics are detected in the higher µg/L range in effluents, lower µg/L range in municipal wastewater and ng/L range in surface, sea and groundwater. The accumulation and persistence of antibiotics in the environment can produce harmful effects, in either aquatic or terrestrial ecosystems. Although present at vestigial levels, antibiotics may lead to increased resistance in bacterial populations, making them ineffective in the treatment of several diseases in the foreseeable future. Therefore, a practical, economic solution needs to be achieved to reduce the daily amounts of antibiotics discharged into the environment. A wide range of chemical and physical methods for the removal of organic compounds can be employed. Depending on the pollutant concentration in the effluent and the cost of the process, different methods may be chosen [7].

Biological processes are the most widely used at conventional wastewater treatment plants [8,9,10]. However, new alternatives have emerged due to the low efficiencies of these methods and the impossibility of implementing them at times. Oxidation processes such as chlorination [11] and the advanced oxidation process [12, 13, 14, 15] are oxidative methods that could be applied to fluctuating rate compositions. However, they have a number of drawbacks, such as producing toxic products and being pH-dependent, besides the high cost of equipment and high energy requirements to power the process. Membrane processes such as reverse osmosis, nano- and ultrafiltration [16] are effective for reducing high levels of dissolved salts, but present limitations with respect to the removal of organic compounds. They are sensitive to temperature, the organic material and the concentration of the dissolved salts, which can lead to deterioration of the membrane structure. The adsorption process is widely used in industry to remove organic contaminants. This technique has the advantage of removing analytes instead of producing more dangerous metabolites [17, 18]. The most widely used adsorbents are granular carbons (GACs), although they present the drawbacks of their cost and difficulty of regeneration. Interest in alternative adsorbents has accordingly grown aimed at finding new low-cost adsorbents [19].

Polymer resins are becoming more widely used in wastewater treatment due to their low cost, easy regeneration and selective removal of pollutants. Adams[2] and Choi[3] studied the use of polymeric resin to remove sulfonamides and tetracyclines, obtaining high removal efficiencies (90% for sulfonamides and >80% for tetracyclines). Vergili[20] studied the adsorption of carbamazepine, propyphenazone and sulfamethoxazole using a polymeric resin, Lewatit VP OC 1163. This resin showed a high adsorption capacity for pharmaceuticals with low solubility.

The antibacterial sulfonamides sulfamethoxazole (SMX) and sulfamethazine (SMZ) are common antibiotics used to treat urinary tract infections in humans and animals. They prevent the formation of dihydrofolic acid, a compound that bacteria must be able to produce in order to survive. They are the most frequently detected sulfonamides in municipal sewage. Studies carried out in 1988 by the National Centre for Toxicological Research indicated that SMZ is carcinogenic and that thyroid tumors developed in rats and mice after they received 2.4-4.8 ppm of SMZ in their diet over 2 years.

The aim of the present study was to investigate the feasibility of ion exchange treatment of effluents from pharmaceuticals plants containing mixtures of sulfonamides such as sulfamethoxazole (SMX) and sulfamethazine (SMZ) and their competition in the process of ion exchange in mixtures. Lewatit MP500, a macroporous strong anion exchange resin was tested to determine its capacity to retain SMX and SMZ in mixtures, comparing the results with those previously obtained for each compound individually. Equilibrium and kinetics were studied in order to characterize the removal process. The adsorption equilibrium constants were determined using a modified extended Langmuir model for multicomponent equilibrium sorption. The kinetics was analyzed using two models: a film mass transfer model and the pore diffusion model. Finally, several loading and elution cycles were performed in a fixed bed column to assess the behavior of the resin in an industrial operation. The breakthrough curves of the loading and elution steps were fitted using a fixed-bed adsorption model.

The effectiveness of ion exchange operation in batch experiments using mixtures of sulfamethoxazole (SMX) and trimethoprim (TMP) and their competition were studied as these two compounds are generally administered in combination at a ratio of 1:5 (TMP: SMX).

2. Materials and methods

2.1. Materials

Sulfamethoxazole (purity>98 % w/w), sulfamethazine (purity ≥99% w/w) and trimethoprim (purity ≥99% w/w) were purchased from Sigma-Aldrich. The chemical properties of sulfamethoxazole are: molecular formula: $C_{10}H_{11}N_3O_3S$; melting point: 171 ºC, molecular weight: 253.28 g/mol; dissociation constants: pKa_1= 1.6 (aromatic amine) and pKa_2= 5.7(sulfonate nitrogen); octanol/water partition coefficient: log K_{ow}= 0.89; solubility in water: 610 mg/L at 37ºC; from Hazardous Substances Data Bank (HSDB). For sulfamethazine, its chemical properties are: molecular formula: $C_{12}H_{14}N_4O_2S$; melting point: 197ºC; molecular weight: 278.33 g/mol; dissociation constants: pKa_1= 2.65 (aromatic amine) and pKa_2= 7.65 (sulfonate nitrogen); octanol/water partition coefficient: log K_{ow}= 0.14; solubility in water: $1.5 \cdot 10^3$ mg/L (29ºC) and $1.92 \cdot 10^3$ mg/L (37ºC), solubility increases with increasing pH; from HSBD. The chemical properties of trimethoprim are: molecular formula: $C_{14}H_{18}N_4O_3$; molecular weight: 290.32 g /mol; dissociation constants pKa= 7.12; octanol/water partition coefficient: log K_{ow} = 0.91; solubility in water: 400 mg/l at 25º C; from HSBD.

Methanol (HPLC grade) was used for liquid chromatography and ultra-pure water was prepared in a Milli-Q purification system. The filters used for filtration were obtained from Millipore (0.45 µm PVDF for samples) and Whatman (0.22 µm PTFE for the mobile phase). Stock solutions were prepared by dissolving the pharmaceutical in distilled water. Experiments were carried out at pH values of pharmaceuticals in solutions, pH= 5.0-5.5, monitoring the pH over time to check that remaining constant during the essays.

A commercial organic polymeric resin, Lewatit MP500, manufactured by Lanxess (Lenntech) was used as the ion exchange resin. The strong base resin Lewatit MP500 has a quaternary amine (macroporous type I) and a crosslinked polystyrene matrix. The main properties of the resin are shown in Table 1.

Table 1 Characteristics of Lewatit MP500 anion-exchange resin[a]

General description	
Ion form	Cl^-
Functional group	Quaternary amine (type I)
Matrix	Crosslinked polystyrene
Polymer structure	Macroporous
Bead side >90% (mm)	0.47(±0.06)
Density (g/mL)	1.06
Total capacity (min.eq/L)	1.1

[a] Information provided by the manufacturer.

2.2. Analytical methods

Determination of sulfamethoxazole, sulfamethazine and trimethoprim in the samples was performed by HPLC (Agilent 1200) using a column Mediterranean sea18 (5µm x 25 cm x 46 cm, plus a reverse-phase column from Waters) combined with UV detection. The wavelength used for detection was 270 nm. Prior to HPCL analysis, the samples were filtered through 0.45 µm PVDF filters. The mobile phase consisted of eluent A (0.1% TFA in methanol) and eluent B (0.1% TFA in water). The method comprised a binary gradient from 30% solution A to 95% solution B. The column compartment temperature was 40ºC. Run time: 12 min. Post

time: 3 min. Injection volume: 20µL. Analysis was performed at flow rate of 0.7 mL/min. The retention times in mixtures of SMX+SMZ were 8.9 min for SMX and 9.2 for SMZ; and in mixtures of SMX+TMP, 8.5 for TMP and 9.2 for SMX.

2.3. Adsorption Studies

2.3.1. Batch Experiments

Batch experiments were carried out at room temperature in cylindrical stirred tanks at a stirring rate of 300 rpm. The resin was conditioned by contacting it with a solution of NaOH 1 M with an L/S ratio (volume of liquid (mL)/ mass of resin (g)) of 20, 2 times, 20 minutes each time. Next, the resin was washed with distilled water twice for 5 minutes each time with a ratio L/S= 50, and then separated from the solution.

The resin was subsequently contacted with the loading solution. The L/S ratio was adjusted by maintaining the volume of solution (300 mL) and varying the amount of resin. The contact time was 120 minutes in all tests; this time being considered sufficient to reach operating equilibrium. The volume of the samples extracted from the tank each time was 2 mL, which did not change the volume of the solution appreciably. The concentration of SMX, SMZ and TMP ions in the resin was determined by mass balance, calculating the difference between the initial and final amount of charged ions in the solution.

2.3.2. Column Experiments

Continuous flow adsorption experiments were carried out in a glass column with an internal diameter of 1.1 cm and a total length of the tube of 25 cm. The column was prepared by packing it with 2 grams of wet resin (3 cm). Solutions were pumped through the column by a peristaltic pump (Masterflex) in down-flow mode.

To condition the resin in the fixed bed, a solution of NaOH 1M was pumped through the column for 20 minutes at a flow rate of 11 mL/min. Distilled water was then fed through the column at a flow rate of 11 mL/min for 15 minutes to wash the resin.

Two loading stages using synthetic solutions of SMX and SMZ in an equal mass concentration of 200 and 300 mg/L of each compound were carried out at a down-flow rate of 4.5 mL/min and 5.1 mL/min, respectively. The effluent samples were collected (4 mL approximately) at specified times intervals (5-10 minutes) and measured by HPLC to monitor the evolution of the SMZ and SMX concentration with time. Breakthrough curves were plotted until the concentration at the outlet of the column effluent reached the initial concentration of the feed solution. After adsorption, distilled water was fed through the column to wash it and remove any unabsorbed ions on the adsorbent surface or entrapped between adsorbent particles.

After each loading stage, an elution stage was carried out by pumping a solution of NaOH 0.5M through the column at a down-flow-rate of between 4.2 mL/min and 5.3 mL/min, respectively. Effluent samples were collected at the outlet of the column every 5-10 minutes, monitoring the evolution of the concentration with time. The elution curve was plotted until no SMZ or SMX concentration was detected at the outlet of the column.

3. Results and discussion

3.1. Batch equilibrium study

In order to assess the behavior of the MP500 resin under different L/S ratios (500, 800, 1000, 1200, 1500 and 1800), several runs were carried out to obtain the appropriate L/S ratio, in which different amounts of resins were loaded with 300 mL of the SMZ + SMX synthetic solution at a concentration of 100 mg/L of each pharmaceutical, monitoring the concentration over time until reaching equilibrium. A mass balance was used to determine the equilibrium compositions of the resin and the solution phase. The results show that an L/S ratio of 1000 was

suitable to obtain concentrations of 23.2 mg SMX/L and 82.3 mg SMZ/L at equilibrium, with an overall operational capacity of 22.2 mg SMZ/g wet resin and 74.1 mg SMX/g wet resin. This L/S ratio was accordingly chosen for all the subsequent equilibrium and kinetic tests.

For the equilibrium experiments, the MP500 resin was contacted with different SMX and SMZ solution concentrations at a 1:1 ratio of SMX and SMZ (30, 50, 80, 100, 150, and 200 mg/L), employing an L/S ratio (volume of liquid (mL)/mass of resin (g)) = 1000. The results show that equilibrium is reached in all cases in approximately 120 minutes. The adsorption capacities and equilibrium concentrations values obtained in binary system were shown in Table 2.

Table 2 Equilibrium concentrations (C_{ei}) and adsorption capacities (q_{ei}) for SMX and SMX in binary system in batch essays.

C0-SMX + SMZ (mg/L)	Ce-SMX (mg/L)	Ce-SMZ (mg/L)	qe-SMX (mg/g wet resin)	qe-SMZ (mg/g wet resin)
30	5.7	13.7	22.9	14.0
50	10.1	27.4	37.2	19.0
80	15.9	52.7	61.5	20.9
100	23.2	82.3	74.1	22.2
150	31.7	125.8	114.1	19.3
200	56.5	178.5	129.9	21.5

In previous trials using each compound separately, the adsorption capacities obtained using concentrations of 50 mg/L of each compound were 54.2 mg SMX/g wet resin and 40.1 mg SMZ/g wet resin; while in trials using concentrations of 150 mg/L, the results were 134 mg SMX/g wet resin and 82.6 mg SMZ/g wet resin. Therefore, if we compare the results of these compounds in single trials and in trials where they were combined in a mixture, it can be seen that the resin has more affinity for SMX than for SMZ, there being a greater decrease in the capacity of adsorption in mixtures in the case of SMZ than in the case of SMX. Higher adsorption capacities for SMX were obtained in all trials involving mixtures.

The Langmuir sorption isotherm is the best known and the most widely used isotherm for the sorption of a solute from a liquid solution:

$$q_{ei} = \frac{K_L \cdot C_{ei}}{1 + a_L \cdot C_{ei}} \quad (1)$$

where K_L is the Langmuir equilibrium constant (L/mg), a_L is the Langmuir constant related to the energy of adsorption(mg/L), q_{ei} is the amount of component i adsorbed by resin at equilibrium (mg/g wet resin) and C_{ei} is the solution equilibrium concentration of specie i (mg/L). The Langmuir constants K_L and a_L can be determined from a linearized form of Langmuir equation. The monolayer capacity of the Langmuir isotherm, Q_m, is given as:

$$Q_m = \frac{K_L}{a_L} \quad (2)$$

Multicomponent equilibrium studies have passed through many stages of development. However, none of the multicomponent equilibrium studies has dealt with competitive adsorption and only a few have addressed the selectivity of the adsorption process. Extensions of several isotherms were used to model the experimental data, namely the extended Langmuir equation and the Jain and Snoeyink modified extended Langmuir model [21]. If there are two solutes present together in the sorption system, the extended Langmuir (EL) equation, using a linear transform method (LTFM), is:

$$q_{ei}=\frac{K_{Li}\cdot C_{ei}}{1+\sum a_{Li}C_{ei}} \quad (3)$$

For example, using components 1 and 2:

$$q_{e1}=\frac{K_{L1}\cdot C_{e1}}{1+a_{L1}\cdot C_{e1}+a_{L2}\cdot C_{e2}} \quad (4)$$

$$q_{e2}=\frac{K_{L2}\cdot C_{e2}}{1+a_{L1}\cdot C_{e1}+a_{L2}\cdot C_{e2}} \quad (5)$$

where q_{e1} and q_{e2} are the amounts of solutes 1 and 2 sorbed per unit of sorbent at equilibrium concentrations C_{e1} and C_{e2}, respectively, and K_{Li} and a_{Li} are the Langmuir isotherm constant. These Langmuir equations are simple extensions of the single-component Langmuir isotherms used to account for multicomponent sorption. They assume that each component adsorbs onto the surface according to ideal solute behavior under homogeneous conditions with no interaction or competition between molecules taking place. The values of K_L and a_L for SMX and SMZ in single system (obtained in previous works) and in binary system are presented in Table 3 .The extended Langmuir model gave a good correlation between experimental data and predicted data for SMZ but not good for SMX. The monolayer saturation capacity in binary system for SMX and SMZ was 277 mg SMX/g wet resin and 25 mg SMZ/g wet resin, while in single system was 263 mg SMX/g wet resin and 110 mg SMZ/g wet resin. In the presence of both compounds, the resin has more affinity for SMX than for SMZ, and interaction competition in adsorption process between these two species are significant.

Table 3 Extended Langmuir and Join and Snoeyink modified extended Langmuir isotherm constants for SMX and SMZ in single and binary system

	K_L(L/g resin)	a_L(L/mg)	Q_m(mg/g resin)	R^2
single component system				
SMX	4.54	0.017	263	0.997
SMZ	4.73	0.043	110	0.995
SMX + SMZ binary system				
SMX	4.34	0.016	277	0.9985
SMZ	2.52	0.101	25	0.9991

Jain and Snoeyink[22] investigated competitive sorption from aqueous bicomponent solutions of organic sorbates and developed a model that predicts sorption equilibria in such non ideal systems. According to Jain and Snoeyink, the Langmuir theory for binary sorbate systems is based on sorption without competition. Therefore, to account for competition in the Langmuir theory, the Jain-Snoeyink model proposed adding an additional term to the extended Langmuir equation:

$$q_{e1}=\frac{(Q_{m1}-Q_{m2})a_{L1}C_{e1}}{1+a_{L1}C_{e1}}+\frac{Q_{m2}a_{L1}C_{e1}}{1+a_{L1}C_{e1}+a_{L2}C_{e2}} \quad (6)$$

$$q_{e2}=\frac{Q_{m2}a_{L2}C_{e2}}{1+a_{L1}C_{e1}+a_{L2}C_{e2}} \quad (7)$$

where Q_{mi} is the monolayer saturation capacity for the Langmuir isotherm. The first term on the right hand side of Eq. (6) refers to the amount of species 1 adsorbed without competition with 2, while the second term gives the amount of species 1 adsorbed in competition with 2, as described by applying the competition to the Langmuir model. The additional term in Eq. (6) is

the Langmuir expression for the number of molecules of solute 1 which are sorbed without competition on the surface, the terms being proportional to $(Q_{m1} - Q_{m2})$, where $Q_{m1} > Q_{m2}$. By means of Eq. (7), the number of molecules of solute 2 sorbed on the sorbent surface (proportional to Q_{m2} and in competition with solute 1) can be calculated from the extended Langmuir equation.

Figure 1 shows the comparison between experimental data and predictions based on the Jain and Snoeyink modified extended Langmuir model for SMX and SMZ in binary solutions.

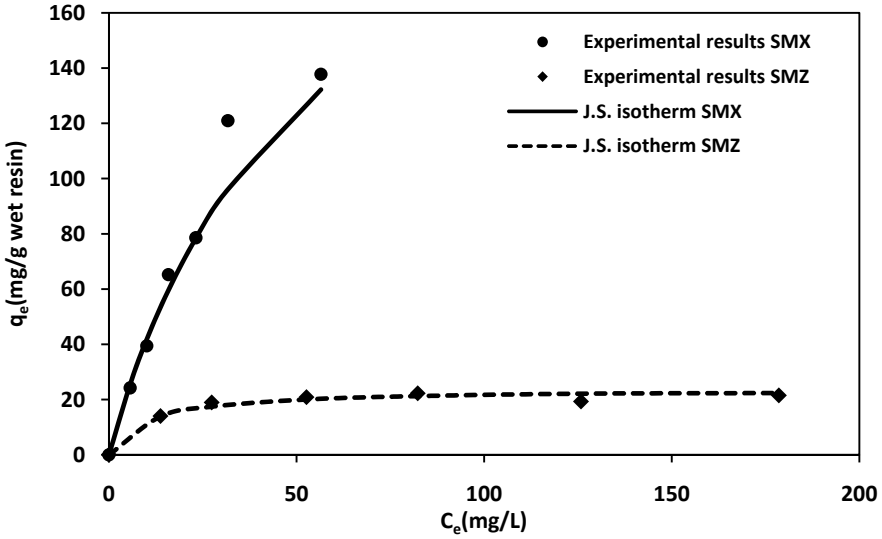

Figure 1 Comparison of experimental data and values predicted by the Join and Snoeyink (J.S.) modified extended Langmuir for SMX and SMZ in mixtures

The develop equilibrium equations were evaluated using Chi-square analysis [23] and non linear regression analysis. Eq. (8) shows how to calculated χ^2. The advantage of the Chi-square analysis is that all equilibrium equations can be compared at the same abscissa and ordinate. If the data predicted by the model were similar to experimental data, χ^2 (mg/g resin) would be small and vice versa.

$$\chi^2 = \sum_{i=1}^{N} \frac{\left(q_{eq,exp} - q_{eq,cal}\right)^2}{q_{eq,cal}} \tag{8}$$

$q_{eq,cal}$ is the equilibrium capacity obtained from a model (mg/g resin); $q_{eq,exp}$ the equilibrium capacity obtained from experiments (mg/g resin) and N number measurements.

Eq. (9) shows the average percentage error (Ɛ) used in the non-linear regression analysis [24]. The error between the experimental data and the predicted data were calculated using Eq. (9)

$$\varepsilon(\%) = \frac{\sum_{i=1}^{N} \left|\left(q_{eq,exp} - q_{eq,cal}\right)/q_{eq,exp}\right|}{N} x\ 100 \tag{9}$$

Also to quantify the agreement between the model predictions and the experimental data observations, an objective function (*Ei*) relating the experimental and the predicted component uptake may be defined as [25]:

$$E_i = \sum_{j=1}^{Q} \left(\frac{q_i^{exp} - q_i^{model}}{q_i^{exp}} \right)^2 \quad (10)$$

where Q if the number of data points: j=1…Q, and q_i^{exp} and q_i^{model} are the experimental and the predicted sorption capacities.

The Table 4 shows the experimental values and the calculated values for the extended Langmuir model and Jain and Snoeyink modified extended Langmuir model using the values of Q_{mi} and a_{Li} obtained for SMX and SMZ in mixtures and their respective error functions. The correlation between the predicted and experimental data for Jain and Snoeyink extended Langmuir model was good, which means there is competition between SMX and SMZ for adsorption sites.

Table 4 Experimental and calculated values from Extended Langmuir and Jain and Snoeyink (J.S.) Extended Langmuir models for SMX and SMZ in binary system

$q_{e\text{-}SMX}$ (exp.) mg/g	$q_{e\text{-}SMX}$ (cal. E.L.) mg/g	$q_{e\text{-}SMX}$ (cal J.S.) mg/g	$q_{e\text{-}SMZ}$ (exp.) mg/g	$q_{e\text{-}SMX}$ (cal E.L.) mg/g	$q_{e\text{-}SMZ}$ (cal. J.S.) mg/g
22.9	9.9	25.6	14.0	14.0	13.9
37.2	11.1	41.9	19.0	17.6	17.4
61.5	10.5	59.7	20.9	20.2	20.0
74.1	10.4	78.4	22.2	21.4	21.3
114.1	9.7	96.1	19.3	22.3	22.2
129.9	12.3	132.2	21.5	22.6	22.4
$\chi 2$	0.62	1.15		2975.93	0.25
Ɛ(%)	5.82	8.50		79.63	6.03
Ei	0.035	0.06		3.89	0.03

χ^2= Chi- square analysis (mg/g); Ɛ (%)=average percentage error; Ei= objective function (dimensionless)

Batch experiments using SMX and TMP were carried out in order to study whether there is also competition in the process of adsorption, as occurred in the case of SMX and SMZ, as these compounds are generally found together at a ratio 1:5 (TMP:SMX). Trials were carried out using the same L/S ratio (volume of liquid (mL)/mass of resin (g)) = 1000, varying the concentration of SMX and TMP between 30-200 mg/L of each compound. The concentration of TMP was kept constant in all trials. The Lewatit MP500 resin has no affinity for TMP, while the concentration of SMX decreased in a similar way as in the trials with mixtures of SMX+SMZ, obtaining a maximum adsorption capacity $Q_{T\ Langmuir\text{-}SMX}$= 254 mg SMX/g wet resin and the Langmuir constants $a_{L\text{-}\ SMX}$= 0.012 L/mg and $K_{L\text{-}SMX}$=3.06 L/g resin. Thus, although TMP was not adsorbed by the resin, its presence in the solution did not affect the capacity to adsorb SMX. The evolution of the concentrations of both compounds over time is shown in Figure 2.

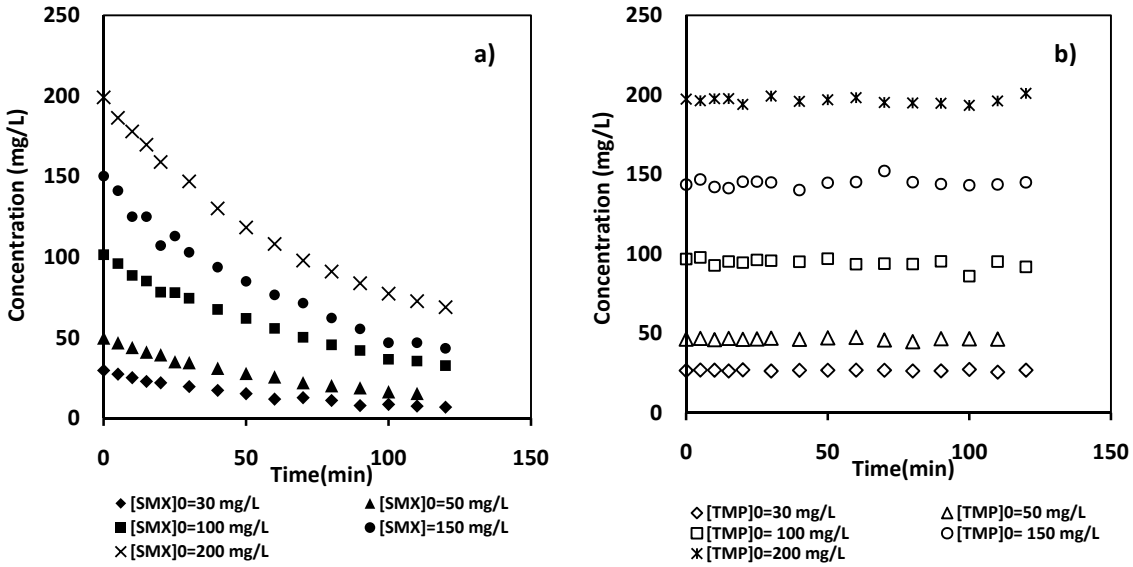

Figure 2 Evolution of the concentration of SMX (a) and TMP (b) in mixtures over time

3.2. Batch kinetics study

Kinetics experiments were carried out in batch mode with an L/S ratio=1000 (mL solution/g wet resin) monitoring the SMZ and SMX concentration over time from the initial time to equilibrium for all solutions. After 120 minutes, the solution concentration of SMX and SMZ does not change substantially, so operational equilibrium may be assumed. The experiments were conducted in a stirred tank with synthetic solutions of SMX and SMZ at concentrations of 30, 50, 80, 100, 150, 200 and 250 mg/L of each compound.

The concentration profiles was modeled using the pore diffusion kinetics model to determine the mass transfer mechanisms [26] due to under our operating conditions, such as well stirred solution (300 rpm), it would be expected that rate-determining step is the particle diffusion control [27].

Pore Diffusion Model. This model [28] considers the resin to be a porous matrix. The model is described by the following equations:

- Mass balance inside the particle:

$$\frac{\partial q_i(R,t)}{\partial t} = \frac{\partial q_{ei}(R,t)}{\partial t} + \varepsilon_i \frac{\partial C_{pi}(R,t)}{\partial t} = \frac{1}{R^2}\left[\frac{\partial}{\partial R} R^2 \varepsilon_i D_p \frac{\partial C_{pi}(R,t)}{\partial t}\right] \qquad (11)$$

where q_{ei} is the pore concentration of specie i, C_{pi} is the pore solution concentration of specie i, ε_i is the resin porosity, and D_p is the pore diffusivity.

- Mass balance in the solution:

$$\varepsilon_i V(C_{iT} - C_i(t)) = (1-\varepsilon_i) V \overline{q_{ei} + \varepsilon_i C_{pi}(t)} \qquad (12$$

where C_{iT} is the initial concentration of species i in solution and V is the volume of solution.

- Average concentration in the particle:

$$\overline{q_{ei} + \varepsilon_i C_{pi}}(t) = \frac{3}{R_0^3}\int_0^R R^2 \left(q_{ei} + \varepsilon_i C_{pi}\right)(R,t)\,dR \qquad (13)$$

where R is the radial coordinate and R_0 is the radius of the particle.

The initial and boundary conditions needed to solve the systems are:

- Initial conditions:

$$C_{pi}(R,0)= 0 \quad (14)$$

- Boundary conditions:

$$\text{In R} = 0 \rightarrow \left.\frac{\partial C_{pi}(R,t)}{\partial R}\right|_{R=0} = \left.\frac{\partial q_i(R,t)}{\partial R}\right|_{R=0} \quad (15)$$

$$\text{At the interphase (R=}R_0) \rightarrow C_{pi}(R_0, t) = C_i(t) \quad (16)$$

This model included the measured isotherm in which was not included the amount just retained in the pores of the resin. A FORTRAN subroutine, PDECOL [29] was used to solve these equations. The subroutine uses the method of orthogonal collocation on finite elements to solve the system of non-linear differential equations. The diffusivity values obtained were $D_{p\ SMX} = 3.2 \cdot 10^{-10}$ cm^2/s and $D_{p\ SMZ} = 6.8 \cdot 10^{-9} cm^2/s$ with average function error $\varepsilon(\%)$ calculated as Eq.(17), $\varepsilon(\%)_{SMX} = 6.3$ and $\varepsilon(\%)_{SMZ} = 3.9$. It can be observed that the order of magnitude of the diffusivity values is similar for each compound.

$$\varepsilon(\%) = \frac{\sum_{i=1}^{N}\left|\left(C_{i,exp} - C_{i,cal}\right)/C_{i,exp}\right|}{N} \text{ x } 100 \quad (17)$$

Figure 3 shows the fit of the experimental results to this model with diffusivity values obtained. The good agreement between experimental data and the theoretical prediction shows the goodness of the model. Comparing the values obtained in single compound trials ($D_{p\ SMX\ alone} = 2.6 \cdot 10^{-10} cm^2/s$ and $D_{p\ SMZ\ alone} = 2.6 \cdot 10^{-10}$ cm^2/s) with these results, the diffusivity values for SMX are seen to be similar, having the same order of magnitude, while in the case of SMZ in mixtures, the values of diffusivity increased slightly.

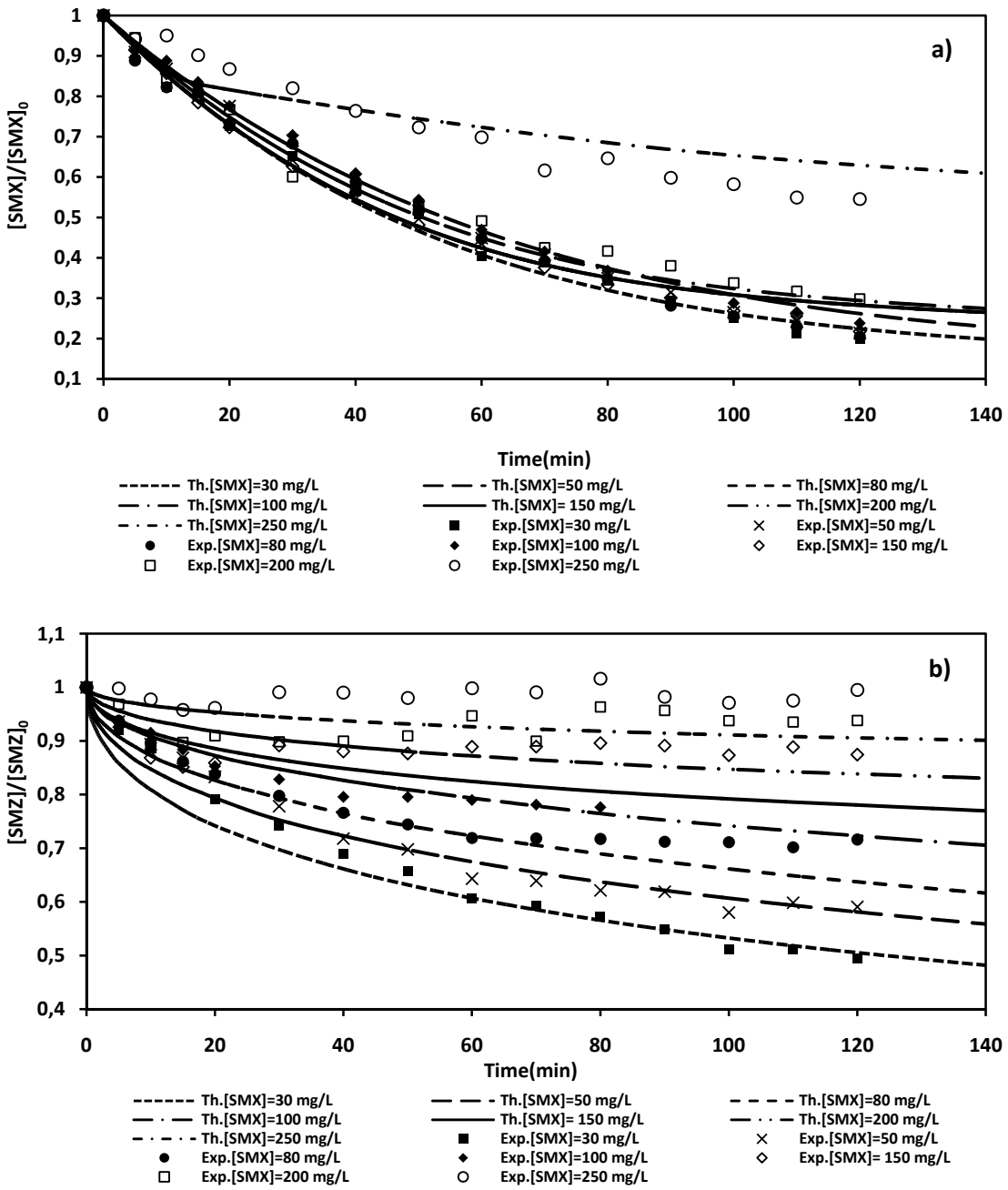

Figure 3 Fitting of kinetic data using the pore diffusion model for SMX (a) + SMZ (b) in mixtures

3.3. Fixed Bed Operation

Breakthrough Curves from Loading and Elution Stages. After studying the equilibrium and kinetics, tests were conducted in a fixed bed column using synthetic solutions of SMX+SMZ at concentrations of 200 and 300 mg/L of each compound to obtain the breakthrough curves.

Initially, fixed bed operation in column was tested using a synthetic solution of 200 mg/L of each compound, a volume of resin 1.9 mL, and flow rate of 4.5 mL/min. The breakthrough curve for the loading step shows a pronounced jump in SMZ concentration at 100 minutes, i.e., a compressive front, reaching the initial sample concentration in 250 minutes. At

this time, the concentration of the SMX at the outlet of the column was only 25 mg/L SMX, however, the breakthrough point for SMX not being reached in 400 minutes of operating. This is because the resin has more affinity for SMX than for SMZ, so SMX is retained more by the resin than SMZ, which exits the column outlet first. Retention of the resin packed in the column was calculated by numerical integration of the area under the breakthrough curves of the loading stage. The operational capacity found in the bed at 400 minutes of operating was 189 mg SMZ/mL resin and 188 mg SMX/mL resin.

Resin life is one of the key parameters for determining the kind of resin to be applied in industrial production. After adsorption, the resin was regenerated with NaOH 0.5 M at a flow rate of 4.2 mL/min. The elution curve presents a high elution peak in the first minutes of the elution step, reaching a concentration peak of 3877 mg SMZ/L and 2820 mg SMX/L and diminishing quickly to reach a negligible concentration at the outlet at 240 minutes; hence, 100% SMX and SMZ were recovered in the elution step. The good capacity of the MP500 resin to concentrate the solute has thus been proved, which is very interesting for reducing sulfonamides present in wastewater from drug manufacturers.

After this first cycle of loading and elution steps in column, another cycle was carried out with SMX and SMZ using a concentration of 300 mg/L of each compound at a flow rate of 5.1 mL/min to see how the resin operates. In this cycle, there is no increase or pronounced jump in SMZ concentration over time. SMZ was detected at the column outlet from the first minutes of operation onwards, reaching the initial sample concentration in 180 minutes. In the case of SMX, this compound began to be detected at 60 minutes of operating, the concentration subsequently continuing to increase very slowly. After 1000 minutes of operating, a concentration of 270 mg SMX/L was obtained at the outlet, less than the initial concentration; hence, the resin was not completely saturated. As in the previous cycle, it can be seen that the resin has more affinity for retaining SMX than SMZ. The retention capacity of the resin was 769 mg SMX/mL resin and 189 mg SMZ/mL resin. The resin was then regenerated with a solution of NaOH 0.5M at a down-flow rate of 5.1 mL/min, reaching a concentration of 3704 mg SMX/L in the first minutes, decreasing to 90 mg SMX/L in 240 minutes and achieving complete removal after 600 minutes of operating, with 100% recovery of SMX. In the case of SMZ, no peak was detected in the first minutes of operation for the reason that the concentration decreased very quickly, detecting less than 100 mg SMZ/L at the outlet from the first minutes of operating and achieving complete removal in 180 minutes, with 100% recovery of SMZ. The breakthrough curves of the two cycles for the loading and elution steps are shown in Figure 4.

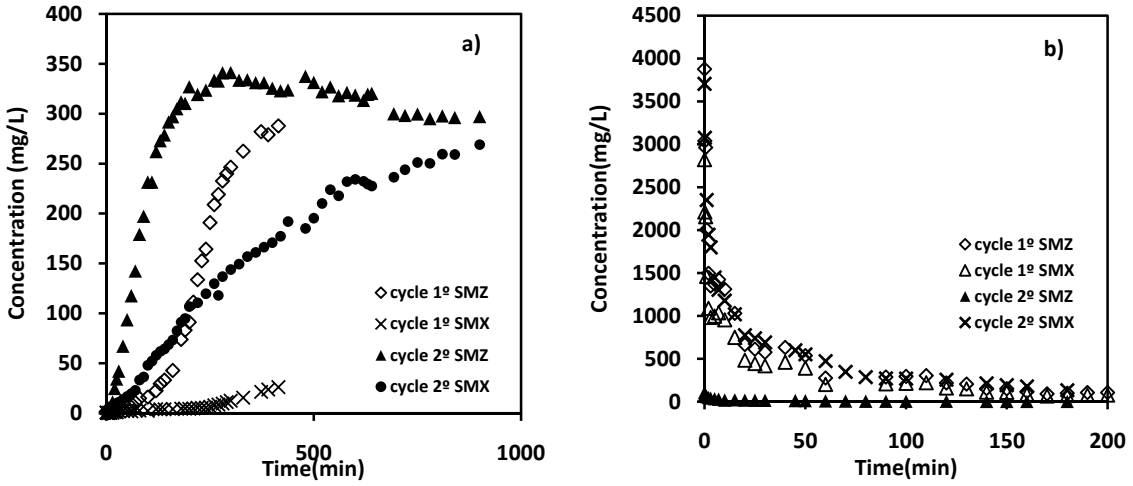

Figure 4 (a) Loading breakthrough curves for cycle 1 (conditions: $[SMX+SMZ]_0$= 200 mg/L SMX+SMZ; flow rate = 4.5 mL/min) and cycle 2 (conditions $[SMX+SMZ]_0$= 300 mg/L, flow rate = 5.1 mL/min);**(b)** elution curves for cycles 1 and 2, conditions: flow rates cycle 1= 4.2 mL/min and cycle 2= 5.1 mL/min)

Comparing these results with those obtained in single trials for each compound individually in column, it can be observed that there is no decrease in adsorption capacity. In single trials, using an initial concentration of 200 mg/L and a flow rate of 11 ml/min, an adsorption capacity of 194 mg SMX/mL resin and 140 mg SMZ/mL resin was obtained.

3.4. Fixed Bed Model

The analysis of the loading and elution curves obtained from fixed bed experiments was carried out considering a model developed by Costa[33] and used by Fernandez et al.[34,35]This model was used to simulate the breakthrough curves of loading and elution in a laboratory column. The model takes into account aspects of equilibrium and kinetics, axial dispersion in the column and no film transfer resistance. The developed model can be seen in López et al. [36].

To solve the fixed bed model, parameters such as bed porosity, particle porosity, equilibrium constant of Constant Separation Factor isotherm whose equation was used in previous work [36], diffusivities in the pores and the capacity of the resin must be known. All these parameters were determined for the system in previous batch experiments. The equations of the proposed model in this case are:

- Conservation of the mass of solute in the solution:

$$\frac{1}{Pe}\frac{\partial^2 x_i(z^*,\theta_{st})}{\partial z^{*2}} - \frac{\partial x_i(z^*,\theta_{st})}{\partial z^*} = \frac{\partial x_i(z^*,\theta_{st})}{\partial \theta_{st}} + \frac{15\varepsilon_i(1-\varepsilon_l)N_D}{\varepsilon_l}\left[x_i(z^*,\theta_{st}) - x_{pi(z^*,\theta_{st})}\right] \quad (18)$$

- Conservation of the mass of solute inside the particles:

$$\frac{\partial x_{pi}(z^*,\theta_{st})}{\partial \theta_{st}} = \frac{15\varepsilon_i N_{Di}}{\varepsilon_i + \dfrac{K_i\, {}^{q_{Ti}}/_{C_{Ti}}}{\left(1+(K_i-1)x_{Pi}(z^*,\theta_{st})\right)^2}}\left[x_i(z^*,\theta_{st}) + x_{pi(z^*,\theta_{st})}\right] \quad (19)$$

obtained by the relationship:

$$\frac{\partial q_i}{\partial t} = \frac{\partial q_i}{\partial C_i}\frac{\partial C_i}{\partial t} \quad (20)$$

In which $\partial q_i/\partial C_i$ was obtained by differentiating the equilibrium isotherm.

- Boundary conditions in the solution

$$z^* = 0 \quad x_i(z^*, \theta_{st}) = x_{Ti} \tag{21}$$

$$z^* = L \quad \frac{\partial x_i(z^*,\theta_{st})}{\partial z^*} = 0 \tag{22}$$

- Initial conditions:

$$\theta_{st}=0 \quad \partial x_i(z^*,\theta_{st}) = x_{Ti} \text{ en } z^*=0 \tag{23}$$

$$\theta_{st}=0 \quad x_i(z^*,\theta_{st}) \text{ depends on washing } \forall z^*>0 \tag{24}$$

The spatial coordinate inside the column is normalized by L, the length of the column, and time by the stoichiometric time, t_{st}, i.e. the time for the resin to become completely saturated. N_D is the number of intraparticle mass transfer units ($N_D = \tau D_p/R_0$), with $\tau = L/u_i$, special time. *Pe* is the Peclet number $Pe = u_i L/D_{AX}$. The axial dispersion parameter was not available for the laboratory column, so it was considered the sole parameter model fit. A FORTRAN subroutine, PDECOL [29] was used to solve the differential equation system proposed for the fixed bed model.

The values of the different parameters used in this study are given in Table 5. The axial dispersion calculated as a fitting parameter in the loading steps was 0.5 cm^2/s for SMZ and 0.1 cm^2/s for SMX in the first cycle, and 3 cm^2/s for SMZ and SMX in the second cycle. In the elution steps the axial dispersion was 43 cm^2/s for SMX and SMZ in the two cycles. The experimental and theoretical loading and elution breakthrough curves are shown in Figure 5 and Figure 6, respectively. A good correlation can be observed between the experiment results and the numerical solution of the fixed bed model for the loading and elution stages, thus demonstrating the validity of the model.

Table 5 Fixed bed operating parameters of the studied system

	1st cycle	1st cycle	2nd cycle	
	SMX	SMZ	SMX	SMZ
Bed Porosity	0.5			
Particle Porosity	0.34			
Equilibrium Constant	15.8	41.3	15.8	41.3
Equilibrium Constant OH^-	0.063	0.024	0.063	0.024
Diffusivity in pores (cm^2/s)	$9\cdot10^{-7}$	$3\cdot10^{-9}$	$3.3\cdot10^{-8}$	$2.8\cdot10^{-9}$
Bed Height (cm)	3			
Retention Capacity (g/L wet resin)	188	189	769	189

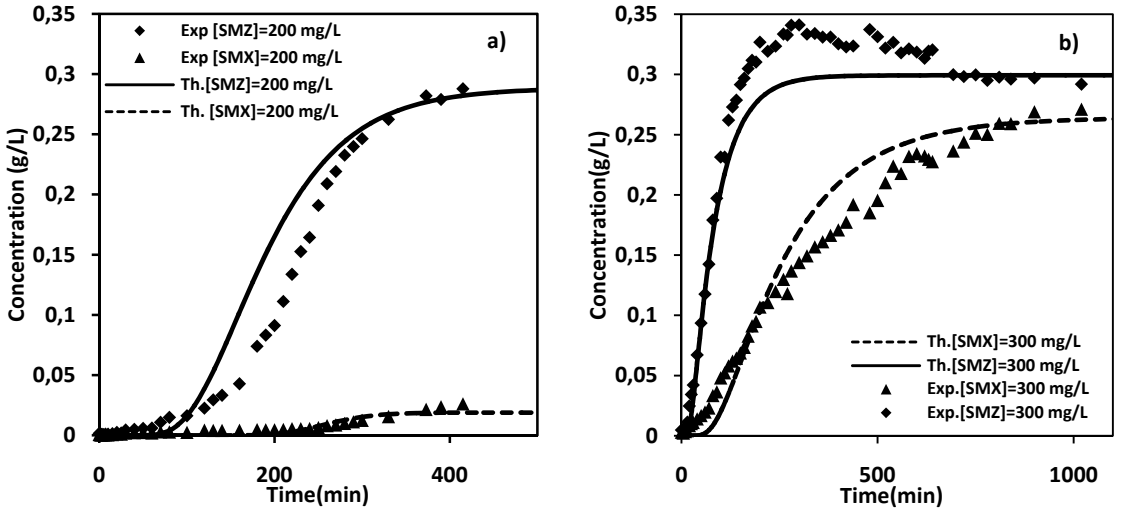

Figure 5 Experimental and theoretical loading curves for SMX+SMZ from synthetic solutions onto the Lewatit MP500 resin in a fixed bed column. Conditions: **(a)** $[SMX+SMZ]_0$= 200 mg/L of each compound, flow rate: 4.5 mL/min; **(b)** [SMX+SMZ]0= 300 mg/L of each compound, flow rate 5.1 mL/min; volume resin 1.9 mL (Z=3 cm)

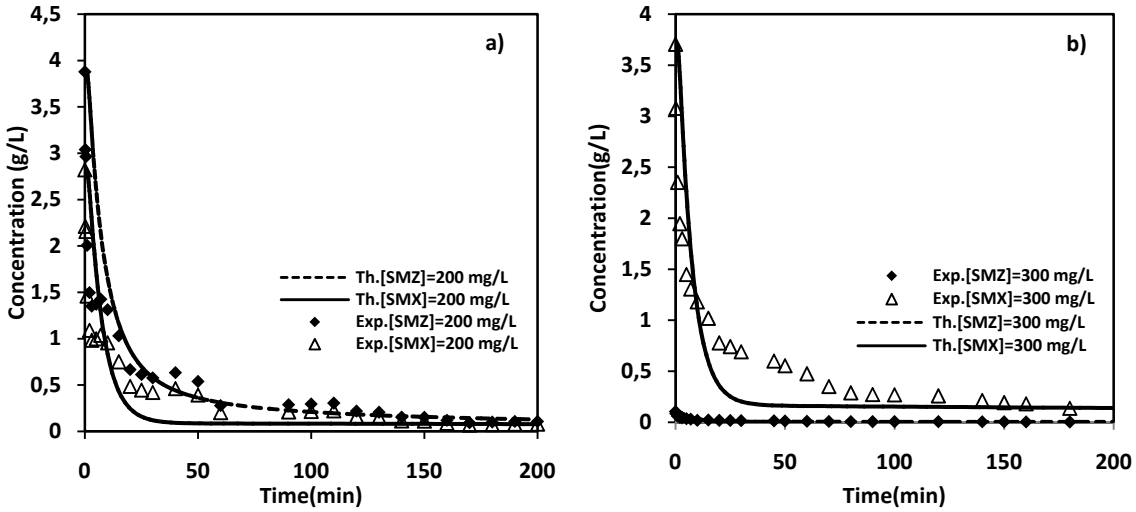

Figure 6 Experimental and theoretical elution curves for SMX+SMZ from synthetic solutions, using NaOH 0.5M as the eluent in a fixed bed column. Conditions: **(a)** $[SMX+SMZ]_0$= 200 mg/L of each compound; flow rate= 4.2 ml/min; **(b)** $[SMX+SMZ]_0$= 300 mg/L of each compound; flow rate= 5.1 ml/min, volume resin:1.9 mL (Z=3 cm).

4. Conclusions

The removal of mixtures of SMX (sulfamethoxazole) and SMZ (sulfamethazine) using a strong anionic resin (Lewatit MP500) was carried out successfully. Experiments were carried out in batch mode using binary synthetic solutions of SMX and SMZ in an equal mass concentration of between 30-250 mg/L of each compound, with an L/S ratio=1000 (volume of liquid (mL)/mass of resin (g)) determined in previous trials as suitable for calculating the retention capacity of the resin. The adsorption process was relatively fast, equilibrium being

reached in 120 minutes. The experimental data were fitted to Extended Langmuir Model and the Jain and Snoeying Extended Langmuir Model for multicomponent systems. The values of the equilibrium constant were $a_{L\ SMX}$= 0.016 L/mg, $K_{L\ SMX}$= 4.34 L/g wet resin and $a_{L\ SMZ}$= 0.101 L/mg, $K_{L\ SMZ}$=2.52 L/g wet resin, and the maximum adsorption capacities were $Q_{m\ SMX}$= 277 mg SMX/g wet resin and $Q_{m\ SMZ}$= 25 mg SMZ/g wet resin. The resin thus presents more affinity for SMX than for SMZ. The combined effects of the two compounds on the Lewatit MP500 resin were competitive. The Jain and Snoeyink Modified Extended Langmuir model described the adsorption equilibrium of SMX and SMZ in a binary mixture well. Although TMP in combination with SMX was not adsorbed by the Lewatit MP500 resin, its presence did not affect the resin's capacity to adsorb SMX. The pore diffusion model was tested to fit kinetic data, obtaining average intraparticle diffusivity values of $3.2 \cdot 10^{-10}$ cm^2/s for SMX and $6.8 \cdot 10^{-9}$ cm^2/s for SMZ.

Two column loading and elution cycles were carried out using synthetic solutions of 200 and 300 mg/L of each compound and a solution of NaOH 0.5 M as eluent. The retention capacity of the resin and the ability of the eluent were successfully evaluated. The results show that the resin is a very effective adsorbent for removing SMX and SMZ, obtaining a higher capacity of adsorption for SMX and recovering 100% of both compounds in the elution steps. Fixed bed operation was simulated using a proposed model that takes into account axial dispersion, equilibrium and kinetic parameters for the system under study. The numerical solution of the model shows good agreement between the experimental data and predicted values for the loading and elution curves, thus demonstrating the validity of the model. Taking into account the equilibrium, kinetic and fixed bed results reported in this paper, it may be concluded that the Lewatit MP500 resin is effective in removing SMX and SMZ present in effluents from STPs.

Acknowledgments

Financial supports of Ana María López from FICYT "Severo Ochoa Programme" grant (Gobierno Regional del Principado de Asturias, Spain) are gratefully acknowledged.

References

1. Kümmerer, K. Significance of antibiotics in the environment. J. Antimicrob. Chemother. **2003**, *52*, 5-7.
2. Adams, C.; ASCE, M.; Wang, Y.; Loftin, K.; Meyer, M. Removal of antibiotics from surface and distilled water in conventional water treatment processes. J. Environ. Eng. **2002**, *128*, 253-260
3. Choi, K.-J.; Son, H.-J.; Kim, S.-H. Ionic treatment for removal of sulphonamide and tetracycline classes of antibiotic. Sci. Total Environ. **2007,** *387*, 247-256 (2007).
4. Xu, W.; Zhang, G.; Zou, S.C.; Li, X.D.; Liu, Y.C. Determination of selected antibiotics in the Victoria Harbour and the Pearl River, South China using high-performance liquid chromatography-electrospray ionization tandem mass spectrometry. Environ. Pollut. **2007**, *145*, 672-679.
5. Mompelat, S.; LeBot, B.; Thomas, O. Occurrence and fate of pharmaceutical products and by-products, from resource to drinking water. Environ. Int. **2009**, *35***,** 803-814.
6. Díaz-Cruz, M.; Barceló, D. Environmental behavior and analysis of veterinary and human drugs in soils, sediments and sludge. Trends Anal. Chem. **2007**, *22*, 340-351.
7. Homen V.; Santos, L. Degradation and removal methods of antibiotics from aqueous matrices-A review. Journal of Environment Management **2011**, *92*, 2304-2347.
8. Göbel, A.; McArdell, C.S.; Joss, A.; Siegrist, H.; Giger, W. Fate of sulfonamides, macrolides and trimethoprim in different wastewater treatment technologies. Sci. Total Environ. **2007**, *372*, 361-371.
9. Stackelberg, P.E.; Gibs, J.; Furlong, E.T.; Meyer, M.T.; Zaugg, S.D.; Lippincott, R.L. Efficiency of conventional drinking water treatment processes in removal of pharmaceuticals and other organic compounds. Sci. Total Environ.**2007**, *377*, 255-272.
10. Vieno, N.M.; Harkki, H.; Tuhkanen, T.; Kronberg, L. Occurrence of pharmaceuticals in river water and their elimination in a pilot scale drinking water treatment plant. Environ. Sci. Technol. **2007**, *41*, 5077-5084.

11. Acero, J.L.; Benitez, F.J.; Real, F.J.; Roldan, G. Kinetics of aqueous chlorination of some pharmaceuticals and their elimination from water matrices. Water Res. **2007**, *44*, 4158-4170.
12. Andreozzi, R.; Canterino, M.; Marotta, R.; Paxeus, N. Antibiotic removal from wastewaters: the ozonation of amoxicillin. J. Hazard. Mater. **2005**, *122*, 243-250.
13. Balcioğlu, L.A.; Ötker, M. Treatment of pharmaceutical wastewater containing antibiotics by O_3/H_2O_2 processes. Chemosphere **2003**, *50*, 85-95.
14. Trovó, A.G.; Nogueira, R.F.P.; Agüera, A.; Sirtori, C.; Fernández-Alba, A.R. Photodegradation of sulfamethoxazole in various aqueous media: persistence, toxicity and photoproducts assessment. Chemosphere **2009**, *77*, 1292-1298.
15. Pérez-Moya, M.; Graells, M.; Castells, G.; Amigó, J.; Ortega, E.; Buhigas, G.; Pérez, L.M.; Mansilla. H.D. Characterization of the degradation performance of the sulfamethazine antibiotic by Photo-Fenton process. Water Res. **2010**, *44*, 2533-2540.
16. Li, S.Z.; Li, X.-Y.; Wang, D.-Z. Membrane (RO-UF) filtration for antibiotic wastewater treatment and recovery of antibiotics, Sep. Purif. Technol. 2004, *34* (1-3), 109-114.
17. Putra, E.K.; Pranowo, R.; Sunarso, J.; Indraswati, N.; Ismadji, S. Performance of activated carbon and bentonite for adsorption of amoxicillin from wastewater: mechanism, isotherms and kinetics, Water Res. **2009**, *43*, 2419-2430.
18. Rivera-Utrilla, J.; Prados-Joya, G.; Sánchez Polo, M.; Ferro Garcia, M.A.; Bautista-Toledo, I. Removal of nitroimidazole antibiotics from aqueous solution by adsorption/bioadsorption on activated carbon, J. Hazard. Mater. **2009**, *170*, 298-305.
19. Crisafully, R.; Milhome, M.A.L.; Cavalcante, R.M.; Silveira, E.R.; De Keukeleire, D.; Nascimiento, R.F. Removal of some polycyclic aromatic hydrocarbons from petrochemical wastewater using low-cost adsorbent of natural origin. Bioresour. Technol. **2008**, *99*, 4515-4519.
20. Vergili, I.; Barlas, H. Removal of selected pharmaceutical compounds from water by an organic polymer resin. Journal of Scientific & Industrial Research **2009**, *68*, 417-425.
21. Choy, K.K.H.; Porter, J.F.; McKay, G. Langmuir Isotherm Models Applied to the Multicomponent Sorption of Acid Dyes from Effluent onto Activated Carbon. J. Chem. Eng. Data **2009**, *45*, 575-584.
22. Jain. J.S.; Snoeyink, V.L. Adsorption from Bisolute Systems on Active Carbon. J. Water Pollut. Control Fed. **1973**, *45*, 2463-2479.
23. Yuh SH. Selection of optimum sorption isotherm. Carbon **2004**, *42*, 2113-2130.
24. Aksu Z.; Tunç O. Application of biosorption for penicillin G removal comparison with activated carbon. Process Biochem. **2004**, *40*, 831-847.
25. Shallcross, M.; Herrmann, C.C.; Mccoy, B. J. An improved model for the prediction of multicomponent ion exchange equilibria. Chem. Eng. Sci. **1988**, *43*, 279-288.
26. Boyd, G.E.; Adamson, A.W.; Myers, L.S. The exchange adsorption from aqueous solutions by organic zeolites. II. Kinetics, Journal of the American Chemical Society **1947**, *69***,** 2836-2848.
27. .Helfferich, F. *Ion Exchange*; McGraw-Hill: New York, **1962**.
28. Rodrigues, A.E. Tondeur, D. *Percolation Processes: Theory and Applications.* NATO ASI Series; Martinuous Nijhoff Publishers, **1981**.
29. Madsen, N.K., Sincovec, R.F.: Algorithm 540: PDECOL, General Collocation Software for Partial Differential Equations [D3]. ACM Transactions on Mathematical Software (TOMS) **1979**, *5* (3), 326-351.
30. Reid, R.C.; Praustniz, J.M.; Poling, B.E. The properties of Gases and Liquids, McGraw-Hill, New York, **1988**.
31. Wilke, C.R.; Chang, P. Correlation of diffusion coefficients in dilute solutions. AIChE J. **1955**, *1* (2), 264-270.
32. LeBas, G. *The molecular Volumes of Liquid Chemical Compounds*; Longmans & Green: New York, **1915**.
33. Costa, C. Rodrigues, A. Design of cyclic fixed-bed adsorption processes. Part I: Phenol adsorption on polymeric adsorbents. AIChE Journal **1985**, *31* (10), 1645-1654.
34. Fernández, A.; Rendueles, M.; Rodrigues, A.; Díaz, M. Co-ion behavior at high concentration cationic ion exchange. Ind. Eng. Chem. Res. **1994**, *33* (11), 2789-2794.
35. Fernández, A.; Rodrigues, A.E.; Díaz, M. Modelling of Na/K Exchange in Fixed Beds with Highly Concentrated Feed. Chem. Eng. J. **1994**, *54*, 17-22.
36. López, A.M.; Rendueles, M.; Díaz, M. Sulfamethoxazole removal from synthetic solutions by ion Exchange using a strong anionic resin in fixed bed. Solvent Extraction and Ion exchange **2013**, *31*, 763-781.

4.5. TRATAMIENTO DE LOS CONDENSADOS DEL GAS DE COQUERÍA CON RESINAS ANIÓNICAS: RETENCIÓN DE TIOCIANATO Y FENOL

En este subapartado se recogen los resultados referentes a la eliminación de tiocianato y fenol de aguas residuales mediante resinas de intercambio aniónicas.

Como ya se señalado en el apartado de consideraciones teóricas 2.2., las aguas residuales de los condensados del gas de coquería presentan una elevada carga contaminante de tiocianatos y fenoles. Debido a las deficiencias en los métodos biológicos para eliminar este tipo de contaminantes y a los elevados costes que suponen otros métodos de tratamiento, en este trabajo se ha planteado el intercambio iónico como una alternativa para eliminar estos compuestos. En el artículo de investigación que a continuación se presenta se ha empleado dos resinas aniónicas comerciales, Lewatit MP500 y Lewatit M610, para eliminar tiocianatos y fenoles presentes en aguas residuales. Se ha estudiado el equilibrio y la cinética del proceso de intercambio iónico, y se han realizado varias etapas de carga y elución en columna, para verificar la regeneración de la resina tras la adsorción y la capacidad de concentrar del eluyente.

Artículo: Treatment of condensates of gas coke by anionic exchange resins: thiocyanate and phenol retention

Situación: artículo publicado en *Solvent Extraction and Ion Exchange* (Taylor & Francis)

Referencia:

López, A.M.; Rendueles, M.; Díaz. M. Treatment of condensates of gas coke by anionic exchange resins: thiocyanate and phenol retention. *Solvent Extraction and Ion Exchange*, 30: 212-227, 2012.

Solvent Extraction and Ion Exchange, 30: 212–227, 2012

ISSN: 0736-6299 print / 1532-2262 online
DOI: 10.1080/07366299.2011.609379

Taylor & Francis
Taylor & Francis Group

TREATMENT OF CONDENSATES OF GAS COKE BY ANIONIC EXCHANGE RESINS: THIOCYANATE AND PHENOL RETENTION

Ana María López, Manuel Rendueles, and Mario Díaz
Department of Chemical Engineering and Environmental Technology, University of Oviedo, Oviedo, Spain

In coke production plants one of the most important wastewaters generated comes from the condensates of the gas coke pipelines which contains important quantities of toxic components such as phenols or thiocyanates. These contaminants can be treated by ion exchange. In this work, thiocyanate and phenol has been retained on strong anionic resins: Lewatit MP500 and Lewatit M610. Equilibrium and kinetics were studied and equilibrium constants and diffusivity values determined using different models. Breakthrough curves from the load and elution steps were carried out in order to evaluate the ion exchange operation in fixed bed. In the elution step the contaminants could be concentrated four times permitting their treatment. The results allow the determinination of the feasibility of ion exchange operations to diminish the thiocyanate and phenol concentration producing a final wastewater that can be used as treatment in the biological depuration of plants without poisoning the active sludges.

Keywords: ***Ion exchange, coke gas condensates, thiocyanate, fixed bed operation***

INTRODUCTION

The main aqueous wastes generated in coke production plants are the condensates of the gas coke generated. This effluent contains very high pollutant organic charges. The effluent is generated in the range of 0.25–0.30 m^3/ton of coke. The toxicity is caused by compounds such as phenols, cyanides, thiocyanates, ammonia, sulfides, chlorides, as well as small amounts of polyaromatic hydrocarbons and heterocyclic nitrogen compounds. Thiocyanate is the most serious hazardous substance contained in the condensates due to it high concentration and its strong effects on both the environment and human life.[1–3]

Several works have been published on the removal of thiocyanate using physical and chemical methods such as adsorption onto activated carbon,[4] surfactant modified coir pith,[5] calcined hydrotalcite,[6] alkaline chloration,[7] oxidation by ion,[8–14] ozone,[15] electrosorption,[16–17] separation through liquid membranes,[18] and the most widespread is biological treatment[19–22] but this method requires long residence times,

Address correspondence to Mario Díaz, Department of Chemical Engineering and Environmental Technology, University of Oviedo, Julian Claveria 8 Oviedo, 33001, Spain. E-mail: mariodiaz@uniovi.es

large tank capacities, and the microorganisms are extremely sensitive to factors such as the pH and the temperature. Some recent studies have been carried out by Dizge[23] in a batch-mode operation using an anion exchange resin Purolite A-250, finding an adsorption capacity of 191.20 mg/g at 323 K and a pH of 8. Thiocyanate can be removed from a wastewater stream by biological processes at concentrations of approximately 500 mg/L, but over these concentrations microorganisms can be poisoned. In the coke plants effluents, phenol is always present. Its concentration is usually lower than thiocyanate concentration, but this is also a problematic compound that must be treated in the wastewaters.

Ion exchange is one of the methods used for the removal of several ionic toxic substances from industrial and municipal wastewaters.[23–24] Adsorption technology has been currently used extensively for the removal of organic and inorganic micropollutants from aqueous solutions. Activated carbon is the most widely used for the removal of a variety of organics from water, but its main disadvantage is the high regeneration cost and the production of carbons fines, due to the brittle nature of carbons used for the removal of organic species. Nowadays, polymeric adsorbents have been viewed as a practical alternative to activated carbon for efficient removal of organic pollutants. Regeneration of the resin can be accomplished by simple, nondestructive means such as solvent washing, thus providing the potential for solute recovery.

A complete study of the removal of phenol from aqueous solution was evaluated by Costa[24] using a nonfuntionalized hyper-cross-linked polymer Macronet MN200 and two ion exchange resins, Dowex XZ (strong anion resin) and AuRIX 100 (weak anion exchange) determining equilibrium, kinetics, and phenol elution.

The objective of this study was to investigate the feasibility of the ion exchange operation for the treatment of the wastewaters produced in the condensation of coke gas generated in coke plants. Two anionic resins (Lewatit MP500 and Lewatit M610 manufactured by Lanxess) were tested to determine their capacity to retain thiocyanate and phenol, the two main toxic compounds of the condensates. Kinetics and equilibrium parameters for the removal of thiocyanate from coke condensates wastewaters are studied in order to characterize the operation. The adsorption equilibrium constants were determined using Langmuir and the Constant Separation Factor isotherms. Kinetics was analyzed using two models: a film mass transfer model and the pore diffusion models. Finally, several operational cycles of load and elution will be carried out in fixed bed to evaluate the behavior of the resin in an industrial operation.

MATERIALS AND METHODS

Solutions

An industrial wastewater from condensates of the coal gasification plants was simulated for initial tests. Synthetic solutions of concentrations 400 mg/L of SCN^- prepared with KSCN (Sigma-Aldrich, St. Louis, MO, USA) and solutions mixtures of 400 mg/L SCN^- and 100 mg/L of phenol also were prepared. The pH of these solutions was approximately 9. The real wastewater was supplied by a coke production plant in Asturias (Spain), in this real wastewater the average concentration of the thiocyanate and phenol was 500 and 100 mg/L approximately. The condensates were obtained from the pipelines of the coke gas in the distribution lines. The condensates were filtrated with a 0.45 μm mesh filter, and stored at room temperature.

Table 1 Characteristics of Lewatit MP500 and Lewatit M610.

General description	Lewatit MP500	Lewatit M610
Ion form	Cl^-	Cl^-
Funtional group	Quaternary amine (type I)	Tertiary amine (type II)
Matrix	Crosslinked polystyrene	Crosslinked polystyrene
Polymer Estructure	Macroporous	Gel
Bead side > 90% (mm)	0.47(± 0.06)	0.6(± 0.05)
Density (g/mL)	1.06	1.1
Water retention (%)	62	45–60
Total capacity (min.eq /L)	1.1	1.25
Temperature stability (°C)	–20/100	1/70
pH range stability	0/14	0/14
Storability of product (min. years)	2	2
Temperature range storability (°C)	–20/40	1/40

Resins

Two anionic resins were tested, the strong base resin Lewatit MP500 with a quaternary amine (macroporous type I) functional group and the strong base resin Lewatit M610 with ternary amine (gel-type II). Both resins have a crosslinked polystyrene matrix and are manufactured by Lanxess. The main properties of the resins are shown in Table 1.

Experimental Methods

Batch Experiments. Runs were carried out at room temperature in cylindrical stirred tanks of 1000 mL volume at 300 rpm. All the conditioning and loading of the resin experiments were carried out contacting 4 g of each resin with a solutions of NaOH 0.5 M (100 mL) 2 times, 20 min each time. After conditioning, the resins were washed with 100 mL of distilled water twice for 5 min each time and were then separated from the solution.

The resin was subsequently contacted with the loading solution. The L/S ratio (volume of liquid (mL)/mass of resin (g)) was adjusted by varying the volume of the solution and maintaining the amount of the resin. The contact time was 1 hour in all tests; this time was considered sufficient to reach operative equilibrium. The volume of the samples extracted from the tank each time was 5 mL, which did not substantially change the volume of the solution. The concentration of SCN^- and phenol ions in the resins was determined by mass balance, calculating the difference between the initial and final quantity of the charged ions in the solution.

Column Experiments. Continuous flow adsorption experiments were carried out in a glass column consisting of an internal diameter of 3.2 cm and a total length of the tube of 25 cm. Columns were prepared packing 15 grams of wet resin M610 (1.7 cm height of the bed) and 30 grams of resin MP500 (3.5 cm height of the bed) in each case. Resin M610 presents a high flow resistance in comparison with MP500; for this reason the M610 fixed bed was compacted using a minor quantity of resin. Solutions were pumped through the column by a peristaltic pump (Masterflex) in a down-flow mode.

To perform the conditioning of the resin in the fixed bed a solution of NaOH 1 M was pumped through the column during 20 minutes at a flow rate of 16 mL/min. Afterwards, distilled water was fed through the column at a flow rate of 20 mL/min during 15 minutes to wash the resin.

The load stage was carried out also with down-flow at a desired flow rate in each assay. The effluent samples were collected (10 mL approximately) at specified times intervals (5–10 minutes) and analyzed to follow the evolution of thiocyanate and phenol concentration with time. The breakthrough curve was followed until the thiocyanate and the phenol concentration in the outlet of the column effluent reached the initial concentration of the solution feed.

Finally, after charge, the elution stage was carried out pumping through the column a solution of NaOH 0.5 M also with down-flow. The effluent samples were collected every 5–10 minutes to follow the evolution of the concentration with time. The elution curve was followed until no thiocyanate and phenol concentration was detected at the outlet of the column.

Analytical Methods

To determine the concentration of thiocyanate in water the standard method of the iron complex (Fe^{3+}) was used.[25] Thiocyanate reacts with ferric ions at a pH < 2 to form a colored complex, which was determined by colorimetry at 460 nm in a UV/Vis spectrophotometer. The ferric nitrate solution used for the reaction between Fe^{3+} and SCN^- to form the red complex was prepared dissolving 404 g of ferric nitrate ($Fe(NO_3)_3 \cdot 9H_2O$) in 800 mL of distilled water. 80 mL of concentrated nitric acid was added to this solution, well mixed, and diluted to a final volume of 1L with distilled water. For every 50 mL of thiocyanate sample 2.5 mL of ferric nitrate solution was added and well mixed. Within 5 minutes the absorbance of the solution at 460 nm in a 5.0 cm cell was determined using water as blank. The absorbance plot was linear with a regression of 0.999.

Phenol analysis was carried out colorimetrically using the method of 4-aminoantipyrine[25] at a wavelength of 510 nm. Phenolic compounds react with 4-aminoantipyrine in the presence of potassium ferrocyanide to form a colored antipyrine dye. A stock phenol solution was prepared dissolving 1 g phenol in distilled water and diluted to 1000 mL. A standard phenol solution was made dissolving 100 mL stock solution with distilled water until 1L volume. A series of 100 mL phenol standards were prepared with concentration ranging from 1 mg/L to 20 mg/L. Distilled water was used as blank. The sample, the blank, and the standards were treated as follows: for every 5 mL of sample 0.1 mL NH_4Cl solution (50 g NH_4Cl diluted to 1L) were added and adjusted to the pH between 9.8–10.2 with NH_3. Next, 0.1 mL 4-aminoantipyrine solution (1 g 4-aminoantipyrine diluted to 50 mL) was added and mixed well. Then, 0.1 mL $K_3Fe(CN)_6$ solution (8 g $K_3Fe(CN)_6$ diluted to 100 mL) was added and well mixed. After 5 min, the absorbance of the solution was determined at 510 nm in a 5 cm cell. The absorbance plot was linear with a regression of 0.999.

RESULTS AND DISCUSSION

Batch Equilibrium Study

In order to compare the retention capacity of the MP500 and M610 resins for thiocyanate under different L/S ratios (100, 150, 200, and 250), several runs were carried out to obtain the appropriate ratio L/S to carry out the next equilibrium experiments. In these previous runs 4 g of each resin were contacted with different volumes of a 400 mg/L thiocyanate synthetic solution during 90 minutes, measuring the final thiocyanate

concentration to determine the retention capacity of the resin. The results show that an operative L/S of 150 (mL solution/g of wet resin) was sufficient to reach complete saturation of the resin. In these conditions 84% of the thiocyanate in solution is retained in both resins. This L/S ratio was chosen for batch equilibrium and kinetic experiments.

Several runs were carried out to obtain the capacities of the resins. MP500 and M610 resins were contacted with different thiocyanate solution concentrations (200, 400, 600, and 800 mg/L of thiocyanate) with ratio L/S = 150. The results show that in all cases the equilibrium is reached in approximately 45 minutes.

Two different models, Langmuir and the Constant Separation Factor (CSF) isotherms, were used to define the relationship between the loading capacity and the solution concentration. The equation of the Langmuir isotherm is

$$q_i = \frac{K_{eq} \cdot q_t \cdot C_i}{1 + K_{eq} \cdot C_i} \tag{1}$$

where K_{eq} K_e is the equilibrium constant; q_t is the maximum capacity of the resin, and C_i is the solution concentration of species i. For the Constant Separation Factor isotherm, the equation is:

$$q_i = \frac{K_{eq} \cdot q_t \cdot C_i}{C_t + (K_{eq} - 1) \cdot C_i} \tag{2}$$

where C_t is the minimum thiocyanate equilibrium concentration in the solution with a saturated resin.

The fitting of the experimental results to the Langmuir and the CSF isotherms are shown in Fig. 1. The equilibrium constants and the maximum capacity absorption were obtained. Table 2 summarizes the parameters obtained for the two equilibrium models. It can be seen that the CSF isotherms show good correlation between the experimental results and predicted values.

The equilibrium results allow the observation of the good performance of the two resins for the retention of the studied anions, presenting very favorable isotherms as can be seen when taking into account the values of the equilibrium constants obtained in the two models. In both the tested isotherms the equilibrium constants are always higher (more favorable for thiocyanate retention) for the Lewatit M610 resin.

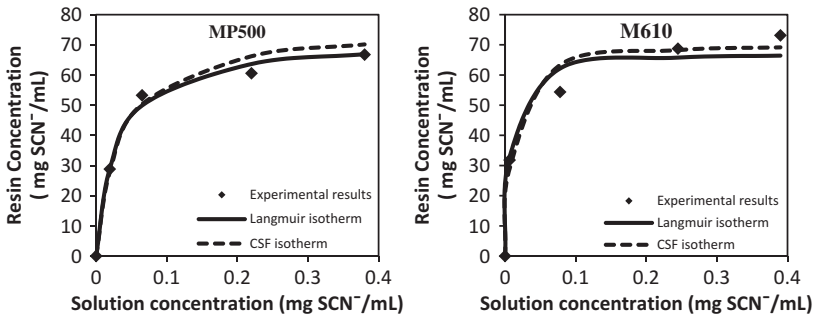

Figure 1 Comparison of experimental data with predicted values from Langmuir and Constant Separation Factor isotherms.

Table 2 Isotherms parameters obtained for both resins.

	MP500 resin		M610 resin	
	Langmuir isotherm	FSC isotherm	Langmuir isotherm	FSC isotherm
K_{eq}	34.75	17.37	148	44.86
q_t (mg SCN^-/mL resin)	71.95	71.95	67.57	69.21
C_t (mg SCN^-/mL solution)	—	0.551	—	0.405

Batch Kinetics Study

The kinetics experiments were carried out in batch experiments with L/S ratio of 150 (mL solution/g wet resin) following the thiocyanate concentration with time from the initial contacting time to 60 minutes, time estimated as sufficient to reach the equilibrium. It was observed that after 45 minutes, the solution concentration of thiocyanate does not change substantially. The experiments were carried out in a stirred tank with synthetic solutions of initial concentrations 200, 400, 600, and 800 mg/L of thiocyanate. Synthetic solutions of mixtures of 400 mg/L of thiocyanate and 100 mg/L of phenol and assays with real wastewater from condensates containing approximately 400 mg/L of SCN^- and 15 mg/L of phenol were also carried out.

The concentration profiles of the thiocyanate in solution with time can be modeled using the film mass transfer and the pore diffusion kinetics models in order to determine the mass transfer mechanisms.[26–27]

Film Mass Transfer Model. In this model the retention of the thiocyanate is assumed to be limited by the external surface of the particle.[28] The behavior of this model can be described by the following equations:

$$\frac{dq_i}{dt} = K_f\, a_p \left(C_i - C^*\right) \tag{3}$$

where q_i is the concentration of specie i in the resin at time t, K_f is the mass transfer coefficient in the fluid phase (cm/s), C^* is the equilibrium thiocyanate concentration in the solution, and a_p is the specific surface area. The total surface area per unit of volume. $K_f\, a_p$ can be considered as K the mass transfer apparent constant. The mass balance of the system can be written as follows:

$$V_L C_i + V_r q_i = V_L C_0 \tag{4}$$

where V_L is the volume of liquid; V_r is the volume of resin and C_0 is the initial thiocyanate concentration in solution. By integrating Eq. (3) and introducing Eq. (4) the following equation is obtained:

$$q_i(t) = C_0\,(V_L/V_r)\left(1 - \frac{C^*}{C_0}\right)\left(1 - \exp\left(\frac{-Kt}{V_L/V_r}\right)\right. \tag{5}$$

The mass transfer constant, K, can be determined by linear regression using the experimental data, fitting these to Eq. (3). The anion exchange beads are of constant size with

Table 3 Mass transfer constant for thiocyanate calculated by film mass transfer for both the resins.

	MP500 resin		M610 resin	
Experiments	K (min^{-1})	K_f (cm/s)	K (min^{-1})	K_f (cm/s)
Synthetic solution, $C_{0\,SCN^-} = 200$ mg/L	0.164	$2.1 \cdot 10^{-5}$	0.166	$2.8 \cdot 10^{-5}$
Synthetic solution, $C_{0\,SCN^-} = 400$ mg/L	0.1648	$2.1 \cdot 10^{-5}$	0.1893	$3.2 \cdot 10^{-5}$
Synthetic solution, $C_{0\,SCN^-} = 600$ mg/L	0.2197	$2.9 \cdot 10^{-5}$	0.2057	$3.4 \cdot 10^{-5}$
Synthetic solution, $C_{0\,SCN^-} = 800$ mg/L	0.3271	$4.3 \cdot 10^{-5}$	0.3265	$5.4 \cdot 10^{-5}$
Synthetic solution SCN^- + phenol	0.1184	$1.5 \cdot 10^{-5}$	0.1614	$2.7 \cdot 10^{-5}$
Wastewater	0.1804	$2.4 \cdot 10^{-5}$	0.1814	$3.0 \cdot 10^{-5}$

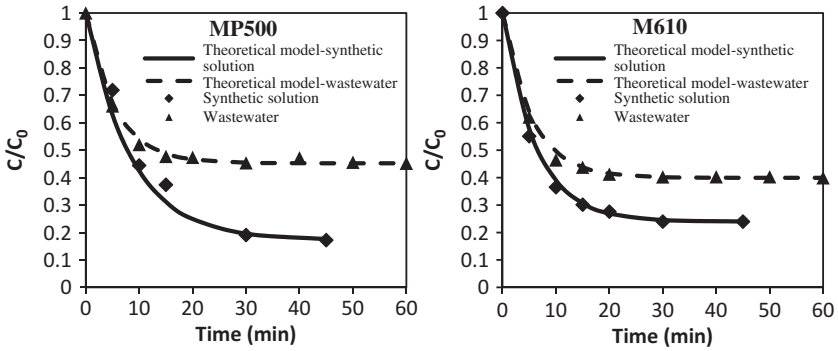

Figure 2 Fitting of kinetics data using the film mass transfer model for synthetic mixture solutions of 400 mg/L of SCN^- and 100 mg/L of phenol and wastewater.

a spherical geometry; therefore $K_f = K/a_p$. Then the fitting of the experimental results for thiocyanate concentration to Eqs. (4) and (5) will give the mass transfer constant of the system. The values obtained for the mass transfer constants for the two studied resins and the different solutions tested are summarized in Table 3. As an example, Fig. 2 graphically shows the fitting of the experimental data to the model for the mixture of thiocyanate and phenol and the industrial condensate.

Pore Diffusion Model. This model[29] considers the resin as a porous matrix. The model is described by the following equations:

- Mass balance inside the particle:

$$\frac{\partial q_i(R,t)}{\partial t} = \frac{\partial q_{ei}(R,t)}{\partial t} + \varepsilon_i \frac{\partial C_{pi}(R,t)}{\partial t} = \frac{1}{R^2}\left[\frac{\partial}{\partial R} R^2 \varepsilon_i D_p \frac{\partial C_{pi}(R,t)}{\partial t}\right] \tag{6}$$

where q_{ei} is the pore concentration of specie i, C_{pi} is the pore solution concentration of specie i, ε_i is the resin porosity, and

$$D_p q_{ei} + \varepsilon_i C_{pi}(t) = \frac{3}{R_0^3} \int_0^R R^2 \left(q_{ei} + \varepsilon_i C_{pi}\right)(R,t)\, dR$$

is the pore diffusivity.

- Mass balance in the solution:

$$\varepsilon_i V(C_{iT} - C_i\,(t) = (1-\varepsilon_i)\overline{V_{q_{ei}} + \varepsilon_i C_{pi}(t)} \tag{7}$$

where C_{iT} is the initial concentration of species i in solution and V is the volume of solution

- Average concentration in particle:

$$\overline{q_{ei} + \varepsilon_i C_{pi}}(t) = \frac{3}{R_0{}^3} \int_0^R R^2 \left(q_{ei} + \varepsilon_i C_{pi}\right)(R,t)\, dR \tag{8}$$

where R is the radial coordinate and R_0 is the radius of the particle.

The initial and boundary conditions needed to solve the systems are:

- Initial conditions:

$$C_{pi}\,(R,0) = 0 \tag{9}$$

- Boundary conditions:

$$\text{In R} = 0 \rightarrow \frac{\partial C_{pi}\,(R,t)}{\partial R}\bigg|_{R=0} = \frac{\partial q_i\,(R,t)}{\partial R}\bigg|_{R=0} \tag{10}$$

At the interphase

$$(\text{R} = \text{R}_0) \rightarrow \text{C}_{pi}(\text{R}_{0,}\ \text{t}) = \text{Ci(t)} \tag{11}$$

A FORTRAN subroutine, PDECOL,[30] was used to solve these equations. The subroutine uses the method of finite elements to solve the system of non-linear differential equations. Table 4 shows the diffusivity values obtained in the fitting of the experimental data to the model for all the experiments carried out.

Figure 3 shows the fit of the experimental results to this model using the diffusivity values of Table 4 for the mixture of thiocyanate and phenol and the industrial condensate

Table 4 Pore diffusivities for thiocyanate calculated by pore diffusion model by both resins.

Experiments	D_p (cm^2/s) MP500 resin	D_p (cm^2/s) M610 resin
Synthetic solution, $C_{0\,SCN^-} = 200$ mg/L	$1.7 \cdot 10^{-7}$	$2.8\ 10^{-7}$
Synthetic solution, $C_{0\,SCN^-} = 400$ mg/L	$4.7 \cdot 10^{-7}$	$4.7 \cdot 10^{-7}$
Synthetic solution, $C_{0\,SCN^-} = 600$ mg/L	$4.2 \cdot 10^{-7}$	$4.2 \cdot 10^{-7}$
Synthetic solution, $C_{0\,SCN^-} = 800$ mg/L	$4.2 \cdot 10^{-7}$	$4.2 \cdot 10^{-7}$
Synthetic solution SCN^- + phenol	$8.3 \cdot 10^{-8}$	$2.2 \cdot 10^{-7}$
Wastewater	$4.4 \cdot 10^{-7}$	$4.4 \cdot 10^{-7}$

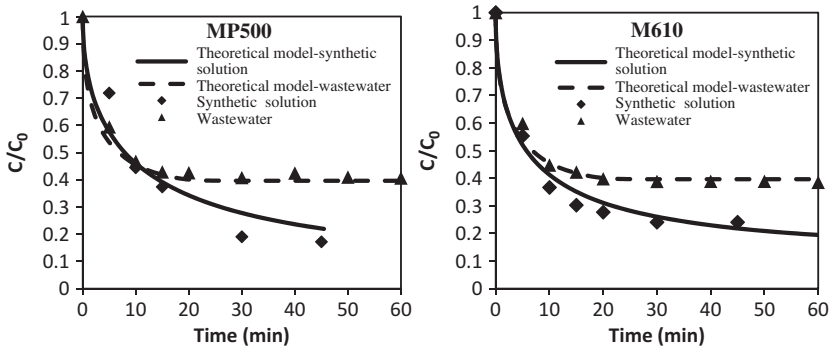

Figure 3 Fitting of kinetics data using the pore diffusion model for synthetic mixture solutions of 400 mg/L of SCN^- and 100 mg/L of phenol and wastewater.

experiments. The good agreement between experimental data and the theoretical prediction shows the goodness of the model. The diffusivity values of the thiocyanate are similar for all the tests, being lower for the mixture of thiocyanate and phenol, due to the competition of the ions to access to the resin pores.

Rate-Controlling Step. In order to identify the rate-controlling step (diffusion inside the solid particles or diffusion in the film surrounding the particles) of the ion exchange process, a method proposed by Helfferich[28] was used. This model constitutes a method to predict the rate-controlling step that theoretically reflects the effect of the ion exchange capacity solution concentration, particle diameter, film thickness, film mass transfer coefficient, pore diffusivity, D_p, and separation constant parameter. The criteria are based on the following expression:

$$\frac{q_T D_p \delta}{C_T D^{\infty} R_0}\left(5 + 2\alpha_{A/B}\right) \tag{12}$$

When the obtained value of this factor is below 1, particle diffusion control exists; otherwise, if the value is above 1, film diffusion control can be deduced. In this expression, δ is the thickness of the film, which can be calculated as:

$$\delta = \frac{2R_0}{Sh} \tag{13}$$

where Sh is the Sherwood number.

$$Sh = \frac{K_f d_p}{D} \tag{14}$$

where K_f is the mass transfer coefficient in cm/s and can be calculated from the mass transfer model. $K_f = K/a_p$, where a_p is the specific surface area, the total surface area per unit of volume that is calculated assuming spherical particles, $a_p = 3/R_0$. D^{∞} is the diffusivity coefficient in the film and $\alpha_{A/B}$ is the separation factor. The manufacturer's parameters of the resin[28] as well as the values previously calculated can be seen in Table 5.

Table 5 Manufacturer's parameters of the resin and data calculated by theoretical models.

Resin parameters	MP500	M610	Equilibrium calculated data	MP500	M610
R_0(cm)	0.024	0.03	q_T (mg SCN^-/mL)	71.75	69.21
ε_i	0.34	0.34	C_T (mg SCN^-/mL)	0.551	0.405
ρ (g/cm^3)	1.06	1.1	K_{eq}	17.37	44.86
a_p (cm^{-1})	128	100			
D^∞ (Helfferich, 1962)	$0.72 \cdot 10^{-5}$		$\alpha_{A/B}$ [28]	13	

Using the values of Tables 3, 4, and 5, the Sherwood number and the film thickness were obtained, and once all the parameters were known, they were introduced in Eq. (12). In all cases the value of Helfferich's factor is much higher than 1; therefore, the diffusion through the film around the spheres is the rate-controlling step.

Fixed Bed Operation

Breakthrough Curves from Load and Elution Stages. After studying the equilibrium and kinetics, fixed fed column runs were conducted to obtain the breakthrough curves. For these tests initially synthetic solutions of thiocyanate were used, then mixtures of thiocyanate and phenol, and finally industrial wastewaters.

Initially the operation in fixed column was checked using synthetic solutions of SCN^-. In both resins, the breakthrough curves of the load step have some scattered results, showing a sharp increase in concentration with time, and reaching the initial sample concentration in 240 minutes for resin MP500 and in 440 minutes for resin M610 as can be seen in Fig. 4. It must be indicated that these saturation times are obtained with a volume bed of 15 mL for M610 and 30 mL for MP500. Even with these conditions the saturation time is higher for M610, showing its good performance.

The retention of the resins packed in the column was calculated by numerical integration of the area under the breakthrough curves of the load stage. The operative capacity found in the bed was 54 mg/mL resin for MP500 and 121 mg/mL resin for the M610, showing the better behavior of Lewatit M610 for this ion exchange operation.

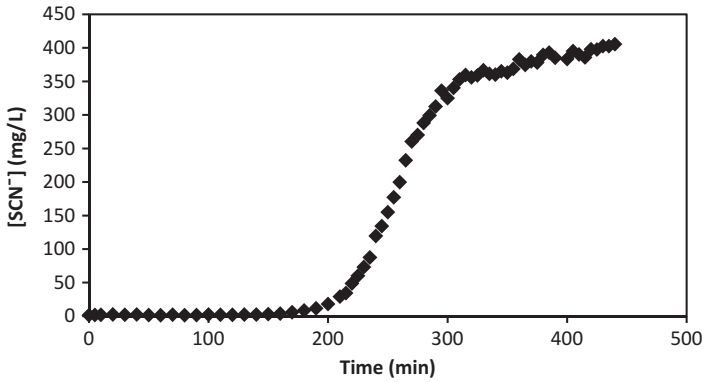

Figure 4 Breakthrough curve for the sorption of SCN^- in Lewatit M610 ion exchange resin (conditions: C0 SCN^- = 400 mg/L; flow rate = 15 mL/min).

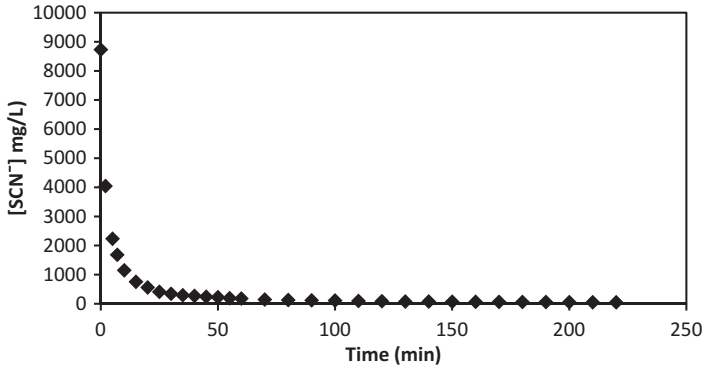

Figure 5 Elution using NaOH of Lewatit M610 loaded with a synthetic solution of SCN^- (flow rate = 15 mL/min).

After adsorption, the resin was regenerated with NaOH 0.5 M. The elution curves for the two resins present a high elution peak in the first minutes of the elution step. For resin MP500 the peak reach a concentration of 2900 mg/L in the first minutes, diminishing quickly to reach a complete elution of thiocyanate in 100 minutes approximately. The elution curve for resin M610 is presented in Fig. 5. In this figure, an elution peak reaching a concentration of 8800 mg/L can also be observed in the first few minutes of the elution, and a complete elution can be reached in 100 minutes. So it has been proven the good capacity of both resin to concentrate the solute, which is very interesting to reduce the toxic effluent in subsequent treatments to carry out the elimination or recovery of thiocyanate.

In order to evaluate the effectiveness of the elution it can carry out a mass balance to thiocyanate, calculating the mass thiocyanate recovered in the elution step and comparing it with the mass thiocyanate retained in the breakthrough step. In 100 minutes 87% of the thiocyanate was recovered for both resins. After regeneration, distilled water was fed through the column to wash the resin, eliminating the NaOH and ions present in the interstitial volume of the bed.

Subsequent runs were carried out loading the fixed beds with a synthetic solution formed by a mixture of 400 mg/L of thiocyanate and 100 mg/L of phenol. Figure 6 shows the breakthrough curves obtained for this mixture. The curves show a sharp increase in concentration with time. The retention capacity of the resins was 30 mg SCN^-/mL resin and 11 mg phenol/mL resin for MP500; and 106 mg SCN^-/mL resin and 15 mg phenol/mL resin for M610. So, the higher capacity of the resin Lewatit M610 was also determined. In the breakthrough curves, there was a displacement of the phenol front by the thiocyanate within the fixed bed so that a peak of elution of phenol was observed ahead of the thiocyanate front. This fact could allow the selective separation of thiocyanate and phenol.

After loading of the mixture solution, the column was regenerated again. Figure 7 shows the elution curves for the two resins. In both resins, in 100 minutes the concentration of thiocyanate at the outlet of the column was less than 150 mg/L; and in 240 minutes the concentration was less than 80 mg/L. In the resin MP500 a concentration of 4600 mg/L of SCN^- is reached in the elution peak while in resin M610 the peak reached a concentration of 7900 mg/L of SCN^-. The thiocyanate recovered was 63% for the MP500 resin and 92% for the M610 resin. In the case of phenol, in 40 minutes the concentration at the outlet of the

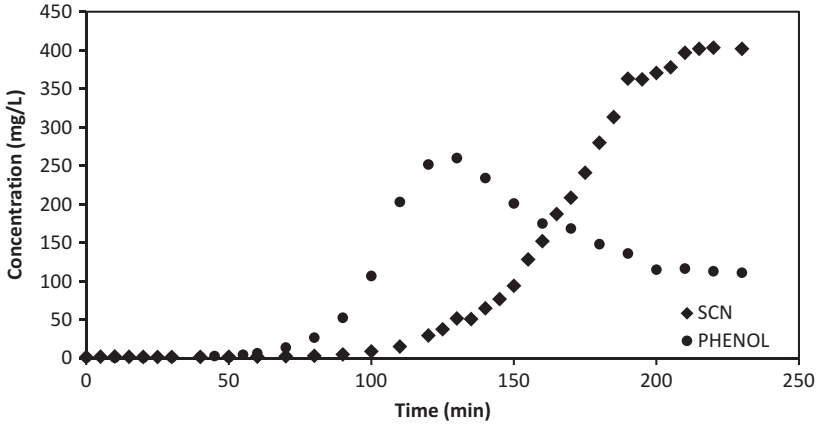

Figure 6 Breakthrough curve for the sorption of SCN^- and phenol in Lewatit MP500 ion exchange resin (conditions: C0 SCN^- = 400 mg/L; C0 PHENOL = 100 mg/L; flow rate = 15 mL/min).

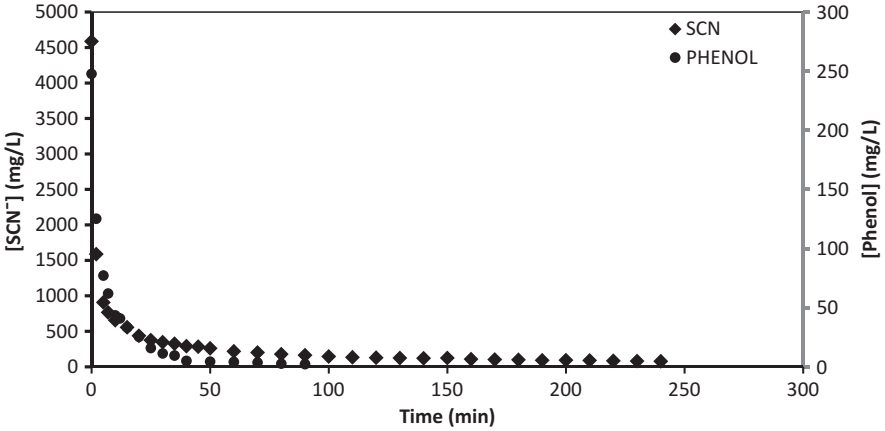

Figure 7 Elution using NaOH of Lewatit MP500 loaded with a synthetic solution mixtures of 400 mg/L of SCN^- and 100 mg/L of phenol (flow rate = 15 mL/min).

column was less than 5 mg/L in resin MP500 and reached a concentration of 250 mg/L, while at the same time for the resin M610 the concentration was less than 30 mg/L and reached a concentration of 430 mg/L in the elution peak.

Fixed Bed Operation with Industrial Wastewater. The final design of the ion exchange operation must be carried out testing the behavior of the resin with the industrial wastewater, obtained from the condensates of the gas coke. Thus it is interesting not only to check the capacity of the resin in industrial operation conditions but also to check the resin physical resistance with time after several operational load / elution cycles.[31]

Five stages of load and elution were carried out using synthetic solutions of SCN^- (stages 1 and 2), mixture of SCN^- and phenol (stage 3), and wastewater (stages 4 and 5) to see the operation of the resins.

In stages 4 and 5, the resins were loaded with wastewater previously filtrated from coke gas condensate containing 400 mg/L of SCN^- and 15 mg/L of phenol approximately.

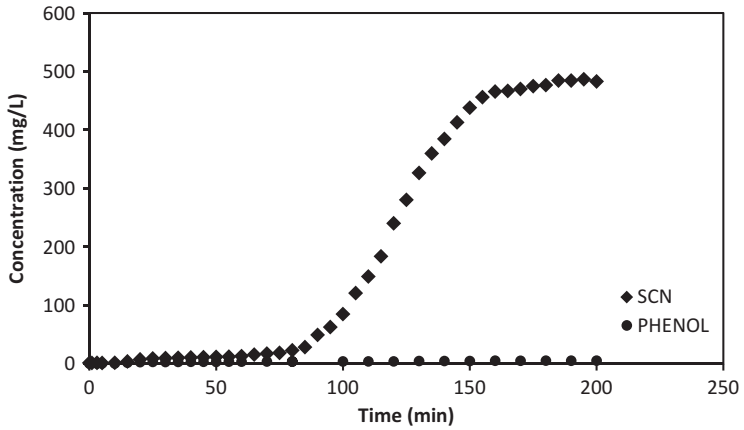

Figure 8 Breakthrough curve for the sorption of SCN^- and phenol present in wastewater using M610 ion exchange resin (flow rate = 16 mL/min).

For the resin MP500, the curve shows scattered results, and an increase or pronounced jump of the concentration with time, reaching the concentration of the initial sample in 130 minutes was not observed. However, for the resin M610 the curve shows a pronounced increase, that is, a more compressive front. The breakthrough curve for this resin was less sharp than in the case of synthetic solutions, reaching complete saturation in 200 minutes. Figure 8 shows the breakthrough curve of the fifth load cycle for the Lewatit M610.

The fifth elution step for Lewatit M610 is shown in Fig. 9. After several operation cycles the elution peak remains well formed reaching a concentration near 3600 mg/L in the elution peak, so the operation is well stabilized with no loss of capacity. For the resin MP500, similar results were found, with an elution peak of 950 mg/L of thiocyanate. For both of the resins the recovery of thiocyanate was near 100%, so the operation was stabilized after five operational cycles.

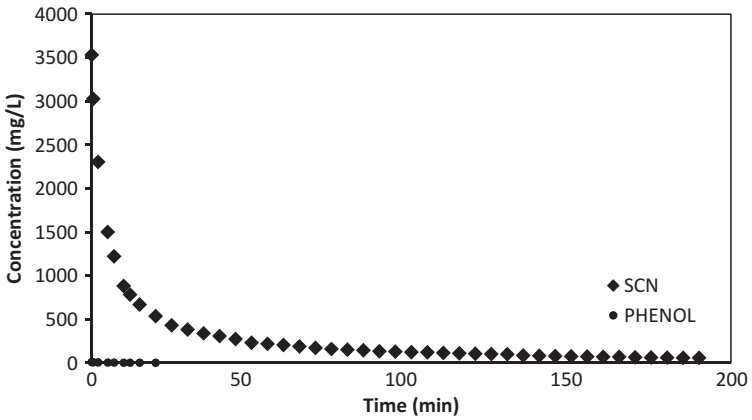

Figure 9 Elution curve using NaOH of Lewatit M610 loaded with wastewater (flow rate = 16 mL/min) after five load-elution cycles.

Table 6 Results of load with wastewater and elution with NaOH 0.5 M stages.

Resin	Stage	Load SCN^- (mg)	SCN^- recovered (mg)	Capacity (mg SCN^- / mL resin)	Recovery (%)
MP500	4	294	267	10.4	91
	5	267	250	9.5	91
M610	4	940	921	68.9	98
	5	848	833	62.2	98

In the case of phenol for industrial wastewater, variations in phenol concentration between loading and elution stages were not observed.

The results of the capacity of the resins in the stages with wastewater are summarized in Table 6. A slight decrease in the retention capacity for the two resins can be observed, but after 5 cycles the resin can be considered to be well stabilized because the quantity of the ions charged and eluted are the same. In this table the better capacity of Lewatit M610 in comparison with MP500 for the treatment of the effluent is evident.

CONCLUSIONS

The removal of thiocyanate from aqueous solutions and coke gas condensate wastewater using two strong anionic resins (Lewatit MP500 and Lewatit M610) was carried out successfully. Experiments in batch were carried out using synthetic solutions of 400 mg/L of thiocyanate, synthetic solutions containing mixtures of 400 mg/L of thiocyanate, and 100 mg/L of phenol and industrial wastewater containing 400 mg/L of thiocyanate and 15 mg/L of phenol approximately with and L/S ratio = 150 (volume of liquid (mL)/mass of resin (g)) determined in previous assays as adequate for calculating the retention capacity of the resins. The results were similar in both resins although a slightly higher capacity was obtained with resin M610. To study the adsorption equilibrium, the experimental data were fitted to the Langmuir and Constant Separation Factor isotherms. The values of the equilibrium constant for CSF isotherm were 17.37 for resin MP500 and 44.86 for resin M610.

In order to determine the rate-controlling step of the process, the mass transfer coefficient and the intraparticle diffusivity were obtained from experimental data. The film mass transfer model was used to calculate the mass transfer constant, obtaining values between $1.5{\cdot}10^{-5}$ and $4.3{\cdot}10^{-5}$ cm/s for resin MP500 and $2.7{\cdot}10^{-5}$ to $5.4{\cdot}10^{-5}$ cm/s for resin M610. The pore diffusion model was also tested to fit kinetics data, obtaining the diffusivity values between $8.3{\cdot}10^{-8}$ and $4.4{\cdot}10^{-7}$ cm^2/s for resin MP500 and $2.2{\cdot}10^{-7}$ to $4.4{\cdot}10^{-7}$ for resin M610. The Helfferich method for predicting the rate-controlling step showed that the adsorption of thiocyanate onto Lewatit MP500 and M610 resins are controlled by mass transfer through liquid film.

Successive cycles of loading and elution in column were carried out with synthetic solutions and wastewater using Lewatit MP500 and M610 resins and a solution of NaOH 0.5 M as eluent. The retention capacities of the resins and the ability of the eluent were evaluated. The breakthrough curves obtained for synthetic solution were sharp and NaOH were determined as a good eluent because the thiocyanate can be concentrated nearly five times after elution permitting an easier final treatment of this compound. For synthetic mixtures of thiocyanate/phenol the breakthrough curves that the thiocyanate front displaces

in the phenol front can be useful for the separation of phenol and thiocyanate if necessary. Finally, the ion exchange resins were tested with the real industrial coke condensates after several load / elution cycles in the fixed bed columns. The shape of the breakthrough curves is adequate to permit the viability of the ion exchange operation for the treatment of the effluent. The elution of the thiocyanate with NaOH gives a good elution peak, concentrating the contaminant compounds and completely eluting the ions.

In conclusion, taking into account the equilibrium, kinetics, and fixed bed results shown in this work it can be concluded that the resin Lewatit M610 is more effective than Lewatit MP500 to remove thiocyanate from industrial coke condensates. The two resins can be used to design the ion exchange process to eliminate thiocyanate and phenol from the condensates of gas coke plants allowing the waste of the ion exchange effluent in the treatment plants without risk for the microbiological sludge.

REFERENCES

1. Luthy, R G. Cyanide and thiocyanate in coal gasification wastewaters. J. Water Pollut. Control Fed. **1979**, *51*, 2267–2282.
2. Luthy, R G. Treatment of coal coking and gasification wastewaters. J. Water Pollut. Control. Fed. **1981**, *53*, 325–339.
3. Rancaño, A. *Biological Treatment of Coke Wastewaters*. PhD Thesis. Universidad de Oviedo (Spain), 2000.
4. Kononova, O.N.; Kholmogorov, A.G.; Danilenko, N. V.; Goryaeva, N. G.; Shatmykh, K.A.; Kachin, S.V (2007). Recovery of silver from thiosulfate and thiocyanate leachsolutions by adsorptionon anion exchange resins and activated carbon. Hydrometallurgy **2007**, *88*, 189–195.
5. Namasivayam, C.; Sangeetha, D. Kinetic studies of adsorption of thiocyanate onto ZnCl2 activated carbon from coir pith, an agricultural solid waste. Chemosphere **2005**, *60*, 1616–1623.
6. Li, Y.; Gao, B.; Wu, T.; Chen, W.; Li, X.; Wang, B. Adsorption kinetics for removal of thiocyanate from aqueous solution by calcined hydrotalcite. Colloids and Surfaces A **2008**, *325*, 38–43.
7. Balawejdar, E.K. A macromolecular N, N-dichloro-sulfonamide as oxidant for thiocyanates. Eur. Polym. J. **2002**, *36*, 1137–1143.
8. Sharma, V; Burnett, C; O´Connor; Cabelli, D. Iron (VI) and iron (V) of thiocyanate. Environ. Sci. and Technol. **2002**, *36*, 4182–4186.
9. Vicente, J; Díaz, M. Thiocyanate wet oxidation. Environ. Sci. Technol.. **2003a**, *37*, 1452–1456.
10. Vicente, J; Diaz, M. Thiocyanate/phenol wet oxidation interactions. Environ. Sci. Technol. **2003**b, *37*, 1457–1462.
11. Vicente, J; Díaz, M. Treatment of coke effluents by wet oxidation (I). Ingeniería Química. **2004**, *36*(412), 142–161.
12. Vicente, J; Díaz, M. Treatment of coke effluents by wet oxidation (II). Ingeniería Química. **2004**, *36*(413), 188–209.
13. Vicente, J; Rosal, R; Díaz, M. Catalytic wet oxidation of phenol with homogeneous iron salts. J. Chem. Technol. Biotechnol. **2005**, *80*, 1031–1035.
14. Christy, A; Egeberg, P. Oxidation of thiocyanate by hydrogen peroxide- a reaction kinetic study by capillary electrophoresis. Talanta. **2000**, *51*, 1049–1058.
15. Van Leeuwen, J. Badriyha, B.; Vaczi, S. Investigation into ozonation of coal coking processing wastewater for cyanide, thiocyanate and organic removal. Ozone Sci. Eng. **2003**, *25*, 273–283.
16. Rong, C.; Xien, H. Electrosorption of thiocyanate anions on active carbon felt electrode in dilute solution. J. Colloid Interface Sci. **2005**, *290*, 190–195.
17. Ayranci, E.; Conway, B. E. Adsorption and electrosorption of ethyl xanthate and thiocyanate anions at high-area carbon cloth electrodes studied by in situ UV spectroscopy: Development of procedures for wastewater purification. Anal. Chem. **2001**, *73*, 1181–1189.

18. Kobya, M.; Topcu, N.; Demircioglu, N. Kinetic analysis of coupled transport of thiocyanate ions through liquid membranes at different temperatures. J. Membr. Sci. **1997**, *130*, 7–15.
19. Staib, C.; Lant, P. Thiocyanate degradation during activated sludge treatment of coke-ovens wastewater. Biochem. Eng. J. **2007**, *34*, 122–130.
20. Vazquez, I.; Rodriguez, J.; Marañón, E.; Castrillón, L.; Fernández, Y. Simultaneous removal of phenol, ammonium and thiocyanate from coke wastewater by aerobic biodegradation. J. Hazard. Mater. **2006**, *137*, 1773–1780.
21. Vázquez, I.; Rodríguez, J.; Marañón, E.; Castrillón, L.; Fernández, Y. Study of the aerobic biodegradation of coke wastewater in two and three-step activated sludge process. J. Hazard. Mater. **2006**, *137*, 1681–1688.
22. Jeong, Y; Chung, J. Simultaneous removal of COD, thiocyanate, cyanate and nitrogen from coal process wastewater using fluized biofilm process. Process Biochemi. **2006**, *41*, 1141–1147.
23. Dizge, N.; Dermirbas, E.; Kobya, M. Removal of thiocyanate from aqueous solutions by ion exchange resins. J. Hazard. Mater. **2009**, *166*, 1367–1376.
24. Costa, C.; Rodrigues, A. Intraparticle diffusion of phenol in macroreticular adsorbents: modeling and experimental study of batch and CSTR adsorbents. Chem. Eng. Sci. **1985**, *40* (6), 983–993.
25. APHA-AWWA-WPCF. *Standard Methods for the Examination of Water and Wastewater*, 19th Edn.; Washington, DC, 1992.
26. Boyd, G. E.; Adamson, A. W.; Myers, L. S. The exchange adsorption from aqueous solutions by organic zeolites. II. Kinetics. J. Am. Chem. Soc. **1947**, *69*, 2836–2848.
27. Boyd, G. E.; Schubert, J.; Adamson, A. W. The exchange adsorption of ions from aqueous solutions by organic zeolites. I. Ion-exchange equilibria. J. Am. Chem. Soc. **1947**, *69*(11), 2818–2829.
28. Helfferich, F. *Ion Exchange*; McGraw-Hill: New York, 1962.
29. Rodrigues, A. E.; Tondeur, D. Percolation Processes: Theory and Applications; NATO ASI Series; 1981, pp 31–81.
30. Madsen, N. K.; Sincovec, R. F. ACM Trans. Math. Software (TOMS). **1979**, *3*, 326–351.
31. Bachiller, D.; Torre, M.; Rendueles, M (2004). Cyanide recovery by ion exchange from gold ore waste effluents containing copper. Min. Eng. **2004**, *17*, 767–774.
32. Bolto, B. A.; Pawlosky, L. *Wastewaters Treatment by Ion Exchange*; E & F. N. Spon Ltd.: London, 1987.

4.6. SÍNTESIS DE POLÍMEROS DE 2-DIETILAMINOETIL METACRILATO EN FORMA DE ESFERAS, CARACTERIZACIÓN FISICO-QUÍMICA Y CAPACIDAD PARA RETENER ANTIBIÓTICOS

Debido a la necesidad de crear materiales adsorbentes de bajo coste, selectivos y fácilmente regenerables, capaces de retener compuestos que se encuentran en baja concentración en las aguas como es el caso de los antibióticos, pero que es necesario eliminar para cumplir con la legislación vigente en materia de aguas, se ha decidido sintetizar polímeros de metacrilato por las ventajas que presentan frente a otros materiales poliméricos como fácil funcionalización y se puede trabajar tanto a pH ácido como básico.

En la publicación que se incluye a continuación, se ha descrito el proceso de síntesis y caracterización llevado a cabo en el laboratorio para la obtención de polímeros de metacrilato en forma de esferas mediante fotopolimerización. Se describe el protocolo seguido en la síntesis y los resultados obtenidos en la caracterización física. Asimismo, se ha estudiado la capacidad de estos polímeros para retener un antibiótico, sulfametoxazol, presente en disoluciones acuosas. Posteriormente, con el polímero con el que se ha obtenido mayor capacidad de retención se ha estudiado el equilibrio y la cinética del proceso de intercambio iónico en tanque agitado, determinándose las constantes de equilibrio y cinéticas.

También se ha analizado su comportamiento en columna, para ello se han llevado a cabo sucesivos ciclos de carga y elución, determinándose las capacidades de retención, la eficacia del eluyente en el proceso de regeneración, y se han modelizado las curvas de ruptura obtenidas ajustándolas a un modelo de lecho fijo.

Artículo: Synthesis of 2-(diethylamino)ethyl methacrylate-based microspheres. Physico-chemical characterization and chromatographic performance for antibiotic adsorption

Situación: artículo bajo revisión en *Separation and Purification Technology*

Synthesis of 2-(diethylamino)ethyl methacrylate-based microspheres. Physico-chemical characterization and chromatographic performance for antibiotic adsorption.

Ana María López Fernández[a], María A. Villa-García[b], Manuel Rendueles[a] and Mario Díaz[a]

[a]*Department of Chemical and Environmental Engineering, University of Oviedo, Oviedo, Spain*

[b]*Department of Organic and Inorganic Chemistry, University of Oviedo, Oviedo, Spain*

Abstract

In order to obtain new resins suitable for antibiotic adsorption, copolymeric beads of 2-(diethylamino)ethyl methacrylate-co-ethyleneglycol dimethacrylate (DEAEM-co-EGDMA) were synthesized by suspension polymerization. The monomers were dissolved in acetonitrile (ACN) and polyvinylpyrrolidone (PVP) was used as stabilizer of the suspension system. Cyclohexanol and poly(ethylene glycol) (PEG) of 1 kDa were used as porogens. Physical characterization showed that the polymers consist of macroporous micro spheres exhibiting a unimodal particle size distribution and good thermal stability. Chromatographic characterization using sulfamethoxazole (SMX) as model antibiotic was carried out both in batch and in column-packed experiments. The Langmuir model described successfully the SMX removal. The copolymer showed very good retention capacity, 101 mg SMX/g wet resin, which is equivalent to 220 mg SMX/g dry resin. Kinetic parameters were determined using the pore diffusion model. Finally, several cycles of loading and elution were performed in a fixed bed column. Breakthrough curves of loading and elution were fitted using a fixed bed adsorption model, the good results obtained confirm the validity of this model.

Keywords: methacrylate copolymers, sulfamethoxazole, equilibrium, kinetics, fixed bed operation

1. Introduction

Human and veterinary antibiotics are frequently found in aquatic environments and soil. These drugs are introduced into the environment through waste effluents of manufacturing processes, excreta, disposal of unused or expired drugs and accidental spills during manufacturing or distribution [1, 2]. The presence of pharmaceuticals in the environment is due to the fact that these contaminants are not completely removed during waste water treatment in sewage treatment plants (STPs), and drinking water treatment plants (DWTPs).

Sulfamethoxazole (SMX), a sulfonamide commonly used to treat a wide variety of bacterial infections, is the antibiotic most frequently detected in municipal sewage [3-5]. It is no biodegradable and its persistence in the environment is larger than one year.

The presence in the environment, even in low concentrations, of antibiotics and other pharmaceuticals may result in the development of adverse effects in terrestrial and aquatic organisms, and also increased bacterial resistance that can lead to decreased effectiveness of these drugs [6-11]. Therefore, there is a need to optimize and improve current technologies used in STP and DWTP for the elimination of drug residues and, especially, for the treatment of pharmaceutical industrial wastewater [12, 13]. Treatment options which are typically considered for the removal of emerging contaminants include: adsorption [14], advanced oxidation processes (AOPS) [15-19], nanofiltration (NF), and reverse osmosis (RO) membranes [20].

However, the shortcomings of most of these methods are: high investments and maintenance costs, secondary pollution and also the complicated procedures involved in the treatment.

Adsorption processes do not add undesirable by-products, and have been found to be superior to other techniques for wastewater treatment in terms of simplicity of design and operation. Among the different materials used as adsorbents, activated carbon (AC) [21, 22] has been used for the removal of different types of emerging compounds, but their use is sometimes restricted due to the high cost. Furthermore, although exhausted AC can be regenerated for further use, the regeneration results in a loss of carbon and lower adsorption capacity.

The use of polymeric resins for wastewater treatment has the advantages of lower costs, easy regeneration and selective removal of pollutants, in comparison with the low selectivity shown by activated carbon, which adsorbs organic chemicals indiscriminately [23]. Since most drugs are present in ionic form, ion exchange chromatography using polymeric supports can be effective for the removal of ionic antibiotics [24]. Additional advantage of the polymeric chromatographic supports for adsorption of ionic drugs, as an alternative to activated carbon, is due to the inefficient removal of electrically charged or hydrophilic pharmaceuticals by AC [25].

Aminomethacrylate-based polymers can behave as good adsorbents for retention of anionic contaminants due to the presence of amine functional groups. The tertiary amine function allows attaching charged species, since it can be easily transformed into a quaternary amine creating cationic centers [26]. A variety of aminomethacrylate monomers were used for the synthesis of polymeric membranes suitable for retention and separation in different fields such as waste water purification [27], solid phase extraction [28], drug delivery systems [29], protein recovery and purification [30-32] and biochemical sensors[33,34], among others.

Different requirements must be taken into account when designing a chromatographic separation medium. The chemical nature of the separation medium controls the type of chromatography, but a number of other features of the support such as mechanical and chemical resistance, rigidity and porosity are of great importance in order to achieve good chromatographic properties.

Macroporous polymer beads, obtained by dispersion and suspension polymerization techniques, provide high capacities, excellent solvent tolerance and good physical properties. However, for ion exchange chromatography in packed column experiments, because the larger particles accumulate near the walls and the smaller ones towards the center during the column filling process, it is very important to employ particles as uniform in size as possible [35,36].

Porosity of the chromatographic support usually plays a substantial role in the adsorption capacity, because it increases the adsorption surface and, hence, the number of adsorption sites. It was reported that the textural properties of the polymers can be modified by the solvents used in the polymerization mixture and the presence of porogenic agents [37–42]. It was also found that polymeric porogens significantly enhanced the permeability of the polymers, since the extraction of the linear polymeric porogen generates larger pores in the polymer structure [43-45].

This paper reports the synthesis, characterization and chromatographic behavior for antibiotic retention of copolymeric beads of 2-(diethylamino)ethyl methacrylate-

co-ethyleneglycol dimethacrylate (DEAEM-co-EGDMA). The polymeric beads were obtained by suspension polymerization, photoinitiated with azobiscyclohexane carbonitrile (ACCN), of a monomer mixture consisting of 40% DEAEM and 60% EGDMA dissolved in acetonitrile (ACN). Polyvinylpyrrolidone (PVP) was used as stabilizer of the suspension system. Cyclohexanol (sample A) and poly(ethylene glycol) (PEG) of 1 kDa (sample B) were used as porogens. Physico-chemical characterization of the polymers was carried out using different techniques: SEM microscopy, thermal gravimetric (TG) and differential thermal analysis (DTA), nitrogen adsorption-desorption isotherms, and mercury intrusion porosimetry. The chromatographic properties were tested using the antibiotic sulfamethoxazole, both in batch and in column-packed experiments. The kinetic curves were analyzed using the pore diffusion kinetics model. Finally, several cycles of loading and elution were performed in a fixed bed

column. Breakthrough curves of loading and elution were fitted using a fixed bed adsorption model.

2. Materials and Methods

2.1. Reagents

Sulfamethoxazole (purity>98% w/w), 2-(Diethylamino)ethyl methacrylate (99%), ethylene glycol dimethacrylate (98%) and the initiator 1,1´-azobis(cyclohexane–carbonitrile) (98%) were purchased from Aldrich (UK) and used without further purification. Acetonitrile (HPLC grade) and polyvinylpirrolidone (PVP) were purchased from Sigma-Aldrich. Poly(ethylene glycol) with molecular weight 1 kDa (Fluka) and cyclohexanol (Sigma-Aldrich) were used as porogenic agents. Methanol (HPLC grade, Sigma) was used for liquid chromatography and ultra-pure water was obtained with a Milli-Q purification system. Polyvinylidene difluoride (PVDF) membrane syringe filters of 0.45 µm (Millipore) were used to eliminate polymer particles in SMX analysis.

2.2. Polymer synthesis

A variety of polymers with DEAEM as functional monomer were prepared using mixtures with different compositions of monomer (DEAEM) and crosslinker (EGDMA) and two porogenic agents: cyclohexanol and the linear polymeric porogen poly(ethylene glycol) (1 kDa). To determine the optimum polymerization conditions different assays were run using different reaction times, agitation speed and temperature.

The resin with the higher retention capacity was synthesized using the following procedure: a mixture with a composition of monomer/crosslinker (DEAEM: EGDMA) 40:60 (mol%) was dissolved in acetonitrile, containing the initiator and cyclohexanol as porogen. The composition of the polymer was calculated with the base of 32 g of crosslinker (EGDMA). The solvent (ACN) was 50% (mass) of the total monomer and solvent mixture, while initiator was 1% (mass). The composition of the polymerization mixture is shown in Table 1. The organic phase was dispersed in an aqueous phase containing 1% of polyvinylpyrrolidone (PVP) as suspension stabilizer; the ratio of organic/aqueous phase was 1:3. The polymerization mixture was transferred to a UV irradiation reactor, UV-Laboratory Reactor System 2 (Peschl), and photopolymerization was carried out for 3 hours under vigorous stirring to avoid coalescence and agglomeration of the beads during the polymerization reaction, stirring speed was 900 rpm. The polymerization temperature was kept at 30 ºC by using water cooling. The intensity of the UV lamp was 0.163 W/cm^2. The polymer particles obtained were washed with water, separated by centrifugation and dried overnight at 60ºC.

Table 1. Polymers composition

Aqueous phase	1% PVP	
Organic phase	Polymers	
	A	B
DEAEM:EGDMA(mol %)	40:60	40:60
EGDMA(g)	32	32
DEAEM(g)	20	20
ACN(g)	52	52
ACCN (g)	1.040	1.040
Cyclohexanol(mL)	20	---
PEG 1kDa(g)	---	2
organic/aqueous ratio	1:3	1:3

2.3. Techniques of characterization

The diameter and surface features of the polymer microspheres after drying were observed by a JSM-6610 scanning electron microscope (SEM) (JEOL, Japan) operating at 20 kV. The sample was placed on a metal stub with double-sided conductive adhesive tape and was coated with a thin gold film using a Balzers SCD 004 equipment.

Particle size distributions of the polymer beads were determined by laser light scattering using a Mastersizer S long bench apparatus (Malvern Instruments Ltd., UK), provided with a 300RF lens capable of measuring particle sizes ranging from 0.05 to 900 µm. Nitrogen adsorption-desorption isotherm at 77 K was obtained with a Micromeritics ASAP 2020 instrument, using static adsorption procedures, the sample was previously degassed in vacuum at 130 ºC. Macroporosity and total pore volume were measured by mercury intrusion porosimetry with a Micromeritics Autopore IV instrument, performed under pressure values from 0.1 to 60.000 psia on samples previously evacuated. Thermal analysis was carried out using a Mettler SDTA851e with a Mettler TA-4000 TG-50 type thermobalance. Samples (40-50 mg) were heated in alumina crucibles, under nitrogen atmosphere, with a heating rate of 10ºC/min from 25° to 1000°C.

2.4. Analytical Method

Analysis of sulfamethoxazole concentrations in the samples after adsorption was performed by HPLC chromatography (Agilent 1200) combined with an UV detection system, using a reverse phase column (Mediterranean Sea: 18, 5µm x 25 cm x 46 cm). The wavelength used for detection was 270 nm. Prior to the analysis by HPCL the samples were filtered with 0.45 µm PVDF filters. The mobile phase consisted on a mixture of two solutions containing 0.1% trifluoro acetic acid (TFA) dissolved in methanol (solution A) and 0.1% TFA in water (solution B); isocratic conditions were used and the ratio of both eluents was: 60% of solution A and 40% of B. The column temperature was 40ºC, run time 10 minutes, and the injection volume 20 µL. The analysis was performed at a flow rate of 0.7 mL/min, being the retention time 4.9 minutes.

2.5. Batch separation media

The ion exchange properties of the polymeric beads for SMX retention were tested using batch and packed column experiments. The resin was conditioned by dispersing it twice in 1M solution of NaOH, using a liquid/solid ratio = 20 (volume of solution (mL)/mass of resin (g)) and contact time 20 m. Then, it was thoroughly washed with distilled water and filtered.

Sulfamethoxazole adsorption experiments were carried out in duplicate, at 20ºC, in an Erlenmeyer flask. In all the experiments 0.5 g of the activated resin were mixed with 400 mL of aqueous solutions of SMX (pH= 5), prepared by dissolving different amounts of the antibiotic in distilled water. The suspensions were stirred at 300 rpm for 2 hours, time necessary to reach the adsorption equilibrium. Blank experiments were run in parallel under the same experimental conditions. Using a liquid/solid ratio of 800 $mL \cdot g^{-1}$, which was previously established as the most convenient value, it was obtained the adsorption isotherm by changing the initial SMX concentrations.

2.6. Packed column separation media

Continuous flow ion exchange experiments were carried out in a glass column, internal diameter of 1.1 cm, filled with 2 grams of wet resin (0.9 g of dry resin), being the compacted bed height of 3 cm. The packed column was activated by pumping through (Masterflex 7554-60 pump) a 1 M solution of NaOH for 20 minutes at a flow rate of 6 mL/min. Then, distilled water was passed through it at a flow rate of 6 mL/min during 15 minutes. Breakthrough curves were obtained by pumping through the column SMX solutions containing 100, 200 and 300 mg SMX/L, at a flow rate of 6 mL/min. Samples for analysis were collected every at time intervals

between 5 to 10 minutes. Once the column had been saturated, distilled water was pumped through it at a flow rate of 6 mL/min to wash away any antibiotic not retained by the functional groups of the resin. After washing, the retained SMX was eluted by pumping through the column a solution of 0.5 M NaOH, at a flow rate of 5 mL/min

3. Results and discussion

In order to obtain a good chromatographic support for SMX anionic exchange, several assays were run under different polymerization conditions. In all cases suspension photo polymerization was used, and polyvinylpyrrolidone was employed as stabilizer of the copolymerization suspension, because by modifying its concentration it is possible to obtain beads with the desired particle size distribution [46]. Moreover, this stabilizer is easily removed from the beads surface. However, variables such as the composition of the monomers mixture, polymerization temperature and time, or type (cyclohexanol and poly(ethylene glycol) 1 kDa) and percentage of porogenic agents were considered. It was found that the best retention capacity was obtained when cyclohexanol was used as porogen. These assays lead us to conclude that the polymerization conditions described under the experimental section, were the most adequate to obtain macroporous beads of 2-(diethylamino)ethyl methacrylate-co-ethyleneglycol dimethacrylate with good chromatographic behavior for the retention of SMX. The white micro spheres synthesized have a bulk density of 0.486 g/ml and are hygroscopic.

3.1. SEM microscopy

Morphologic analysis of the beads was performed with a scanning electron microscope. Figure 1 shows micrographs of the samples taken with a magnification of 220x. The SEM images of samples A and B, Figure 1(a) and 1(b) respectively, reveal that the copolymer beads are spherical, but the particle size distributions are dependent on the type of porogen used. Cyclohexanol favors the formation of microspheres with more homogeneous average sizes. However, when using the polymeric porogen poly(ethylene glycol) 1 kDa, both larger and smaller micro spheres were obtained, being the beads size distribution more heterogeneous, therefore, resin B was less adequate to be used as chromatographic support.

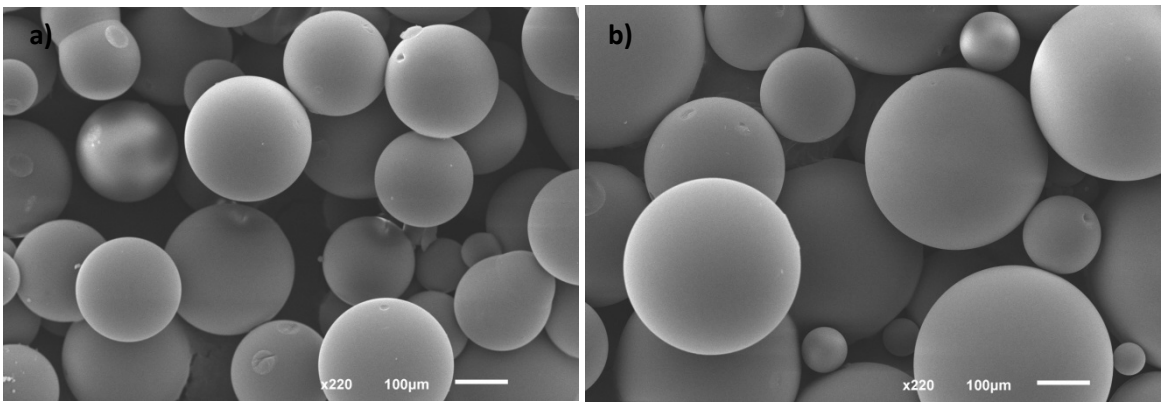

Figure 1. SEM images of the resins obtained using as porogen: a) cyclohexanol, b) PEG 1kDa

3.2. Particle size distribution

The importance of using particles as uniform in size as possible to increase the efficiency of the columns has already been reported [35, 36]. For this reason the polymer microspheres were analyzed in a Mastersizer laser granulometer (Malvern Instruments). Figure 2 shows that the size distribution curves obtained using both porogens were quite symmetric; the formation of polymer microspheres smaller than 100 µm was negligible. The polymer beads exhibit a unimodal particle size distribution with a maximum at 326 µm for the microspheres synthesized in the presence of cyclohexanol, sample A, and a maximum at 435 µm for those obtained using PEG 1kDa, sample B. The presence of the polymeric porogen in the polymerization mixture favors the formation of both larger and smaller size beads, being the particle size distribution more heterogeneous.

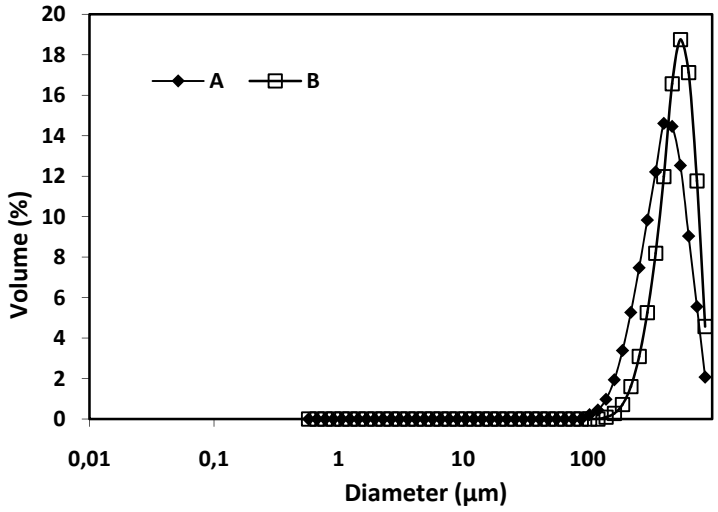

Figure 2. Particle size distribution curves of samples A and B

3.3. Thermal analysis

TG and DTG curves of sample A are shown in Figure 3. TG plot of both polymers shows the absence of any significant mass loss below 200 ºC; above this temperature takes place a continuous mass loss due to the polymer decomposition that is completed at ~ 470 ºC. The DTG curve shows that the polymer decomposition takes place in three steps. The first, with a maximum at 300 ºC, corresponds to the elimination of the amine groups, the mass loss corresponding to this step is 10.3 %; at higher temperature takes place the polymer decomposition at two different mass loss rates, with DTG peaks at 350 ºC and 440 ºC.

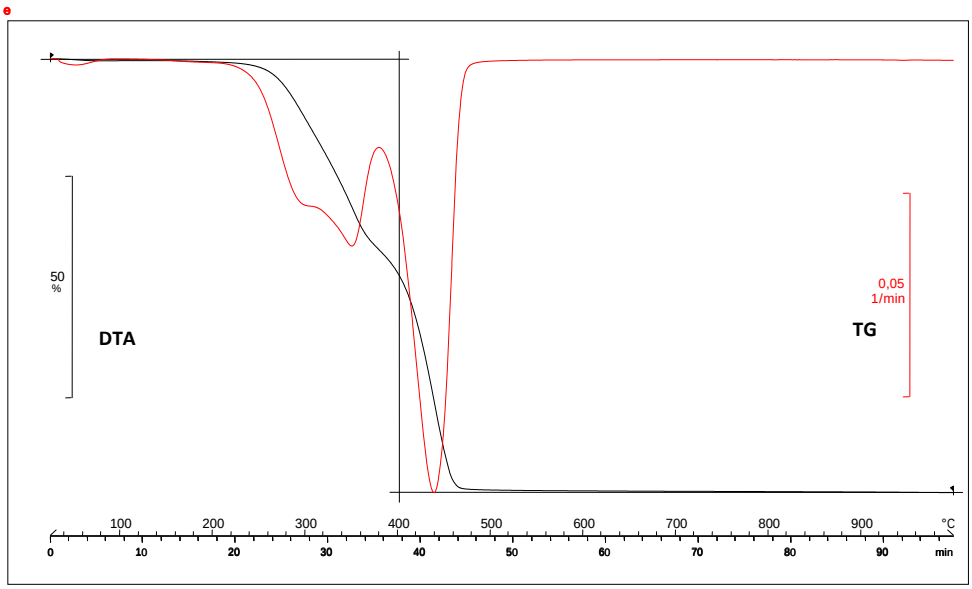

Figure 3. TG and DTG curves of sample A heated under nitrogen at 10ºC/min.

3.4. Textural properties

The porous structure of the chromatographic supports is one of the fundamental features required to achieve good retention capacity, large pores promote a rapid mass transfer that improves the kinetics of adsorption. In Figure 4 is shown the nitrogen adsorption-desorption isotherm at 77 K corresponding to the microspheres obtained using cyclohexanol as porogen (sample A). Nitrogen uptake is negligible at relative pressures lower than 0.85, indicating the absence of micro or mesoporosity. The profile of the isotherms is typical of a type II of the BDDT classification [47] and is characteristic of both macroporous and non-porous materials that only exhibit external surface area.

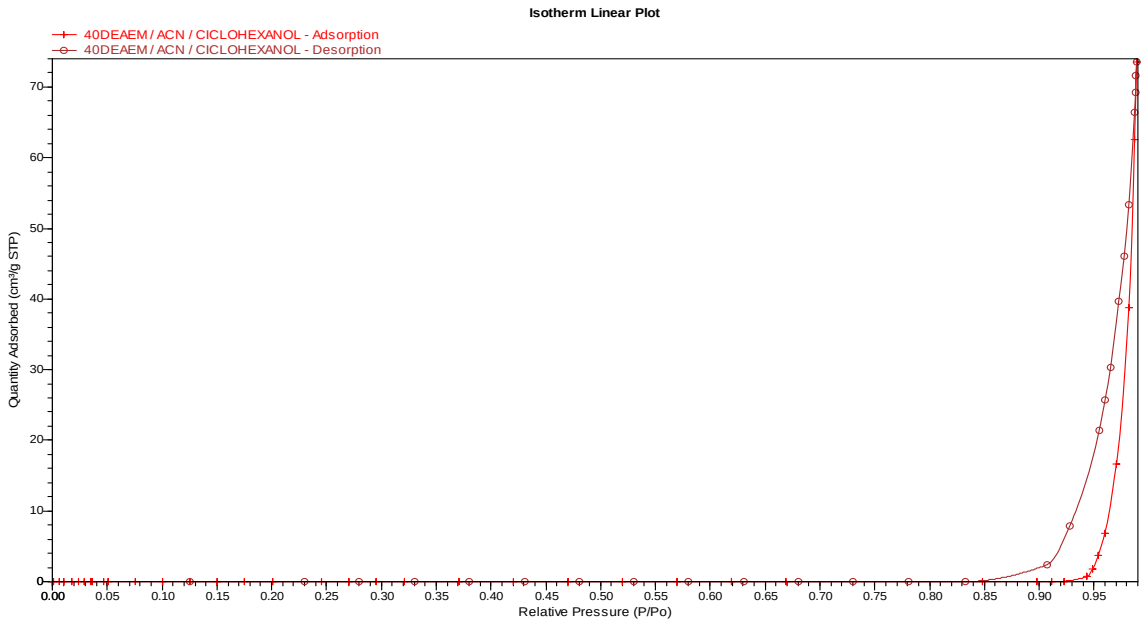

Figure 4. N_2 adsorption-desorption isotherm at 77 K of sample A.

Macroporosity of the polymers was analyzed by mercury intrusion porosimetry. The pore size distribution profiles of the beads obtained using cyclohexanol as porogen (sample A) and PEG 1 kDa (sample B), are shown in Figures 5 and 6. Sample A displays a bimodal pore size distribution with a first maximum at 600 µm and a second maximum at 800 µm, being the cumulative pore volume 1.071 mL/g. The large pore sizes indicate that the porosity is due to inter particle spacing, rather than pores within the structure. The pore size distribution of sample B shows maxima at 22 and 42 µm due to the presence of very large macropores, and also a peak at 700 µm due to inter particle spacing, the cumulative pore volume of this sample is 0.753 mL/g. The presence of the polymeric porogen in the polymerization mixture favors the formation of macroporous larger sized beads.

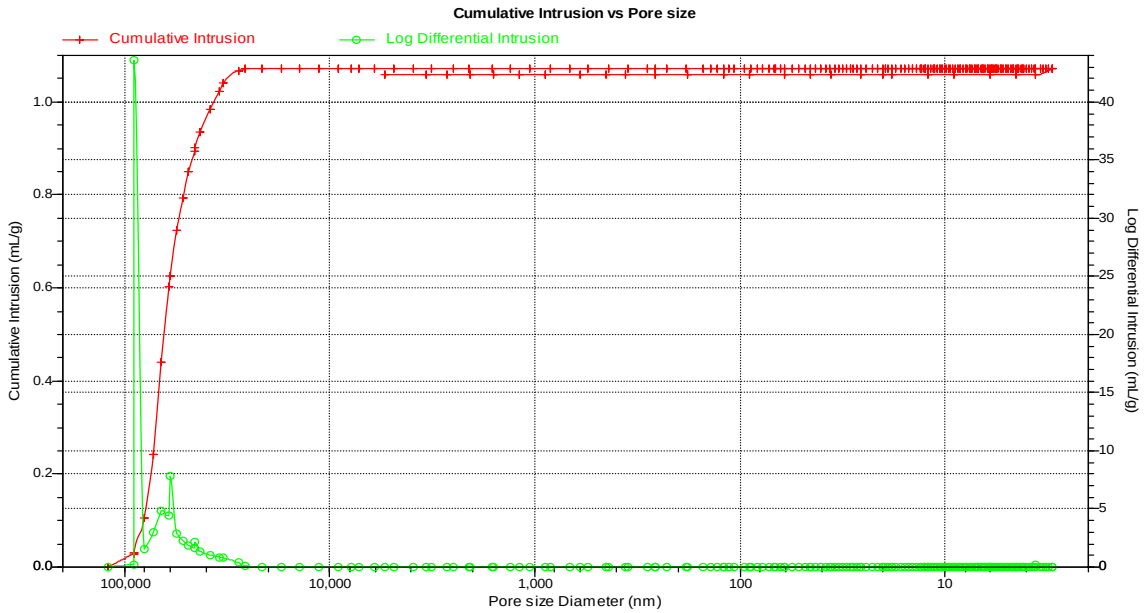

Figure 5. Pore size distribution profile of sample A measured by mercury porosimetry

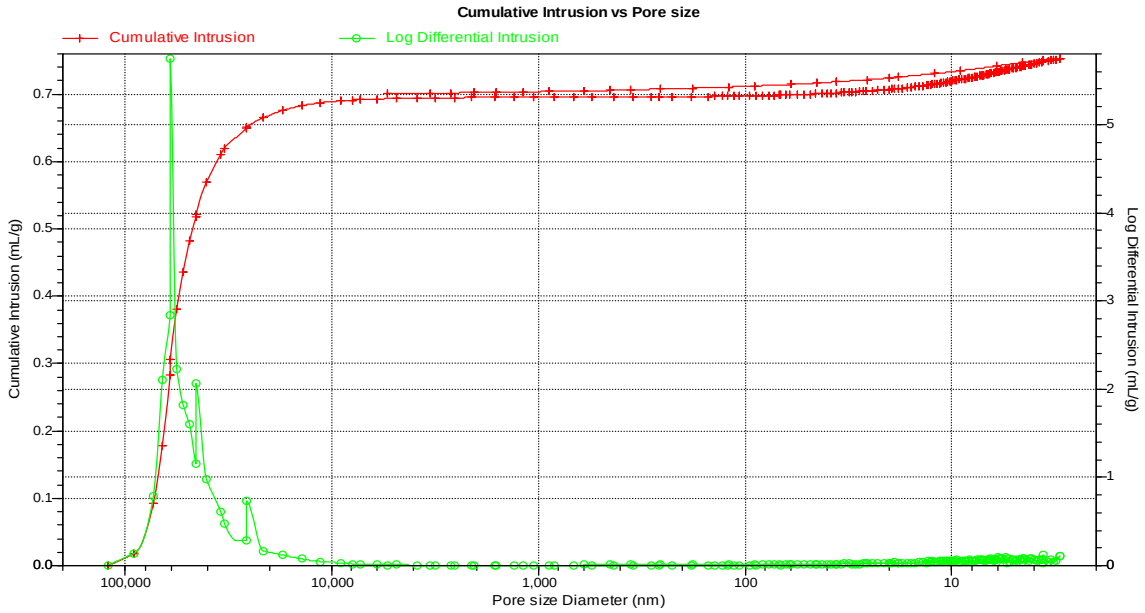

Figure 6. Pore size distribution profile of sample B measured by mercury porosimetry

3.5. Chromatographic properties

3.5.1. Batch equilibrium study

In order to evaluate the retention capacity of samples A and B, SMX adsorption experiments were performed in duplicate at pH 5 and 20 ºC. Both resins were sieved and particles with sizes between 100 µm and 355 µm were used in all the assays. Preliminary experiments were run dispersing 0.5 g of both resins in an aqueous solution containing 100 mg/L of SMX, using a liquid/solid ratio of 200 and two hours contact time. The adsorption capacities obtained were: 17.7 mg SMX /g wet resin for sample A, and 8.2 mg SMX/g wet resin

for sample B. The resin obtained using cyclohexanol as porogen showed considerably higher retention capacity than sample B, which is probably due to the fact that this resin with smaller bead sizes has larger surface area than sample B and, as a consequence, a larger number of functional groups are accessible to the antibiotic. Therefore, all the chromatographic assays were run using sample A as adsorbent for SMX retention.

The adsorption isotherm obtained under the conditions already described is depicted in Figure 7, and it shows typical Langmuir characteristics. The SMX uptake increases with the concentration and finally reaches a plateau. According to the Langmuir isotherm theory that assumes monolayer coverage of adsorbate over a homogeneous adsorbent surface, at equilibrium a saturation point is reached where no further adsorption/desorption can take place. The Langmuir equation is expressed as:

$$q_e = \frac{K_L \cdot C_e}{1 + a_L \cdot C_e} \tag{1}$$

where q_e is the equilibrium SMX concentration on the adsorbent (mg g^{-1}), C_e is the equilibrium liquid phase concentration (mgL^{-1}), K_L is the Langmuir constant (L·mg^{-1}), a_L is related to the energy of adsorption. The monolayer capacity of the Langmuir isotherm, Q_m is given as:

$$Q_m = \frac{K_L}{a_L} \tag{2}$$

Q_m is a constant related to the area occupied by a monolayer of adsorbate, reflecting the adsorption capacity of the resin (mg SMX/g wet resin).

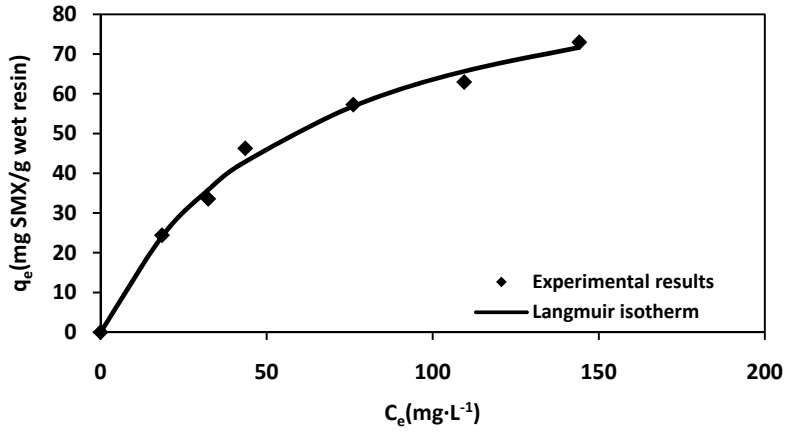

Figure 7. SMX adsorption isotherm

The Langmuir constants K_L and a_L were determined from a linear form of the Langmuir equation, represented by equation (3).

$$\frac{C_e}{q_e} = \frac{a_L}{K_L} C_e + \frac{1}{K_L} \tag{3}$$

Experimental data were fitted to equation (3), obtaining the following values for Langmuir parameters: K_L=1.71 L·g^{-1}, a_L= 0.017 L·mg^{-1} and Q_m = 101 mg SMX/g wet resin, equivalent to 220 mg SMX/g dry resin. The linear correlation coefficient was 0.9865.

To quantify the agreement between the model predictions and experimental data, the equilibrium equations were evaluated using Chi-square analysis [48] and non-linear regression analysis, equation (4). If the data predicted by the model is similar to experimental data, χ^2 (mg/g wet resin) will be small, and vice versa.

$$\chi^2 = \sum_{i=1}^{N} \frac{\left(q_{eq,exp} - q_{eq,cal}\right)^2}{q_{eq,cal}} \quad (4)$$

where $q_{(eq,cal)}$ is the equilibrium capacity obtained from a model (mg/g wet resin), $q_{(eq,exp)}$ is the equilibrium capacity obtained from experiments (mg/g wet resin), and N is the number of measurements. Eq. (5) shows the average percentage error (Ɛ) used in the non-linear regression analysis [49]. The errors between experimental data and predicted data were calculated using Eq. (5). The values obtained were χ^2=0.55 and $\mathcal{E}$=3.6%.

$$\varepsilon(\%) = \frac{\sum_{i=1}^{N}\left|\left(q_{eq,exp} - q_{eq,cal}\right)/q_{eq,exp}\right|}{N} \text{x } 100 \quad (5)$$

3.5.2. Batch kinetics study

The SMX adsorption process was monitored until equilibrium time was reached. After 120 minutes there were no substantial changes of the SMX concentration and operational equilibrium could be assumed. The ion exchange experiments were conducted in a stirred tank using initial concentrations of 50, 75, 100, 150, 200 and 250 mg/L SMX. The concentration profiles were modeled using the pore diffusion model to determine the mass transfer mechanisms [50]. Under our operating conditions it could be expected that the rate determining step was particle diffusion.

Pore Diffusion Model. This model [51] considers the resin to be a porous matrix. The model is described by the following equations:

- Mass balance inside the particle:

$$\frac{\partial q_i(R,t)}{\partial t} = \frac{\partial q_{ei}(R,t)}{\partial t} + \varepsilon_i \frac{\partial C_{pi}(R,t)}{\partial t} = \frac{1}{R^2}\left[\frac{\partial}{\partial R} R^2 \varepsilon_i D_p \frac{\partial C_{pi}(R,t)}{\partial t}\right] \quad (6)$$

where q_{ei} is the pore concentration of specie i, C_{pi} is the pore solution concentration of specie i, ε_i is the resin porosity, and D_p is the pore diffusivity.

- Mass balance in the bulk solution:

$$\varepsilon_i V(C_{iT} - C_i(t) = (1-\varepsilon_i) V \overline{q_{ei} + \varepsilon_i C_{pi}(t)} \quad (7)$$

where C_{iT} is the initial concentration of species i in solution, and V is the solution volume.

- Average concentration in particles:

$$\overline{q_{ei} + \varepsilon_i C_{pi}}(t) = \frac{3}{R_0^3}\int_0^R R^2 \left(q_{ei} + \varepsilon_i C_{pi}\right)(R,t)\,dR \quad (8)$$

where R is the radial coordinate, and R_0 is the particle radius. The initial and boundary conditions needed to solve the systems are:

- Initial conditions:

$$C_{pi}(R,=0) \tag{9}$$

- Boundary conditions:

$$\text{In R} = 0 \rightarrow \left.\frac{\partial C_{pi}\,(R,t)}{\partial R}\right|_{R=0} = \left.\frac{\partial q_i\,(R,t)}{\partial R}\right|_{R=0} \tag{10}$$

$$\text{At the inter phase } (\text{R} = \text{R}_0) \rightarrow \text{C}_{\text{pi}}(\text{R}_0, \text{t}) = \text{C}_\text{i}(\text{t}) \tag{11}$$

A FORTRAN subroutine, PDECOL [52], was used to solve these equations. The subroutine uses the orthogonal collocation on finite elements method to solve the non-linear differential equations. The average diffusivity value obtained was $3.1 \cdot 10^{-9}$ cm^2/s, with an average error of $\mathcal{E}$= 4.7 %. Figure 8 shows the good agreement found between experimental data and theoretical values obtained using the pore diffusion model.

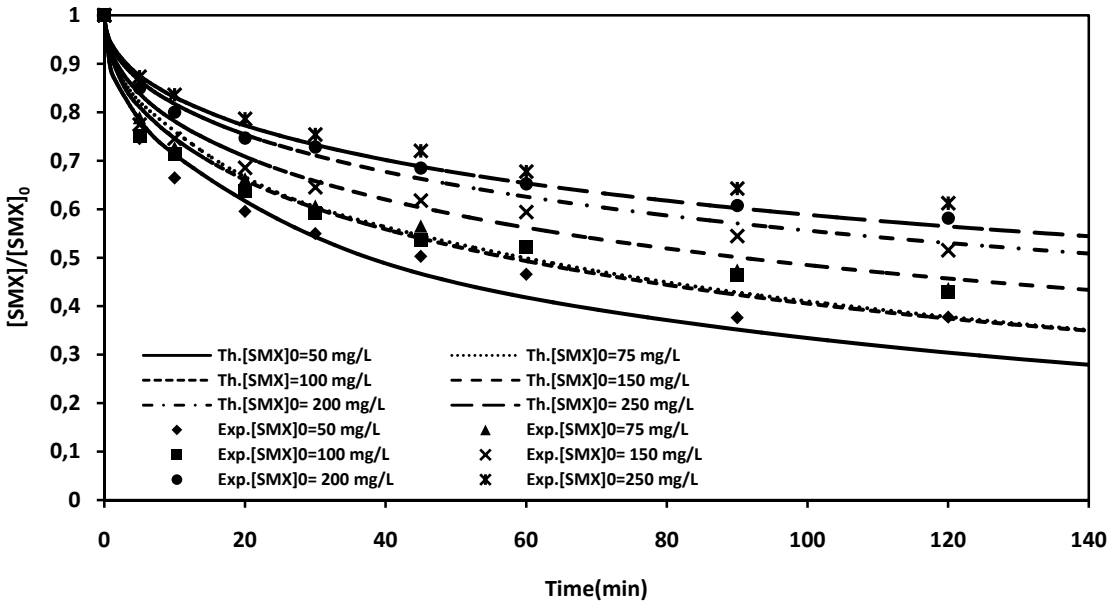

Figure 8. Kinetic curves obtained in batch and theoretical curves obtained using the pore diffusion model. Concentration range 50-250 mg SMX/L

3.6. Packed column experiments

The adsorption properties of the polymer were also studied in packed column experiments using 2 g of wet resin (0.9 g of dry resin), being the compacted bed height 3 cm. Column operation was initially tested by passing through a SMX solution containing 100 mg/L, at a flow of 6 mL/min. Breakthrough curves (Figure 9) were obtained by passing through the conditioned column SMX solutions with concentration of 100, 200 and 300 mg /L, at a flow rate of 6 mL/min. The retention capacity of the resin was calculated by numerical integration of the area under the breakthrough curve.

The first stage of loading was carried out with the solution whose concentration was 100 mg/L; the value obtained for the retention capacity from the breakthrough curve was 66 mg SMX/g wet resin.

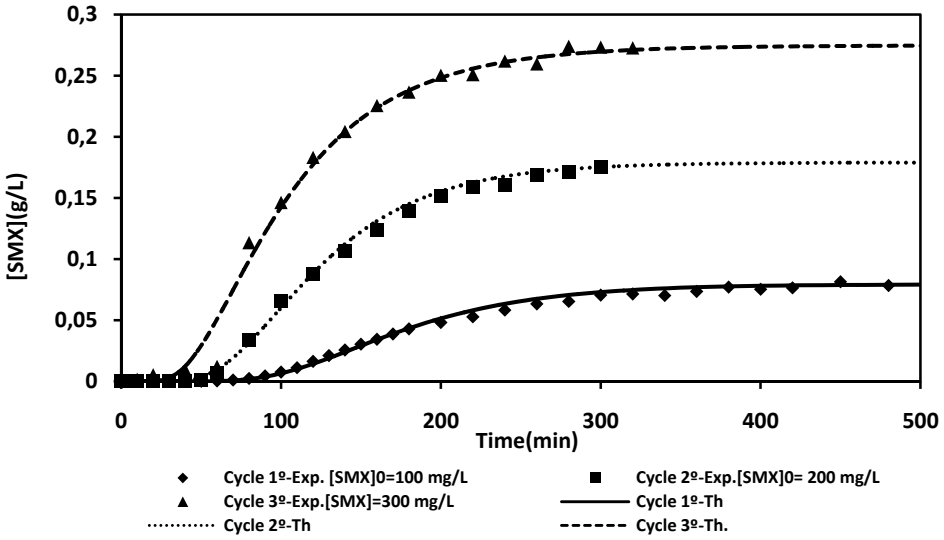

Figure 9. Experimental and theoretical breakthrough curves for SMX. Flow rate: 6 mL/min.

The resin was regenerated by passing through a 0.5 M solution of NaOH, at a flow rate of 5 mL/min. The elution curve is presented in Figure 10; it shows that SMX concentration in the eluate increases quickly at the initial stage of elution, being the SMX concentration 600 mg/L after 5 minutes, then the concentration decreases quickly and total elution is completed after 40 minutes. The resin shows a very good performance to concentrate the antibiotic in the initial stages of elution; SMX concentration in the eluate was ~ 6 times higher than in the loading solution, which is very interesting for industrial operation. In order to evaluate the effectiveness of the elution, a mass balance was carried out by integrating the area under the elution curve. It was found that the mass of SMX eluted was the same as the mass loaded, obtained by integrating the area under the loading curve. Complete SMX recovery was achieved in 40 minutes.

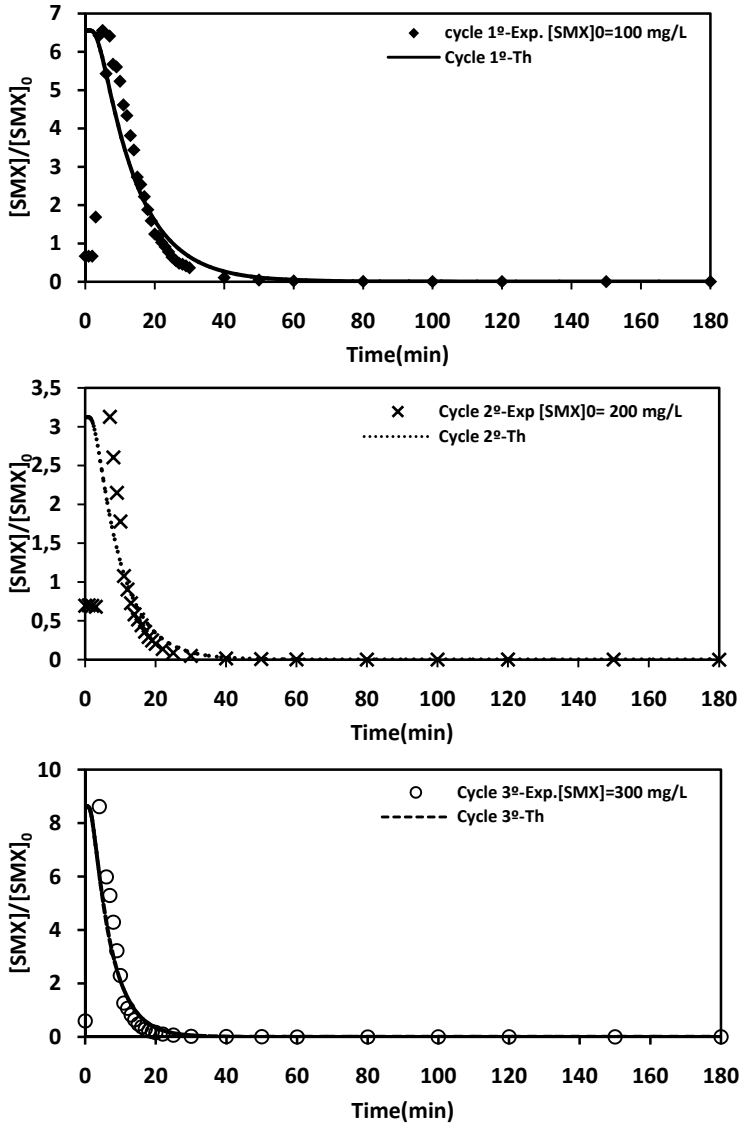

Figure 10. Experimental and theoretical elution curves for SMX using NaOH 0.5 M as eluant. Flow rate: 5 mL/min.

After the first stage of loading and elution, two more cycles were carried out to study the behavior of the resin after several cycles. SMX solutions with concentration of 200 and 300 mg/L were used in the second and third cycles, respectively. The breakthrough curves, Figure 9, show a rapid increase in SMX retention after 60 minutes, complete saturation of the column is reached in 300 minutes. The retention capacities of the resin were 91 mg SMX/g wet resin and 108 mg SMX/g wet resin in the second and third cycle, respectively. Elution curves corresponding to the second and third cycle (Figure 10) reveal that SMX concentration in the eluate increases quickly at the initial stage of elution, reaching a concentration of 620 mg/L in the second cycle and 2497 mg/L in the third cycle. In both cases total elution is completed after 40 minutes. Complete SMX recovery was achieved in all cycles. The results obtained show that the resin is an effective adsorbent to remove SMX. The retention capacity does not decrease after successive cycles, achieving a 100% recovery in all cases. The resin showed a very good performance to concentrate the antibiotic in the initial stages of elution; in the last cycles SMX concentration was 8 times higher in the eluate than in the loading solution, which favors an easier recovery of this compound.

3.7. Fixed bed model

Analysis of the loading and elution curves obtained from fixed bed experiments was carried out using a model developed by Costa [53] and used by Fernandez et al. [54] to simulate load and elution breakthrough curves in a laboratory column. The model considers equilibrium and kinetic aspects, axial dispersion in the column and assumes absence of film transfer resistance. Complete development of this model was reported by López et al. [55]. To solve the fixed bed model, parameters such as bed porosity, particle porosity, equilibrium constants, diffusivities in the pores and resin capacity must be known. All these parameters were previously determined for the system. The bed porosity was calculated in previous assays and the particle porosity was determined from the resin characterization. The axial dispersion value was not available for the laboratory column, so it was considered the only parameter to fit.

The values of the different parameters used in this study are shown in Table 2. The value calculated for axial dispersion was between 0.8-1.3 cm^2/s in the loading steps and between 0.4-0.8 cm^2/s in the elution steps. Experimental and theoretical load and elution breakthrough curves are shown in Figure 9 and Figure 10, respectively. Good agreement was found between experimental results and theoretical values obtained using the fixed bed model, both for the load and elution stages, thus demonstrating the validity of the model.

Table 2. Fixed bed operational parameters

Flow rate(mL/min)	6 (in load) 5 (in elution)
Bed Porosity(ε_l)	0.5
Particle Porosity (ε_i)	0.52
Equilibrium Constant SMX ($K_{eq\text{-}CSF}$)	11.3
Equilibrium Constant OH^-	0.09
Diffusivity in pores (cm^2/s)	$2.0 \cdot 10^{-9}$ (in load) $4.0 \cdot 10^{-9}$ (in elution)
Bed High(cm)	3
Retention Capacity of SMX (g SMX/L wet resin)	66-108

4. Conclusions

In this study, polymeric beads of 2-(Diethylanino)ethyl metacrylate-co-ethylene glycol dimethacrylate (DEAEM-co-EGDMA) were obtained by suspension polymerization, using as porogenic agents cyclohexanol and PEG 1kDa. The beads were tested as chromatographic supports to retain the contaminant sulfamethoxazole, frequently found in aquatic environments.

The presence of porogenic agents in the polymerization mixture did not generate small pores, the polymeric micro spheres obtained were macroporous or non porous. The nature of the porogens used conditioned the size and the particle size distribution of the beads. The presence of the polymeric porogen PEG 1kDa in the polymerization mixture favors the formation of both larger and smaller beads than those obtained using cyclohexanol. Thermal analysis revealed that the copolymers are stable below 200 ºC. Analysis of the porosity by mercury intrusion porosimetry showed the presence of very large pore sizes that can be attributed to inter particle spacing, rather than pores within the structure.

The resin obtained using cyclohexanol (sample A) as porogen showed considerably higher retention capacity, about twice higher than that exhibited by the resin obtained using PEG 1 kDa (sample B). This is probably due to the smaller bead sizes of sample A, which implies that the surface area of this resin is larger and, as a consequence, a larger number of functional groups are accessible to SMX.

Langmuir isotherm described the SMX adsorption process of polymer A. The resin has a high SMX retention capacity, up to 101 mg SMX/g wet resin, which is equivalent to 220 mg SMX/g dry resin. Kinetic parameters were determined using the pore diffusion model, obtaining a value for the pore diffusivity constant $D_p = 3.1 \cdot 10^{-9}$ cm^2/s.

The adsorption properties of the polymer were also studied in a fixed bed column, performing three successive cycles of loading and elution, obtaining in all the cycles a good retention capacity and complete elution of the antibiotic. Furthermore, the resin showed a very good performance to concentrate the antibiotic in the initial stages of elution, which favors an easier recovery of this contaminant.

Finally, it was obtained a good agreement between experimental breakthrough curves and the theoretical ones obtained using the fixed bed model, demonstrating the viability of the model. From the analysis of the chromatographic data, it can be concluded that this resin is highly effective for removing SMX in effluents of STPs.

Acknowledges

Financial supports of Ana María López from FICYT "Severo Ochoa Programme" grant (Gobierno del Principado de Asturias) are gratefully acknowledged.

References

1. M. Díaz-Cruz, D. Barceló, Environmental behavior and analysis of veterinary and human drugs in soils, sediments and sludge, Trends Anal. Chem. 22 (2007) 340-351.
2. D.G.J. Larsson, C. de Pedro, N. Paxeus, Effluents from drug manufactures contains extremely high levels of pharmaceuticals. J. Hazard. Mater. 148(2007) 751-755.
3. W. Xu, G. Zhang, S.C. Zou, X.D. Li, Y.C. Liu, Determination of selected antibiotics in the Victoria Harbor and the Pearl River, South China using high-performance liquid chromatography-electrospray ionization tandem mass spectrometry, Environ. Pollut. 145 (2007) 672-679.
4. A. Göbel, C.S. McArdell, A. Joss, H. Siegrist, W. Giger, Fate of sulfonamides, macrolides and trimethoprim in different wastewater treatment technologies. Sci. Total Environ. 372 (2007) 361-371.
5. K.J. Choi, S.G. Kim, C.W. Kim, S.H. Kim, Determination of antibiotics compounds in water by on-line SPE.LC/MSD, Chemosphere 66(&) 2007, 977-984.
6. Adams, C., Wang, Y., Loftin, K., and Meyer, M.T., Removal of antibiotics from surface and distilled water in conventional water treatment processes, J. Environ. Eng. 128 (2002) 253-260.
7. N. Le-Minh, S.J. Khan, J.E. Drewes, R.M. Stuetz, Fate of antibiotics during municipal water recycling treatment processes, Water Research 44(15) (2010) 4295-4323.
8. M. Carballa, F. Omil, J.M. Lema, M. Llompart, C. García, I. Rodriguez, M. Gómez, and T. Ternes, Behaviour of pharmaceuticals and personal care products in a sewage treatment plant of northwest Spain, Water Science and Technology 52 (2005) 29-35.
9. T.A. Ternes, M. Meisenheimer, D. McDowell, F. Sacher, H.-J. Brauch, B. Haist-Gulde, G. Preus, U. Wilme, N. Zulei-Seibert, Removal of pharmaceuticals during drinking water treatment. Environ. Sci. Technol. 36 (2002) 3855-3863.
10. P.E. Stackelberg, J. Gibs, E.T. Furlong, M.T. Meyer, S.D. Zaugg, R.L. Lippincott, Efficiency of conventional drinking water treatment processes in removal of pharmaceuticals and other organic compounds. Sci. Total Environ. 377 (2007) 255-272.
11. N.M. Vieno, H. Harkki, T. Tuhkanen, L. Kronberg, Occurrence of pharmaceuticals in river water and their elimination in a pilot scale drinking water treatment plant, Environ. Sci. Technol. 41 (2007), 5077-5084.
12. V. Homen and L. Santos, Degradation and removal methods of antibiotics from aqueous matrices-A review, Journal of Environment Management 92 (2011) 2304-2347.
13. M. Grassi, G. Kaykioglu, V. Belgiorno, G. Lofrano, Removal of Emerging Contaminants from Water and Wastewater by Adsorption Process, in: G. Lofrano(ed.) Emerging Compounds Removal from Wastewater, SpringBriefs in Green Chemistry for Suitainability, 2012, pp. 15-37.
14. T. Xuan Bui, H. Choi, Adsorptive removal of selected pharmaceutical by mesoporous silica SBA-15. Journal of Hazardous Materials 168 (2009) 602-608.
15. J.L. Acero, F.J. Benitez, F.J. Real, G. Roldan, Kinetics of aqueous chlorination of some pharmaceuticals and their elimination from water matrices, Water Res. 44 (2007) 4158-4170.

16. R. Andreozzi, M. Canterino, R. Marotta, N. Paxeus, Antibiotic removal from wastewaters: the ozonation of amoxicillin. J. Hazard. Mater. 122 (2005) 243-250.
17. L.A. Balcioğlu, M. Ötker, Treatment of pharmaceutical wastewater containing antibiotics by O_3/H_2O_2 processes, Chemosphere 50 (2003) 85-95.
18. A.G. Trovó, R.F.P. Nogueira, A. Agüera, C. Sirtori, A.R. Fernández-Alba, Photodegradation of sulfamethoxazole in various aqueous media: persistence, toxicity and photoproducts assessment, Chemosphere 77 (2009) 1292-1298.
19. M. Pérez-Moya, M. Graells, G. Castells, J. Amigó, E. Ortega, G. Buhigas, L.M. Pérez, H.D. Mansilla. Characterization of the degradation performance of the sulfamethazine antibiotic by Photo-Fenton process, Water Res. 44 (2010) 2533-2540.
20. S.Z. Li, X.-Y. Li, D.-Z. Wang, Membrane (RO-UF) filtration for antibiotic wastewater treatment and recovery of antibiotics, Sep. Purif. Technol. 34 (1-3) (2004) 109-114.
21. E.K. Putra, R. Pranowo, J. Sunarso, N. Indraswati, S. Ismadji, Performance of activated carbon and bentonite for adsorption of amoxicillin from wastewater: mechanism, isotherms and kinetics, Water Res. 43 (2009) 2419-2430.
22. J. Rivera-Utrilla, G. Prados-Joya, M. Sánchez Polo, M.A. Ferro Garcia, I. Bautista-Toledo, Removal of nitroimidazole antibiotics from aqueous solution by adsorption/bioadsorption on activated carbon, J. Hazard. Mater. 170 (2009) 298-305.
23. I. Vergili, H. Barlas, Removal of selected pharmaceutical compounds from water by an organic polymer resin. Journal of Scientific & Industrial Research 68 (2009) 417-425.
24. K.-J. Choi, H.-J. Son; S.-H. Kim, Ionic treatment for removal of sulphonamide and tetracycline classes of antibiotic, Sci. Total Environ. 387 (2007) 247-256.
25. E. Çalişkan S. Göktürk, Adsorption Characteristics of Sulfamethoxazole and Metronidazole on Activated Carbon, Separation Science and Technology 45 (2010) 244-255.
26. J.M. Cervantes-Uc, J.V. Cauich-Rodríguez, W.A. Herrera-Kao, H. Vázquez-Torres, A. Marcos-Fernández, Thermal degradation behabiour of polymethacrykates containing amine side groups, Polym. Degrad. Stabil. 93 (2008) 1891-1900.
27. Y.V. Bune, A.P. Sheninker, Y.S. Bogachev, I.L. Zhuravleva, E.N. Teleshov, Radical polymerization of diethylaminoethyl methacrylate and its salts in various solvents, European Polymer Journal, 27 (6) (1991) 509-513.
28. A. Guerreiro, A. Soares, E. Piletska, B. Mattiasson, S. Piletsky, Preliminary evaluation of new polymer matrix for solid-phase extraction of nonylphenol from water samples, Anal. Chim. Acta 612 (2008) 99-104.
29. M.T. Am Ende, D. Hariharan, N.A. Peppas. Factors influencing drug and protein transport and release from ionic hydrogels, React. Polym. 25 (1995) 127-137.
30. S. Barral, A. Guerreiro, M. A. Villa-García, M Rendueles, M. Díaz, Synthesis of 2-(diethylamino)ethyl mehacrylate-based polymers. Effect of crosslinking degree, porogen and solvent on the textural properties and protein adsorption performance, Reactive & Functional Polymers 70(2010) 890-899.
31. C.H. Hu, T.-C., Chou, Albumin molecularly imprinted polymer with high template affinity- Prepared by systematic optimization in mixed organic/aqueous media, Microchem Journal 91 (2009) 53-58.
32. C. Boyer, G. Boutevin, J.J. Robin, B. Boutevin, Study of the telomerization of dimethylaminoethylmethacrylate (DMAEMA) with mercaptoethanol. Application to the synthesis of a new macromonomer, Polymer 45 (23) (2004) 7863-7876.
33. S. Piletsky, E. Piletskaya, T.L. Panasyuk, A.V. El'skaya, R. Levi, I. Karube, G. Wulff, Imprinted membranes for sensor technology-opposite behavior of covalently and noncovalently imprinted membranes, Macromolecules 31 (7) (1998) 2137-2140.
34. X. Zhang, J. Xia, Controlled/"Living" Radical Polymerization of 2-(Dimethylamino)ethyl Methacrylate, Macromolecules 31 (15) (1998) 5167-5169.
35. M. Sarker, G. Guiochon, Study of the operation conditions of axial compression columns for preparative chromatography. J. Chromatogr. A 709 (1995) 227-239.
36. M. Sarker, A.M. Katti, G. Guiochon, Consolidation of the packing materials in chromatographic columns under dynamic axial compression. II Consolidation and breakage of several packing materials. J. Chromatogr. A 719 (1996) 275-289.
37. F. Svec, J.M.J. Fréchet, Kinetic control of pore formation in macroporous polymers. The formation of "molded" porous materials with high flow characteristics for separations or catalysis J. Chem. Mater. 7 (1995) 707-715.

38. C.D. Vianna-Soares, C.J. Kim, M.R. Borenstein, Hydrophilic Porous Hydroxypropyl Methacrylate–Ethyleneglycol Dimethacrylate Packing Materials Suitable for Use in Size Exclusion Chromatography, J. Porous Mater. 9 (1) (2002) 67-75.
39. J. Hradil, D. Horák, Characterization of pore structure of PHEMA-based slabs, React. Funct. Polym. 62 (1) (2005) 1-9.
40. I. Chianella, K. Karim, E.V. Piletska, C. Preston, S.A. Piletsky, Computational design and synthesis of molecularly imprinted polymers with high binding capacity for pharmaceutical applications - model case: adsorbent for abacavir, Anal. Chim. Acta 559 (2006) 73-77.
41. F. Wu, Y. Zhu, Z. Jia, Preparation of dye‑ligand affinity chromatographic packings based on monodisperse poly(glycidylmethacrylate-co-ethylenedimethacrylate) beads and their chromatographic properties, J. Chromatogr. A 1134 (1–2) (2006) 45-50.
42. C.F. Jasso-Gastinel, S. García-Enríquez, L.J. González-Ortiz, Synthesis and Characterization of Anionic Exchange Resins with a Gradient in Polymer Composition for the PS-co-DVB/PDEAMA-co-DVB System, Polym. Bull. 59 (6) (2008) 777-785.
43. A. Ferreira, M. Bigan, D. Blondeau, Optimization of a polymeric HPLC phase: poly(glycidyl methacrylate‑co-ethylene dimethacrylate): Influence of the polymerization conditions on the pore structure of macroporous beads, React. Funct. Polym. 56 (2003) 123-136.
44. T.A. Sergeyeva, S.A. Piletsky, E.V. Piletska, O.O. Brovko, L.V. Karabanova, L.M. Sergeeva, A.V. El'skaya, A.P.F. Turner, In situ formation of porous molecularly imprinted polymer membranes, Macromolecules 36 (19) (2003) 7352-7357.
45. R.H. Schmidt, K. Mosbach, K. Haupt, A simple method for spin coating molecularly imprinted polymer films of controlled thickness and porosity, Adv. Mater. 16 (8) (2004) 719-722.
46. L. Morejón, L. Mendizábal, J. A. Delgado, N. Davidenko, F. López-Dellamary, R. Manríquez, M. P. Ginebra, F. J. Gil, J. A. Planell, Synthesis and characterization of poly(methyl methacrylate-styrene) copolymeric beads for bone cements, Latin American Applied Research 35 (2005)175-182.
47. S. Brunauer, L.S. Deming, W.S: Deming, E. Teller, On a theory of the Van der Waals adsorption of gases, J. Am. Chem. Soc. 62 (1940) 1723-32.
48. SH, Yuh, Selection of optimum sorption isotherm. Carbon, 42 (2004) 2113-2130.
49. Z. Aksu,O. Tunç, Application of biosorption for penicillin G removal comparison with activated carbon, Process Biochem. 40 (2004) 831-847.
50. F. Helfferich, Ion Exchange, McGraw-Hill, New York, 1962.
51. A.E. Rodrigues, D. Tondeur, Percolation Processes: Theory and Applications, NATO ASI Series, 1981, pp. 31-81.
52. N.K. Madsen, R.F. Sincovec, Algorithm 540: PDECOL, General Collocation Software for Partial Differential Equations [D3], ACM Transactions on Mathematical Software (TOMS) 5 (3) (1979) 326-351.
53. C. Costa, A. Rodrigues, Design of cyclic fixed-bed adsorption processes. Part I: Phenol adsorption on polymeric adsorbents, AIChE Journal 31(10) (1985) 1645-1654.
54. A. Fernández, A.E. Rodrigues, M. Díaz, Modelling of Na/K Exchange in Fixed Beds with Highly Concentrated Feed, Chem. Eng. J. 54 (1994) 17-22.
55. A.M. López, M. Rendueles, M. Díaz, Sulfamethoxazole Removal from Synthetic Solutions by Ion Exchange using a Strong Anionic Resin in Fixed Bed, Solvent Extraction and Ion exchange 31 (2013**)** 763-781.

4.7. RETENCIÓN DE SULFAMETAZINA Y MEZCLAS DE SULFAMETOXAZOL Y SULFAMETAZINA MEDIANTE INTERCAMBIO IÓNICO EN POLÍMEROS DE METACRILATO

En el trabajo que se incluye a continuación, se presentan los resultados obtenidos en el proceso de intercambio iónico de sulfametazina y de mezclas de sulfametoxazol y sulfametazina presentes en disoluciones acuosas, empleando polímeros de metacrilato sintetizados en forma de esferas mediante fotopolimerización.

Se describe el proceso de síntesis de la resina llevado a cabo y su caracterización. Se realizaron experimentos de equilibrio y cinética en tanque agitado empleando disoluciones acuosas de sulfametazina. También se llevaron a cabo ensayos empleando mezclas de sulfametoxazol y sulfametazina para estudiar la competitividad en el proceso de intercambio iónico. Los resultados obtenidos se ajustaron a isotermas de adsorción para sistemas individuales y para sistemas binarios, y la cinética se describió empleando el modelo de difusión en poros. A su vez, se estudió la operación en columna empleando disoluciones de sulfametazina, y mezclas de sulfametoxazol y sulfametazina. Se determinaron las capacidades de adsorción, las eficacias en el proceso de regeneración de la resina, y se modelizaron las curvas de ruptura obtenidas empleando un modelo de lecho fijo.

Artículo: Retention of sulfamethazine and sulfamethoxazole mixtures onto anionic ion exchange polymethacrylate resin

Situación: artículo bajo revisión.

RETENTION OF SULFAMETHAZINE AND SULFAMETHOXAZOLE IN MIXTURES ONTO ANIONIC ION EXCHANGE POLYMETHACRYLATE RESIN

Ana María López Fernández[a], María-A. Villa-García[b], Manuel Rendueles[a,*] and Mario Díaz[a]

[a] *Department of Chemical and Environmental Engineering, University of Oviedo, Oviedo, Spain*

[b] *Department of Organic and Inorganic Chemistry, University of Oviedo, Oviedo, Spain*

Abstract

The removal of sulfamethoxazole (SMX) and sulfamethazine (SMZ) from synthetic solutions using copolymeric beads of 2-(diethylamino)ethyl methacrylate-co-ethyleneglycol dimethacrylate (DEAEM-co-EGDMA) synthesized by photopolymerization have been studied in this work. The resin retention capacities in single system of SMZ and in binary mixtures of SMX and SMZ were determined in batch assays. Equilibrium data were analyzed using the Langmuir isotherm for single system, showed good retention capacity 41.2 mg SMZ/g wet resin (equivalent to 91.5 mg SMZ/g dry resin). The Extended Langmuir Model and the Jain and Snoeyink Modified Extended Langmuir Model were used for binary systems, being this last model more adequate to describe the competitive adsorption process. Kinetics was described using the pore diffusion model, determining the pore diffusivities. Finally, several load and elution cycles using synthetic solutions of SMZ and mixtures of SMX and SMZ were carried out in a fixed bed column. Higher retention capacities were obtained for SMX, and 100% of both compounds were recovered in elution steps. The breakthrough curves of load and elution were simulated using a fixed bed model. A good correlation between experimental dates and numerical results demonstrated the validity of this model.

Keywords: polymethacrylate, sulfamides, isotherms, kinetics, fixed bed operation

1. Introduction

The use of human and veterinary antibiotics are increased and pharmaceuticals and personal and care products have been detected in effluent of sewage treatment plants, in surface water and groundwater worldwide due to these contaminants cannot be removed completely in STPs, and persist in the environment, causing adverse effects on living organisms and an increase in the percentage of drug-resistance bacteria 1,2.

Sulfamethoxazole and sulfamethazine are bacteriostatic antibiotics sulfonamides commonly used to treat urinary tract infections in human and animals and they are some of the most detected antibiotics in sewage, agricultural wastewater, surface water and influent and treated water of drinking water treatment plants 3-6. For these reason, there is a need to optimize and improve current technologies used in STP and DWTP for elimination pharmaceutical residues, especially for industrial wastewater and purifying surface water in DWTP 7-10. Treatment options which are typically considered for the removal of emerging contaminants include adsorption 11,12, advanced oxidation processes (AOPs)13-17, nanofiltration and reverse osmosis membranes 18. However, the shortcomings of most of these methods are: high investment and maintenance costs, secondary pollution and complicated procedure involved in the treatment.

Adsorption process, although does not add undesirable by-products and is easy in terms of design and operation, is restricted due to high cost and loss of adsorption capacity after regeneration process (ACs) 19-21.

Since most of the antibiotics are present in ionic form, ionic exchange using chromatography support treatment can be effective for removing them. Polymeric resins are becoming more common in wastewater treatment due to low cost, easy regeneration and selective removal of pollutants, in comparison with the low selectivity shown by activated carbon, which adsorbs organic chemicals indiscriminately. Additional advantage of the polymeric chromatographic supports for adsorption of ionic drugs, as an alternative to activated carbon, is due to the inefficient removal of electrically charged or hydrophilic pharmaceuticals by AC [22]. Vergili [23] studied the removal of carbamazepine, propyphenazone and sulfamethoxazole by and organic polymer resin Lewatit VPOC 1163, and Choi [24] used ionic treatment (MIEX treatment) for removal sulfonamides and tetracyclines antibiotics. In previous works, the removal of SMX in solutions was studied using Lewatit MP500 a macroporous resin with quaternary amine as functional group, which showed good results 25.

Aminomethacrylate-based polymers can behave as good adsorbents for retention of anionic contaminants due to the presence of amine functional groups. The tertiary amine function allows attaching charged species, since it can be easily transformed into a quaternary amine creating cationic centers 26. A variety of aminomethacrylate monomers were used for the synthesis of polymeric membranes suitable for retention and separation in different fields such as waste water purification 27, solid phase extraction 28, drug delivery systems 29, protein recovery and purification 30-32 and biochemical sensors 33,34, among others.

Macroporous polymer beads, obtained by dispersion and suspension polymerization techniques, provide high capacities, excellent solvent tolerance and good physical properties. However, for ion exchange chromatography in packed column experiments, it is very important to employ particles as uniform in size as possible, due to the larger particles accumulate near the walls and the smaller ones towards the center during the column filling process 35,36.

This paper report the synthesis, characterization and chromatography behavior for antibiotic retention of copolymeric beads of 2-(diethylamino)ethyl methacrylate-co-ethyleneglycol dimethacrylate (DEAEM-co-EGDMA). Physical-chemical characterization of polymer was carried out using different techniques and the chromatography support was tested using the antibiotic sulfamethazine (SMZ), due to the adsorption of other antibiotic, SMX, onto this polymer was studied previously. Likewise, the polymer was tested using mixtures of both sulfamides SMX and SMZ in equal proportion of each compound, to study the competition in the adsorption process by the active sites of the polymer, so they commonly appear in real waters mixed. Polymer was tested in both, batch and column-packed experiments. Equilibrium and kinetics was studied for individual and binary systems in batch. Finally, several operational cycles of loading and elution were performed in a fixed bed column, fitting the breakthrough curves to a fixed bed adsorption model.

2. Materials and methods

2.1. Reagents

Sulfamethoxazole and sulfamethazine (purity>98% w/w), 2-(diethylamino)ethyl methacrylate (99%), ethylene glycol dimethacrylate (98%) and the initiator 1,1´-azobis(cyclohexane–carbonitrile) (98%) were purchased from Aldrich (UK) and used without further purification. Acetonitrile (HPLC grade) and polyvinylpirrolidone (PVP) were purchased from Sigma-Aldrich. Cyclohexanol (Sigma-Aldrich) were used as porogenic agent. Methanol (HPLC grade, Sigma) was used for liquid chromatography and ultra-pure water was obtained with a Milli-Q purification system. Polyvinylidene difluoride (PVDF) membrane syringe filters of 0.45 μm (Millipore) were used to eliminate polymer particles in SMX and SMZ analysis.

2.2. Polymer synthesis

The resin was synthesized using the following procedure: a mixture with a composition of monomer/crosslinker (DEAEM: EGDMA) 40:60 (mol%) was dissolved in acetonitrile, containing the initiator and cyclohexanol as porogen. The composition of the polymer was calculated with the base of 32 g of crosslinker (EGDMA). The solvent (ACN) was 50% (mass) of the total monomer and solvent mixture, while initiator was 1% (mass). The composition of the polymerization mixture is shown in Table 1. The organic phase was dispersed in an aqueous phase containing 1% of polyvinylpyrrolidone (PVP) as suspension stabilizer; the ratio of organic/aqueous phase was 1:3. The polymerization mixture was transferred to a UV irradiation reactor, UV-Laboratory Reactor System 2 (Peschl), and photopolymerization was carried out for 3 hours under vigorous stirring to avoid coalescence and agglomeration of the beads during the polymerization reaction, stirring speed was 900 rpm. The polymerization temperature was kept at 30 ºC by using water cooling. The intensity of the UV lamp was 0.163 W/cm^2. The polymer particles obtained were washed with water, separated by centrifugation and dried overnight at 60ºC.

Table 1. Polymers composition

Aquatic phase	1% PVP
Organic phase	
DEAEM:EGDMA (mol %)	40:60
EGDMA(g)	32
DEAEM(g)	20
ACN(g)	52
ACCN (g)	1.040
Cyclohexanol(mL)	20
PEG 1kDa(g)	---
Organic:aquatic ratio	1:3

2.3. Polymer characterization

The diameter and surface features of the polymer microspheres after drying were observed by JSM-6610 scanning electron microscope (SEM) (JEOL, Japan) operating at 20 kV. Particle size distributions of the polymer beads were determined by laser light scattering using a Mastersizer S long bench apparatus (Malvern Instruments Ltd., UK), provided with a 300RF lens capable of measuring particle sizes ranging from 0.05 to 900 µm. Thermal analysis was carried out using a Mettler SDTA851e with a Mettler TA-4000 TG-50 type thermobalance. Samples (40-50 mg) were heated in alumina crucibles, under nitrogen atmosphere, with a heating rate of 10ºC/min from 25° to 1000 °C. Nitrogen adsorption-desorption isotherm at 77 K was obtained with a Micromeritics ASAP 2020 instrument, using static adsorption procedures, the sample was previously degassed in vacuum at 130 ºC. Macroporosity and total pore volume were measured by mercury intrusion porosimetry with a Micromeritics Autopore IV instrument, performed under pressure values from 0.1 to 60.000 psia on samples previously evacuated.

2.4. Analytical methods

Determination of sulfamethoxazole and sulfamethazine in the samples after adsorption were performed by HPLC (Agilent 1200) using a reverse phase column (Mediterranean sea18, 5µm x 25 cm x 46 cm, from Teknokroma) combined with UV detection at 270 nm. Prior to the analysis by HPLC, the samples were filtered with 0.45 µm PVDF filters. The mobile phase consisted in a mixtures of two solutions containing 0.1% of trifluoro acetic (TFA) in methanol (solution A) and 0.1% of TFA in water (solution B). The method for SMZ alone was isocratic: 60% solution A and 40% solution B. Run time: 10 min. The retention of SMZ was 5.1 min. The method for SMX and SMZ mixed was a binary gradient from 30% solution A to 95% solution

B. Run time: 12 min. Post time: 3 min. The retention times in mixtures of SMX and SMZ were 7.5 min for SMX and 8.9 min for SMZ. The column compartment temperature was 40ºC. Injection volume: 20µL. Analysis was performed at flow rate of 0.7 mL/min.

2.5. Chromatography properties

The chromatographic properties of the polymeric beads for the retention of SMZ in individual system and SMX and SMZ in binary system were tested in batch and column-packed experiments

2.5.1. Batch Separation media

The resin was conditioned by dispersing it twice in 1M solution of NaOH, using a liquid/solid ratio = 20 (volume of solution (mL)/mass of resin (g)) and contact time 20 minutes. Then, it was thoroughly washed with distilled water and filtered.

Adsorption experiments using sulfamethazine and mixtures of sulfamethoxazole and sulfamethazine in equal proportion of each compound were carried out in duplicate, at 20ºC, in an Erlenmeyer flask of 500 mL. In all experiments 0.5 g of activated resin were mixed with 400 mL of aqueous solutions of SMZ (pH=6.5) and mixtures of SMX and SMX in equal proportion of each compound (pH=6) respectively, prepared by dissolving different amounts of the antibiotics in distilled water. The suspension was stirred at 300 rpm for 2 hours, time necessary to reach the adsorption equilibrium. The adsorption isotherms for individual (SMZ) and binary (SMX+SMZ) systems were obtained changing the initial concentration and using a liquid/solid ratio of 800 (mL solution/g wet resin), previously established as the most convenient value. To follow the evolution of the concentration over time, 2 mL samples were extracted from the tank each time, which did not change the volume of the solution appreciably.

2.5.2. Column-packed separation media

Continuous flow adsorption experiments were carried out in a glass column, internal diameter of 1.1 cm, filled with 3.6 grams of wet resin (1.7 g of dry resin), being the compacted bed height of 3 cm. The packed column was activated by pumping through (Masterflex 7554-60 pump) a 1 M solution of NaOH for 20 minutes at a flow rate of 6 mL/min. Then, distilled water was passed through it at a flow rate of 6 mL/min for 15 minutes. Breakthrough curves were obtained by pumping through the column SMZ solutions containing 100, 200 and 300 mg/L at a flow rate of 6 mL/min. Likewise, 3 grams of wet resin (1.4 g of dry resin) was packed in the column and activated following the same procedure. Then, SMX and SMZ mixtures solutions containing 100, 200, 300 and 400 mg/L of each compound were pumped through the column at a flow rate of 6 mL/min. Samples for analysis were collected every at time intervals between 5 to 10 minutes. Once the column had been saturated, distilled water was pumped through it at a flow rate of 6 mL/min to wash away any antibiotic not retained by the functional groups of the resin. After washing, the retained SMX and SMZ was eluted by pumping through the column a solution of 0.5 M NaOH, at a flow rate of 5 mL/min.

3. Results and discussion

The polymerization conditions of chromatographic support were described under the experimental section. The white micro spheres synthesized have a bulk density of 0.486 g/mL and are hygroscopic, 1 gram of wet resin equivalent to 0.45 grams of dry resin. The polymer characterization and its chromatographic properties for SMX and SMZ retention are described below:

3.1. Physico-Chemical characterization of the polymer

3.1.1. SEM microscopy

Morphologic analysis of the beds was performed with a scanning electron microscope. Figure 1 shows micrograph of the sample taken with a magnification of 220x. The SEM image reveals that the copolymer beads are spherical with quite homogeneous average sizes.

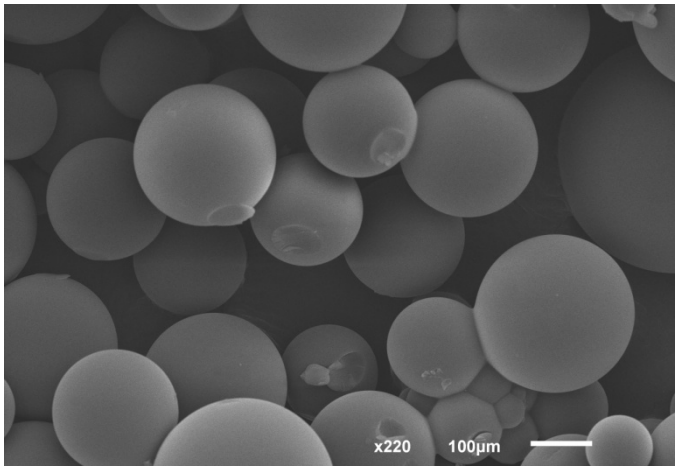

Figure 1. SEM image of DEAEM-co-EGDMA

3.1.2. Particle size distribution

The importance of using uniform particles to increase the efficiency of the columns has been reported 35,36. Therefore, the polymer microspheres were analyzed in a Mastersizer laser granulometer (Malvern Instruments). Figure 2 shows that the size distribution curve obtained is quite symmetric. The polymer beads exhibit a unimodal particle size distribution with a maximum at 326 µm.

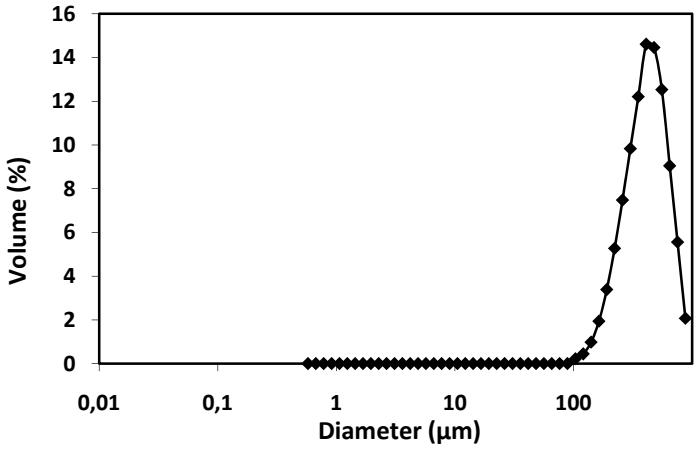

Figure 2. Particle size distribution of the resin

3.1.3. Textural properties

The porous structure of the chromatographic supports is one of the fundamental features required to achieve good retention capacity, large pores promote a rapid mass transfer that improves the kinetics of adsorption. In Figure 3 is shown the nitrogen adsorption-desorption isotherm at 77 K. Nitrogen uptake is negligible at relative pressures lower than 0.85, indicating the absence of micro or mesoporosity. The profile of the isotherms is typical of a type II of the BDDT classification 37 and is characteristic of both macroporous and non-porous materials that only exhibit external surface area.

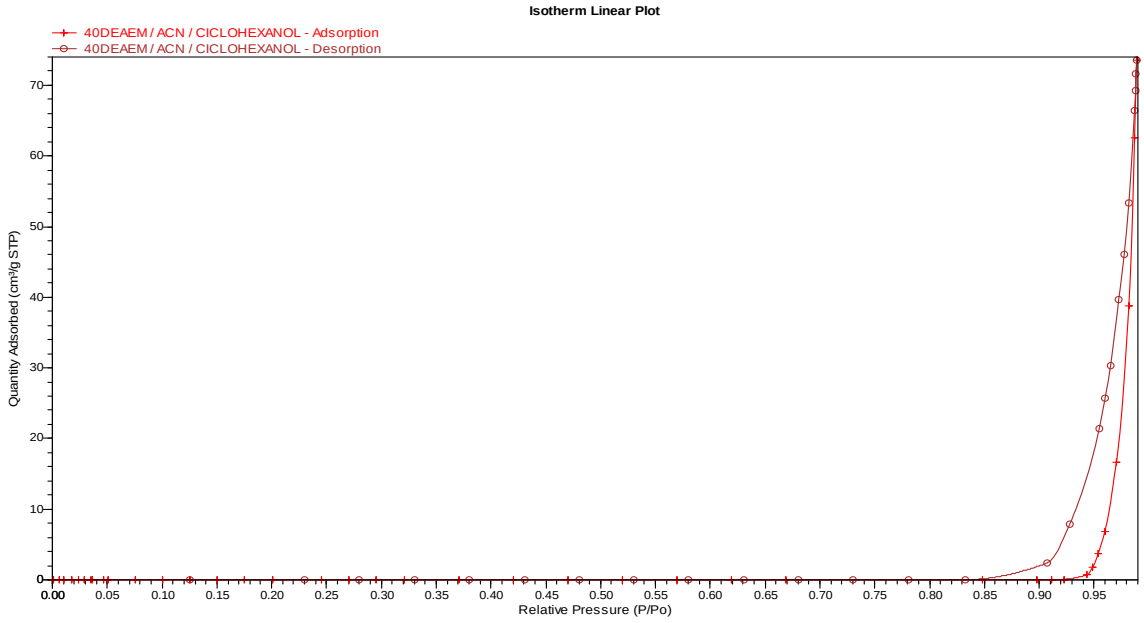

Figure 3. N_2 adsorption-desorption isotherm

Macroporous of polymer was analyzed by mercury intrusion porosimetry. Figure 4 shows the pore size distribution profile of beads synthesized. It presents a first maximum at 600 µm and a second maximum at 800 µm, being the cumulative pore volume 1.071 mL/g. The large pore sizes indicate that the porosity is due to inter particle spacing, rather than pores within the structure.

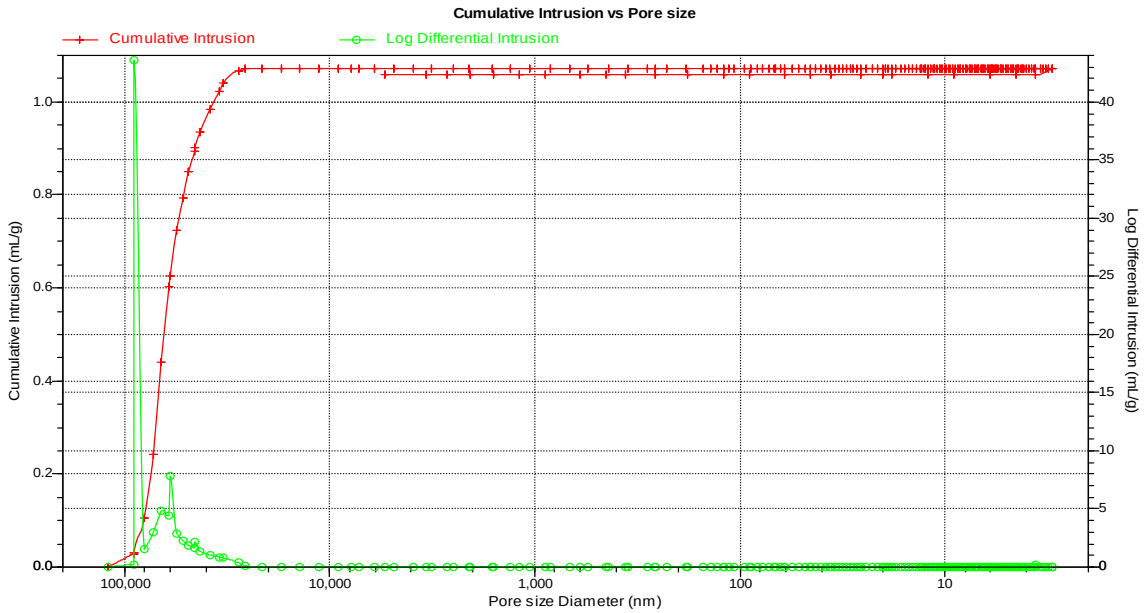

Figure 4. Pore size distribution profile measured by mercury porosimetry

3.1.4. Thermal analysis

TG and DTG curves of the resin, displayed in Figure 5, show the absence of any significant mass loss below 200 ºC, above this temperature takes places a continuous mass loss due to the polymer decomposition that is completed at ~ 470 ºC. The DTG curves shows that the polymer decomposition takes places in three steps. The first, with a maximum at 300 ºC, corresponds to elimination of amine groups, which corresponding to 10.3% mass loss, and above this temperature takes places the polymer decomposition.

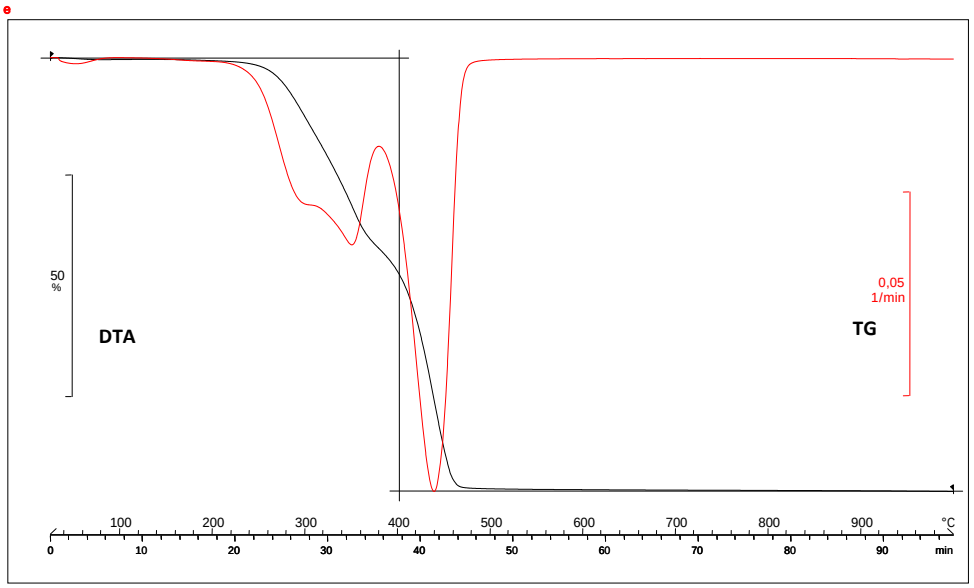

Figure 5. TG and DTA curves from thermal analysis

3.2. Chromatographic properties

3.2.1. Batch equilibrium studies

3.2.1.1. SMZ in single system

In order to evaluate the SMZ retention capacity of the resin, several runs were carried out at pH= 6 and 20ºC. Preliminary experiments were performed to obtain the appropriate liquid/solid ratio, being as suitable a liquid/solid ratio of 800 (mL solution/mass of wet resin).

Next, adsorption experiments were carried out varying the initial concentration between 50 and 250 mg/L SMZ in the conditions already described. The adsorption isotherm obtained, Figure 6a, shows typical Langmuir characteristics. The SMZ uptakes increases with the initial concentration and finally reached a plateau. According to the Langmuir isotherm theory that assumes monolayer coverage of adsorbate over a homogeneous adsorbent surface, at equilibrium a saturation point is reached where no further adsorption/desorption can take place. The Langmuir equation is expressed as:

$$q_e = \frac{K_L \cdot C_e}{1 + a_L \cdot C_e} \quad (1)$$

where q_e is the equilibrium SMZ concentration on the adsorbent (mg g^{-1}), C_e is the equilibrium liquid phase concentration (mg·L^{-1}), K_L (L·g^{-1}) indicates the solute adsorptivity, a_L is related to the energy of adsorption. The monolayer capacity of the Langmuir isotherm, Q_m is given as:

$$Q_m = \frac{K_L}{a_L} \quad (2)$$

where a_L is Langmuir constant for energy of sorbent (L·mg^{-1}), K_L is Langmuir constant (L·g^{-1}) and Q_m is a constant related to the area occupied by a monolayer of adsorbate, reflecting the adsorption capacity of the resin (mg SMZ/g wet resin).

Experimental data were fitted to a linear form of Langmuir equation, obtaining the Langmuir parameters K_L, a_L and the monolayer capacity, Q_m. The values obtained for these parameters are K_L= 0.35 L·g^{-1}, a_L= 0.0084 L·mg^{-1} and Q_m = 41.2 mg SMZ/g wet resin, equivalent to 91.5 mg/g dry resin, with a linear correlation coefficient 0.98.

To quantify the agreement between the model predictions and experimental data, the proposed equilibrium equations were evaluated using Chi-square analysis 38 and non-linear regression analysis. Eq. (3) shows how to calculate χ^2. If the data predicted by the model is similar to experimental data, χ^2 (mg/g wet resin) will be small, and vice versa.

$$\chi^2 = \sum_{i=1}^{N} \frac{(q_{eq,exp} - q_{eq,cal})^2}{q_{eq,cal}} \quad (3)$$

where $q_{eq,cal}$ is the equilibrium capacity obtained from a model (mg/g wet resin), $q_{eq,exp}$ is the equilibrium capacity obtained from experiments (mg/g wet resin), and N is the number of measurements. Eq. (4) shows the average percentage error (Ɛ) used in the non-linear regression analysis 39. The errors between experimental data and predicted data were calculated using Eq. (4). The values obtained were χ^2= 0.095 and ε= 2.86 %.

$$\varepsilon(\%) = \frac{\sum_{i=1}^{N} \left| (q_{eq,exp} - q_{eq,cal})/q_{eq,exp} \right|}{N} \text{x } 100 \quad (4)$$

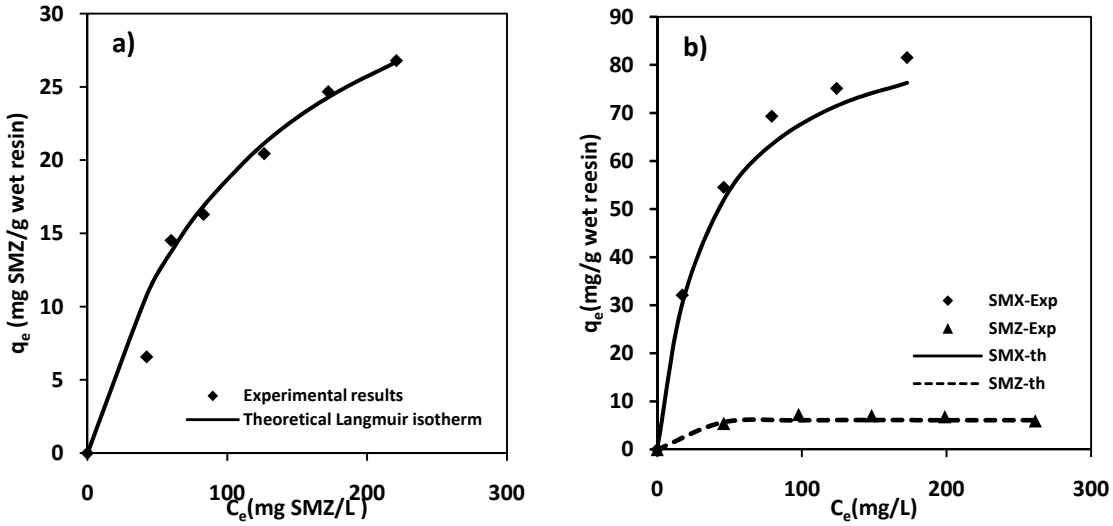

Figure 6. a) SMZ Langmuir adsorption isotherm in single system. **b)** Jain and Snoeyink modified Extended Langmuir isotherm for SMX and SMZ in the binary system

3.2.1.2. SMX and SMZ in binary system

In order to evaluate the efficacy of the resin synthesized to exchange SMX and SMZ in mixtures of synthetic solution, several runs were carried out using concentrations of SMX and SMZ between 50-250 mg/L of each compound in equal proportion and a liquid/solid ratio of 800 mL solution/g wet resin. The adsorption capacities obtained and the equilibrium liquid phase concentrations reached are showed in Figure 6b. The resin has more affinity to retain SMX than SMZ when the two compounds are together in solution. This agree with the results obtained in single assays where obtained higher adsorption capacities for SMX.

The process was modeled using the Extended Langmuir (EL) Model for multicomponent system 40. This model assumed: i) a homogeneous surface with respect to the energy of adsorption, ii) no interaction between adsorbed species and iii) that all adsorption sites are equally to all adsorbed species. However, the failure of the fit using the EL model, with average percentage error for SMX and SMZ of $\mathcal{E}_{SMX}$ = 82% and $\mathcal{E}_{SMZ}$ = 9% respectively, suggested that the binary adsorption might be competitive.

Jain and Snoeyink 41 investigated competitive sorption from aqueous bicomponent solutions of organic sorbates and developed a model that predicts sorption equilibrium in such non ideal systems. According to Jain and Snoeyink, the Langmuir theory for binary sorbate systems is based on sorption without competition. Therefore, to account for competition in the Langmuir theory, the Jain-Snoeyink model proposed to add an additional term to the extended Langmuir equation.

$$q_{e1} = \frac{(Q_{m1} - Q_{m2})a_{L1}C_{e1}}{1 + a_{L1}C_{e1}} + \frac{Q_{m2}a_{L1}C_{e1}}{1 + a_{L1}C_{e1} + a_{L2}C_{e2}} \quad (5)$$

$$q_{e2} = \frac{Q_{m2}a_{L2}C_{e2}}{1 + a_{L1}C_{e1} + a_{L2}C_{e2}} \quad (6)$$

where K_L and a_L are the Langmuir isotherm constants, Q_{mi} is the monolayer saturation capacity for the Langmuir isotherm. The first term on the right hand side of the Eq. (5) refers to the amount of species 1 adsorbed without competition with 2, while the second term gives the amount of species 1 adsorbed in competition with 2, as described by applying the competition to the Langmuir model. The additional term of Eq. (5) is the Langmuir expression for the number

of molecules of solute 1 which are sorbed without competition on the surface, and the terms is proportional to $(Q_{m1} - Q_{m2})$, where $Q_{m1} > Q_{m2}$. By Eq (6) the number of molecules of solute 2 sorbed on the sorbent surface (proportional to Q_{m2} and in competition with solute 1) can be calculated from the extended Langmuir equation. The Langmuir constants K_L and a_L can be determined using a linear transform method. The Table 2 shows the constants and the monolayer capacities for single component data and for the binary monolayer capacities.

Table 2. Langmuir Sorption Isotherm Constant for SMX and SMZ in single and binary system

		K_L(L/g resin)	a_L(L/mg)	Q_0(mg/g wet resin)	R^2
Single component system	SMX	1.71	0.017	101	0.9865
	SMZ	0.35	0.0084	41.2	0.9862
Binary system	SMX	2.76	0.028	98.1	0.9991
	SMZ	0.82	0.113	7.3	0.9879

The Figure 6b shows the comparison between experimental data and predictions based on the Jain and Snoeyink modified extended Langmuir model for SMX and SMZ in binary solutions. The correlation between the prediction and experimental data are good, with average percentage error of $\mathcal{E}_{SMX}$ = 6% and $\mathcal{E}_{SMZ}$ = 9%, that means, there are competition for adsorption sites between SMX and SMZ.

3.2.2. Batch kinetics studies

The process of adsorption was monitored until equilibrium was reached in single system of SMZ, and in binary system of SMX and SMZ. After 120 minutes, the solution concentration of each component does not change, so operational equilibrium can be assumed. The ion exchange operation was taken from the loading batch assays conducted in stirred tanks with synthetic solution of SMZ and mixtures synthetic solutions of SMX and SMZ in ratio 1:1 in concentrations of 50, 100, 150, 200, and 250 mg/L. The concentration profiles can modeled using the pore diffusion kinetics model to determine the mass transfer mechanisms 42 due to under our operating conditions, such as well stirred solution (300 rpm), it would be expected that rate-determining step is the particle diffusion control 43.

Pore diffusion Model. This model 44 considers the resin as a porous matrix. The developed model was described in previous work 25. The diffusivity values obtained for SMX and SMZ in single system were $D_{p\,SMX} = 3 \cdot 10^{-9}$ cm^2/s (obtained in previous work), $D_{p\,SMZ} = 9 \cdot 10^{-9}$ cm^2/s, with an average percentage error Ɛ= 2.7%. The values obtained in binary system were $D_{p\,SMX} = 5 \cdot 10^{-8}$ cm^2/s and $D_{p\,SMZ} = 7.6 \cdot 10^{-9}$ cm^2/s, with the average percentages error of $\mathcal{E}_{SMX}$= 6.8% and $\mathcal{E}_{SMZ}$= 1.2%. It can observe that the diffusivity values for each compound in single assays have the same order of magnitude, but in mixtures the diffusivity for SMX is higher than for SMZ.

Figure 7a-b shows the fit of the experimental results to this model with the diffusivity values obtained in binary systems. The good agreement between experimental data and the theoretical prediction shows the goodness of the model.

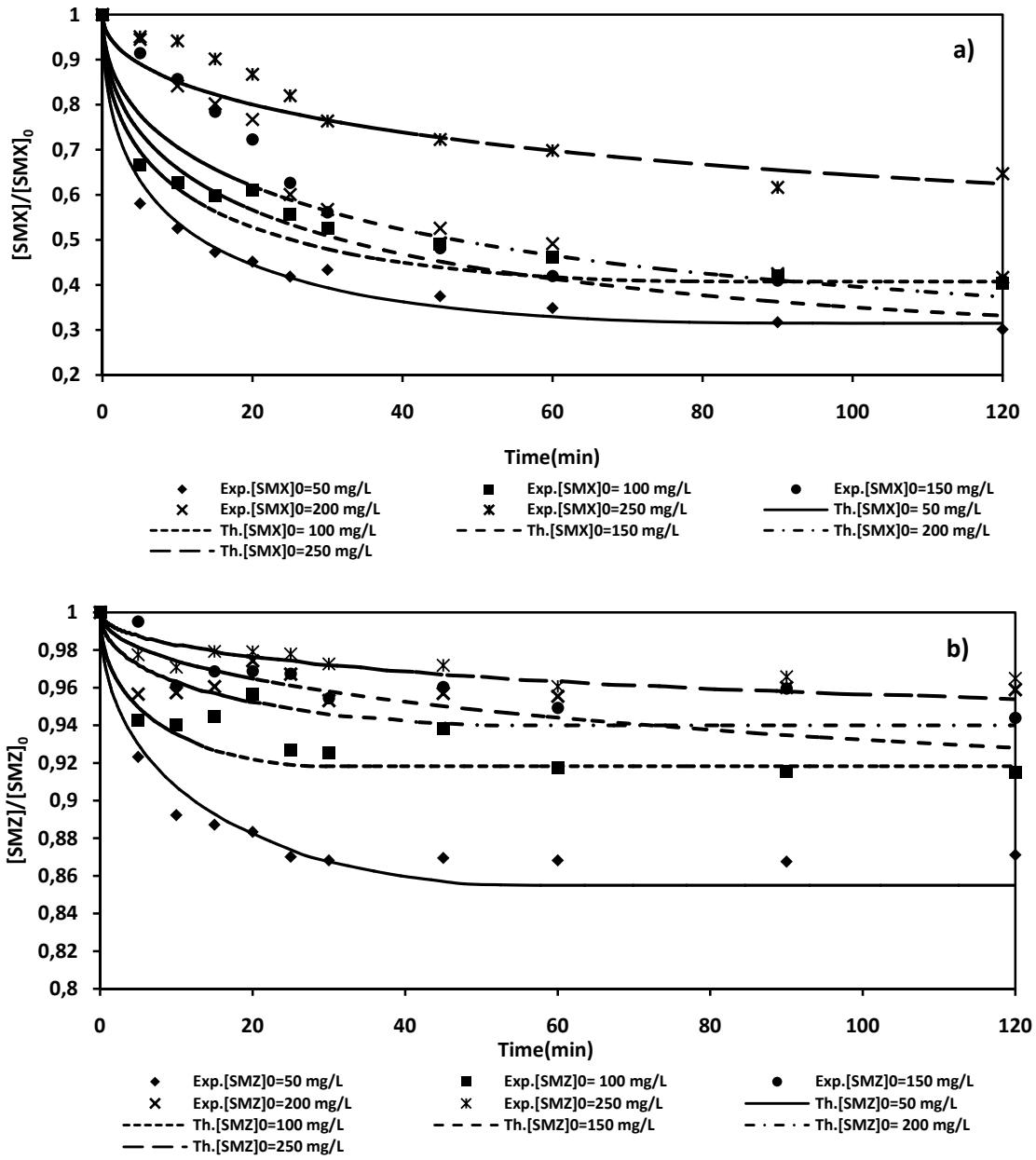

Figure 7. Fitting of kinetics data using the pore diffusion model for the adsorption of SMX **(a)** and SMZ **(b)** synthetic solutions in binary system with concentrations range 50-250 mg/L of each one

3.3. Fixed Bed Column

Breakthrough Curves from the Load and Elution Stages. After studying the equilibrium and kinetics of the process, tests were conducted in a fixed bed column using synthetic solutions of SMZ at concentrations of 100, 200 and 300 mg/L and mixtures synthetic solutions of SMX and SMZ at concentrations of 100, 200, 300 and 400 mg/L of each compound in equal proportion, to obtain the breakthrough curves.

Initially, the column was packed with 3.6 grams of wet resin (equivalent to 1.7 grams of dry resin). After conditioning it, the resin was loaded using a synthetic solution of 100 mg/L SMZ with a flow rate 6 mL/min for 320 minutes. The breakthrough curve showed dispersive results with no pronounced jump in the concentration with time because it was detected

concentration at the outlet of the column in the first minutes of operation, and after 10 minutes, the concentration increased quickly until reach complete saturation of the resin in 200 minutes. The retention of the resin packed in the column was calculated by numerical integration of the area under the load breakthrough curve. The operative capacity was 10.2 mg SMZ/g wet resin. After loading, the resin was regenerated for determining if this resin can be applied in an industrial operation, using a solution of NaOH 0.5M at a flow rate of 5 mL/min for 180 minutes. The elution curve showed a high elution peak in the first minutes, reaching a concentration of 1330 mg/L, and decreasing quickly to achieve a completely elimination in 60 minutes and recovering 100% of SMZ retained. The resin shows a very good performance to concentrate the antibiotic in the initial stages of elution; SMZ concentration in the eluate was ~ 13 times higher than in the loading solution, which is very interesting for industrial operation.

After this first cycle, other two cycles of loading and elution were carried out using concentrations of 200 and 300 mg/L SMZ. As in the first cycle, there was detected concentration at the outlet of the column in the first minutes of operation. In the second cycle, in which was used an initial concentration of 200 mg/L, after 180 minutes, complete saturation of the resin was achieved. The retention capacity was 18.4 mg SMZ/grams wet resin. In elution step, as happened in the first cycle, a high elution peak were detected, reaching a concentration of 2500 mg/L and decreasing until complete elution in 40 minutes. In the last cycle of SMZ, using an initial concentration of 300 mg/L, the resin saturated in 180 minutes, with a retention capacity of 21 mg SMZ/grams wet resin. In the third elution step, as in the other cycles, all SMZ retained were recovered in 60 minutes.

The retention capacity for SMX in column obtained in previous work in the same operating conditions was five times higher than the retention capacity for SMZ. That is in accord with the results obtained in batch, where the resin demonstrated more affinity for SMX than for SMZ. Figure 8a and 8b shows the breakthrough curves of load and elution steps for SMZ.

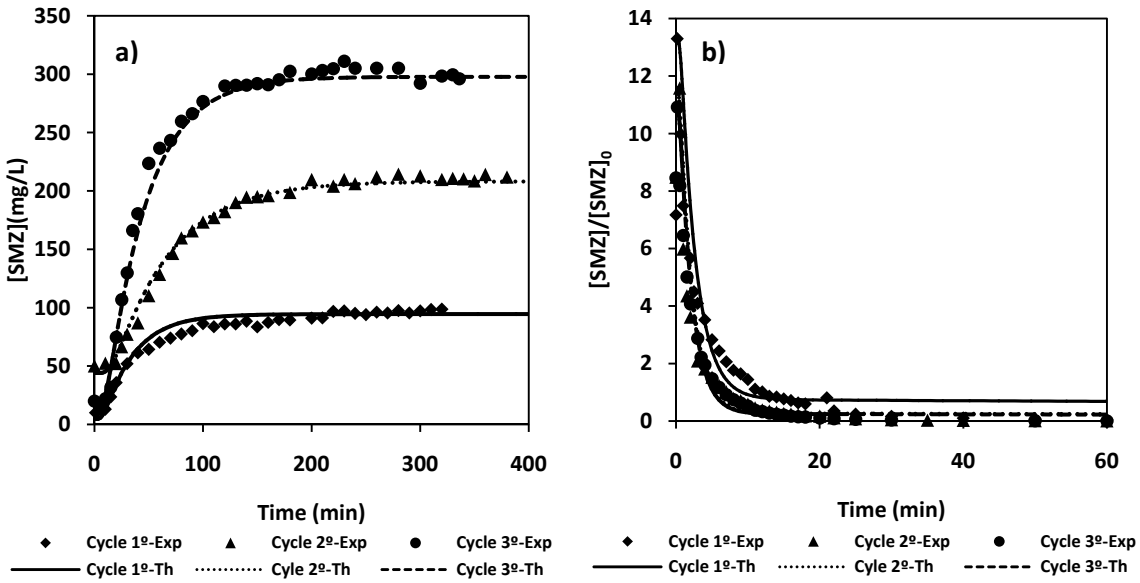

Figure 8. a) Experimental and theoretical loading **(a)** and elution **(b)** breakthrough curves for SMZ in single system from synthetic solutions, in a fixed bed column. Conditions: initial load concentrations: cycle 1º= 100 mg/L; cycle 2º= 200 mg/L; cycle 3º= 300 mg/L, flow rate load= 6 mL/min, mass wet resin= 3.6 grams, Z= 3 cm. Elution: NaOH 0.5 M solution, flow rate elution= 5 mL/min

Likewise, experiments in column were carried out using mixtures synthetic solutions of SMX and SMZ in equal proportion at concentrations of 100, 200, 300 and 400 mg/L of each one, to compare the results with the obtained with each compound individually, and analyze the competition between them in the adsorption process by the actives sites of the resin. In this case, the column was packed with 3 grams of wet resin (1.4 grams of dry resin). Next conditioning it, the column was loaded with a solution of 100 mg/L of each one with a flow rate of 6 mL/min for 6 hours. The breakthrough curves showed that while SMZ was detected at the outlet of the column in the first minutes, reaching the feed concentration in 200 minutes, SMX was adsorbed totally, reaching the breakthrough point at 300 minutes. After 360 minutes of operation, the concentration detected at the outlet was only 16 mg SMX/L. The retention capacities were 11 mg SMZ/g wet resin and 80 mg SMX/g wet resin. After loading, the resin was regenerated. In elution step, both compounds were eluted totally after 60 minutes, reaching a much higher elution peak for SMX due to the resin adsorbed much more SMX than SMZ.

After this first stage, other three cycles were carried out using concentrations of 200, 300 and 400 mg/L of each compound. In the second load stage, using an initial concentration of 200 mg/L of each one, the breakthrough curve obtained for SMZ was similar at the first cycle, detecting concentration at the outlet in the first minutes of operation and saturating the resin by SMZ in 120 minutes. In the case of SMX, the breakthrough point was at 200 minutes, increasing quickly, reaching a concentration of 170 mg/L at the outlet in 345 minutes of operation. The retention capacities obtained were 20 mg SMZ/g wet resin and 126 mg SMX/g wet resin. In the second elution step, the two compounds were eluted in 60 minutes, reaching a high elution peak for SMX and recovering 100% of SMX and SMZ.

In the third cycle, the resin was loaded with a solution of 300 mg/L approximately of each compound. In the case of SMZ the profile of breakthrough curve is the same as in the other cycles, reaching a complete saturation in 120 minutes. For SMX, the breakthrough point was at 170 minutes, reaching in 345 minutes the concentration of initial feed. The retention capacities were in this case 22 mg SMZ/g wet resin and 89 mg SMX/g wet resin. In the elution step, in 60 minutes both compound were removed, recovering 100% of SMX and SMZ retained.

Finally in the last cycle, using an initial concentration of 400 mg/L of each compound approximately, the complete saturation was achieved in 180 minutes for SMZ, while for SMX the breakthrough point was in 90 minutes, reaching in 330 minutes a concentration next to the feed solution. The retention capacities were 14 mg SMZ/g wet resin and 142 mg SMX/g wet resin. In elution step, in 60 minutes both compounds were recovered totally. Figures 9 and 10a-b show the breakthrough curves of loading and elution steps of the fourth cycles, respectively.

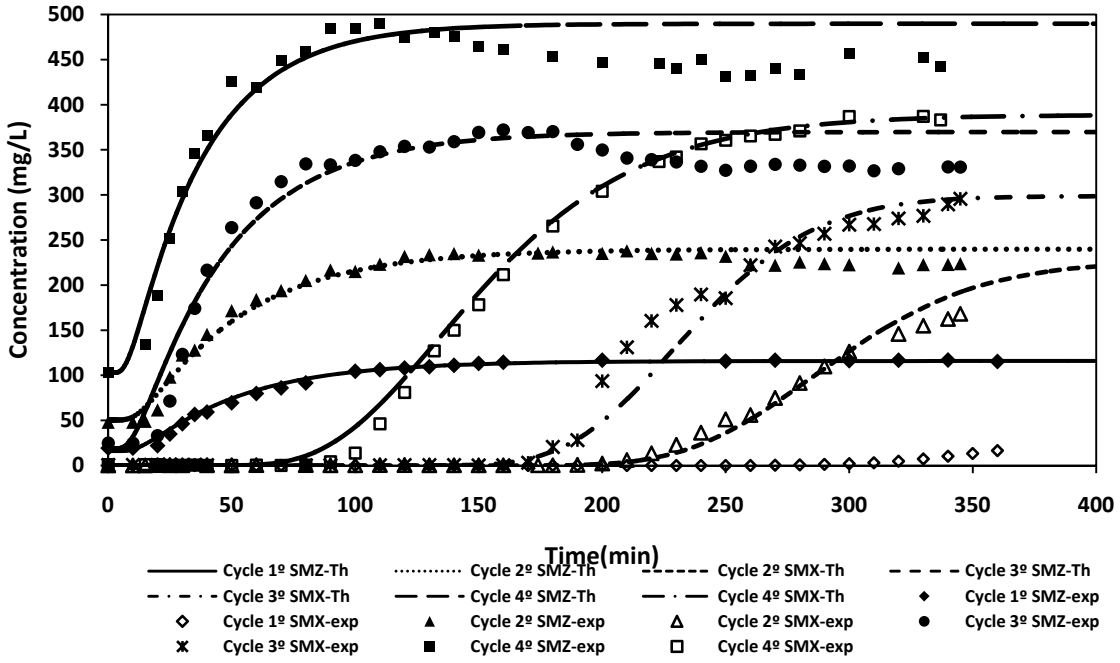

Figure 9. Experimental and theoretical load breakthrough curves for mixtures of SMX and SMZ in ratio 1:1 from mixtures synthetic solutions, in a fixed bed column. Conditions: initial concentrations: cycle 1º= 100 mg/L; cycle 2º= 200 mg/L; cycle 3º= 300 mg/L; cycle 4º= 400 mg/L, flow rate= 6 mL/min, mass wet resin= 3 grams, Z= 2.5 cm

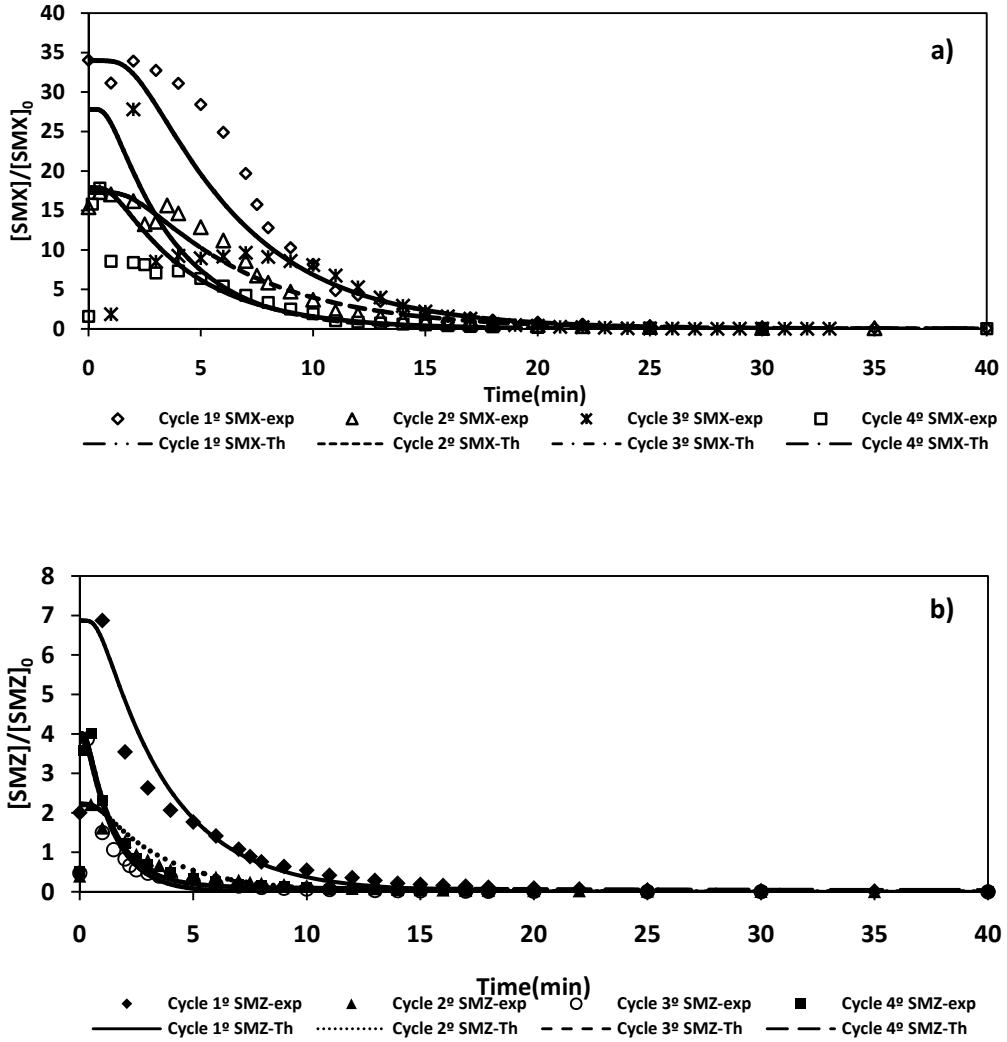

Figure 10. Experimental and theoretical elution breakthrough curves for SMX **(a)** and SMZ **(b)** in ratio 1:1 from mixtures synthetic solutions, using NaOH 0.5 M as eluant in a fixed bed column. Conditions: initial concentrations: cycle 1º= 100 mg/L; cycle 2º= 200 mg/L; cycle 3º= 300 mg/L; cycle 4º= 400 mg/L, flow rate= 5 mL/min, mass wet resin= 3 grams, Z= 2.5 cm

3.4. Fixed Bed Model

The analysis of the fixed bed experiments in the cases of the load and elution curves was carried out considering a model developed by Costa 45 and used by Fernandez et al. 46. This model was used to simulate the load and elution breakthrough curves in a laboratory column. The model takes into account equilibrium and kinetics aspects, axial dispersion in the column and no film transfer resistance. The developed model can be seen in López et al. 25. To solve the fixed bed model, parameters such as bed porosity, particle porosity, equilibrium constants, diffusivities in the pores and the capacity of the resin must be known. All these parameters were determined for the system previously. The bed porosity was calculated in previous assays and the particle porosity was determined from the resin characterization. The axial dispersion parameter was not available for the laboratory column, so it was considered the sole parameter model fit.

The values of the different parameters used in this study and the axial dispersion calculated as a fitting parameter for load and elution stages for SMZ in single system; and in the assays for SMX and SMX in binary system are shown in Table 3. The experimental and theoretical load and elution breakthrough curves for single system is shown in Figures 8a and 8b respectively, and for binary system is shown in Figures 9 and 10a-b, respectively. A good correlation can be seen between experimental results and the numerical solution of the fixed bed model for the load and elution stages, demonstrating the validity of the model.

Table 3. Fixed bed operating parameters

	Single system	Binary system	
	SMZ	SMX	SMZ
K_{eq}	2.71	18.7	77.7
Q_t(mg/g wet resin)	35.5	92.8	6.95
Diffusivity in pores (cm^2/s)	$9 \cdot 10^{-9}$	$7.6 \cdot 10^{-9}$	$5 \cdot 10^{-8}$
D_{AX} (cm^2/s) load	10	10	0.5
D_{AX} (cm^2/s) elution	1.2	0.6	1.7
Retention Capacity (mg/g wet resin) 1st cycle	10.2	---	16
Retention Capacity (mg/g wet resin) 2nd cycle	18.2	126	20
Retention Capacity (mg/ g wet resin) 3st cycle	21	89	22
Retention Capacity (mg/ g wet resin) 4nd cycle	---	142	14
Flow (mL/min)load	6		
Flow (mL/min) elution	5		
Bed Porosity (ε_l)	0.5		
Particle porosity (ε_i)	0.52		
Bed High(cm)	3	2.5	

4. Conclusions

The removal of SMZ and mixtures of SMX and SMZ from aqueous solutions using copolymeric beads of 2-(diethylamino)ethyl metacrylate-co-ethyleneglycol dimethacrylate (DEAEM-co-EGDMA) synthesized by photopolymerization was carried out successfully. Batch experiments were conducted using synthetic solutions between 50 and 250 mg/L of SMZ and mixtures of SMX and SMZ in ratio 1:1 with a liquid/solid ratio of 800 (mL solution/g wet resin) determined previously as adequate. The results show that the resin has much higher retention capacity for SMX than for SMZ in mixtures solutions. Equilibrium data of SMZ in single system was fitted using Langmuir isotherm, obtaining a maximum adsorption capacity of 41.2 mg SMZ/g wet resin (91.5 mg SMZ/g dry resin). In the binary system, the combined effects of the two compounds onto the polymer were competitive. The equilibrium dates were fitted using the Extended Langmuir Model and the Jain and Snoeyink Modified Extended Langmuir Model. The last model was more adequate to describe the binary component adsorption equilibrium. The maximum uptakes of SMZ and SMZ in binary system were 98.1 and 7.3 mg/g wet resin respectively, equivalent to 218 mg SMX/g dry resin and 16.3 mg SMZ/g dry resin. The kinetics adsorption was described successfully using the pore diffusion model, determining the constants pore diffusivity D_p for SMX and SMZ in single and binary systems.

Successive cycles of loading and elution in a fixed bed column were performed with synthetic solutions of SMZ and mixtures solutions of SMZ and SMZ in equal proportion, using a solution of NaOH 0.5M as eluant. The retention capacities and the ability of the eluant were evaluated. The shape of the breakthrough curves obtained showed the viability of the ion exchange operation using the resin synthesized to remove and separate SMX and SMZ from mixtures solutions. Furthermore, NaOH was found as adequate eluant, recovering 100% of both compounds in elution steps and concentrating the solute after elution, permitting an easier treatment of these compounds. Fixed bed operation was simulated using a fixed bed model

showed good agreement between experimental data and predicted values by the model, demonstrating its viability.

Acknowledgements

Financial supports of Ana María López Fernández from PhD fellowship Severo Ochoa Programme (Gobierno del Principado de Asturias) are gratefully acknowledged.

References

1. M. Díaz-Cruz, D. Barceló, Environmental behavior and analysis of veterinary and human drugs in soils, sediments and sludge, Trends Anal. Chem. 22 (2007) 340-351.
2. T. A Ternes, M. Meisenheimer, D. McDowell, F. Sacher, H. J. Brauch;, B. Haist-Gulde, G. Preus, U. Wilme, N. Zulei-Seibert. Removal of pharmaceuticals during drinking water treatment. Environ. Sci. Technol. 36 (2002) 3855-3863.
3. C. Adams, M. ASCE, Y. Wang, K. Loftin, M. Meyer, Removal of antibiotics from surface and distilled water in conventional water treatment processes, J. Environ. Eng. 128 (2002) 253-260.
4. N. Le-Minh, S.J. Khan, J.E. Drewes, R.M. Stuetz, Fate of antibiotics during municipal water recycling treatment processes, Water Research 44(15) (2010) 4295-4323.
5. M. Carballa; F. Omil; J.M. Lema; M. Llompart; C. García;I. Rodriguez; M. Gómez; T. Ternes. Behaviour of pharmaceuticals and personal care products in a sewage treatment plant of northwest Spain. Water Science and Technology 52 (8) (2005) 29-35.
6. N. Kemper. Veterinary antibiotics in the aquatic and terrestrial environment. Ecological Indicators 8 (2008) 1-13
7. V. Homen and L. Santos, Degradation and removal methods of antibiotics from aqueous matrices-A review, Journal of Environment Management 92 (2011) 2304-2347.
8. A. Göbel, C.S. McArdell, A. Joss, H. Siegrist, W. Giger, Fate of sulfonamides, macrolides and trimethoprim in different wastewater treatment technologies. Sci. Total Environ. 372 (2007) 361-371.
9. P.E. Stackelberg, J. Gibs, E.T. Furlong, M.T. Meyer, S.D. Zaugg, R.L. Lippincott, Efficiency of conventional drinking water treatment processes in removal of pharmaceuticals and other organic compounds. Sci. Total Environ. 377 (2007) 255-272.
10. N.M. Vieno, H. Harkki, T. Tuhkanen, L. Kronberg, Occurrence of pharmaceuticals in river water and their elimination in a pilot scale drinking water treatment plant, Environ. Sci. Technol. 41 (2007) 5077-5084.
11. M. Grassi, G. Kaykioglu, V. Belgiorno, G. Lofrano, Removal of Emerging Contaminants from Water and Wastewater by Adsorption Process, in: G. Lofrano(ed.) Emerging Compounds Removal from Wastewater, SpringBriefs in Green Chemistry for Suitainability, 2012, pp. 15-37.
12. Xuan Bui, T., Choi, H. Adsorptive removal of selected pharmaceutical by mesoporous silica SBA-15. Journal of Hazardous Materials 168 (2009) 602-608
13. J.L. Acero, F.J. Benitez, F.J. Real, G. Roldan, Kinetics of aqueous chlorination of some pharmaceuticals and their elimination from water matrices, Water Res. 44 (2007) 4158-4170.
14. R. Andreozzi, M. Canterino, R. Marotta, N. Paxeus, Antibiotic removal from wastewaters: the ozonation of amoxicillin. J. Hazard. Mater. 122 (2005) 243-250.
15. L.A. Balcioğlu, M. Ötker, Treatment of pharmaceutical wastewater containing antibiotics by O_3/H_2O_2 processes, Chemosphere 50 (2003) 85-95.
16. A.G. Trovó, R.F.P. Nogueira, A. Agüera, C. Sirtori, A.R. Fernández-Alba, Photodegradation of sulfamethoxazole in various aqueous media: persistence, toxicity and photoproducts assessment, Chemosphere 77 (2009) 1292-1298.
17. M. Pérez-Moya, M. Graells, G. Castells, J. Amigó, E. Ortega, G. Buhigas, L.M. Pérez, H.D. Mansilla. Characterization of the degradation performance of the sulfamethazine antibiotic by Photo-Fenton process, Water Res. 44 (2010) 2533-2540.
18. S.Z. Li, X.-Y. Li, D.-Z. Wang, Membrane (RO-UF) filtration for antibiotic wastewater treatment and recovery of antibiotics, Sep. Purif. Technol. 34 (1-3) (2004) 109-114.
19. E.K. Putra, R. Pranowo, J. Sunarso, N. Indraswati, S. Ismadji, Performance of activated carbon and bentonite for adsorption of amoxicillin from wastewater: mechanism, isotherms and kinetics, Water Res. 43 (2009) 2419-2430.
20. J. Rivera-Utrilla, G. Prados-Joya, M. Sánchez Polo, M.A. Ferro Garcia, I. Bautista-Toledo, Removal of nitroimidazole antibiotics from aqueous solution by adsorption/bioadsorption on activated carbon, J. Hazard. Mater. 170 (2009) 298-305.

21. W. Lertpaitoonpan; S.K. Ong; T.B. Moorman. Effect of organic carbon and pH on soil sorption of sulfamethazine. Chemosphere 76(2009) 558-564.
22. E. Çalişkan S. Göktürk, Adsorption Characteristics of Sulfamethoxazole and Metronidazole on Activated Carbon, Separation Science and Technology, 45(2010) 244-255.
23. I. Vergili, H. Barlas, Removal of selected pharmaceutical compounds from water by an organic polymer resin. Journal of Scientific & Industrial Research 68 (2009) 417-425.
24. K.-J. Choi, H.-J. Son; S.-H. Kim, Ionic treatment for removal of sulphonamide and tetracycline classes of antibiotic, Sci. Total Environ. 387 (2007) 247-256.
25. A.M. López; M. Rendueles; M. Díaz. Sulfamethoxazole removal from synthetic solutions by ion Exchange using a strong anionic resin in fixed bed. Solvent Extraction and Ion exchange 31 (2013) 763-781.
26. J.M. Cervantes-Uc, J.V. Cauich-Rodríguez, W.A. Herrera-Kao, H. Vázquez-Torres, A. Marcos-Fernández, Thermal degradation behavior of polymethacrylates containing amine side groups, Polym. Degrad. Stabil. 93 (2008) 1891-1900.
27. Y.V. Bune, A.P. Sheninker, Y.S. Bogachev, I.L. Zhuravleva, E.N. Teleshov, Radical polymerization of diethylaminoethyl methacrylate and its salts in various solvents, European Polymer Journal, 27 (6) (1991) 509-513.
28. A. Guerreiro, A. Soares, E. Piletska, B. Mattiasson, S. Piletsky, Preliminary evaluation of new polymer matrix for solid-phase extraction of nonylphenol from water samples, Anal. Chim. Acta 612 (2008) 99-104.
29. M.T. Am Ende, D. Hariharan, N.A. Peppas. Factors influencing drug and protein transport and release from ionic hydrogels, React. Polym. 25 (1995) 127-137.
30. S. Barral, A. Guerreiro, M. A. Villa-García, M rendueles, M. Díaz, Synthesis of 2-(diethylamino)ethyl methacrylate-based polymers. Effect of crosslinking degree, porogen and solvent on the textural properties and protein adsorption performance, Reactive & Functional Polymers 70(2010) 890-899.
31. C.H. Hu, T.-C., Chou, Albumin molecularly imprinted polymer with high template affinity- Prepared by systematic optimization in mixed organic/aqueous media, Microchem Journal 91 (2009) 53-58.
32. C. Boyer, G. Boutevin, J.J. Robin, B. Boutevin, Study of the telomerization of dimethylaminoethylmethacrylate (DMAEMA) with mercaptoethanol. Application to the synthesis of a new macromonomer, Polymer 45 (23) (2004) 7863-7876.
33. S. Piletsky, E. Piletskaya, T.L. Panasyuk, A.V. El'skaya, R. Levi, I. Karube, G. Wulff, Imprinted membranes for sensor technology-opposite behavior of covalently and noncovalently imprinted membranes, Macromolecules 31 (7) (1998) 2137-2140.
34. X. Zhang, J. Xia, Controlled/"Living" Radical Polymerization of 2-(Dimethylamino)ethyl Methacrylate, Macromolecules 31 (15) (1998) 5167-5169.
35. M. Sarker, G. Guiochon, Study of the operation conditions of axial compression columns for preparative chromatography. J. Chromatogr. A 709 (1995) 227-239.
36. M. Sarker, A.M. Katti, G. Guiochon, Consolidation of the packing materials in chromatographic columns under dynamic axial compression. II Consolidation and breakage of several packing materials. J. Chromatogr. A 719 (1996) 275-289.
37. S. Brunauer, L.S. Deming, W.S: Deming, E. Teller, On a theory of the Van der Waals adsorption of gases, J. Am. Chem. Soc. 62 (1940) 1723-32.
38. SH, Yuh, Selection of optimum sorption isotherm. Carbon, 42 (2004) 2113-2130.
39. Z. Aksu,O. Tunç, Application of biosorption for penicillin G removal comparison with activated carbon, Process Biochem. 40 (2004) 831-847.
40. L.A.V. Butler; C. Ockrent. Studies in ELectrocapillarity. Part III. The Surface Tensions of Solutions Containing Two Surface-Active Solutes. J. Phys. Chem. 34, (1930) 2841-2845.
41. J.S. Jain; V.L. Snoeyink. Adsorption from Bisolute Systems on Active Carbon. J. Water Pollut. Control Fed. 45 (1973), 2463-2479.
42. G.E. Boyd, A.W. Adamson, L.S. Myers, The exchange adsorption from aqueous solutions by organic zeolites. II. Kinetics, Journal of the American Chemical Society 69 (1947) 2836-2848.
43. F. Helfferich, Ion Exchange, McGraw-Hill, New York, 1962.
44. A.E. Rodrigues, D. Tondeur, Percolation Processes: Theory and Applications, NATO ASI Series, 1981, pp. 31-81.
45. C. Costa, A. Rodrigues, Design of cyclic fixed-bed adsorption processes. Part I: Phenol adsorption on polymeric adsorbents, AIChE Journal 31(10) (1985) 1645-1654.
46. A. Fernández, A.E. Rodrigues, M. Díaz, Modelling of Na/K Exchange in Fixed Beds with Highly Concentrated Feed, Chem. Eng. J. 54 (1994) 17-22.

4.8. RETENCIÓN Y SEPARACIÓN DE TIOCIANATO Y FENOL EN DISOLUCIONES SINTÉTICAS MEDIANTE INTERCAMBIO IÓNICO EMPLEANDO RESINA DE POLIMETACRILATO OBTENIDA MEDIANTE FOTOPOLIMERIZACIÓN

Debido a que previamente se había estudiado el proceso de intercambio iónico de tiocianato y fenol con resinas comerciales, en este trabajo se ha querido evaluar el proceso de intercambio iónico de ambos compuestos empleando en este caso polímeros de metacrilato sintetizados en el laboratorio.

En el trabajo que se incluye a continuación, se presentan los resultados obtenidos de los estudios de equilibrio y cinética llevados a cabo en tanque agitado con disoluciones sintéticas de tiocianato, y mezclas de tiocianato y fenol, empleando como adsorbente un polímero de metacrilato obtenido previamente mediante fotopolimerización. La síntesis de la resina se describe brevemente, ya que se ha desarrollado ampliamente junto con su caracterización en el trabajo incluido en el apartado 4.6.

Se evaluó la influencia del pH en el proceso de adsorción. Se estudió el equilibrio y la cinética del proceso de intercambio iónico en tanque agitado, y se determinaron las capacidades de retención. El equilibrio de intercambio iónico se describió empleando isotermas de adsorción para sistemas de un solo componente y modelos basados en isotermas de adsorción modificadas para sistemas multicomponentes, para describir el comportamiento del sistema binario tiocianato y fenol. A su vez, la cinética del proceso se describió empleando los modelos cinéticos de primer orden y de segundo orden. También se estudió la operación en columna, empleando disoluciones sintéticas de tiocianato, de fenol y mezclas de tiocianato y fenol. Se determinaron las capacidades de retención en columna y la eficacia del eluyente en las etapas de regeneración.

Artículo: Retention and separation of thiocyanate and phenol from synthetic solutions by ion exchange with polymethacrylate resin from photopolymerization

Situación: en elaboración.

RETENTION AND SEPARATION OF THIOCYANATE AND PHENOL FROM SYNTHETIC SOLUTIONS BY ION EXCHANGE WITH POLYMETHACRYLATE RESIN FROM PHOTOPOLYMERIZATION

Ana María López Fernández[a], María A. Villa-García[b], Manuel Rendueles[a] and Mario Díaz[a]

[a]*Department of Chemical and Environmental Engineering, University of Oviedo, Oviedo, Spain*

[b]*Department of Organic and Inorganic Chemistry, University of Oviedo, Oviedo, Spain*

Abstract

The adsorption of thiocyanate and phenol in mixtures in aqueous solutions onto copolymer beads of 2-(diethylamino)ethyl methacrylate-co-ethyleneglycol dimethacrylate (DEAEM-co-EGDMA) synthesized by photopolymerization were investigated in batch-mode operation to assess the possible used of this adsorbent. The effects of parameters such as pH and thiocyanate and phenol concentrations were studied. The equilibrium was studied using the Langmuir isotherm in individual thiocyanate system, and using modified models of Langmuir equation to predict the multicomponent adsorption system: the extended Langmuir, the Jain and Snoeyink extended Langmuir and the P-factor. The maximum adsorption capacity obtained were 16.3 mg SCN^-/g wet resin (36.2 mg SCN^-/g dry resin) in single system and 14.7 mg SCN^-/g wet resin (32.7 SCN^-/g dry resin) and 25 mg phenol/g wet resin (55.6 mg phenol/g dry resin) in binary system. The kinetics was analyzed using the first-order and second-order kinetics models, determining the rate constants. The kinetics results correlated well with second-order model. Finally, several cycles of loading and elution were performed in a fixed bed column.

Keywords: methacrylate copolymer, thiocyanate, equilibrium, kinetics, fixed-bed column

1. Introduction

Coke industrial wastewater contains considerable amounts of toxic compounds such as CN^-, SCN^-, phenols, ammonia, sulfides, chlorides, as well as small amounts of polyaromatic hydrocarbons and heterocyclic aromatic compounds. The main waste is the condensates of the gas coke generated. Thiocyanate is the most serious hazardous substances contained in the condensates due to the high concentration and strong effects on the environmental and human life [1,2,3]. It affects the thyroid gland, reducing the ability of the gland to produce hormones necessary the normal function of the body [4,5,6]. Therefore, it is necessary to treat this wastewater before discharged in the environment. Biological treatments have been applied to reduce the pollutant load, but after this treatment, the concentrations of thiocyanate and phenols in the wastewater exceeded the limits established by state and regional regulations regarding direct discharge into watercourses and into public sewage system, which means alternative method is required to remove these compounds [7]. Adsorption onto activated carbon[8], reverse osmosis [9], oxidation [10,11], ozone [12], electrosorption [13,14] are processes that have been employed for removal thiocyanate and phenol, but these methods have disadvantages as long residence times, large tank capacities and high economic costs. Adsorption is one efficient method for the removal of thiocyanates from wastewater. Many adsorbents such as Fe(III)/(II) hydroxide, $ZnCl_2$ coir pith carbon and calcined hydrotalcite have been tested for

adsorption of thiocyanates [8,15,16]. Activated carbon is widely used for the removal of a variety of organic compounds from water, but the main disadvantaged is the high cost and loss of adsorption capacity after regeneration. Of the various methods available, the ion exchange process has been chosen for the present study since it is low cost, low energy requirements, simplicity in design and operation, and easy regeneration. Furthermore, adsorbent resins are considered the most promising owing to their chemical stability and ability to control surface chemistry and it is one of the methods used for the removal of toxic substances from industrial and municipal wastewater [17].

Removal of thiocyanate and phenol have been studied in several works using polymeric resins For example, removal of thiocyanate using a strong anionic resin (Purolite A-230) was evaluated by Dizge [18], Caetano [19] studied the removal of phenol using two ion exchange resins, Dowex XZ (strong anionic resin) and AuRX 100 (weak anion exchange resin) and Costa studied the diffusion of phenol in macroreticular adsorbents 20. Our research group investigated in previous works 21 the removal of thiocyanate and phenol from condensates of gas coke using two anionic exchange resins, Lewatit MP500, an amine quaternary and macroporous structure, and Lewatit M610 an amine tertiary and gel structure, obtaining good results.

Aminomethacrylate-based polymers can behave as good adsorbents for retention of anionic contaminants due to the presence of amine functional groups. The tertiary amine function allows attaching charged species, since it can be easily transformed into a quaternary amine creating cationic centers 22. A variety of aminomethacrylate monomers were used for the synthesis of polymeric membranes suitable for retention and separation in different fields such as waste water purification [23], solid phase extraction [24], drug delivery systems [25], protein recovery and purification [26-28] and biochemical sensors [29,30], among others.

The objective of this study was to test the adsorption behavior of copolymer beads of 2-(diethylamino)ethyl methacrylate-co-ethyleneglycol dimethacrylate (DEAEM-co-EGDMA) for the uptake of thiocyanate and phenol from aqueous solutions. The polymeric beads were obtained by suspension polymerization, photoinitiated with azobiscyclohexane carbonitrile (ACCN), of a monomer mixture consisting of 40% DEAEM and 60% EGDMA dissolved in acetonitrile (ACN). Polyvinylpyrrolidone (PVP) was used as stabilizer of the suspension system. Cyclohexanol was used as porogen. Physico-chemical characterization of the polymer using different techniques: SEM microscopy, thermal gravimetric (TG) and differential thermal analysis (DTA), nitrogen adsorption-desorption isotherms, and mercury intrusion porosimetry and their behavior for antibiotic retention were described in previous work. The pH effect in the thiocyanate adsorption process was evaluated in batch assays. Equilibrium and kinetics parameters for the removal of thiocyanate and phenol from aqueous solutions were studied. The adsorption equilibrium constants were determined using the Langmuir isotherm in the case of single thiocyanate trials and some Langmuir isotherms models (Extended Langmuir, Jain and Snoeyink Extended Langmuir Model and P-Factor) were applied to the multicomponent sorption of thiocyanate and phenol from mixtures synthetic solutions. The adsorption kinetic was determined using first order and second order kinetic models.

2. Materials and methods

2.1. Reagents

Synthetic solutions of thiocyanate prepared with KSCN (Panreac) and phenol (Sigma, Aldrich) were prepared in distilled water. Acetonitrile (HPLC grade) was used for liquid chromatography and ultra-pure water was prepared in a Milli-Q purification system. The filters used for filtration samples were obtained from Millipore (0.45 μm PVDF).

The materials used for the synthesis were 2-(diethylamino)ethyl methacrylate (DEAEM) (99%), ethylene glycol dimethacrylate (EGDMA) (98%), 1,1’ azobis (cyclohexanecarbonitrile) (ACCN), acetonitrile (ACN), cyclohexanol, polyvinylpirrolidone (PVP). All of them were purchased by Sigma Aldrich.

2.2. Polymer synthesis

The synthesis and characterizations of the resin were described in previous works. The resin was synthesized using the following procedure: a mixture with a composition of monomer/crosslinker (DEAEM: EGDMA) 40:60 (mol%) was dissolved in acetonitrile, containing the initiator and cyclohexanol as porogen. The composition of the polymer was calculated with the base of 32 g of crosslinker (EGDMA). The solvent (ACN) was 50% (mass) of the total monomer and solvent mixture, while initiator was 1% (mass). The organic phase was dispersed in an aqueous phase containing 1% of polyvinylpyrrolidone (PVP) as suspension stabilizer; the ratio of organic/aqueous phase was 1:3. The polymerization mixture was transferred to a UV irradiation reactor, UV-Laboratory Reactor System 2 (Peschl), and photopolymerization was carried out for 3 hours under vigorous stirring to avoid coalescence and agglomeration of the beads during the polymerization reaction, stirring speed was 900 rpm. The polymerization temperature was kept at 30 ºC by using water cooling. The intensity of the UV lamp was 0.163 W/cm^2. The polymer particles obtained were washed with water, separated by centrifugation and dried overnight at 60ºC.

The polymers were characterized by thermal analysis, nitrogen adsorption-desorption isotherms, mercury intrusion porosimetry and SEM microscopy. The composition of the polymerization mixture is shown in Table 1 along with some parameters obtained in the characterization. The white micro spheres synthesized are hygroscopic, because 1 gram of wet resin is equivalent to 0.45 grams of dry resin.

Table 1. Polymers composition and characterization parameters

Composition	
Aquatic phase	1% PVP
Organic phase	
DEAEM:EGDMA (mol %)	40:60
EGDMA(g)	32
DEAEM(g)	20
ACN(g)	52
ACCN (g)	1.040
Cyclohexanol (mL)	20
Organic:aquatic ratio	1:3
Some characterization parameters	
Diameter particle (µm)	326
Thermal established (ºC)	<200
Bulk density (g/mL)	0.486
Apparent density (g/mL)	1.013

2.3. Analytical methods

Determination of thiocyanate and phenol in the samples was performed by HPLC (Agilent 1200) combined with UV detection using a reverse phase column Mediterranean sea18 (5µm x 25 cm x 46 cm, from Teknokroma). The wavelength used for detection was 210 nm. Prior to HPCL analysis, the samples were filtered through 0.45 µm PVDF filters. The mobile phase consisted in a mixture of two solutions: acetonitrile (solution A) and 0.4% phosphoric acid in water (solution B). The method comprised a binary gradient from 30% solution A to 95% solution B. The column compartment temperature was 40ºC. Run time: 12 min. Post time: 3 min. Injection volume: 20µL. Analysis was performed at flow rate of 0.7 mL/min. The retention times in mixtures of thiocyanate and phenol were 5 min for thiocyanate and 8.8 min for phenol.

2.4. Sorption experiments in batch

Thiocyanate and phenol adsorption experiments were carried out at room temperature in Erlenmeyer flasks of 250 mL at stirring rate of 300 rpm. The resin was conditioned by contacting it with a solution of NaOH 1M with an L/S ratio (volume of liquid (mL)/ mass of resin (g)) of 20, 2 times, 20 minutes each time. Next, the resin was washed with distilled water twice for 5 minutes with a ratio L/S= 50, and then separated from the solution.

The experiments were carried out at different pH solutions (3, 8 and 11) of thiocyanate to study the pH effect in the adsorption process. The initial pH of the thiocyanate solution in distilled water was 8, then the pH was modified adding HCl 1M or NaOH 0.05M respectively. 0.5 grams of wet resin previously conditioning was put in contact with 100 mL of thiocyanate solutions at concentration 100 mg/L, with pH 3, 8 and 11. The contact time was 120 minutes in all tests, sufficient to reach operative equilibrium. The volume of the samples extracted from the tank each time was 2 mL, which did not change the volume of the solution appreciably. The concentration of SCN^- ion in the resin was determined by mass balance, calculating the difference between initial and final amount of charged ions in the solution.

Experiments in batch were carried out at pH 3, where it was obtained higher SCN^- retention capacities, using a liquid/solid ratio of 200 (100 mL solution and 0.5 grams of wet resin) and initial concentrations of 50, 100, 150, 200 and 250 mg/L of SCN^- to assess the resin adsorption capacity; and assays using solutions of thiocyanate and phenol at concentrations in the range between 50 to 250 mg/L of each compound in equal proportion, monitoring the concentration of each compound over time for 120 minutes.

2.5. Packed column separation media

Continuous flow ion exchange experiments were carried out in a glass column, internal diameter of 1.1 cm, filled with 2 grams of wet resin (0.9 g of dry resin), being the compacted bed height of 3 cm. The packed column was activated by pumping through (Masterflex 7554-60 pump) a 1 M solution of NaOH for 20 minutes at a flow rate of 6 mL/min. Then, distilled water was passed through it at a flow rate of 6 mL/min during 15 minutes. Breakthrough curves were obtained by pumping through the column thiocyanate solutions containing 110 and 220 mg SCN^-/L, phenol solutions containing 110 and 220 mg phenol/L, and mixture solutions containing 110 and 220 mg/L of each compound in equal proportion, at a flow rate of 6 mL/min approximately. Samples for analysis were collected every at time intervals between 5 to 10 minutes. Once the column had been saturated, distilled water was pumped through it at a flow rate of 6 mL/min to wash away any compound not retained by the functional groups of the resin. After washing, the retained compounds were eluted by pumping through the column a solution of 0.5 M NaOH, at a flow rate of 5 mL/min approximately.

3. Results and discussion

3.1. Retention capacity in batch

3.1.1. Effect of pH

In this experiment, 0.5 g of wet resin was treated with 100 mL of 100 mg/L thiocyanate solutions at different pH values (3, 8 and 11). The experiments were carried out for 2 hours but the equilibrium was reached in 60 minutes in all assays. The results obtained for the removal of SCN^- ions at different pH have been shown in Figure 1. As can be seen, at pH 11 the resin did not show any removal of SCN^- ions. With increasing pH of solution less anion will be available to be exchanged by SCN^- ions in the solution. The removal percentage of SCN^- at pH =3 was 54%, and at pH= 8 was 39%.

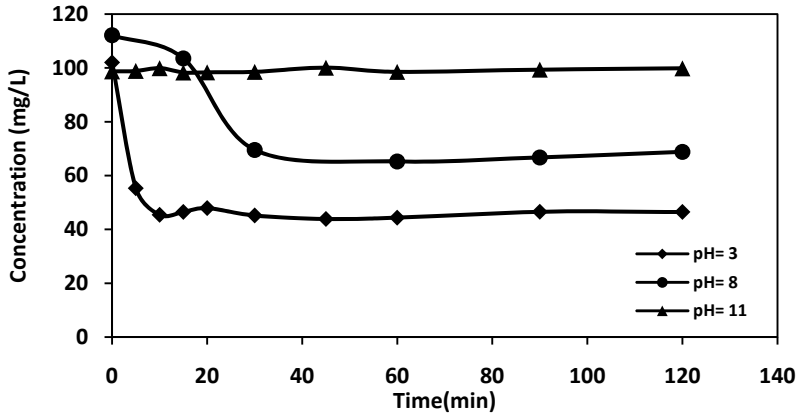

Figure 1. The effect pH on the removal of SCN^-

3.1.2. Batch equilibrium study

Several runs were carried out to obtain the adsorption capacities of the resin. Resin was contacted with different thiocyanate concentrations (50, 100, 150, 200 and 250 mg/L) at pH=3. The results showed that in all cases the equilibrium was achieved in 20 minutes.

The adsorption isotherm obtained under the conditions already described is depicted in Figure 2, it shows typical Langmuir characteristics. The thiocyanate uptake increases with the concentration and finally reaches a plateau. According to the Langmuir isotherm theory that assumes monolayer coverage of adsorbate over a homogeneous adsorbent surface, at equilibrium a saturation point is reached where no further adsorption/desorption can take place. The Langmuir equation is expressed as:

$$q_e = \frac{K_L \cdot C_e}{1 + a_L \cdot C_e} \tag{1}$$

where q_e is the equilibrium SCN^- concentration on the adsorbent (mg g^{-1}), C_e is the equilibrium liquid phase concentration (mg·L^{-1}), K_L (L·mg^{-1}) indicates the solute adsorptivity, a_L is related to the energy of adsorption. The monolayer capacity of the Langmuir isotherm, Q_m is given as:

$$Q_m = \frac{K_L}{a_L} \tag{2}$$

where a_L is Langmuir constant for energy of sorbent (L·mg^{-1}), K_L is Langmuir constant (L·mg^{-1}) and Q_m is a constant related to the area occupied by a monolayer of adsorbate, reflecting the adsorption capacity of the resin (mg SCN^-/g wet resin).

A linear transform method (LTFM) was used to find the Langmuir constant. The Langmuir constants K_L and a_L can be determined from a linearized form of Langmuir Eq. (1), represented by Eq. (3).

$$\frac{C_e}{q_e} = \frac{a_L}{K_L} C_e + \frac{1}{K_L} \tag{3}$$

Experimental data were fitted to LTFM Langmuir equation, Eq. (3), obtaining the Langmuir parameters K_L, a_L and the monolayer capacity, Q_m. The values obtained for these parameters are K_L= 4.11 L·g^{-1}, a_L= 0.252 L·mg^{-1} and Q_m = 16.3 mg SCN^-/g wet resin (36.2 mg SCN^-/g dry resin), with a linear correlation coefficient 0.967.

To quantify the agreement between the model predictions and experimental data, the proposed equilibrium equations were evaluated using Chi-square analysis [31] and non-linear

regression analysis. Eq. (4) shows how to calculate χ^2. If the data predicted by the model is similar to experimental data, χ^2 (mg/g wet resin) will be small, and vice versa.

$$\chi^2 = \sum_{i=1}^{N} \frac{\left(q_{eq,exp} - q_{eq,cal}\right)^2}{q_{eq,cal}} \tag{4}$$

where $q_{(eq,cal)}$ is the equilibrium capacity obtained from a model (mg/g wet resin), $q_{(eq,exp)}$ is the equilibrium capacity obtained from experiments (mg/g wet resin), and N is the number of measurements. Eq. (5) shows the average percentage error (Ɛ) used in the non-linear regression analysis [32]. The errors between experimental data and predicted data were calculated using Eq. (5). The values obtained were χ^2= 0.5 and $\mathcal{E}$= 7.3%.

$$\varepsilon(\%) = \frac{\sum_{i=1}^{N}\left|\left(q_{eq,exp} - q_{eq,cal}\right)/q_{eq,exp}\right|}{N} \text{x } 100 \tag{5}$$

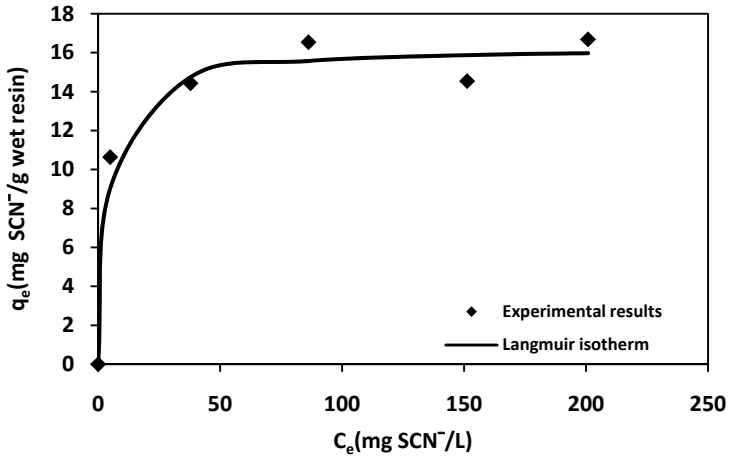

Figure 2. SCN^- adsorption isotherm in single system

Experiments in batch using synthetic mixtures solutions of thiocyanate and phenol were carried out at concentrations of 50, 100, 150, 200 and 250 mg/L of each compound in equal proportion to obtain the resin adsorption capacities in mixtures. The resin (0.5 grams) was put in contact with 100 mL of each solution for 2 hours. The equilibrium was achieved in 20 minutes. To describe the multicomponent equilibrium sorption, extension of several isotherms were used to model the experimental data, namely the Extended Langmuir equation, Jain and Snoeyink Extended Langmuir model, and the P-factor.

Extended Langmuir Equation. Buttler and Ockrent [33] were the first to develop the Langmuir model for competitive adsorption. This model assumed i) homogeneous surface with respect to the energy of adsorption, ii) no interaction between adsorbed species, and iii) all adsorption sites are equal available to all adsorbed species.

$$q_{e1} = \frac{K_{Li} \cdot C_{ei}}{1 + \sum a_{Li} C_{ei}} \tag{6}$$

For example, using components 1 and 2:

$$q_{e1} = \frac{K_{L1} \cdot C_{e1}}{1 + a_{L1} \cdot C_{e1} + a_{L2} \cdot C_{e2}} \tag{7}$$

$$q_{e2}=\frac{K_{L2}\cdot C_{e2}}{1+a_{L1}\cdot C_{e1}+a_{L2}\cdot C_{e2}} \quad (8)$$

where K_L and a_L are the Langmuir isotherm constants. The Langmuir constants K_L and a_L can be determined using a linear transform method. The Table 2 shows the constants and the monolayer capacities for single component data and for the binary monolayer capacities. The quality of the fit using EL isotherm for SCN^- was rather good, but the quality of fits for phenol was very poor. The average percentages error for SCN^- and phenol were ε_{SCN^-}= 9.8%, ε_{phenol}= 79.8%, and the χ values were χ_{SCN^-}= 2.3, χ_{phenol}= 353. The failure of the EL model suggested that the binary adsorption might be competitive.

Table 2. Extensions Langmuir isotherm parameters for SCN^- in individual and binary system with phenol

		K_L(L/g resin)	a_L(L/mg)	Q_0(mg/g wet resin)	R^2
Individual system	SCN^-	4.11	0.252	16.3	0.967
Binary system	SCN^-	1.41	0.095	14.71	0.987
	Phenol	0.075	0.003	25	0.872

Jain and Snoeyink [34] investigated competitive sorption from aqueous bicomponent solutions and developed a model that predicts sorption equilibrium in such non ideal systems. According to Jain and Snoeyink, the Langmuir theory for binary sorbate systems is based on sorption without competition. Therefore, to account for competition in the Langmuir theory, the Jain-Snoeyink model proposed to add an additional term to the extended Langmuir equation.

$$q_{e1}=\frac{(Q_{m1}-Q_{m2})a_{L1}C_{e1}}{1+a_{L1}C_{e1}}+\frac{Q_{m2}a_{L1}C_{e1}}{1+a_{L1}C_{e1}+a_{L2}C_{e2}} \quad (9)$$

$$q_{e2}=\frac{Q_{m2}a_{L2}C_{e2}}{1+a_{L1}C_{e1}+a_{L2}C_{e2}} \quad (10)$$

where Q_{mi} is the monolayer saturation capacity for the Langmuir isotherm. The first term on the right hand side of the Eq. (9) refers to the amount of species 1 adsorbed without competition with 2, while the second term gives the amount of species 1 adsorbed in competition with 2, as described by applying the competition to the Langmuir model. The additional term of Eq. (9) is the Langmuir expression for the number of molecules of solute 1 which are sorbed without competition on the surface, and the terms is proportional to $(Q_{m1}-Q_{m2})$, where $Q_{m1}>Q_{m2}$. By Eq. (10) the number of molecules of solute 2 sorbed on the sorbent surface (proportional to Q_{m2} and in competition with solute 1) can be calculated from the extended Langmuir equation. Again, the prediction between the experimental data and theoretical data for SCN^- is rather good, but in the case of phenol is fairly poor. The Jain and Snoeyink not provided an improvement over the data predicted by the extended Langmuir isotherm equation. The average percentages error for SCN^- and phenol were ε_{SCN^-}= 9.8%, ε_{phenol}= 49.3% and the χ values were χ_{SCN^-}= 2.3, χ_{phenol}= 29.4. Overall the Jain and Snoeyink modified extended Langmuir model cannot be used to predict multicomponent sorption onto resin.

P-factor. This method is another correlative technique that has been developed by McKay and Al Duri [35] based on introducing a lumped capacity factor, P_i

$$P_i=\frac{(K_{L,i}/a_{Li})_{single\ solute}}{(K_{L,i}/a_{Li})_{multisolute\ solute}} \quad (11)$$

where (K_{Li}/a_{Li}) is the monolayer capacity for component *i* in a single solute and multisolute systems respectively. This model assumes a Langmuir isotherm; hence, for each component *i*, the multicomponent isotherm is describes as:

$$q_{e,i,multi} = \frac{1}{P_i} \frac{K_{L,i}}{1 + a_{Li} C_{e,i,multi}} \quad (12)$$

The P-factor is a simplified approach that may be adopted to compare and correlate single-component sorption isotherms with those of the multicomponent systems. The results present in Table 2 show that the Langmuir equation correlates the single-solute and multisolute data over a wide concentration range, since each set of data has a correlation coefficient > 0.9. Consequently, it was decided to use the P-factor to correlate single-component and multicomponent isotherms using the Langmuir constants of K_L and a_L. The constant K_L represents the ratio of the kinetics parameters, and a_L is linked to the thermodynamic properties of the system through the enthalpy of adsorption.

The capacity P-factor for SCN^- and phenol in binary system were P_{SCN^-}= 1.1 and P_{phenol}= 1.05. The prediction for SCN^- and phenol using P-factor is shown in Figure 3. The agreement between the predicted SCN^- and phenol concentration and the experimental data in binary system is good. It provides a major improvement over the data predicted by the extended Langmuir isotherm equation and Jain and Snoeyink modified extended Langmuir model, with the average percentage error of ε_{SCN^-}= 9.7%, ε_{phenol}= 10.5%; and χ_{SCN^-}= 2.2, χ_{phenol}= 2.0.

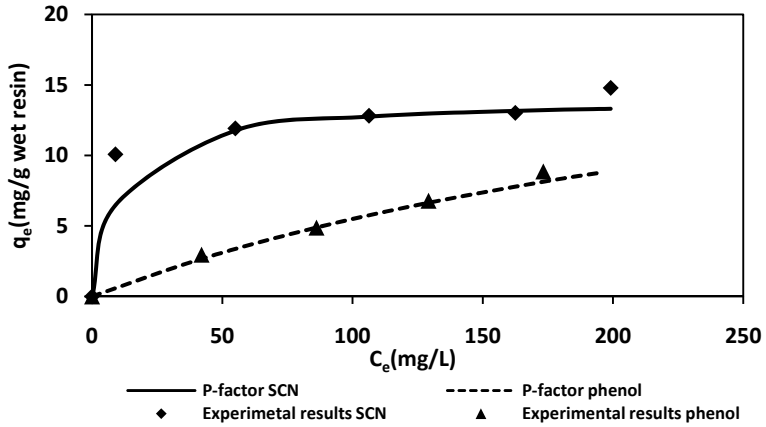

Figure 3. P-factor isotherm analysis for SCN^- and phenol in binary system.

3.1.3. Batch kinetics studies

The process of adsorption was monitored from the initial time to equilibrium time in all solutions in single system of SCN^- and in binary system of SCN^- and phenol. After 120 minutes, the solution concentration of each component does not change, so operational equilibrium can be assumed. The ion exchange operation was taken from the loading batch experiments conducted in stirred tanks with synthetic solution of SCN^- and synthetic mixtures solutions of SCN^- and phenol in ratio 1:1 at concentrations 50, 100, 150, 200, and 250 mg/L of each component. The concentration profiles of SCN^- and phenol were analyzed using first-order and second-order kinetics models.

First-order kinetics model. The kinetics data of thiocyanate are analyzed using the Lagergren first-order rate equation [36]:

$$\log(q_e - q_t) = log q_e - \frac{K_1 t}{2.303} \quad (13)$$

where q_e and q_t are the amounts of thiocyanate adsorbed (mg/g) at equilibrium and at time t, respectively, and k_1 is the rate constant of first–order adsorption (min^{-1}). The q_e and the rate constants k_1 were calculated from the slope and intercept of the plot of $\log(q_e-q_t)$ vs. t. It was found that the calculated q_e values do not agree with the experimental q_e values. This suggests that the adsorption of thiocyanate does not follow first-order kinetics.

Second-order kinetics model. Ho and McKay [37] and [38] proposed a pseudo-second order equation and assumed that the sorption rate is proportional to the number of active sites occupied onto the sorbent; the kinetic rate law is expressed as:

$$\frac{t}{q} = \frac{1}{K_2 q_e^2} + \frac{t}{q_e} \tag{14}$$

where K_2 is the rate constant of second-order adsorption (g mg^{-1} min^{-1}). The second-order rate constant K_2 and the q_e values were calculated from the slope and intercept of the plots t/q vs. t (Figure 4). It was found that the calculated q_e values agree well with the experimental q_e values (see Table 3). This suggested that the adsorption of thiocyanate did follow the second-order kinetics model. Similar has been observed by Dizge [18] in the adsorption of thiocyanate by used anion-exchange resin Purolite A-250, and Namasivayam [8] by used $ZnCl_2$ activated coir pith carbon.

Table 3. Second-order adsorption rate constants and comparison of calculated and experimental q_e values for different initial thiocyanate concentrations in individual system. Conditions: mass wet resin= 0.5 g, volume solution = 100 mL, pH= 3.0.

Initial SCN^- conc. (mg L^{-1})	q_e exp (mg g^{-1})	K_2 (g mg^{-1} min^{-1})	q_e cal (mg g^{-1})
50	10.633	0.270	10.672
100	14.428	0.167	14.472
150	16.533	0.096	16.611
200	14.536	0.133	14.684
250	16.685	0.265	16.474

The adsorption kinetics for thiocyanate and phenol in binary system were assessed using the second-order kinetics model. The second-order rates constants K_2 and the q_e values were calculated for both compounds like in the case of thiocyanate in single system. The K_2 and q_e values obtained for SCN^- and phenol in binary system are shown in Table 4 and the experimental data fitted to the second-order kinetics model are shown in Figure 5. It was found that the q_e values calculated agree with the q_e experimental results. Therefore the adsorption of thiocyanate and phenol did follow the second-order kinetics.

Table 4. Second-order adsorption rate constant and comparison of the calculated and experimental q_e values for different initial thiocyanate and phenol concentrations in binary systems. Conditions: mass wet resin= 0.5 g, volume solution = 100 mL, pH= 3.0.

	Second-order kinetics for SCN^-				Second-order kinetics for phenol			
Initial conc. (mg L^{-1})	q_e exp (mg g^{-1})	K_2 (g mg^{-1} min^{-1})	q_e cal (mg g^{-1})	R^2	q_e exp (mg g^{-1})	K_2 (g mg^{-1} min^{-1})	q_e cal (mg g^{-1})	R^2
50	10.633	0.270	10.672	1	2.961	1.528	2.936	0.9993
100	14.428	0.167	14.472	0.9999	4.877	0.895	4.876	0.9995
150	16.533	0.096	16.611	0.9999	6.784	0.165	6.789	0.9996
200	14.536	0.133	14.684	0.9997	8.859	0.302	8.937	0.9992
250	16.685	0.265	16.474	0.999	12.927	0.072	13.123	0.9994

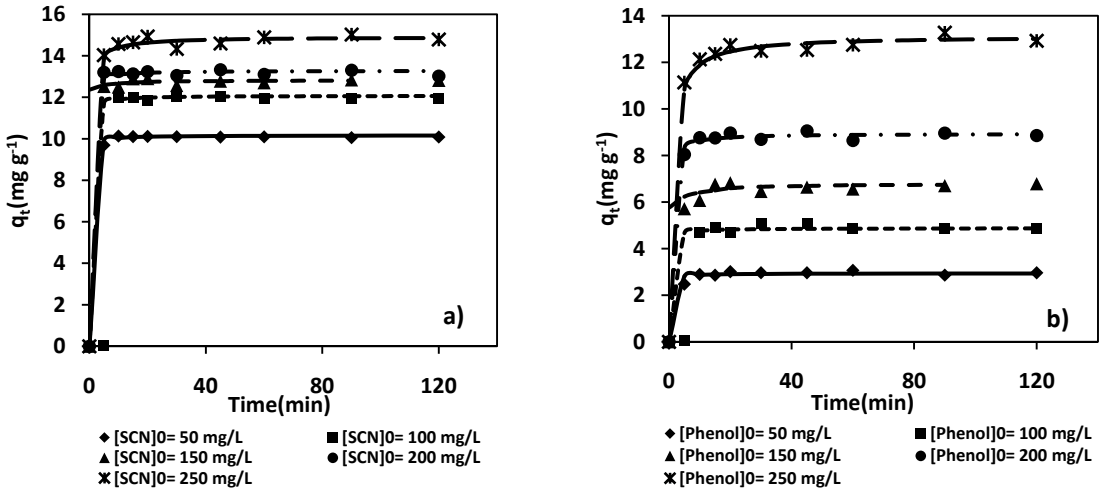

Figure 4. Kinetics of thiocyanate **(a)** and phenol **(b)** adsorption in binary system on resin fitted to second-order kinetics model. Conditions: mass wet resin: 0.5 g, volume solutions= 100 mL, pH=3.0

3.2. Packed column experiments

The adsorption properties of the polymer were also studied in packed-column experiments using 3.2 g of wet resin (1.5 g of dry resin). Column operation was initially tested by passing through SCN^- solutions containing 110 mg/L at pH 3 and down-flow rate of 5.8 mL/min. Breakthrogh curve (Figure 6) obtained showed a concentration profile constant during the loading step in both cycles, with lower concentration than the initial sample. Another cycle was carried out in column packing 2 grams of wet resin (0.9 g of dry resin) and passing through the column a thiocyanate solution containing 220 mg/L at pH 3 and flow rate of 5.6 mL/min. The shape of the breakthroughs (Figure 6) curve obtained are similar than previous cycle. This decrease in the concentration may be due to a dilution phenomenon caused by wash water, and not due to SCN^- retention onto the resin. The reason of this is that although the initial solution of SCN^- was adjusted at pH 3, the resin was conditioned with NaOH 1M, so when the solution pass through the column, its pH increases, and as it was demonstrated previously, at high pH, SCN^- was not retained.

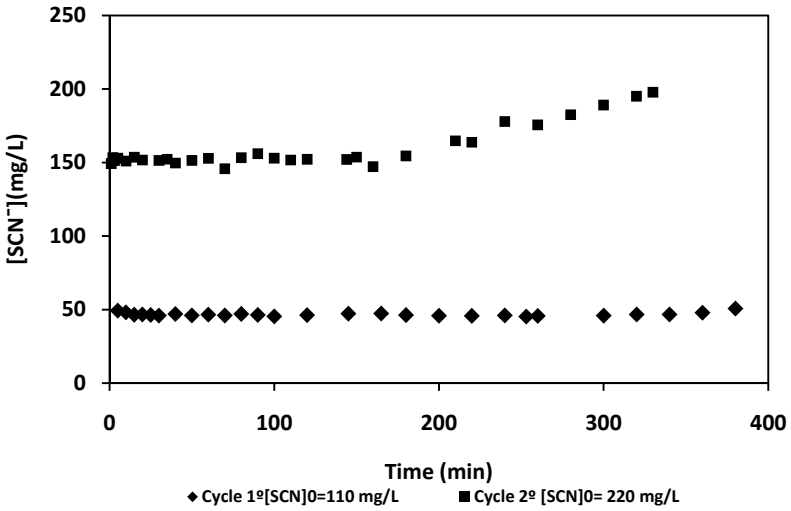

Figure 5. Breakthrough curves for 1st and 2nd cycles. Conditions: Loading (a): cycle 1º: $[SCN^-]_0$= 110 mg/L, pH=3, flow rate 5.8 ml/min, mass wet resin: 3.2 g; cycle 2º: $[SCN^-]_0$= 220 mg/L, pH=3, flow rate: 5.6 ml/min, mass wet resin: 2 grams.

Adsorption of phenol was performed in packed-column using 2 grams of wet resin (0.9 grams of dry resin). Phenol solutions containing 110 and 220 mg/L in third and fourth cycles, both at pH=3, were pumping through the column at flow rates of 6.3 and 6 mL/min, respectively. The breakthrough curves obtained (Figure 7a) show a rapid increase in phenol retention after 10 minutes, complete saturation of the column is reached in 60 minutes in both cycles. The retention capacities of the resin were 6 mg phenol/g wet resin and 14.4 mg phenol/g wet resin in the third and fourth cycle, respectively. After loading stages, the resin was regenerated by passing through a 0.5 M solution of NaOH, at a flow rate of 5 mL/min approximately in both cycles. Elution curves corresponding to the third and fourth cycle (Figure 7b) reveal that phenol concentration in the eluate increases quickly at the initial stage of elution, reaching a concentration of 195 mg/L in the first cycle and 450 mg/L in the second cycle. Concentration in the eluate was ~ 2 times higher than in the loading solution, which is very interesting for industrial operation. In both cases total elution is completed after 10 minutes. Complete phenol recovery was achieved in both cycles. The results obtained show that the resin is an effective adsorbent to remove phenol.

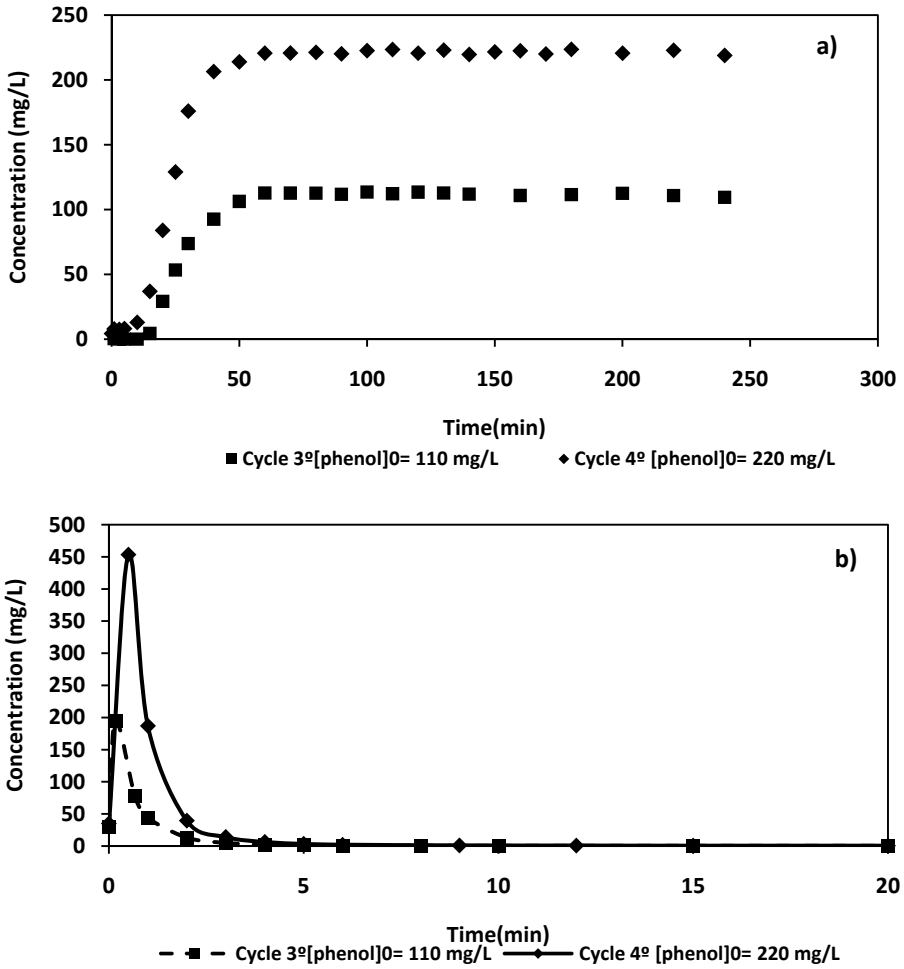

Figure 6. Loading and elution curves for 3th and 4th cycles. Conditions **(a)**: Loading: cycle 3º: $[phenol]_0$= 110 mg/L, pH=3, flow rate 6.3 mL/min, mass wet resin: 2 grams; cycle 4º: $[phenol]_0$= 220 mg/L, pH=3, flow rate: 6.0 mL/min, mass wet resin: 2 grams. Elution **(b)**: NaOH 0.5 M as eluant, flow rate 3º cycle= 5.0 mL/min; flow rate 4º cycle= 5.0 mL/min.

Adsorption of mixtures thiocyanate/phenol solutions were carried out in packed column using 2 grams of wet resin. Thiocyanate/phenol solutions at concentrations of 110 and 220 mg/L at pH 3, of each compound in equal proportion were pumping through the column at down-flow rate of 6.9 and 6.5 mL/min, respectively. The shape of the breakthrough curves (Figure 8a) obtained was similar at obtained in individual systems. Phenol breakthrough curves show a rapid increase in phenol retention after 10 minutes, complete saturation of the column is reached in 60 minutes in both cycles. The adsorption capacities obtained were 7 and 7.2 mg phenol/g wet resin in the fifth and sixth cycles respectively. Thiocyanate breakthrough curves show a concentration profile constant in both cycles, like in individual system. Therefore, thiocyanate was not retained, and the decrease in the concentration is due to dilution effect by wash water. A reason that phenol was retained and not thiocyanate may be is that thiocyanate adsorption is more pH dependent than phenol. Thiocyanate only is adsorbed at low pH whereas phenol is retained in a wide range of pH, so any increase in the pH causes that thiocyanate is not adsorbed whereas phenol is adsorbed. Although thiocyanate is not retained, this resin could allow the selective separation of thiocyanate and phenol in mixtures.

After loading stages, the resin was regenerated by passing through a 0.5 M solution of NaOH, at flow rate of 4.8 mL/min and 5.8 mL/min in the fifth and sixth elution cycles, respectively. Elution curves (Figure 8b-c) show that total elution is completed after 20 minutes.

Complete phenol recovery was achieved in both cycles. The results obtained in column show that the resin is an effective adsorbent to remove phenol and for selective separation of thiocyanate and phenol in mixtures.

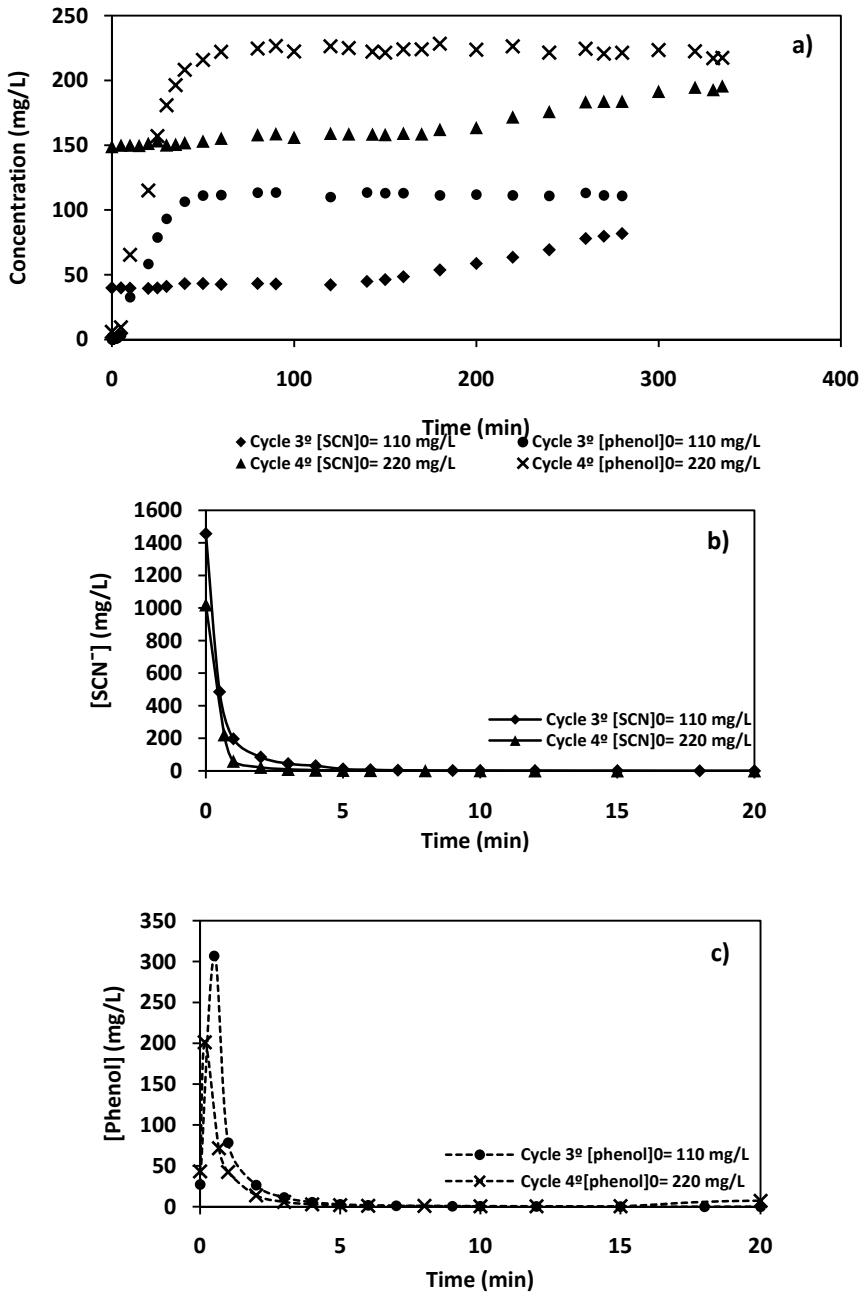

Figure 7. Loading **(a)** and elution **(b, c)** curves for 5th and 6th cycles. Conditions: Loading: cycle 5º: $[SCN^-$ + phenol$]_0$= 110 mg/L, pH=3, flow rate 6.9 ml/min, mass wet resin: 2 grams; cycle 6º: $[SCN^-$ + phenol$]_0$= 220 mg/L, pH=3, flow rate: 6.5 mL/min, mass wet resin: 2 grams. Elution: NaOH 0.5 M as eluant, flow rate 3º cycle= 4.8 mL/min; flow rate 4º cycle= 5.8 mL/min.

4. Conclusions

The removal of thiocyanate and phenol from aqueous solutions onto polymethacrylate beads synthesized by photopolymerization was investigated under different experimental conditions such as pH, and initial SCN^- and phenol concentrations. The optimum conditions for removal SCN^- and phenol from aqueous solutions was at pH 3. The adsorption process in batch was relatively fast and equilibrium was achieved in 20 minutes. To study the equilibrium, the experimental data were fitted to Langmuir isotherms for single SCN^- system. In the case of binary system of SCN^- and phenol, several methods based on the Langmuir isotherm equation were used to determine the best fit model to predict the multicomponent system performance: the Extended Langmuir model, the Jain and Snoeyink Extended Langmuir model and the P-factor. It was found that the P-factor was the better to predict and correlate the experimental data. The maximum SCN^- adsorption capacity obtained was 16.3 mg SCN^-/g wet resin (36.2 mg SCN^-/g dry resin) in single system, and 14.7 mg SCN^-/g wet resin (32.7 mg SCN^-/g dry resin) and 25 mg phenol/g wet resin (55.6 mg phenol/g dry resin) in binary system. Adsorption of SCN^- and phenol by resin followed the second order rate.

The adsorption properties of the polymer were also studied in a fixed bed column, performing successive cycles of loading and elution using thiocyanate, phenol and mixtures thiocyanate/phenol solutions, obtained that the resin is an effective adsorbent to retain phenol and could allow the selective separation of thiocyanate and phenol in mixtures.

Acknowledges

Financial support of Ana María López from FICYT “Severo Ochoa Programme” grant (Gobierno del Principado de Asturias) is gratefully acknowledged.

References

1. Luthy, R.FG. Cyanide and thiocyanate in coal gasification wastewaters. J. Water Pollut. Control Fed. 51 (1979)2267-2282.
2. Luthy, R.G. Treatment of coal coking and coal gasification wastewaters. J. Water Pollut. Control Fed 54(3) (1981) 325-339.
3. Rancaño, A. Biological treatment of Coke Wastewaters. PhD Thesis. Universidad de Oviedo (Spain), 2000.
4. Agency for toxic Substances and Disease Registry (ATSDR) Toxicological profile for Cyanide, Atlanta, GA: U.S. Department of Health and Human Services, Public Health Service, 2006.
5. Greenwood, A.; Earnshaw, A. Chemistry of the Elements, Butterworth-Heinemann, Second Ed., Oxford, 1997.
6. Guy, R.G. Synthesis and Preparative Applications of Thiocyanates, John Wiley, New York, 1977.
7. Vázquez, I.; Rodríguez-Iglesias, J.; Marañón, E.; Castrillón, L.; Álvarez, M. Removal of residual phenols from coke wastewater by adsorption. Journal of Hazardous Materials 147 (2007) 395-400.
8. Namasivayam, C. Sangeetha, D. Kinetics studies of adsorption of thiocyanate onto $ZnCl_2$ activated carbon from coir pith an agricultural solid waste. Chemosphere 60 (2005) 1616-1623
9. Kobya, M.; Topcu, N.; Demisciogly, N. Kinetics analysis of coupled transport of thiocyanate ions through liquid membranes at different temperatures. J. Membr. Sci. 130 (1997) 7-15.
10. Vicente, J; Díaz, M. Thiocyanate/phenol wet oxidations interactions. Environ. Sci. Technol. 37 (2003) 1457-1462.
11. Vicente, J.; Díaz, M. Treatment of coke effluents by wet oxidation. Ingeniería Química 36 (412) (2004) 142-161.
12. Van Leeuwen, J.; Badriyha, B.; Vaczi, S. Investigation into ozonation of coal coking processing wastewater for cyanide, thiocyanate and organic removal. Ozone Sci. Eng. 25(2003) 273-283.
13. Ansari, R.; Fahim, N.K.; Dellavar, A.F. Removal of thiocyanate ions from aqueous solutions using polypyrrole and polyaniline conducting electroactive polymers. J. Iran. Chem. Res. 2 (2009) 163-171.
14. Rong, C.; Xien, H. Electrosorption of thiocyanate anions on active carbon felt electrode in dilute solution. Journal of Colloid and Interface Science 290(2005) 190-195.

15. Namasivayam. C; Prathap, K. Removal of thiocyanate by industrial solid waste Fe(III)/(II) Hydroxide: kinetics and equilibrium studies. J. Environ. Manage. 16 (2006) 267-274.
16. Li, Y.; Yang, X.; Zhang, X. Adsorption removal of thiocyanate from aqueous solution by calcined hidrotalcite. J: Environ. Sci. 18(2006) 23-28.
17. Chubar, I.N.; Samanidou, V.F.; Kouts, V.S.; Gallios, G.G.; Kanibolotsky, V.A.; Strelko, V.V. Zhuravlev, I.Z. Adsorption of fluoride, chloride, bromide, and bromate ions on a novel ion exchanger. J: Colloid Interface Sci. 291 (2005) 67-74.
18. Dizge, N. Demirbas, E. Kobya, M. Removal of thiocyanate from aqueous solutions by ion exchange. Journal of Hazardous Materials 166(2009) 1367-1376.
19. Caetano, M.; Valderrama, C.; Farran, A; Cortina, J.L. Phenol removal from aqueous solution by adsorption and ion exchange mechanisms onto polymeric resins
20. Costa, C.; Rodrigues, A. Intraparticle diffusion of phenol in macroreticular adsorbents: modeling and experimental study of batch and CSTR adsorbents. Chem. Eng. Sci. 40(6) (1985) 983-993.
21. López, A.M.; Rendueles, M. Díaz, M. Treatment of Condensates of Gas Coke by Anionic Exchange Resins: Thiocyanate and Phenol Retention. Solvent Extraction and Ion Exchange 30(2) (2012) 212-227.
22. Cervantes-Uc, J.M; Cauich-Rodríguez, J.V.; Herrera-Kao, W.A.; Vázquez-Torres, H.; Marcos-Fernández, A. Thermal degradation behabiour of polymethacrykates containing amine side groups, Polym. Degrad. Stabil. 93 (2008) 1891-1900.
23. Bune, Y.V.; Sheninker, A.P.; Bogachev, Y.S.; Zhuravleva, I.L.; Teleshov, E.N. Radical polymerization of diethylaminoethyl methacrylate and its salts in various solvents, European Polymer Journal, 27 (6) (1991) 509-513.
24. Guerreiro, A.; Soares, A.; Piletska, E.; Mattiasson, B.; Piletsky, S. Preliminary evaluation of new polymer matrix for solid-phase extraction of nonylphenol from water samples, Anal. Chim. Acta 612 (2008) 99-104.
25. Am Ende, M.T.; Hariharan, D.; Peppas. N.A. Factors influencing drug and protein transport and release from ionic hydrogels, React. Polym. 25 (1995) 127-137.
26. Barral, S.; Guerreiro, A.; Villa-García, M. A.; Rendueles, M.; Díaz, M. Synthesis of 2-(diethylamino)ethyl mehacrylate-based polymers. Effect of crosslinking degree, porogen and solvent on the textural properties and protein adsorption performance, Reactive & Functional Polymers 70(2010) 890-899.
27. Hu, C.H.; Chou, T.-C. Albumin molecularly imprinted polymer with high template affinity- Prepared by systematic optimization in mixed organic/aqueous media, Microchem Journal 91 (2009) 53-58.
28. Boyer, C.; Boutevin, G.; Robin, J.J.: Boutevin, B. Study of the polymerization of dimethylaminoethylmethacrylate (DMAEMA) with mercaptoethanol. Application to the synthesis of a new macromonomer, Polymer 45 (23) (2004) 7863-7876.
29. Piletsky, S.; Piletskaya, E.; Panasyuk, T.L.; El'skaya, A.V.; Levi, R.; Karube, I.; Wulff, G. Imprinted membranes for sensor technology-opposite behavior of covalently and noncovalently imprinted membranes, Macromolecules 31 (7) (1998) 2137-2140.
30. Zhang, X.; Xia, J. Controlled/"Living" Radical Polymerization of 2-(Dimethylamino)ethyl Methacrylate, Macromolecules 31 (15) (1998) 5167-5169.
31. Yuh, SH. Selection of optimum sorption isotherm. Carbon, 42 (2004) 2113-2130.
32. Aksu, Z.; Tunç, O. Application of biosorption for penicillin G removal comparison with activated carbon, Process Biochem. 40 (2004) 831-847.
33. Butler, J.A.V.; Ockrent, C. Studies in Electrocapillarity. Part III. The Surface Tensions of Solutions Containing Two Surface-Active Solutes. J. Phys. Chem. 34 (1930) 2841-2845.
34. Jain, J.S.; Snoeyink, V.L. Adsorption from Bisolute Systems on Active Carbon. J. Water Pollut. Control Fed. 45 (1973) 2463-2479.
35. Choy, K.K-H.; Porter, J.F.; McKay G. Langmuir Isotherms Models Applied to the Multicomponent Sorption of Acid Dyes from Effluent onto Activated Carbon. J. Chem. Eng. Data 45 (2000) 575-584.
36. Lagergren, S. About the theory of so-called adsorption of solute substances, Kungliga Svenska Vetenskapsakademiens. Handlingar. Band, 24 (1898) 1-39.
37. Ho, Y.S.; McKay, G. Pseudo-second model for sorption process. Proc. Biochem. 34 (1999) 451-454.
38. Ho, Y.S. McKay, G. The sorption of lead (II) ions on peat. Water Res. 33 (1999) 578-584.

5. CONCLUSIONES

Los diferentes estudios llevados a cabo durante el desarrollo de esta Tesis nos permiten llegar a las siguientes conclusiones:

- ✓ La eliminación de las sulfamidas sulfametoxazol (SMX) y sulfametazina (SMZ) en disoluciones acuosas se llevó a cabo exitosamente empleando la resina comercial Lewatit MP500 en sistemas individuales y en sistemas binarios de SMX y SMZ. La resina presentó mayor afinidad por el SMX que por el SMZ. Los resultados de equilibrio de ajustaron adecuadamente a las isotermas Langmuir y Factor de Separación Constante (FSC). Las capacidades máximas de adsorción obtenidas fueron 258.5 mg/mL resina (263 mg SMX/g resina húmeda) y 110 mg SMZ/g resina húmeda. En los ensayos realizados con mezclas de ambas sulfamidas, el equilibrio de adsorción de ajustó a un modelo de Langmuir modificado para sistemas multicomponentes (Jain y Snoeyink), demostrando que hay competencia en el proceso de adsorción, obteniendo unas capacidades máximas de adsorción de 277 mg SMX/g resina húmeda y 25 mg SMZ/g resina húmeda. La cinética se describió siguiendo dos modelos de difusión: el modelo de transferencia de masa a través de la película líquida y el modelo de difusión en poros, obteniendo buena concordancia entre los valores experimentales y los predichos por ambos modelos para el SMX y el SMZ. En mezclas, la cinética se ajustó adecuadamente al modelo de difusión en poros.

- ✓ En las etapas de carga y elución llevadas a cabo en columna, empleando disoluciones sintéticas de SMX, SMZ y mezclas de ambos en igual proporción, se obtuvieron buenas capacidades de retención. La forma de la curvas de ruptura demostró la viabilidad para llevar a cabo la separación de las sulfamidas presentes en disolución acuosa. Además el eluyente demostró ser efectivo, recuperando el 100% de ambas sulfamidas en las etapas de elución tanto en sistemas individuales como en mezclas. La operación en columna se modelizó empleando un modelo de lecho fijo, obteniendo buena concordancia entre los valores experimentales y los predichos por el modelo.

- ✓ En los ensayos realizados con SMX en presencia de sales (cloruros, sulfatos y nitratos) empleando la resina Lewatit MP500, la capacidad de adsorción del SMX disminuyó debido a la competencia que existe entre el SMX y las sales por los sitios activos de la resina, pero aún así, se consiguió obtener buena capacidad de retención

del SMX. Los resultados de equilibrio se ajustaron a la isoterma de Langmuir para sistemas multicomponentes, obteniendo los siguientes valores: $K_{eq\text{-}SMX}$= 1.4; $K_{eq\text{-}nitrato}$= 6 mL/mg, $K_{eq\text{-}sulfato}$= 9 mL/mg; Q_0= 105 mg SMX/mL resina. Los datos de cada sal en sistemas individuales se ajustaron correctamente a las isotermas de Langmuir y FSC, obteniendo unas capacidades máximas de adsorción de 35.2 mg Cl^-/mL resina, 76.9 mg SO_4^{2-}/mL resina y 73.8 mg NO_3^-/mL resina. La cinética se ajustó adecuadamente al modelo de transferencia de masa y al modelo de difusión en poros, siendo la etapa controlante del proceso la difusión en poros. Los ensayos en columna empleando mezclas de SMX y sales, demostraron que la resina era capaz de retener SMX a pesar de la presencia de sales, recuperándose el 100% de todos los compuestos en la etapa de elución. El modelo de lecho fijo mostró ser válido para representar el sistema multicomponente, obteniendo buena concordancia entre los valores experimentales y los predichos por el modelo.

- ✓ La eliminación de tiocianato y fenol procedentes de disoluciones acuosas y de aguas residuales de coquería se llevó a cabo exitosamente empleando las resinas aniónicas comerciales Lewatit MP500 y Lewatit M610. Se determinaron los parámetros de equilibrio y cinética del proceso en tanque agitado. Las capacidades de adsorción obtenidas fueron de 72 mg SCN^-/mL resina para MP500 y de 69 mg SCN^-/mL resina para M610. Se determinaron las constantes cinéticas de transferencia de masa y difusividad en poros para ambas resinas. En la operación llevada a cabo en columna se obtuvieron buenas capacidades de retención del tiocianato en disoluciones sintéticas y el eluyente demostró ser eficaz concentrando la disolución inicial, lo que permite un tratamiento final más sencillo. En los ensayos llevados a cabo con disoluciones mezclas de tiocianato y fenol se observó un desplazamiento del frente de fenol por el tiocianato, esto permitiría la separación selectiva del fenol del tiocianato. En los ensayos realizados con aguas residuales, la forma de las curvas de ruptura demostró la viabilidad de la operación de intercambio iónico para eliminar estos contaminantes de las aguas residuales. Finalmente, comparando los resultados obtenidos con ambas resinas se concluyo que era más eficaz la resina Lewatit M610 para eliminar tiocianatos y fenoles presentes en aguas residuales.

- ✓ La síntesis de polímeros de metacrilato en forma de esferas mediante fotopolimerización dio lugar a dos polímeros que difieren en el agente porogénico,

denominados resina A y resina B. La caracterización físico-química de los polímeros demostró que se trata de partículas esféricas con una distribución de tamaños uniforme, cuyos diámetros son 326 µm para A y 435 µm para B, son partículas macroporosas y térmicamente estables hasta 200ºC, a partir de esta temperatura comienza su descomposición, finalizando a los 470ºC.

- ✓ Se probaron las propiedades de estos polímeros para retener SMX en disoluciones acuosas, obteniéndose el doble de capacidad de retención con A que con B. Se llevaron a cabo estudios de equilibrio y cinética empleando la resina A para retener SMX, SMZ, y mezclas de SMX y SMZ en disoluciones acuosas. La resina A demostró tener mayor afinidad por el SMX. Los datos de equilibrio se ajustaron a la isoterma de Langmuir para cada sistema individual, obteniéndose muy buena capacidad de retención para el SMX, 101 mg/g resina húmeda ó 220 mg SMX/g resina seca. Para el SMZ se obtuvo una capacidad de retención de 41.2 mg SMZ/g resina húmeda ó 91.5 mg SMZ/g resina seca. En mezclas de SMX y SMZ, los datos experimentales se ajustaron a la isoterma de Langmuir modificada, obteniéndose unas capacidades de retención de 98.1 mg SMX/g resina húmeda (218 mg SMX/g resina seca) y 7.3 mg SMZ/g resina húmeda (16.3 mg SMZ/g resina seca). La cinética del proceso se ajustó correctamente al modelo de difusión en poros.

- ✓ En los ensayos realizados en columna empleando disoluciones sintéticas de SMX, SMZ y mezclas de ambos, de nuevo se obtuvo mejores capacidades de retención para el SMX que para el SMZ. La capacidad de retención del SMX fue cinco veces superior a la del SMZ en sistemas individuales trabajando en las mismas condiciones de operación, y en mezclas la capacidad de retención del SMX fue muy superior a la del SMZ. En las etapas de elución, se demostró la eficacia del eluyente, recuperándose el 100% de SMX y SMZ en todos los casos. La operación en columna fue modelizada con el modelo de lecho fijo, obteniendo buena concordancia entre los valores experimentales y los predichos por el modelo.

- ✓ Finalmente, se probó la capacidad de la resina A para retener tiocianato y fenol presentes en disoluciones acuosas tanto solos como mezclados. De los estudios realizados sobre la influencia del pH en la adsorción, se concluyó que a pH 3 es cuando se obtiene mejor capacidad de adsorción. Las capacidades de adsorción obtenidas fueron 16.3 mg SCN^-/g resina húmeda (36.2 mg SCN^-/g resina seca) en

el sistema individual, y 14.7 mg SCN^-/g resina húmeda (32.7 mg SCN^-/g resina seca) y 25 mg fenol/g resina húmeda (55.6 mg fenol/g resina seca) en mezclas. El equilibrio de adsorción en mezclas se describió adecuadamente con un modelo basado en la ecuación de Langmuir, P-factor. El proceso de adsorción en mezclas siguió una cinética de segundo orden. A partir de las curvas de ruptura obtenidas en los ensayos realizados en columna, se puede concluir que a pesar de que el tiocianato no es retenido, ya que la disminución que se observa en su concentración fue debida a efectos de dilución, sí es posible la separación del tiocianato del fenol en mezclas empleando esta resina, y el eluyente demostró ser eficaz regenerando la resina, recuperando el 100% del fenol adsorbido.

CONCLUSIONS

Studies conducted during the development of this thesis allow us to reach the following conclusions:

- ✓ Removal of sulfamides, sulfamethoxazole (SMX) and sulfamethazine (SMZ), in aqueous solutions using a commercial resin Lewatit MP500 was carried out successfully both in individual and binary systems. The resin showed more affinity for the SMX than for the SMZ. The equilibrium results were fitted to Langmuir and Constant Separation Factor (CSF) isotherms adequately. The maximum adsorption capacities obtained were 258.5 mg SMX/mL resin (263 mg SMX/g wet resin) and 110 mg SMZ/g wet resin. In the assays performed with mixtures of sulfamides, the ion exchange equilibrium was adjusted to a modified Langmuir model for multicomponent systems (Jain and Snoeyink), demonstrating that exists competition in the adsorption process between sulfamides, obtaining the adsorption capacities of 277 mg SMX/g wet resin and 25 mg SMZ/g wet resin. Kinetics was described using two diffusion models: the film mass transfer model and the pore diffusion model, getting good agreement between experimental and theoretical data by both models for SMX and SMZ. In mixtures, kinetics adsorption was adjusted to the pore diffusion model correctly.

- ✓ In loading and elution stages in column, using synthetic solutions of SMX, SMZ and mixtures of both compounds in equal proportion, good retention capacities were obtained. The shape of the breakthrough curves showed the viability to performer the sulfamides separation. Furthermore, the efficiency of eluent was demonstrated, recovering 100% of both sulfamides, both in individual and mixture systems. The column operation was modeled using a fixed bed model; good agreement between experimental and theoretical data was reached.

- ✓ In the trials with SMX in presence of salts (chlorides, sulfates and nitrates) using Lewatit MP500 resin, the SMX adsorption capacity decreased due to the competition existing between SMX and salts by the active sites of the resin, but even so, good retention capacity was reached. The equilibrium results were adjusted to Langmuir isotherm for multicomponent system, obtaining the values: $K_{eq\text{-}SMX}$= 1.4; $K_{eq\text{-}nitrate}$= 6 mL/mg, $K_{eq\text{-}sulfate}$= 9 mL/mg; Q_0= 105 mg SMX/mL resin. The

experimental values of each salt were fitted to Langmuir and CSF isotherm properly, obtaining the adsorption capacities of 35.2 mg Cl^-/mL resin, 76.9 mg SO_4^{2-}/mL resin and 73.8 mg NO_3^-/mL resin. Kinetics was adjusted to the film mass transfer and the pore diffusion models, being the particle diffusion the rate-controlling step. Column assays using mixtures of SMX and salts demonstrated that the resin was able to retain SMX despite of the presence of salts, recovering 100% of all compounds in elution stage. The fixed bed model showed to be adequate for fitting the multicomponent system, obtaining good agreement between experimental and theoretical data.

- ✓ Removal of thiocyanate and phenol from aqueous solutions and coke wastewaters was carries out successfully using the commercial anionic resins Lewatit MP500 and Lewatit M610. The equilibrium and kinetics parameters were determined in batch. The adsorption capacities were 72 mg SCN^-/mL resin for MP500 and 69 mg SCN^-/mL resin for M610. The film mass transfer constant and the pore diffusivity for both resins was determined, being the mass transfer through the liquid film the rate-controlling step. In column, good retention capacity for thiocyanate in synthetic solutions was obtained, and the eluent showed to be effective, concentrating the initial sample, thus permitting and easier final treatment. In assays using synthetic mixtures of thiocyanate/phenol, the thiocyanate front displaces in the phenol front, thus permitting a selective separation of both compounds. In assays with wastewaters, the shape of breakthrough curves demonstrated the viability of the ion exchange operation for removing these compounds from wastewaters. Finally, comparing the results obtained with both resins was concluded that Lewatit M610 resin is more effective for removing thiocyanates and phenols from wastewaters.

- ✓ Synthesis of methacrylate copolymers beads by photopolymerization resulted in two polymers that differ in the porogen, named A and B. Physico-chemical characterization of polymers showed that consisting in spherical particles exhibiting a unimodal particle size distribution, which diameters were 326 µm for A and 435 µm for B, are macroporous and thermally stable up to 200ºC, from this temperature begins its decomposition, ending at 470ºC.

- ✓ The chromatographic properties of A and B to retain SMX in aqueous solutions were performed; obtaining the double of adsorption capacity with A. Equilibrium

and kinetics studies were carried out with A to retain SMX, SMZ, and mixtures of SMX and SMZ in aqueous solutions. The resin A showed to have more affinity for SMX. The equilibrium data were fitted to Langmuir isotherm for each individual system, obtaining very good retention capacity for SMX, 101 mg SMX/g wet resin, equivalent at 220 mg SMX/g dry resin. For SMZ the retention capacity obtained was 41.2 mg SMZ/g wet resin, equivalent at 91.5 mg SMZ/g dry resin. In mixtures of SMX and SMZ, the experimental data were fitted to modified Langmuir isotherms, obtaining retention capacities of 98.1 mg SMX/g wet resin (218 mg SMX/g dry resin) and 7.3 mg SMZ/g wet resin (16.3 mg SMZ/g dry resin). Kinetics was adjusted to the pore diffusion model correctly.

- ✓ In column assays using SMX, SMZ and mixtures of SMX and SMZ in synthetic solutions, better retention capacities for SMX were obtained than for SMZ, being five times higher the adsorption capacity obtained for SMX in individual system, working under the same operating conditions. In mixtures, the SMX retention capacity was much higher than that of SMZ. In elution steps, the eluent efficiency was proved, recovering 100% of SMX and SMZ in all cases. Column operation was modeled using the fixed bed model, obtaining good agreement between experimental data and those predicted by the model.

- ✓ Finally, the capacity of resin A to retain thiocyanate and phenol present in aqueous solution either alone or mixed was tested. The influence of pH on ion exchange process was studied obtaining at pH 3 the best retention capacities. The values obtained were 16.3 mg SCN^-/g wet resin, equivalent to 36.2 mg SCN^-/g dry resin in the individual system; 14.7 mg SCN^-/g wet resin (32.7 mg SCN^-/g dry resin) and 25 mg phenol/g wet resin (55.6 mg phenol/g dry resin) in mixed trials, respectively. The ion exchange equilibrium in mixtures was adequately described with a model based on the Langmuir equation, the P-factor model. The ion exchange process in mixtures followed second-order kinetics model. From breakthrough curves, it can be concluded that although thiocyanate was not retain, since the decrease in its concentration is due to the dilution effect, it is possible the separation of thiocyanate and phenol in mixtures using this resin. The eluent was effective in resin regeneration, recovering 100% of phenol retained.

6. BIBLIOGRAFÍA

[1] C. Orozco Barrenetxea, A. Perez Serrano, M. N. González Delgado and F. J. Rodríguez Vida, Contaminación Ambiental. Una Visión Desde la Química, Madrid: Thomson, 2002.

[2] M. J. Lopez de Alda, S. Díaz-Cruz, M. Petrovic and D. Barceló, "Liquid chromatography-(tandem) mass spectrometry of selected emerging pollutants (steroid sex hormones, drugs and alkylphenolic surfactants) in the aquatic evironment," *Environmental Science and Technology,* vol. 39, no. 10, pp. 3421-3429, 2003.

[3] I. Rodríguez, J. B. Quintana, J. Carpinteiro, A. M. Carro, R. A. Lorenzo and R. Cela, "Determination of Acod Drugs in Sewage Water by Gas Chromatography-Mass Spectrometry as Tert-Butyldimethylsilyl Derivatives," *Journal of Chromatography A,* vol. 985, pp. 265-274, 2003.

[4] M. Carballa, F. Omil and J. M. Lema, "Removal of Cosmetic Ingredients and Pharmaceuticals in Sewage Primary Treatment," *Water Research,* vol. 39, pp. 4790-4796, 2005.

[5] M. Carballa, F. Omil, J. M. Lema, M. Lompart, C. García-Jares, I. Rodríguez, M. Gomez and T. Ternes, "Behaviour of phamaceuticals, cosmetics and hormones in a sewage treatment plant," *Water Research,* vol. 38, pp. 2918-2926, 2004.

[6] T. A. Ternes, "Ocurrence of drugs in German sewage treatment plants and rivers," *Water Research,* vol. 32, no. 11, pp. 3245-3260, 1998.

[7] A. Boxal, C. Sinclair, K. Fenner, D. Kolpin and S. J. Maund, "When synthetic chemicals degrade in the environment," *Environ Sci Technol,* vol. 38, pp. 368-375, 2004.

[8] B. S. Kirk and D. B. Othmer, Encyclopedia of Chemical Technology, 4th ed., vol. 23, New York: John Wiley and Sons, 1997, pp. 319-323.

[9] D. W. Boening and C. M. Chew, "A critical rewiew: general toxicity and environmental fate of three aqueous cyanide ions and associated ligands," *Water Air Soil Pollut.,* vol. 109, pp. 67-79, 1999.

[10] European Medicines Agency, European Surveillance of Veterinary Antimicobial Consumption (ESVAC), "Sales of veterinarian antimicrobial agents in 25 EU/EEA countries in 2011 (EMA/236501/2013)," vol. 3, 2013.

[11] D. W. Kolpin, M. Skopec, M. T. Meyer, E. T. Furlong and S. D. Zaugg, "Urban contribution of pharmaceuticals and other organic wastewater contaminants to streams during differing flow conditions," *Science of the Total Environment,* vol. 328, no. 1-3, pp. 119-130, 2004.

[12] X. S. Miao, F. Bishay, M. Chen and C. D. Metcalfe, "Ocurrence of antimicrobials in the final effluents of wastewater treatment plants in Canada," *Environmental Science and Technology,* vol. 38, no. 13, pp. 3533-3541, 2004.

[13] M. Gross, M. Petrovic and D. Barceló, "Wastewater treatment plants as a pathway for aquatic contamination by pharmaceuticals in the Ebro river basin (Northeast Spain)," *Environmental Toxicology and Chemistry,* vol. 26, no. 8, pp. 1553-1562, 2007.

[14] M. Edwards, E. Topp, C. D. Metcalfe, H. Li, N. Gottschall, P. Bolton, W. Curnoe, M. Payne, A. Beck, S. Klewegt and D. R. Lapen, "Phamaceutical and personal care products in tile drainage following surface spreading and injection of dewatered municipal biosoilds to an agricultural field," *Science of The Total Environment,* vol. 407, no. 14, pp. 4220-4230, 2009.

[15] L. Sabourin, A. Beck, P. W. Duenk, S. Kleywegt, D. R. Lapen, H. Li, C. D. Metcalfe, M. Payne and E. Topp, "Runoff of pharmaceuticals and personal and care products following application of dewatered municipal biosolids to an agricultural field," *Science of the Total Environment,* vol. 407, no. 16, pp. 4596-4604, 2009.

[16] J. Schwarzbauer, S. Brinker and R. Littke, "Occurrence and alteration of organic contaminants in seepage and leakage water from a waste deposit landfill," *Water Research,* vol. 36, no. 9, pp. 2275-2287, 2002.

[17] J. P. Bound and N. Voulvoulis, "Household disposal of pharmaceuticals as a pathway for aquatic contamination in the United Kingdom," *Environmental Health Perspectives,* vol. 113, no. 12, pp. 1705-1711, 2005.

[18] V. Homen and L. Santos, "Degradation and removal methods of antibiotics from aqueous," *Journal of Environmental Management,* vol. 92, pp. 2304-2347, 2011.

[19] G. R. Boyd, H. Reemtsma, D. A. Grimm and S. Mitra, "Pharmaceuticals and Personal and Care Products (PPCPs) in Surface and Treated Waters of Louisiana,

USA and Ontario, Canada," *The Science of the Total Environment,* vol. 311, pp. 135-149, 2003.

[20] T. A. Ternes, D. Meisenheimer, D. McDowell, F. Sacher, H. J. Brauch, B. Haist-Gulde, G. Preuss, U. Wilme and N. Zulei-Seibert, "Removal of pharmaceuticals during Drinking Water Treatment," *Environmental Science and Technology,* vol. 36, p. 3855, 2002.

[21] P. E. Stackelberg, E. T. Furlong, M. T. Meyer, S. D. Zaugg, A. K. Henderson and D. B. Reissman, "Persistence of Pharmaceutical Compounds and Other Organic Wastewater Contaminants in a Conventional Drinking-Water -Treatment Plant," *Science of the Total Environment,* vol. 329, pp. 99-113, 2004.

[22] O. A. Jones, J. N. Lester and N. Voulvoulis, "Pharmaceuticals: A Threat to Drinking Water?," *Trends in Biotechnology,* vol. 23, no. 4, pp. 163-167, 2005.

[23] C. G. Daughton and T. A. Ternes, "Pharmaceuticals and Personal and Care Products in the Environment: Agents of Subtle Change?," *Environmental Health Perperctives,* vol. 107, no. 6, pp. 907-938, 1999.

[24] J. A. Cortacans Torre, A. Hernández Lehmann, I. Del Castillo González, E. Montes Carmona and A. Hernández Muñoz, "Presencia de fármacos en aguas residuales y eficacia de los procesos convencionales en su eliminación," Cátedra de Ingeriería Sanidad y Ambiente de la E.T.S. Ingenieros de Caminos, Canales y Puertos, Universidad Politécnica de Madrid.

[25] T. Schwartz, W. Kohnen, B. Jansen and U. Obst, "Detection of Antibiotic-Resistant Bacteria and their Resistance Genes in Wastewater, Surface Water, and Drinking Water Biofilms," *FEMS Microbiology Ecology,* vol. 43, pp. 325-335, 2003.

[26] C. H. Huang, J. E. Renew, K. L. Smeby, K. Pinkerston and D. L. Sedlak, "Assessment of Potential Antibiotics Contaminants in Water and Preliminary Occurrence Analysis," *Water Resour Update,* vol. 120, pp. 30-40, 2001.

[27] D. W. Kolpin, E. T. Furlong, M. T. Meyer, E. M. Thurman, S. D. Zaugg, L. B. Barber and H. T. Buxton, "Pharmaceuticals, Hormones, and Other Organic Wastewater Contaminants in U.S. Streams 1999-2000: A National Reconnaissance," *Environmental Science and Technology,* vol. 36, no. 6, pp. 1202-1211, 2002.

[28] S. F. Webb, "A Data Based Perspective on the Environmental Risk Assessment of Human Pharmaceuticals. III- Indirect Human Exposure," in *Pharmaceuticals in the Environment. Sources, Fate, Effects and Risks*, K. Kümmerer, Ed., Heidelberg, Germany, Springer, 2001, pp. 221-230.

[29] "PubChem," National Center for Biotechnology Information (NCBI), [Online]. Available: http://pubchem.ncbi.nlm.nih.gov/.

[30] A. Rancaño, "Tratamiento Biológico de Aguas Residuales de Coquería," Tesis Doctoral, Universidad de Oviedo, 2000.

[31] R. G. Luthy, "Cyanide and Thiocyanate in Coal Gasification Wastewaters," *Journal Water Pollution Control Federation,* vol. 51, pp. 2267-2282, 1979.

[32] K. Y. Chen and J. C. Morris, "Oxidation of Sulfide by O2: Catalysis and Inhibition," *Jour. San. Eng. Div. Proc. Amer. Soc. Civil Engr,* vol. 98, pp. 215-227, 1972.

[33] D. J. O'Brien and F. B. Birkner, "Oxidation of Reduced Sulfur Species in Aqueous Systems," *Division of Environmental Chemistry,* vol. 15, pp. 232-234, 1975.

[34] U.S. Environmental Protection Agency, "ECOTOX Database," [Online]. Available: http://epa.gov/ecotox/.

[35] C. D. Selassie, T. V. DeSoyza, M. Rosario, H. Gao and C. Hansch, "Phenol toxicity in leukemia cells: a radial process," *Chemico-Biological Interactions,* vol. 113, no. 5, pp. 175-190, 1998.

[36] N. Marqué, E. Pocurrull, R. M. Marcé and F. Borrull, "Determination of eleven priority EPA phenolics at ngL-1 levels by on-line solid-phase extraction and liquid clromathography with UV and electrochemical detection," *Chromatography,* vol. 37, no. 3-4, pp. 176-182, 1993.

[37] CITME, "Tratamientos Avanzados de Aguas Residuales Industriales," [Online]. Available: www.madrimasd.org/citme.

[38] C. P. Gomes, M. F. Almeida and J. M. Loureiro, "Gold recovery with ion exchange used resins," *Sep. and Purif. Tech.,* vol. 24, pp. 35-57, 2001.

[39] F. Helfferich, Ion Exchange, New York: McGraw-Hill, 1962.

[40] I. N. Levin, Fisicoquímica, 3ª ed., Madrid: McGraw-Hill, 1991.

[41] J. S. Jain and V. L. Snoeyink, "Adsorption from Bisolute Systems on Activated

Carbon," *J. Water Pollut. Control Fed.,* vol. 45, pp. 2463-2479, 1973.

[42] G. McKay and B. Al Buri, "Simplifed Model for the Equilibrium Adsorption of Dyes from Mixtures using Activated Carbon," *Chem. Eng. Process,* vol. 22, pp. 145-156, 1987.

[43] G. Schay, "On the definition of interfacial excesses in a system consisting of an insoluble solid adsorbent and a binary liqid mixture," *Colloid and Polimer Science,* vol. 26, pp. 888-891, 1982.

[44] J. A. Marinsky, Ion exchange. A series of Advances, New York: Marcel Dekker, Inc, 1966.

[45] G. E. Boyd, A. W. Adamson and L. S. Myers, "The exchange adsorption from aqueous solutions by organic zeolites. II. Kinetics," *J. Am. Chem. Soc.,* vol. 69, no. 11, pp. 2836-2848, 1947.

[46] W. Nernst, *Z. Phys. Chem.,* vol. 47, pp. 52-55, 1904.

[47] M. A. Fernández Fernández, *Análisis de la recuperación de metales por intercambio iónico con resina complejante iminodiacetato,* Oviedo: Tesis Doctoral. Universidad de Oviedo, 1991.

[48] K. Dorfner, Ion Exchangers, Berlin: Walter de Gruyter, 1991.

[49] P. A. Schweitzer, "Section 1.12: Ion Exchange Separations," in *Handbook of Separation Techniques*, New York, McGraw-Hill, 1979.

[50] S. Barral, A. Guerreiro, A. Villa-García, M. Rendueles and M. Díaz, "Synthesis of 2-(diethylamino)ethyl methacrylate-based polymers. Effect of crossliking degree, porogen and solvent on the textural properties and protein adsorption performance," *Reactive & Functional Polymers,* vol. 70, pp. 890-899, 2010.

[51] M. Nevárez, "Optimización del proceso de regeneración de resinas de intercambio para ser utilizadas en el desmineralizador de agua de refinería estatal esmeraldas," Escuela superior politécnicas de Chimborazo, Riobamba, 2009.

[52] FECYT, "Tecnociencia:Especial Resinas de Intercambio iónico," 2001. [Online]. Available: http://www.fecyt.es/especiales/intercambio_ionico/.

[53] D. Whitney, M. McCoy, N. Gordon and N. Afeyan, "Characterization of large-pore polymeric supports for use in perfusion biochromatography," *J. of Chromatogf. A.,* vol. 807, pp. 165-184, 1998.

[54] APHA-AWWA-WPCF, Métodos normalizados para el análisis de aguas potables y residuales, Madrid: Díaz de Santos, 1992.

[55] J. A. Marinsky, "Volume 1. Charper 2," in *Ion exchange. A series of Advances*, New York, Marcel Dekker, Inc, 1966.

7. ANEXOS

7.1. PUBLICACIONES Y APORTACIONES RELACIONADAS CON LA TESIS

7.1.1. Artículos científicos

- **López, A.M.**; Rendueles, M.; Díaz. M. Treatment of condensates of gas coke by anionic exchange resins: thiocyanate and phenol retention. *Solvent Extraction and Ion Exchange*, 30: 212-227, 2012.
- **López, A.M.**; Rendueles, M.; Díaz. M. Sulfamethoxazole removal from synthetic solutions by ion exchange using a strong anionic resin in fixed bed. *Solvent Extraction and Ion Exchange*, 31:763-781, 2013.
- **López, A.M**.; Rendueles, M.; Díaz. M. Sulfamethazine retention from water solutions by ion exchange with a strong anionic resin in fixed bed. *Separation Science and Technology*. Aceptado (Manuscript ID LSST-2013-7165).
- **López, A.M.**; Rendueles, M.; Díaz. M. Competition of salts with sulfamethoxazole in anionic ion exchange process. *Industrial & Engineering Chemistry Research* (Manuscrip ie-2014-001899). Bajo revisión (Manuscript ie-2014-001899).
- **López, A.M.**; Rendueles, M. Díaz. M. Competitive retention of sulfamethoxazole (SMX) and sulfamethazine (SMZ) in a strong anionic ion exchange resin. *Solvent Extraction and Ion Exchange* (N14-16). Bajo revisión (Manuscript N14-16).
- **López, A.M.**; Villa-García, A.; Rendueles, M.; Díaz, M. Synthesis of 2-(diethylamino)ethyl methacrylate-based microspheres. Physico-chemical characterization and chromatographic performance for antibiotic adsorption. Separation and Purification Technology. Bajo revision
- **López, A.M.**; Villa-García, A.; Rendueles, M.; Díaz, M. Retention of sulfamethazine and sulfamethoxazole mixtures onto anionic ion exchange polymethacrylate resin. Bajo revisión
- **López, A.M.**; Villa-García, A.; Rendueles, M.; Díaz, M. Retention and separation of thiocyanate and phenol from synthetic solutions by ion exchange with polymethacrylate resin from photopolymerization. En elaboración.

7.1.2. Contribuciones a congresos

- **López, A.M.**, Hicks, W.; Rendueles, M.; Díaz, M. "Polymetacrilate from photopolymerization for aqueous sulfamethoxazole adsorption"(comunicación oral). XXXIV Reunión Bienal de la Real Sociedad Española de Química. Santander (España). Septiembre 15-18, 2013.
- **López, A.M.**, Rendueles, M.; Díaz, M. "Removal of pharmaceutical contaminants from wastewater by ion exchange" (póster). ANQUE´s ICCE 2012. International Congress of Chemical Engineering. Sevilla (España). Junio 24-27, 2012.
- **López, A.M.**, Rendueles, M., Díaz. M. "Retention of sulfamethoxazole in presence of salts in effluents of sewage treatment plants by ion exchange"(póster). 12th Mediterranean Congress of Chemical Engineering. Barcelona (España). Noviembre 15-18, 2011.
- **López, A.M.,** Rendueles, M., Díaz. M. "Retention of emergent contaminants derivates of antibiotics by ion exchange" póster). 8th European Congress of Chemical Engineering. Berlín (Alemania). Septiembre 25-29, 2011.
- **López, A.M.**, Rendueles, M. Díaz. "Analysis of the treatment of aqueous effluents containing organic/emergent contaminants: Adsorption and Oxidation"(poster). VII ANQUE INTERNATIONAL CONGRESS. Internal Water Cycle: Present and Future. Oviedo (España) Junio 13-16, 2010

7.1.3. Informe sobre el índice de impacto de los artículos de la tesis

Los artículos que conforman la presente memoria han sido publicados en las revistas incluidas en el Science Citation Index(Thomson Reuters), cuyos índices de impacto son los siguientes:

- Solvent Extraction and Ion Exchange (2013)→ 2.375
- Separation Science and Technology (2013)→ 1.16